DIRECT AND INVERSE SCATTERING PROBLEMS FOR ELASTIC WAVES

A Dissertation

Submitted to the Faculty

of

Purdue University

by

Xiaokai Yuan

In Partial Fulfillment of the

Requirements for the Degree

of

Doctor of Philosophy

August 2019

Purdue University

West Lafayette, Indiana

THE PURDUE UNIVERSITY GRADUATE SCHOOL
STATEMENT OF DISSERTATION APPROVAL

Dr. Peijun Li, Chair

Department of Mathematics

Dr. Zhiqiang Cai

Department of Mathematics

Dr. Steven Dong

Department of Mathematics

Dr. Jie Shen

Department of Mathematics

Approved by:

Dr. David Goldberg

Department of Mathematics

To my beloved parents and sister.

ACKNOWLEDGMENTS

First and foremost, I want to thank my advisor Prof. Peijun Li, not only for his patience and invaluable guidance in my academic career development during the past four years, but also for the excellent example he has provided as how to be an extraordinary mathematician and professor. His noble personalities: curiosity, diligence, patience, collaboration, will always encourage me to grow as a mathematician. It will be my lifelong time honor to be his Ph.D. student.

Besides my advisor, I would like to thank my committee members, Prof. Zhiqiang Cai, Prof. Suchuan Dong, and Prof. Jie Shen for their time and helpful comments. I would also like to thank all the professors I met in Purdue who taught me classes and extended the horizon of my knowledge. I also want to acknowledge Prof. Huaian Diao, Prof. Heping Dong, and Prof. Yixian Gao for their collaborations, discussions and suggestions.

I wish to thank my roommate, academic brother and dear friend, Dr. Yue Zhao, for his uncountable help, support and encouragement not only in academic but also in daily life; I also want to thank Chuchu Chen, Wei Deng, Jianliang Li, Xiaofeng Ou, Xu Wang and many other friends at Purdue for their invaluable help and friendship.

Finally, I want to take this chance to thank my parents and my sister for their love and care.

TABLE OF CONTENTS

Page

LIST OF TABLES

LIST OF FIGURES

ABSTRACT

Xiaokai Yuan Ph.D., Purdue University, August 2019. Direct and Inverse Scattering Problems for Elastic Waves. Major Professor: Peijun Li.

In this thesis, both direct and inverse elastic scattering problems are considered. For a given incident wave, the direct problem is to determine the displacement of wave field from the known structure, which could be an obstacle or a surface in this thesis; The inverse problem is to determine the structure from the measurement of displacement on an artificial boundary. In the second chapter, we consider the scattering of an elastic plane wave by a rigid obstacle, which is immersed in a homogeneous and isotropic elastic medium in two dimensions. Based on a Dirichlet-to-Neumann (DtN) operator, an exact transparent boundary condition is introduced and the scattering problem is formulated as a boundary value problem of the elastic wave equation in a bounded domain. By developing a new duality argument, an a posteriori error estimate is derived for the discrete problem by using the finite element method with the truncated DtN operator. The a posteriori error estimate consists of the finite element approximation error and the truncation error of the DtN operator which decays exponentially with respect to the truncation parameter. An adaptive finite element algorithm is proposed to solve the elastic obstacle scattering problem, where the truncation parameter is determined through the truncation error and the mesh elements for local refinements are chosen through the finite element discretization error. In chapter 3, we extend the argument developed in chapter 2 to elastic surface grating problem, where the surface is assumed to be periodic and elastic rigid; Then, we treat the obstacle scattering in three dimensional space; The direct problem is shown to have a unique weak solution by examining its variational formulation. The domain derivative is studied and a frequency continuation method is developed for

the inverse problem. Finally, in chapter 4, a rigorous mathematical model and an efficient computational method are proposed to solve the inverse elastic surface scattering problem which arises from the near-field imaging of periodic structures. The surface is assumed to be a small and smooth perturbation of an elastically rigid plane. By placing a rectangle slab of a homogeneous and isotropic elastic medium with larger mass density above the surface, more propagating wave modes can be utilized from the far-field data which contributes to the reconstruction resolution. Requiring only a single illumination, the method begins with the far-to-near field data conversion and utilized the transformed field expansion to derive an analytic solution for the direct problem, which leads to an explicit inversion formula for the inverse problem; Moreover, a nonlinear correction scheme is developed to improve the accuracy of the reconstruction; Numerical examples are presented to demonstrate the effectiveness of the proposed methods for solving the questions mentioned above.

1. INTRODUCTION

Scattering problems consider the interaction between incident wave and some structures it hits on. Roughly speaking, it can be classified to direct problems and inverse problems. Direct problem considers the wave propagation after a given incident wave scattered by a known structure, in this thesis the structure could be an obstacle or a periodic surface; For a given incident wave, the inverse problem concerns to reconstruct some properties of the structure, like the geometry of the structure, from the measurement on some artificial boundary.

Generally speaking, scattering problems can be acoustic wave scattering, electromagnetic wave scattering and elastic wave scattering. Specifically, in this thesis, we focus our attention on elastic wave scattering which is more complicate due to the coupling of compressional wave and shear wave with different speeds. For time dependent problem, the displacement of elastic wave is governed by

$$-\nabla \cdot \sigma + \rho \partial_t^2 \boldsymbol{U} = 0, \tag{1.1}$$

where ρ is elastic mass density and σ is the stress, vector $\boldsymbol{U}$ is the displacement of elastic wave. In homogeneous and isotropic medium, by Hooke's law

$$\sigma = 2\mu\epsilon + \lambda \operatorname{tr}(\epsilon) I,$$

where λ, μ are Lamé parameters and I is the identity matrix, tr is trace operator and ϵ is strain tensor defined as

$$\epsilon = \nabla \boldsymbol{U} + (\nabla \boldsymbol{U})^{\top}.$$

For time harmonic problem, we assume the solution $\boldsymbol{U}(x,t)$ has form as $\boldsymbol{U}(x,t) = \operatorname{Re}\left\{\boldsymbol{u}(x)e^{-\mathrm{i}\omega t}\right\}$, where ω is angular frequency. Plug it to (1.1), we can get the Navier equation

$$\mu\Delta\boldsymbol{u} + (\lambda+\mu)\nabla\nabla\cdot\boldsymbol{u} + \omega^2\rho\boldsymbol{u} = 0.$$

For simplicity, throughout this thesis, we assume the elastic mass density $\rho = 1$.

The goal of thesis is fourfold:

- Convergence analysis of adaptive finite element method with DtN map for elastic obstacle scattering;
- Convergence analysis of adaptive finite element method with DtN map for elastic periodic surface grating;
- Analysis of direct and inverse elastic obstacle scattering in three-dimensions;
- Numerical algorithm for the inverse elastic surface scattering with a slab.

In Chapter 2, consider the scattering of an elastic plane wave by a rigid obstacle, which is immersed in a homogeneous and isotropic elastic medium in two dimensions. Based on a Dirichlet-to-Neumann (DtN) operator, an exact transparent boundary condition is introduced and the scattering problem is formulated as a boundary value problem of the elastic wave equation in a bounded domain. By developing a new duality argument, an a posteriori error estimate is derived for the discrete problem by using the finite element method with the truncated DtN operator. The a posteriori error estimate consists of the finite element approximation error and the truncation error of the DtN operator which decays exponentially with respect to the truncation parameter. An adaptive finite element algorithm is proposed to solve the elastic obstacle scattering problem, where the truncation parameter is determined through the truncation error and the mesh elements for local refinements are chosen through the finite element discretization error. Numerical experiments are presented to demonstrate the effectiveness of the proposed method.

In Chapter 3, we consider the problem of a time harmonic elastic plane wave by a periodic structure; Transparent boundary condition is introduced to reformulate the unbounded physical problem to a boundary value problem in a bounded domain; Through duality argument and Helmholtz decomposition, the a posteriori error estimate, which consists of finite element error and truncation error of DtN operator

is deduced; Based on the a posteriori error estimate, an adaptive algorithm which determine the TBC truncation parameter and mesh refinement is developed; Some numerical examples are presented to demonstrate the proposed adaptive algorithm works well.

Chapter 4 considers an exterior problem of the three-dimensional elastic wave equation, which models the scattering of a time-harmonic plane wave by a rigid obstacle. The scattering problem is reformulated into a boundary value problem by introducing a transparent boundary condition. Given the incident field, the direct problem is to determine the displacement of the wave field from the known obstacle; the inverse problem is to determine the obstacle's surface from the measurement of the displacement on an artificial boundary enclosing the obstacle. In this chapter, we consider both the direct and inverse problems. The direct problem is shown to have a unique weak solution by examining its variational formulation. The domain derivative is studied and a frequency continuation method is developed for the inverse problem. Numerical experiments are presented to demonstrate the effectiveness of the proposed method.

In Chapter 5, a rigorous mathematical model and an efficient computational method are proposed to solve the inverse elastic surface scattering problem which arises from the near-field imaging of periodic structures. We demonstrate how an enhanced resolution can be achieved by using more easily measurable far-field data. The surface is assumed to be a small and smooth perturbation of an elastically rigid plane. By placing a rectangular slab of a homogeneous and isotropic elastic medium with larger mass density above the surface, more propagating wave modes can be utilized from the far-field data which contributes to the reconstruction resolution. Requiring only a single illumination, the method begins with the far-to-near (FtN) field data conversion and utilizes the transformed field expansion to derive an analytic solution for the direct problem, which leads to an explicit inversion formula for the inverse problem. Moreover, a nonlinear correction scheme is developed to improve the

accuracy of the reconstruction. Results show that the proposed method is capable of stably reconstructing surfaces with resolution controlled by the slab's density.

2. THE DIRECT ELASTIC OBSTACLE SCATTERING PROBLEM

2.1 Introduction

A basic problem in classical scattering theory is the scattering of time-harmonic waves by a bounded and impenetrable medium, which is known as the obstacle scattering problem. It has played a crucial role in diverse scientific areas such as radar and sonar, geophysical exploration, medical imaging, and nondestructive testing. Motivated by these significant applications, the obstacle scattering problem has been widely studied for acoustic and electromagnetic waves. Consequently, a great deal of results are available concerning its solution [37, 80, 82]. Recently, the scattering problems for elastic waves have received ever-increasing attention due to the important applications in seismology and geophysics [11, 75, 76]. For instance, they are fundamental to detect the fractures in sedimentary rocks for the production of underground gas and liquids. Compared with acoustic and electromagnetic waves, elastic waves are less studied due to the coexistence of compressional waves and shear waves that have different wavenumbers [34, 66].

The obstacle scattering problem is usually formulated as an exterior boundary value problem imposed in an open domain. The unbounded physical domain needs to be truncated into a bounded computational domain for the convenience of mathematical analysis or numerical computation. Therefore, an appropriate boundary condition is required on the boundary of the truncated domain to avoid artificial wave reflection. Such a boundary condition is called the transparent boundary condition (TBC) or non-reflecting boundary condition. It is one of the important and active subjects in the research area of wave propagation [19, 44–46, 55, 56, 91]. Since Berenger proposed a perfectly matched layer (PML) technique to solve the time-dependent Maxwell e-

quations [20], the research on the PML has undergone a tremendous development due to its effectiveness and simplicity. Various constructions of PML have been proposed and studied for a wide range of scattering problems on acoustic and electromagnetic wave propagation [18, 26, 33, 51, 58, 92]. The basic idea of the PML technique is to surround the domain of interest by a layer of finite thickness fictitious medium that attenuates the waves coming from inside of the computational domain. When the waves reach the outer boundary of the PML region, their values are so small that the homogeneous Dirichlet boundary conditions can be imposed.

A posteriori error estimates are computable quantities which measure the solution errors of discrete problems. They are essential in designing algorithms for mesh modification which aim to equidistribute the computational effort and optimize the computation. The a posteriori error estimates based adaptive finite element methods have the ability of error control and asymptotically optimal approximation property [4]. They have become a class of important numerical tools for solving differential equations, especially for those where the solutions have singularity or multiscale phenomena. Combined with the PML technique, an efficient adaptive finite element method was developed in [29] for solving the two-dimensional diffraction grating problem, where the medium has a one-dimensional periodic structure and the model equation is the two-dimensional Helmholtz equation. It was shown that the a posteriori error estimate consists of the finite element discretization error and the PML truncation error which decays exponentially with respect to the PML parameters such as the thickness of the layer and the medium properties. Due to the superior numerical performance, the adaptive PML method was quickly extended to solve the two- and three-dimensional obstacle scattering problems [26, 28] and the three-dimensional diffraction grating problem [16], where either the two-dimensional Helmholtz equation or the three-dimensional Maxwell equations were considered. Although the PML method has been developed to solve various elastic wave propagation problems in engineering and geophysics soon after it was introduced [32, 36, 48, 65],

the rigorous mathematical studies were only recently done for elastic waves because of the complex of the model equation [22, 30, 60, 62].

As a viable alternative, the finite element DtN method has been proposed to solve the obstacle scattering problems [61, 63] and the diffraction grating problems [59, 94], respectively, where the transparent boundary conditions are used to truncate the domains. In this new approach, the layer of artificial medium is not needed to enclose the domain of interest, which makes is different from the PML method. The transparent boundary conditions are based on nonlocal Dirichlet-to-Neumann (DtN) operators and are given as infinite Fourier series. Since the transparent boundary conditions are exact, the artificial boundary can be put as close as possible to the scattering structures, which can reduce the size of the computational domain. Numerically, the infinite series need to be truncated into a sum of finitely many terms by choosing an appropriate truncation parameter N. It is known that the convergence of the truncated DtN map could be arbitrarily slow to the original DtN map in the operator norm. The a posteriori error analysis of the PML method cannot be applied directly to the DtN method since the DtN map of the truncated PML problem converges exponentially fast to the DtN map of the untruncated PML problem. To overcome this issue, a duality argument had to be developed to obtain the a posteriori error estimate between the solution of the scattering problem and the finite element solution. Comparably, the a posteriori error estimates consists of the finite element discretization error and the DtN truncation error, which decays exponentially with respect to the truncation parameter N. The numerical experiments demonstrate that the adaptive DtN method has a competitive behavior to the adaptive PML method.

In this chapter, we present an adaptive finite element DtN method and carry out its mathematical analysis for the elastic wave scattering problem. The goal is threefold: (1) prove the exponential convergence of the truncated DtN operator; (2) give a complete a posteriori error estimate; (3) develop an effective adaptive finite element algorithm. This chapter significantly extends the work on the acoustic scattering problem [61], where the Helmholtz equation was considered. Apparently, the tech-

niques differ greatly from the existing work because of the complicated transparent boundary condition associated with the elastic wave equation.

Specifically, we consider a rigid obstacle which is immersed in a homogeneous and isotropic elastic medium in two dimensions. The Helmholtz decomposition is utilized to formulate the exterior boundary value problem of the elastic wave equation into a coupled exterior boundary value problem of the Helmholtz equation. By using a Dirichlet-to-Neumann (DtN) operator, an exact transparent boundary condition, which is given as a Fourier series, is introduced to reduce the original scattering problem into a boundary value problem of the elastic wave equation in a bounded domain. The discrete problem is studied by using the finite element method with the truncated DtN operator. Based on the Helmholtz decomposition, a new duality argument is developed to obtain an a posteriori error estimate between the solution of the original scattering problem and the discrete problem. The a posteriori error estimate consists of the finite element approximation error and the truncation error of the DtN operator which is shown to decay exponentially with respect to the truncation parameter. The estimate is used to design the adaptive finite element algorithm to choose elements for refinements and to determine the truncation parameter N. Since the truncation error decays exponentially with respect to N, the choice of the truncation parameter N is not sensitive to the given tolerance. Numerical experiments are presented to demonstrate the effectiveness of the proposed method.

The chapter is organized as follows. In Section 2.2, the elastic wave equation is introduced for the scattering by a rigid obstacle; a boundary value problem is formulated by using the transparent boundary condition; the corresponding weak formulation is discussed. In Section 2.3, the discrete problem is considered by using the finite element approximation with the truncated DtN operator. Section 2.4 is devoted to the a posteriori error analysis and serves as the basis of the adaptive algorithm. In Section 2.5, we discuss the numerical implementation of the adaptive algorithm and present two numerical examples to illustrate the performance of the

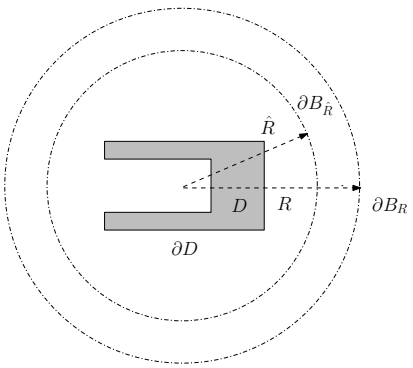

Figure 2.1. Schematic of the elastic wave scattering problem.

proposed method. The chapter is concluded with some general remarks and directions for future work in Section 2.6.

2.2 Problem Formulation

Consider a two-dimensional elastically rigid obstacle D with Lipschitz continuous boundary ∂D, as seen in Figure 2.1. Denote by ν and τ the unit normal and tangent vectors on ∂D, respectively. The exterior domain $\mathbb{R}^2\backslash\overline{D}$ is assumed to be filled with a homogeneous and isotropic elastic medium with a unit mass density. Let $B_R = \{\boldsymbol{x} = (x, y)^\top \in \mathbb{R}^2 : |\boldsymbol{x}| < R\}$ and $B_{\hat{R}} = \{\boldsymbol{x} \in \mathbb{R}^2 : |\boldsymbol{x}| < \hat{R}\}$ be the balls with radii R and $\hat{R}$, respectively, where $R > \hat{R} > 0$. Denote by ∂B_R and $\partial B_{\hat{R}}$ the boundaries of B_R and $R_{\hat{R}}$, respectively. Let $\hat{R}$ be large enough such that $\overline{D} \subset B_{\hat{R}} \subset B_R$. Denote by $\Omega = B_R\backslash\overline{D}$ the bounded domain where the boundary value problem will be formulated.

Let the obstacle be illuminated by an incident wave $\boldsymbol{u}^{\text{inc}}$. The displacement of the scattered field $\boldsymbol{u}$ satisfies the two-dimensional elastic wave equation

$$\mu\Delta\boldsymbol{u} + (\lambda + \mu)\nabla\nabla\cdot\boldsymbol{u} + \omega^2\boldsymbol{u} = 0 \quad \text{in}\,\mathbb{R}^2\backslash\overline{D}, \tag{2.1}$$

where $\omega > 0$ is the angular frequency and λ, μ are the Lamé constants satisfying $\mu > 0, \lambda + \mu > 0$. Since the obstacle is assumed to be rigid, the displacement of the total field $\boldsymbol{u} + \boldsymbol{u}^{\text{inc}}$ vanishes on the boundary of the obstacle, i.e., we have

$$\boldsymbol{u} = \boldsymbol{g} \quad \text{on } \partial D, \tag{2.2}$$

where $\boldsymbol{g} = -\boldsymbol{u}^{\text{inc}}$. In addition, the scattered field $\boldsymbol{u}$ is required to satisfy the Kupradze–Sommerfeld radiation condition

$$\lim_{\rho\to\infty} \rho^{1/2}(\partial_\rho \boldsymbol{u}_{\text{p}} - \mathrm{i}\kappa_1 \boldsymbol{u}_{\text{p}}) = 0, \quad \lim_{\rho\to\infty} \rho^{1/2}(\partial_\rho \boldsymbol{u}_{\text{s}} - \mathrm{i}\kappa_2 \boldsymbol{u}_{\text{s}}) = 0, \quad \rho = |\boldsymbol{x}|, \tag{2.3}$$

where

$$\boldsymbol{u}_{\text{p}} = -\frac{1}{\kappa_1^2}\nabla\nabla\cdot\boldsymbol{u}, \quad \boldsymbol{u}_{\text{s}} = \frac{1}{\kappa_2^2}\mathbf{curl}\,\mathrm{curl}\boldsymbol{u},$$

are the compressional and shear wave components of $\boldsymbol{u}$, respectively. Here

$$\kappa_1 = \frac{\omega}{(\lambda+2\mu)^{1/2}}, \quad \kappa_2 = \frac{\omega}{\mu^{1/2}}$$

are knowns as the compressional wavenumber and the shear wavenumber, respectively. Clearly we have $\kappa_1 < \kappa_2$ since $\mu > 0, \lambda + \mu > 0$. Given a vector function $\boldsymbol{u} = (u_1, u_2)^\top$ and a scalar function u, the scalar and vector curl operators are defined by

$$\mathrm{curl}\boldsymbol{u} = \partial_x u_2 - \partial_y u_1, \quad \mathbf{curl}\, u = (\partial_y u, -\partial_x u)^\top.$$

For any solution $\boldsymbol{u}$ of (2.1), we introduce the Helmholtz decomposition

$$\boldsymbol{u} = \nabla\phi + \mathbf{curl}\,\psi, \tag{2.4}$$

where ϕ, ψ are called the scalar potential functions. Substituting (2.4) into (2.1) yields that ϕ, ψ satisfy the Helmholtz equation

$$\Delta\phi + \kappa_1^2\phi = 0, \quad \Delta\psi + \kappa_2^2\psi = 0 \quad \text{in } \mathbb{R}^2\backslash\overline{D}. \tag{2.5}$$

Taking the dot product of (2.2) with ν and τ, respectively, we get

$$\partial_\nu\phi - \partial_\tau\psi = f_1, \quad \partial_\nu\psi + \partial_\tau\phi = f_2 \quad \text{on } \partial D, \tag{2.6}$$

where $f_1 = -\boldsymbol{g}\cdot\nu$ and $f_2 = \boldsymbol{g}\cdot\tau$. It follows from (2.3) that ϕ, ψ satisfies the Sommerfeld radiation condition

$$\lim_{\rho\to\infty} \rho^{1/2}(\partial_\rho\phi - \kappa_1\phi) = 0, \quad \lim_{\rho\to\infty} \rho^{1/2}(\partial_\rho\psi - \kappa_2\psi) = 0. \tag{2.7}$$

Based on the Helmholtz decomposition, it is easy to show the equivalence of the boundary value problems (2.1)–(2.3) and (2.5)–(2.7). The details are omitted for brevity.

Lemma 2.2.1 *Let $\boldsymbol{u}$ be the solution of the boundary value problem* (2.1)–(2.3)*. Then $\phi = -\kappa_1^{-2}\nabla\cdot\boldsymbol{u}, \psi = \kappa_2^{-1}\mathrm{curl}\boldsymbol{u}$ are the solutions of the coupled boundary value problem* (2.5)–(2.7)*. Conversely, if ϕ, ψ are the solution of the boundary value problem* (2.5)–(2.7)*, then $\boldsymbol{u} = \nabla\phi + \mathbf{curl}\psi$ is the solution of the boundary value problem* (2.1)–(2.3)*.*

Denote by $L^2(\Omega)$ the usual Hilbert space of square integrable functions. Let $H^1(\Omega)$ be the standard Sobolev space equipped with the norm

$$\|u\|_{H^1(\Omega)} = \Big(\|u\|^2_{L^2(\Omega)} + \|\nabla u\|^2_{L^2(\Omega)}\Big)^{1/2}.$$

Define $H^1_{\partial D}(\Omega) = \{u \in H^1(\Omega) : u = 0 \text{ on } \partial D\}$. For any function $u \in L^2(\partial B_R)$, it admits the Fourier series expansion

$$u(R,\theta) = \sum_{n\in\mathbb{Z}} \hat{u}_n(R)e^{\mathrm{i}n\theta}, \quad \hat{u}_n(R) = \frac{1}{2\pi}\int_0^{2\pi} u(R,\theta)e^{-\mathrm{i}n\theta}\mathrm{d}\theta.$$

The trace space $H^s(\partial B_R), s \in \mathbb{R}$ is defined by

$$H^s(\partial B_R) = \{u \in L^2(\partial B_R) : \|u\|_{H^s(\partial B_R)} < \infty\},$$

where $H^s(\partial B_R)$ norm is given by

$$\|u\|_{H^s(\partial B_R)} = \Big(2\pi\sum_{n\in\mathbb{Z}}(1+n^2)^s|\hat{u}_n(R)|^2\Big)^{1/2}.$$

Let $\boldsymbol{H}^1(\Omega) = H^1(\Omega)^2$ and $\boldsymbol{H}^1_{\partial D}(\Omega) = H^1_{\partial D}(\Omega)^2$ be the Cartesian product spaces equipped with the corresponding 2-norms of $H^1(\Omega)$ and $H^1_{\partial D}(\Omega)$, respectively. Throughout the chapter, we take the notation of $a \lesssim b$ to stand for $a \leqslant Cb$, where C is a positive constant whose value is not required but should be clear from the context.

The elastic wave scattering problem (2.2)–(2.3) is formulated in the open domain $\mathbb{R}^2\backslash\overline{D}$, which needs to be truncated into the bounded domain Ω. An appropriate boundary condition is required on ∂B_R.

Define a boundary operator for the displacement of the scattered wave

$$\mathscr{B}\boldsymbol{u} = \mu\partial_r\boldsymbol{u} + (\lambda+\mu)\nabla\cdot\boldsymbol{u}\boldsymbol{e}_r \quad \text{on}\, \partial B_R,$$

where $\boldsymbol{e}_r$ is the unit outward normal vector on ∂B_R. It is shown in [75] that the scattered field $\boldsymbol{u}$ satisfies the transparent boundary condition on ∂B_R:

$$\mathscr{B}\boldsymbol{u} = (\mathscr{T}\boldsymbol{u})(R,\theta) := \sum_{n\in\mathbb{Z}} M_n\boldsymbol{u}_n(R)e^{\mathrm{i}n\theta}, \quad \boldsymbol{u}(R,\theta) = \sum_{n\in\mathbb{Z}}\boldsymbol{u}_n(R)e^{\mathrm{i}n\theta}, \tag{2.8}$$

where $\mathscr{T}$ is called the Dirichlet-to-Neumann (DtN) operator and M_n is a 2×2 matrix whose entries are given in Appendix A.

Based on the transparent boundary condition (2.8), the variational problem for (2.1)–(2.3) is to find $\boldsymbol{u}\in\boldsymbol{H}^1(\Omega)$ with $\boldsymbol{u}=\boldsymbol{g}$ on ∂D such that

$$b(\boldsymbol{u},\boldsymbol{v}) = 0, \quad \forall\boldsymbol{v}\in\boldsymbol{H}^1_{\partial D}(\Omega), \tag{2.9}$$

where the sesquilinear form $b:\boldsymbol{H}^1(\Omega)\times\boldsymbol{H}^1(\Omega)\to\mathbb{C}$ is defined as

$$\begin{aligned} b(\boldsymbol{u},\boldsymbol{v}) = \mu\int_\Omega \nabla\boldsymbol{u}:\nabla\overline{\boldsymbol{v}}\mathrm{d}\boldsymbol{x} + (\lambda+\mu)\int_\Omega(\nabla\cdot\boldsymbol{u})(\nabla\cdot\overline{\boldsymbol{v}})\,\mathrm{d}\boldsymbol{x} \\ -\omega^2\int_\Omega\boldsymbol{u}\cdot\overline{\boldsymbol{v}}\mathrm{d}\boldsymbol{x} - \int_{\partial B_R}\mathscr{T}\boldsymbol{u}\cdot\overline{\boldsymbol{v}}\mathrm{d}s. \end{aligned} \tag{2.10}$$

Here $A:B=\mathrm{tr}(AB^\top)$ is the Frobenius inner product of square matrices A and B.

Following [75], we may show that the variational problem (2.9) has a unique weak solution $\boldsymbol{u}\in\boldsymbol{H}^1(\Omega)$ for any frequency ω and the solution satisfies the estimate

$$\|\boldsymbol{u}\|_{\boldsymbol{H}^1(\Omega)} \lesssim \|\boldsymbol{g}\|_{\boldsymbol{H}^{1/2}(\partial D)} \lesssim \|\boldsymbol{u}^{\mathrm{inc}}\|_{\boldsymbol{H}^1(\Omega)}. \tag{2.11}$$

It follows from the general theory in [3] that there exists a constant $\gamma>0$ such that the following inf-sup condition holds

$$\sup_{0\neq\boldsymbol{v}\in\boldsymbol{H}^1(\Omega)}\frac{|b(\boldsymbol{u},\boldsymbol{v})|}{\|\boldsymbol{v}\|_{\boldsymbol{H}^1(\Omega)}} \geqslant \gamma\|\boldsymbol{u}\|_{\boldsymbol{H}^1(\Omega)}, \quad \forall\boldsymbol{u}\in\boldsymbol{H}^1(\Omega).$$

2.3 The Discrete Problem

Let us consider the discrete problem of (2.9) by using the finite element approximation. Let $\mathcal{M}_h$ be a regular triangulation of Ω, where h denotes the maximum diameter of all the elements in $\mathcal{M}_h$. For simplicity, we assume that the boundary ∂D is polygonal and ignore the approximation error of the boundary ∂B_R, which allows to focus of deducing the a posteriori error estimate. Thus any edge $e \in \mathcal{M}_h$ is a subset of $\partial\Omega$ if it has two boundary vertices.

Let $\boldsymbol{V}_h \subset \boldsymbol{H}^1(\Omega)$ be a conforming finite element space, i.e.,

$$\boldsymbol{V}_h := \left\{ \boldsymbol{v} \in C(\overline{\Omega})^2 : \boldsymbol{v}\big|_K \in P_m(K)^2 \text{ for any } K \in \mathcal{M}_h \right\},$$

where m is a positive integer and $P_m(K)$ denotes the set of all polynomials of degree no more than m. The finite element approximation to the variational problem (2.9) is to find $\boldsymbol{u}^h \in \boldsymbol{V}_h$ with $\boldsymbol{u}^h = \boldsymbol{g}$ on ∂D such that

$$b(\boldsymbol{u}^h, \boldsymbol{v}^h) = 0, \quad \forall \boldsymbol{v}^h \in \boldsymbol{V}_{h,\partial D}, \tag{2.12}$$

where $\boldsymbol{V}_{h,\partial D} = \{\boldsymbol{v} \in \boldsymbol{V}_h : \boldsymbol{v} = 0 \text{ on } \partial D\}$.

In the variational problem (2.12), the DtN operator $\mathscr{T}$ is given by an infinite series. In practical computation, the infinite series must be truncated into a finite sum. Given a sufficiently large N, we define the truncated DtN operator

$$\mathscr{T}_N \boldsymbol{u} = \sum_{|n| \leqslant N} M_n \boldsymbol{u}_n(R) e^{\mathrm{i}n\theta}. \tag{2.13}$$

Using (2.13), we have the truncated finite element approximation: Find $\boldsymbol{u}_N^h \in \boldsymbol{V}_h$ with $\boldsymbol{u}_N^h = \boldsymbol{g}$ on ∂D such that

$$b_N(\boldsymbol{u}_N^h, \boldsymbol{v}^h) = 0, \quad \forall \boldsymbol{v}^h \in \boldsymbol{V}_{h,\partial D}, \tag{2.14}$$

where the sesquilinear form $b_N : \boldsymbol{V}_h \times \boldsymbol{V}_h \to \mathbb{C}$ is defined as

$$\begin{aligned} b_N(\boldsymbol{u}, \boldsymbol{v}) = \mu \int_\Omega \nabla \boldsymbol{u} : \nabla \overline{\boldsymbol{v}} \mathrm{d}\boldsymbol{x} + (\lambda + \mu) \int_\Omega (\nabla \cdot \boldsymbol{u}) (\nabla \cdot \overline{\boldsymbol{v}}) \, \mathrm{d}\boldsymbol{x} \\ -\omega^2 \int_\Omega \boldsymbol{u} \cdot \overline{\boldsymbol{v}} \mathrm{d}\boldsymbol{x} - \int_{\partial B_R} \mathscr{T}_N \boldsymbol{u} \cdot \overline{\boldsymbol{v}} \mathrm{d}s. \end{aligned} \tag{2.15}$$

For sufficiently large N and sufficiently small h, the discrete inf-sup condition of the sesquilinear form b_N may be established by following the approach in [90]. Based on the general theory in [3], the truncated variational problem (2.14) can be shown to have a unique solution $\boldsymbol{u}_N^h \in \boldsymbol{V}_h$. The details are omitted since our focus is the a posteriori error estimate.

2.4 The a Posteriori Error Analysis

For any triangular element $K \in \mathcal{M}_h$, denoted by h_K its diameter. Let $\mathcal{B}_h$ denote the set of all the edges of K. For any edge $e \in \mathcal{B}_h$, denoted by h_e its length. For any interior edge e which is the common side of triangular elements $K_1, K_2 \in \mathcal{M}_h$, we define the jump residual across e as

$$J_e = \mu \nabla \boldsymbol{u}_N^h|_{K_1} \cdot \boldsymbol{\nu}_1 + (\lambda+\mu)\nabla \cdot \boldsymbol{u}_N^h|_{K_1}\boldsymbol{\nu}_1 + \mu \nabla \boldsymbol{u}_N^h|_{K_2} \cdot \boldsymbol{\nu}_2 + (\lambda+\mu)\nabla \cdot \boldsymbol{u}_N^h|_{K_2}\boldsymbol{\nu}_2,$$

where $\boldsymbol{\nu}_j$ is the unit outward normal vector on the boundary of $K_j, j = 1, 2$. For any boundary edge $e \subset \partial B_R$, we define the jump residual

$$J_e = 2\left(\mathscr{T}_N \boldsymbol{u}_N^h - \mu(\nabla \boldsymbol{u}_N^h \cdot \boldsymbol{e}_r) - (\lambda+\mu)(\nabla \cdot \boldsymbol{u}_N^h)\boldsymbol{e}_r\right).$$

For any triangular element $K \in \mathcal{M}_h$, denote by η_K the local error estimator which is given by

$$\eta_K = h_K \|\mathscr{R}\boldsymbol{u}_N^h\|_{\boldsymbol{L}^2(K)} + \left(\frac{1}{2}\sum_{e\in\partial K} h_e \|J_e\|^2_{\boldsymbol{L}^2(e)}\right)^{1/2},$$

where $\mathscr{R}$ is the residual operator defined by

$$\mathscr{R}\boldsymbol{u} = \mu\Delta\boldsymbol{u} + (\lambda+\mu)\nabla(\nabla\cdot\boldsymbol{u}) + \omega^2\boldsymbol{u}.$$

For convenience, we introduce a weighted norm $|||\cdot|||_{\boldsymbol{H}^1(\Omega)}$ which is given by

$$|||\boldsymbol{u}|||^2_{\boldsymbol{H}^1(\Omega)} = \mu\int_\Omega |\nabla\boldsymbol{u}|^2 \mathrm{d}\boldsymbol{x} + (\lambda+\mu)\int_\Omega |\nabla\cdot\boldsymbol{u}|^2\mathrm{d}\boldsymbol{x} + \omega^2\int_\Omega |\boldsymbol{u}|^2\mathrm{d}\boldsymbol{x}. \tag{2.16}$$

It can be verified for any $\boldsymbol{u} \in \boldsymbol{H}^1(\Omega)$ that

$$\min\left(\mu, \omega^2\right)\|\boldsymbol{u}\|^2_{\boldsymbol{H}^1(\Omega)} \leqslant |||\boldsymbol{u}|||^2_{\boldsymbol{H}^1(\Omega)} \leqslant \max\left(2\lambda+3\mu, \omega^2\right)\|\boldsymbol{u}\|^2_{\boldsymbol{H}^1(\Omega)}, \tag{2.17}$$

which implies that the two norms $\|\cdot\|_{\boldsymbol{H}^1(\Omega)}$ and $|||\cdot|||_{\boldsymbol{H}^1(\Omega)}$ are equivalent.

Now we state the main result of this chapter.

Theorem 2.4.1 *Let $\boldsymbol{u}$ and $\boldsymbol{u}_N^h$ be the solution of the variational problem* (2.9) *and* (2.12)*, respectively. Then for sufficiently large N, the following a posterior error estimate holds*

$$\|\boldsymbol{u}-\boldsymbol{u}_N^h\|_{\boldsymbol{H}^1(\Omega)} \lesssim \left(\sum_{K\in\mathcal{M}_h}\eta_K^2\right)^{1/2} + \max_{|n|>N}|n|\left(\frac{\hat{R}}{R}\right)^{|n|}\|\boldsymbol{u}^{\mathrm{inc}}\|_{\boldsymbol{H}^1(\Omega)}.$$

We point out that the a posteriori error estimate consists of two parts: the first part arises from the finite element discretization error; the second part comes from the truncation error of the DtN operator. Apparently, the DtN truncation error decreases exponentially with respect to N since $\hat{R} < R$. In the rest of the chapter, we shall prove the a posteriori error estimate in Theorem 2.4.1.

Denoted by $\boldsymbol{\xi} = \boldsymbol{u} - \boldsymbol{u}_N^h$ be the error between solution of the original variational problem (2.9) and the solution of the finite element approximation to the truncated variational problem (2.12).

Lemma 2.4.2 *Let $\boldsymbol{\xi} = \boldsymbol{u} - \boldsymbol{u}_N^h$, where $\boldsymbol{u}$ and $\boldsymbol{u}_N^h$ are the solutions of the problems* (2.9) *and* (2.12)*, respectively. Then*

$$|||\boldsymbol{\xi}|||^2_{\boldsymbol{H}^1(\Omega)} = \Re b(\boldsymbol{\xi},\boldsymbol{\xi}) + \Re\int_{\partial B_R}(\mathscr{T}-\mathscr{T}_N)\,\boldsymbol{\xi}\cdot\overline{\boldsymbol{\xi}}\mathrm{d}s + 2\omega^2\int_\Omega \boldsymbol{\xi}\cdot\overline{\boldsymbol{\xi}}\mathrm{d}\boldsymbol{x} + \Re\int_{\partial B_R}\mathscr{T}_N\boldsymbol{\xi}\cdot\overline{\boldsymbol{\xi}}\mathrm{d}s \tag{2.18}$$

and

$$\begin{aligned} b(\boldsymbol{\xi},\boldsymbol{v}) + \int_{\partial B_R}(\mathscr{T}-\mathscr{T}_N)\,\boldsymbol{\xi}\cdot\overline{\boldsymbol{v}}\mathrm{d}s &= -b_N(\boldsymbol{u}_N^h,\boldsymbol{v}-\boldsymbol{v}^h) \\ &+ \int_{\partial B_R}(\mathscr{T}-\mathscr{T}_N)\,\boldsymbol{u}\cdot\overline{\boldsymbol{v}}\mathrm{d}s, \quad \forall\boldsymbol{v}\in\boldsymbol{H}^1_{\partial D}(\Omega),\ \boldsymbol{v}^h\in\boldsymbol{V}_{h,\partial D}. \end{aligned} \tag{2.19}$$

Proof Combining (2.16), (2.10), and (2.15), we have from straightforward calculations that

$$\begin{aligned}
|||\boldsymbol{\xi}|||^2_{\boldsymbol{H}^1(\Omega)} &= \mu\int_\Omega \nabla\boldsymbol{\xi} : \nabla\overline{\boldsymbol{\xi}}\mathrm{d}\boldsymbol{x} + (\lambda+\mu)\int_\Omega (\nabla\cdot\boldsymbol{\xi})\left(\nabla\cdot\overline{\boldsymbol{\xi}}\right)\mathrm{d}\boldsymbol{x} + \omega^2\int_\Omega \boldsymbol{\xi}\cdot\overline{\boldsymbol{\xi}}\mathrm{d}\boldsymbol{x} \\
&= \Re b(\boldsymbol{\xi},\boldsymbol{\xi}) + 2\omega^2\int_\Omega \boldsymbol{\xi}\cdot\overline{\boldsymbol{\xi}}\mathrm{d}\boldsymbol{x} + \Re\int_{\partial B_R}\mathscr{T}\boldsymbol{\xi}\cdot\overline{\boldsymbol{\xi}}\mathrm{d}s \\
&= \Re b(\boldsymbol{\xi},\boldsymbol{\xi}) + \Re\int_{\partial B_R}(\mathscr{T}-\mathscr{T}_N)\,\boldsymbol{\xi}\cdot\overline{\boldsymbol{\xi}}\mathrm{d}s + 2\omega^2\int_\Omega \boldsymbol{\xi}\cdot\overline{\boldsymbol{\xi}}\mathrm{d}\boldsymbol{x} + \Re\int_{\partial B_R}\mathscr{T}_N\boldsymbol{\xi}\cdot\overline{\boldsymbol{\xi}}\mathrm{d}s
\end{aligned}$$

and

$$\begin{aligned}
b(\boldsymbol{\xi},\boldsymbol{v}) + \int_{\partial B_R}(\mathscr{T}-\mathscr{T}_N)\,\boldsymbol{\xi}\cdot\overline{\boldsymbol{v}}\mathrm{d}s &= b(\boldsymbol{u},\boldsymbol{v}) - b(\boldsymbol{u}_N^h,\boldsymbol{v}) + \int_{\partial B_R}(\mathscr{T}-\mathscr{T}_N)\,\boldsymbol{\xi}\cdot\overline{\boldsymbol{v}}\mathrm{d}s \\
&= b(\boldsymbol{u},\boldsymbol{v}) - b_N(\boldsymbol{u}_N^h,\boldsymbol{v}) + b_N(\boldsymbol{u}_N^h,\boldsymbol{v}) - b(\boldsymbol{u}_N^h,\boldsymbol{v}) + \int_{\partial B_R}(\mathscr{T}-\mathscr{T}_N)\,\boldsymbol{\xi}\cdot\overline{\boldsymbol{v}}\mathrm{d}s \\
&= b(\boldsymbol{u},\boldsymbol{v}) - b_N(\boldsymbol{u}_N^h,\boldsymbol{v}^h) - b_N(\boldsymbol{u}_N^h,\boldsymbol{v}-\boldsymbol{v}^h) + \int_{\partial B_R}(\mathscr{T}-\mathscr{T}_N)\,\boldsymbol{u}_N^h\cdot\overline{\boldsymbol{v}}\mathrm{d}s \\
&\quad + \int_{\partial B_R}(\mathscr{T}-\mathscr{T}_N)\,\boldsymbol{\xi}\cdot\overline{\boldsymbol{v}}\mathrm{d}s \\
&= -b_N(\boldsymbol{u}_N^h,\boldsymbol{v}-\boldsymbol{v}^h) + \int_{\partial B_R}(\mathscr{T}-\mathscr{T}_N)\,\boldsymbol{u}\cdot\overline{\boldsymbol{v}}\mathrm{d}s.
\end{aligned}$$

which complete the proof. ■

The above result is the error representation formula. In the following, we discuss the four terms in (2.18) one by one. Lemma 2.4.3 gives the a posteriori error estimate for the finite element approximation; Lemma 2.4.6 presents the a posteriori error estimate for the truncation of the DtN operator.

Lemma 2.4.3 *Let $\boldsymbol{u}_N^h$ be the solution of the finite element approximation to the truncated variational problem* (2.12)*. Then*

$$\left|b_N^h(\boldsymbol{u}_N^h,\boldsymbol{v}-\boldsymbol{v}^h)\right| \lesssim \left(\sum_{K\in\mathcal{M}_h}\eta_K^2\right)^{1/2}\|\boldsymbol{v}\|_{\boldsymbol{H}^1(\Omega)},\quad \forall\boldsymbol{v}\in\boldsymbol{H}^1_{\partial D}(\Omega),\ \boldsymbol{v}^h\in\boldsymbol{V}_{h,\partial D}. \tag{2.20}$$

Proof For any $\boldsymbol{v} \in \boldsymbol{H}^1_{\partial D}(\Omega)$ and $\boldsymbol{v}^h \in \boldsymbol{V}_{h,\partial D}$, it follows from the integration by parts that

$$
\begin{aligned}
& -b_N(\boldsymbol{u}_N^h, \boldsymbol{v} - \boldsymbol{v}^h) \\
= & -\sum_{K\in\mathcal{M}_h} \left\{ \mu \int_K \nabla \boldsymbol{u}_N^h : \nabla\big(\overline{\boldsymbol{v}} - \overline{\boldsymbol{v}^h}\big)\mathrm{d}\boldsymbol{x} + (\lambda+\mu)\int_K \big(\nabla\cdot\boldsymbol{u}_N^h\big)\nabla\cdot\big(\overline{\boldsymbol{v}} - \overline{\boldsymbol{v}}^h\big)\mathrm{d}\boldsymbol{x} \right\} \\
& -\sum_{K\in\mathcal{M}_h} \left\{ -\omega^2 \int_K \boldsymbol{u}_N^h \cdot \big(\overline{\boldsymbol{v}} - \overline{\boldsymbol{v}^h}\big)\mathrm{d}\boldsymbol{x} - \int_{\partial B_R\cap\partial K} \mathscr{T}\boldsymbol{u}_N^h \cdot \overline{\boldsymbol{v}} - \overline{\boldsymbol{v}^h}\mathrm{d}s \right\} \\
= & \sum_{K\in\mathcal{M}_h} \left\{ -\int_{\partial K} \big[\mu\nabla\boldsymbol{u}_N^h\cdot\boldsymbol{\nu} + (\lambda+\mu)(\nabla\cdot\boldsymbol{u}_N^h)\boldsymbol{\nu}\big]\cdot\big(\overline{\boldsymbol{v}} - \overline{\boldsymbol{v}^h}\big)\mathrm{d}\boldsymbol{x} + \int_{\partial B_R\cap\partial K} \mathscr{T}\boldsymbol{u}_N^h\cdot\big(\overline{\boldsymbol{v}} - \overline{\boldsymbol{v}^h}\big)\mathrm{d}s \right\} \\
& +\sum_{K\in\mathcal{M}_h} \int_K \big[\mu\Delta\boldsymbol{u}_N^h + (\lambda+\mu)\nabla\nabla\cdot\boldsymbol{u}_N^h + \omega^2\boldsymbol{u}_N^h\big]\cdot\big(\overline{\boldsymbol{v}} - \overline{\boldsymbol{v}^h}\big)\mathrm{d}\boldsymbol{x} \\
= & \sum_{K\in\mathcal{M}_h} \left[\int_K \mathscr{R}\boldsymbol{u}_N^h\cdot\big(\overline{\boldsymbol{v}} - \overline{\boldsymbol{v}^h}\big)\mathrm{d}\boldsymbol{x} + \sum_{e\in\partial K}\frac{1}{2}\int_e J_e\cdot\big(\overline{\boldsymbol{v}} - \overline{\boldsymbol{v}^h}\big)\mathrm{d}s \right].
\end{aligned} \tag{2.21}
$$

We take $\boldsymbol{v}^h = \Pi_h\boldsymbol{v} \in \boldsymbol{V}_{h,\partial D}$, where Π_h is the Scott–Zhang interpolation operator [89], which has the following interpolation estimates

$$
\|\boldsymbol{v} - \Pi_h\boldsymbol{v}\|_{\boldsymbol{L}^2(K)} \lesssim h_K\|\nabla\boldsymbol{v}\|_{\boldsymbol{L}^2(\tilde{K})}, \quad \|\boldsymbol{v} - \Pi_h\boldsymbol{v}\|_{\boldsymbol{L}^2(e)} \lesssim h_e^{1/2}\|\boldsymbol{v}\|_{\boldsymbol{H}^1(\tilde{K}_e)}.
$$

Here $\tilde{K}$ and $\tilde{K}_e$ are the union of all the triangular elements in $\mathcal{M}_h$, which have nonempty intersection with the element K and the side e, respectively. Using the Hölder inequality in (2.21), we get

$$
\big|b_N(\boldsymbol{u}_N^h, \boldsymbol{v} - \boldsymbol{v}^h)\big| \lesssim \left(\sum_{K\in\mathcal{M}_h}\eta_K^2\right)^{1/2}\|\boldsymbol{v}\|_{\boldsymbol{H}^1(\Omega)},
$$

which completes the proof. ■

The following result concerns the trace regularity for functions in $H^1(\Omega)$. The proof can be found in [61].

Lemma 2.4.4 *For any $u \in H^1(\Omega)$, the following estimates hold*

$$
\|u\|_{H^{1/2}(\partial B_R)} \lesssim \|u\|_{H^1(\Omega)}, \quad \|u\|_{H^{1/2}(\partial B_{\tilde{R}})} \lesssim \|u\|_{H^1(\Omega)}.
$$

Lemma 2.4.5 *Let $0 < \kappa_1 < \kappa_2$ and $0 < \hat{R} < R$. For sufficiently large n, the following estimate holds for $j = 1, 2$:*

$$\left| \frac{H_n^{(j)}(\kappa_1 R)}{H_n^{(j)}(\kappa_1 \hat{R})} - \frac{H_n^{(j)}(\kappa_2 R)}{H_n^{(j)}(\kappa_2 \hat{R})} \right| \leqslant \frac{\kappa_2 (\kappa_2 - \kappa_1)}{|n| - 1} \left(R^2 - \hat{R}^2 \right) \left(\frac{\hat{R}}{R} \right)^{|n|},$$

where $H_n^{(1)}$ and $H_n^{(2)}$ are the Hankel functions of the first and second kind with order n, respectively.

Proof Since the Hankel functions of the first and second kind are complex conjugate to each other, we only need to show the proof for the Hankel function of the first kind.

Let J_n and Y_n be the Bessel functions of the first and second kind with order n, respectively. For a fixed $z > 0$, they admit the following asymptotic properties [95]:

$$J_n(z) \sim \frac{1}{\sqrt{2\pi n}} \left(\frac{ez}{2n} \right)^n, \qquad Y_n(z) \sim -\sqrt{\frac{2}{\pi n}} \left(\frac{ez}{2n} \right)^{-n}, \quad n \to \infty. \tag{2.22}$$

Define $S(z) = J_n(z)/Y_n(z)$. A simple calculation yields

$$\begin{aligned} \frac{H_n^{(1)}(zR)}{H_n^{(1)}(z\hat{R})} &= \frac{J_n(zR) + \mathrm{i} Y_n(zR)}{J_n(zR_1) + \mathrm{i} Y_n(z\hat{R})} = \frac{Y_n(zR)}{Y_n(z\hat{R})} \frac{1 - \mathrm{i} \frac{J_n(zR)}{Y_n(zR)}}{1 - \mathrm{i} \frac{J_n(z\hat{R})}{Y_n(z\hat{R})}} \\ &= \frac{Y_n(zR)}{Y_n(z\hat{R})} \frac{1 - \mathrm{i} S_n(zR)}{1 - \mathrm{i} S_n(z\hat{R})} = \frac{Y_n(zR)}{Y_n(z\hat{R})} + \mathrm{i} \frac{Y_n(zR)}{Y_n(z\hat{R})} \frac{S_n(z\hat{R}) - S_n(zR)}{1 - \mathrm{i} S_n(z\hat{R})} \end{aligned} \tag{2.23}$$

By (2.22)–(2.23), we have

$$S_n(z) = \frac{J_n(z)}{Y_n(z)} \sim \frac{\frac{1}{\sqrt{2\pi n}} \left(\frac{ez}{2n} \right)^n}{-\sqrt{\frac{2}{\pi n}} \left(\frac{ez}{2n} \right)^{-n}} \sim -\frac{1}{2} \left(\frac{ez}{2n} \right)^{2n}$$

and

$$\begin{aligned} \left| \frac{H_n^{(1)}(\kappa_1 R)}{H_n^{(1)}(\kappa_1 \hat{R})} - \frac{H_n^{(1)}(\kappa_2 R)}{H_n^{(1)}(\kappa_2 \hat{R})} \right| &\leqslant \left| \frac{Y_n(\kappa_1 R)}{Y_n(\kappa_1 \hat{R})} - \frac{Y_n(\kappa_2 R)}{Y_n(\kappa_2 \hat{R})} \right| + \left| \frac{Y_n(\kappa_1 R)}{Y_n(\kappa_1 \hat{R})} \frac{S_n(\kappa_1 \hat{R})}{1 - \mathrm{i} S_n(\kappa_1 \hat{R})} \right| \\ &+ \left| \frac{Y_n(\kappa_1 R)}{Y_n(\kappa_1 \hat{R})} \frac{S_n(\kappa_1 R)}{1 - \mathrm{i} S_n(\kappa_1 \hat{R})} \right| + \left| \frac{Y_n(\kappa_2 R)}{Y_n(\kappa_2 \hat{R})} \frac{S_n(\kappa_2 \hat{R})}{1 - \mathrm{i} S_n(\kappa_2 \hat{R})} \right| + \left| \frac{Y_n(\kappa_2 R)}{Y_n(\kappa_2 \hat{R})} \frac{S_n(\kappa_2 R)}{1 - \mathrm{i} S_n(\kappa_2 \hat{R})} \right|. \end{aligned}$$

It is easy to verify that

$$\left| \frac{S_n(zR)}{1 - \mathrm{i} S_n(z\hat{R})} \right| \leqslant \left(\frac{ezR}{2n} \right)^{2n}, \quad \left| \frac{S_n(z\hat{R})}{1 - \mathrm{i} S_n(z\hat{R})} \right| \leqslant \left(\frac{ez\hat{R}}{2n} \right)^{2n}$$

and

$$\frac{RzY_n'(zR)}{Y_n(zR)} \sim \frac{z^2R^2}{2(n-1)} - n, \quad \frac{Y_n(zR)}{Y_n(z\hat{R})} \sim \left(\frac{\hat{R}}{R}\right)^{|n|}.$$

Combining the above estimates, we have for $R > \hat{R}$ and $\kappa_2 > \kappa_1$ that

$$\left|\frac{Y_n(\kappa_1 R)}{Y_n(\kappa_1\hat{R})}\frac{S_n(\kappa_1\hat{R})}{1-\mathrm{i}S_n(\kappa_1\hat{R})}\right| + \left|\frac{Y_n(\kappa_1 R)}{Y_n(\kappa_1\hat{R})}\frac{S_n(\kappa_1 R)}{1-\mathrm{i}S_n(\kappa_1\hat{R})}\right| + \left|\frac{Y_n(\kappa_2 R)}{Y_n(\kappa_2\hat{R})}\frac{S_n(\kappa_2\hat{R})}{1-\mathrm{i}S_n(\kappa_2\hat{R})}\right|$$
$$+ \left|\frac{Y_n(\kappa_2 R)}{Y_n(\kappa_2\hat{R})}\frac{S_n(\kappa_2 R)}{1-\mathrm{i}S_n(\kappa_2\hat{R})}\right| \leqslant 2\left(\frac{e\kappa_2 R}{2n}\right)^{2n}\left(\left|\frac{Y_n(\kappa_1 R)}{Y_n(\kappa_1\hat{R})}\right| + \left|\frac{Y_n(\kappa_2 R)}{Y_n(\kappa_2\hat{R})}\right|\right).$$

Define $F(z) = Y_n(zR)/Y_n(z\hat{R})$. By the mean value theorem, there exits $\xi \in (\kappa_1, \kappa_2)$ such that

$$\begin{aligned} F(\kappa_1) - F(\kappa_2) &= F'(\xi)(\kappa_1 - \kappa_2) \\ &= \frac{RY_n'(\xi R)Y_n(\xi\hat{R}) - \hat{R}Y_n(\xi R)Y_n'(\xi\hat{R})}{Y_n(\xi\hat{R})^2}(\kappa_1 - \kappa_2) \\ &= \left(\frac{R\xi Y_n'(\xi R)}{Y_n(\xi R)} - \frac{\hat{R}\xi Y_n'(\xi\hat{R})}{Y_n(\xi\hat{R})}\right)\frac{Y_n(\xi R)}{Y_n(\xi\hat{R})}\frac{\kappa_1 - \kappa_2}{\xi} \\ &\sim \frac{\xi\,(\kappa_1 - \kappa_2)}{2(n-1)}\left(R^2 - \hat{R}^2\right)\frac{Y_n(\xi R)}{Y_n(\xi\hat{R})}. \end{aligned}$$

Therefore,

$$\begin{aligned} \left|\frac{H_n^{(1)}(\kappa_1 R)}{H_n^{(1)}(\kappa_1\hat{R})} - \frac{H_n^{(1)}(\kappa_2 R)}{H_n^{(1)}(\kappa_2\hat{R})}\right| &\leqslant \left|\frac{\xi\,(\kappa_1 - \kappa_2)}{2(n-1)}\right|\left|\left(R^2 - \hat{R}^2\right)\frac{Y_n(\xi R)}{Y_n(\xi\hat{R})}\right| \\ &\quad + 2\left(\frac{e\kappa_2 R}{2n}\right)^{2n}\left(\left|\frac{Y_n(\kappa_1 R)}{Y_n(\kappa_1\hat{R})}\right| + \left|\frac{Y_n(\kappa_2 R)}{Y_n(\kappa_2\hat{R})}\right|\right) \\ &\leqslant \frac{\kappa_2\,(\kappa_2 - \kappa_1)}{|n|-1}\left(R^2 - \hat{R}^2\right)\left(\frac{\hat{R}}{R}\right)^{|n|}, \end{aligned}$$

which completes the proof. ■

Lemma 2.4.6 *Let $\boldsymbol{u} \in \boldsymbol{H}^1(\Omega)$ be the solution of the variational problem* (2.9)*. For any $\boldsymbol{v} \in \boldsymbol{H}^1(\Omega)$, the following estimate holds*

$$\left|\int_{\partial B_R} (\mathscr{T} - \mathscr{T}_N)\,\boldsymbol{u} \cdot \overline{\boldsymbol{v}}\, ds\right| \leqslant C \max_{|n|>N}\left(|n|\left(\frac{\hat{R}}{R}\right)^{|n|}\right)\|\boldsymbol{u}^{\mathrm{inc}}\|_{\boldsymbol{H}^1(\Omega)}\|\boldsymbol{v}\|_{\boldsymbol{H}^1(\Omega)}.$$

where C is a positive constant independent of N.

Proof Recalling the Helmholtz decomposition $\boldsymbol{u} = \nabla\phi + \mathbf{curl}\psi$, we have from the Fourier series expansions in (2.54) that

$$\phi_n(R) = \frac{H_n^{(1)}(\kappa_1 R)}{H_n^{(1)}(\kappa_1 \hat{R})}\phi_n(\hat{R}), \quad \psi_n(R) = \frac{H_n^{(1)}(\kappa_2 R)}{H_n^{(1)}(\kappa_2 \hat{R})}\psi_n(\hat{R}).$$

Comparing the Fourier coefficients of $\boldsymbol{u}$ and ϕ, ψ in the Helmholtz decomposition gives

$$\begin{aligned}
\boldsymbol{u}_n(R) &= \begin{bmatrix} \alpha_{1n}(R) & \frac{\mathrm{i}n}{R} \\ \frac{\mathrm{i}n}{R} & -\alpha_{2n}(R) \end{bmatrix} \begin{bmatrix} \phi_n(R) \\ \psi_n(R) \end{bmatrix} \\
&= \begin{bmatrix} \alpha_{1n}(R) & \frac{\mathrm{i}n}{R} \\ \frac{\mathrm{i}n}{R} & -\alpha_{2n}(R) \end{bmatrix} \begin{bmatrix} \frac{H_n^{(1)}(\kappa_1 R)}{H_n^{(1)}(\kappa_1 \hat{R})} & 0 \\ 0 & \frac{H_n^{(1)}(\kappa_2 R)}{H_n^{(1)}(\kappa_2 \hat{R})} \end{bmatrix} \begin{bmatrix} \phi_n(\hat{R}) \\ \psi_n(\hat{R}) \end{bmatrix} \\
&= \begin{bmatrix} \alpha_{1n}(R) & \frac{\mathrm{i}n}{R} \\ \frac{\mathrm{i}n}{R} & -\alpha_{2n}(R) \end{bmatrix} \begin{bmatrix} \frac{H_n^{(1)}(\kappa_1 R)}{H_n^{(1)}(\kappa_1 \hat{R})} & 0 \\ 0 & \frac{H_n^{(1)}(\kappa_2 R)}{H_n^{(1)}(\kappa_2 \hat{R})} \end{bmatrix} \begin{bmatrix} -\alpha_{2n}(\hat{R}) & -\frac{\mathrm{i}n}{\hat{R}} \\ -\frac{\mathrm{i}n}{\hat{R}} & \alpha_{1n}(\hat{R}) \end{bmatrix} \frac{\boldsymbol{u}_n(\hat{R})}{\Lambda_n(\hat{R})} \\
&= -\frac{1}{\Lambda_n(\hat{R})} \begin{bmatrix} A_{11} & A_{12} \\ A_{21} & A_{22} \end{bmatrix} \boldsymbol{u}_n(\hat{R}),
\end{aligned}$$

where α_{jn}, Λ_n is given in (2.58) and

$$\begin{aligned}
A_{11} &= \frac{H_n^{(1)}(\kappa_1 R)}{H_n^{(1)}(\kappa_1 \hat{R})}\alpha_{1n}(R)\alpha_{2n}(\hat{R}) - \frac{n^2}{R\hat{R}}\frac{H_n^{(1)}(\kappa_2 R)}{H_n^{(1)}(\kappa_2 \hat{R})}, \\
A_{12} &= \frac{H_n^{(1)}(\kappa_1 R)}{H_n^{(1)}(\kappa_1 \hat{R})}\alpha_{1n}(R)\frac{\mathrm{i}n}{\hat{R}} - \frac{\mathrm{i}n}{R}\alpha_{1n}(\hat{R})\frac{H_n^{(1)}(\kappa_2 R)}{H_n^{(1)}(\kappa_2 \hat{R})}, \\
A_{21} &= \frac{H_n^{(1)}(\kappa_1 R)}{H_n^{(1)}(\kappa_1 \hat{R})}\alpha_{2n}(\hat{R})\frac{\mathrm{i}n}{R} - \frac{\mathrm{i}n}{\hat{R}}\alpha_{2n}(R)\frac{H_n^{(1)}(\kappa_2 R)}{H_n^{(1)}(\kappa_2 \hat{R})}, \\
A_{22} &= \frac{H_n^{(1)}(\kappa_2 R)}{H_n^{(1)}(\kappa_2 \hat{R})}\alpha_{1n}(\hat{R})\alpha_{2n}(R) - \frac{n^2}{R\hat{R}}\frac{H_n^{(1)}(\kappa_1 R)}{H_n^{(1)}(\kappa_1 \hat{R})}.
\end{aligned}$$

By Lemma 2.4.5, we have

$$\begin{aligned}
|A_{11}| &\leqslant \left|\frac{H_n^{(1)}(\kappa_1 R)}{H_n^{(1)}(\kappa_1 \hat{R})}\right| \left|\alpha_{1n}(R)\alpha_{2n}(\hat{R}) - \frac{n^2}{R\hat{R}}\right| + \frac{n^2}{R\hat{R}} \left|\frac{H_n^{(1)}(\kappa_1 R)}{H_n^{(1)}(\kappa_1 \hat{R})} - \frac{H_n^{(1)}(\kappa_2 R)}{H_n^{(1)}(\kappa_2 \hat{R})}\right| \\
&\leqslant \left(\frac{\hat{R}}{R}\right)^{|n|} \left|\left(\frac{\kappa_1^2 R}{2(n-1)} - \frac{n}{R}\right)\left(\frac{\kappa_2^2 \hat{R}}{2(n-1)} - \frac{n}{\hat{R}}\right) - \frac{n^2}{R\hat{R}}\right| \\
&\quad + \frac{n^2}{R\hat{R}} \frac{\kappa_2\left(\kappa_1 - \kappa_2\right)}{|n|-1}\left(R^2 - \hat{R}^2\right)\left(\frac{R_1}{R}\right)^{|n|} \\
&\leqslant \kappa_2\left(\kappa_2 - \kappa_1\right)\left(R^2 - \hat{R}^2\right)\frac{2|n|}{R\hat{R}}\left(\frac{\hat{R}}{R}\right)^{|n|} \leqslant C|n|\left(\frac{\hat{R}}{R}\right)^{|n|},
\end{aligned}$$

where C is a positive constant independent of n. Similarly, it can be shown that there exists a positive constant C independent of n such that

$$|A_{ij}| \leqslant C|n|\left(\frac{\hat{R}}{R}\right)^{|n|}, \quad i,j = 1,2.$$

The proofs are omitted for brevity. Combining the above estimates and Lemma 2.7.1, we obtain

$$\left|\boldsymbol{u}^{(n)}(R)\right| \leqslant C|n|\left(\frac{\hat{R}}{R}\right)^{|n|}\left|\boldsymbol{u}^{(n)}(\hat{R})\right|.$$

Combining the above estimate with Lemma 2.4.4 and (2.11) yields

$$\begin{aligned}
&\left|\int_{\partial B_R} \left(\mathscr{T} - \mathscr{T}_N\right)\boldsymbol{u}\cdot\overline{\boldsymbol{v}}\mathrm{d}s\right| \\
&\quad = 2\pi R \sum_{|n|>N} \begin{bmatrix} -\frac{\mu}{R} + \frac{\omega^2}{\Lambda_n}\alpha_{2n}(R) & \mathrm{i}n\left(-\frac{\mu}{R} + \frac{\omega^2}{\Lambda}\frac{1}{R}\right) \\ -\mathrm{i}n\left(-\frac{\mu}{R} + \frac{\omega^2}{\Lambda}\frac{1}{R}\right) & -\frac{\mu}{R} + \frac{\omega^2}{\Lambda}\alpha_{1n}(R) \end{bmatrix} \boldsymbol{u}_n(R)\cdot\overline{\boldsymbol{v}_n(R)} \\
&\quad \lesssim 2\pi R \sum_{|n|>N}\left(\frac{\hat{R}}{R}\right)^{|n|} |n|\left(|n|^{1/2}\boldsymbol{u}_n(\hat{R})\right)\left(|n|^{1/2}\overline{\boldsymbol{v}_n(R)}\right) \\
&\quad \leqslant C\max_{|n|>N}\left(|n|\left(\frac{\hat{R}}{R}\right)^{|n|}\right)\|\boldsymbol{u}\|_{\boldsymbol{H}^{1/2}(\partial B_{\hat{R}})}\|\boldsymbol{v}\|_{\boldsymbol{H}^{1/2}(\partial B_R)} \\
&\quad \leqslant C\max_{|n|>N}\left(|n|\left(\frac{\hat{R}}{R}\right)^{|n|}\right)\|\boldsymbol{u}\|_{\boldsymbol{H}^1(\Omega)}\|\boldsymbol{v}\|_{\boldsymbol{H}^1(\Omega)} \\
&\quad \leqslant C\max_{|n|>N}\left(|n|\left(\frac{\hat{R}}{R}\right)^{|n|}\right)\|\boldsymbol{u}^{\mathrm{inc}}\|_{\boldsymbol{H}^1(\Omega)}\|\boldsymbol{v}\|_{\boldsymbol{H}^1(\Omega)},
\end{aligned}$$

which completes the proof. ■

In Lemma 2.4.6, it is shown that the truncation error of the DtN operator decay exponentially with respect to the truncation parameter N. The result implies that N can be small in practice. The following result is to estimate the last term in (2.18).

Lemma 2.4.7 *For any $\delta > 0$, there exists a positive constant $C(\delta)$ independent of N such that*

$$\Re \int_{\partial B_R} \mathscr{T}_N \boldsymbol{\xi} \cdot \overline{\boldsymbol{\xi}} \mathrm{d}s \leqslant C(\delta) \|\boldsymbol{\xi}\|^2_{\boldsymbol{L}^2(B_R \backslash B_{\hat{R}})} + \frac{R}{\hat{R}} \delta \|\boldsymbol{\xi}\|^2_{\boldsymbol{H}^1(B_R \backslash B_{\hat{R}})}.$$

Proof Using (2.13), we get from a simple calculation that

$$\Re \int_{\partial B_R} \mathscr{T}_N \boldsymbol{\xi} \cdot \overline{\boldsymbol{\xi}} \mathrm{d}s = 2\pi R \, \Re \sum_{|n| \leqslant N} (M_n \boldsymbol{\xi}_n) \cdot \overline{\boldsymbol{\xi}_n}.$$

Denote $\hat{M}_n = (M_n + M_n^*)/2$. Then $\Re \, (M_n \boldsymbol{\xi}_n) \cdot \overline{\boldsymbol{\xi}_n} = \big(\hat{M}_n \boldsymbol{\xi}_n\big) \cdot \overline{\boldsymbol{\xi}_n}$. It is shown in [75] that $\hat{M}_n$ is negative definite for sufficiently large $|n|$, i.e., there exists $N_0 > 0$ such that $\big(\hat{M}_n \boldsymbol{\xi}_n\big) \cdot \overline{\boldsymbol{\xi}_n} \leqslant 0$ for any $|n| > N_0$. Hence

$$\Re \int_{\partial B_R} \mathscr{T}_N \boldsymbol{\xi} \cdot \overline{\boldsymbol{\xi}} \mathrm{d}s = 2\pi R \sum_{|n| \leqslant \min(N_0, N)} \big(\hat{M}_n \boldsymbol{\xi}_n\big) \cdot \overline{\boldsymbol{\xi}_n} + 2\pi R \sum_{N \geqslant |n| > \min(N_0, N)} \big(\hat{M}_n \boldsymbol{\xi}_n\big) \cdot \overline{\boldsymbol{\xi}_n} \tag{2.24}$$

Here we define

$$\sum_{N > |n| > \min(N_0, N)} \big(\hat{M}_n \boldsymbol{\xi}_n\big) \cdot \overline{\boldsymbol{\xi}_n} = 0, \quad N > N_0.$$

Since the second part in (2.24) is non-positive, we only need to estimate the first part which consists of finite terms. Moreover we have

$$\begin{aligned} \Re \int_{\partial B_R} \mathscr{T}_N \boldsymbol{\xi} \cdot \overline{\boldsymbol{\xi}} \mathrm{d}s &\leqslant 2\pi R \sum_{|n| \leqslant \min(N_0, N)} \big(\hat{M}_n \boldsymbol{\xi}_n\big) \cdot \overline{\boldsymbol{\xi}_n} \\ &\leqslant C \sum_{|n| \leqslant \min(N_0, N)} |\boldsymbol{\xi}_n|^2 \leqslant C \|\boldsymbol{\xi}\|^2_{\boldsymbol{L}^2(\partial B_R)}. \end{aligned}$$

Consider the annulus

$$B_R \backslash B_{\hat{R}} = \{(r, \theta) : \hat{R} < r < R, \, 0 < \theta < 2\pi\}.$$

For any $\delta > 0$, it follows from Young's inequality that

$$\begin{aligned}
(R-\hat{R})|u(R)|^2 &= \int_{\hat{R}}^{R} |u(r)|^2 \mathrm{d}r + \int_{\hat{R}}^{R}\int_{r}^{R} \frac{\mathrm{d}}{\mathrm{d}t}|u(t)|^2 \mathrm{d}t\mathrm{d}r \\
&\leqslant \int_{\hat{R}}^{R} |u(r)|^2 \mathrm{d}r + (R-\hat{R})\int_{\hat{R}}^{R} 2|u(r)||u'(r)|\mathrm{d}r \\
&= \int_{\hat{R}}^{R} |u(r)|^2 \mathrm{d}r + (R-\hat{R})\int_{\hat{R}}^{R} 2\frac{|u(r)|}{\sqrt{\delta}}\sqrt{\delta}|u'(r)|\mathrm{d}r \\
&\leqslant \int_{\hat{R}}^{R} |u(r)|^2 \mathrm{d}r + \delta^{-1}(R-\hat{R})\int_{\hat{R}}^{R} |u(r)|^2 \mathrm{d}r + \delta(R-\hat{R})\int_{\hat{R}}^{R} |u'(r)|^2 \mathrm{d}r,
\end{aligned}$$

which gives

$$|u(R)|^2 \leqslant \left[\delta^{-1} + (R-\hat{R})^{-1}\right]\int_{\hat{R}}^{R} |u(r)|^2 + \delta\int_{\hat{R}}^{R} |u'(r)|^2 \mathrm{d}r.$$

On the other hand, we have

$$\begin{aligned}
\|\nabla u\|^2_{\boldsymbol{L}^2(B_R\backslash B_{\hat{R}})} &= 2\pi\sum_{n\in\mathbb{Z}}\int_{\hat{R}}^{R}\Big(r|u_n'(r)|^2 + \frac{n^2}{r}|u_n(r)|^2\Big)\mathrm{d}r, \\
\|u\|^2_{L^2(B_R\backslash B_{\hat{R}})} &= 2\pi\sum_{n\in\mathbb{Z}}\int_{\hat{R}}^{R} r|u_n(r)|^2\mathrm{d}r.
\end{aligned}$$

Using the above estimates, we have for any $u \in H^1(B_R\backslash B_{\hat{R}})$ that

$$\begin{aligned}
&\|u\|^2_{L^2(\partial B_R)} = 2\pi R\sum_{n\in\mathbb{Z}}|u_n(R)|^2 \\
&\leqslant 2\pi R\left[\delta^{-1} + (R-\hat{R})^{-1}\right]\sum_{n\in\mathbb{Z}}\int_{\hat{R}}^{R}|u_n(r)|^2 + 2\pi R\delta\sum_{n\in\mathbb{Z}}\int_{\hat{R}}^{R}|u'(r)|^2\mathrm{d}r \\
&\leqslant 2\pi\left[\delta^{-1} + (R-\hat{R})^{-1}\right]\frac{R}{\hat{R}}\sum_{n\in\mathbb{Z}}\int_{\hat{R}}^{R} r|u_n(r)|^2\mathrm{d}r + 2\pi\delta\frac{R}{\hat{R}}\sum_{n\in\mathbb{Z}}\int_{\hat{R}}^{R}\Big(r|u_n'(r)|^2 + \frac{n^2}{r}|u_n(r)|^2\Big)\mathrm{d}r \\
&\leqslant 2\pi\left[\delta^{-1} + (R-\hat{R})^{-1}\right]\frac{R}{\hat{R}}\|u\|^2_{L^2(B_R\backslash B_{\hat{R}})} + \delta\frac{R}{\hat{R}}\|\nabla u\|^2_{L^2(B_R\backslash B_{\hat{R}})} \\
&\leqslant C(\delta)\|u\|^2_{L^2(B_R\backslash B_{\hat{R}})} + \frac{R}{\hat{R}}\delta\|\nabla u\|^2_{L^2(B_R\backslash B_{\hat{R}})}.
\end{aligned}$$

Therefore,

$$\begin{aligned}
\Re\int_{\partial B_R}\mathscr{T}_N\boldsymbol{\xi}\cdot\overline{\boldsymbol{\xi}}\mathrm{d}s &\leqslant C\|\boldsymbol{\xi}\|^2_{\boldsymbol{L}^2(\partial B_R)} \leqslant C(\delta)\|\boldsymbol{\xi}\|^2_{\boldsymbol{L}^2(B_R\backslash B_{\hat{R}})} + \frac{R}{\hat{R}}\delta\int_{\Omega}|\nabla\boldsymbol{\xi}|\mathrm{d}\boldsymbol{x} \\
&\leqslant C(\delta)\|\boldsymbol{\xi}\|^2_{\boldsymbol{L}^2(B_R\backslash B_{\hat{R}})} + \frac{R}{\hat{R}}\delta\|\boldsymbol{\xi}\|^2_{\boldsymbol{H}^1(B_R\backslash B_{\hat{R}})},
\end{aligned}$$

which completes the proof. ■

To estimate the third term on the right hand side of (2.18), we consider the dual problem

$$b(\boldsymbol{v},\boldsymbol{p}) = \int_\Omega \boldsymbol{v}\cdot\overline{\boldsymbol{\xi}}\mathrm{d}\boldsymbol{x}, \quad \forall \boldsymbol{v}\in \boldsymbol{H}^1_{\partial D}(\Omega). \tag{2.25}$$

It is easy to check that $\boldsymbol{p}$ is the solution of the following boundary value problem

$$\begin{cases} \mu\Delta\boldsymbol{p} + (\lambda+\mu)\nabla\nabla\cdot\boldsymbol{p} + \omega^2\boldsymbol{p} = -\boldsymbol{\xi} & \text{in } \Omega, \\ \boldsymbol{p} = 0 & \text{on } \partial D, \\ \mathscr{B}\boldsymbol{p} = \mathscr{T}^*\boldsymbol{p} & \text{on } \partial B_R, \end{cases} \tag{2.26}$$

where $\mathscr{T}^*$ is the adjoint operator to the DtN operator $\mathscr{T}$. Letting $\boldsymbol{v} = \boldsymbol{\xi}$ in (2.25), we obtain

$$\|\boldsymbol{\xi}\|^2_{\boldsymbol{L}^2(\Omega)} = b(\boldsymbol{\xi},\boldsymbol{p}) + \int_{\partial B_R} (\mathscr{T}-\mathscr{T}_N)\,\boldsymbol{\xi}\cdot\overline{\boldsymbol{p}}\mathrm{d}s - \int_{\partial B_R} (\mathscr{T}-\mathscr{T}_N)\,\boldsymbol{\xi}\cdot\overline{\boldsymbol{p}}\mathrm{d}s. \tag{2.27}$$

To evaluate (2.27), we need to explicitly solve system (2.26), which is very complicate due to the coupling of the compressional and shear wave components. We consider the Helmholtz decomposition to the boundary value problem (2.25). Let

$$\boldsymbol{\xi} = \nabla\xi_1 + \mathbf{curl}\xi_2,$$

where $\xi_j, j=1,2$ has the Fourier series expansion

$$\xi_j(r,\theta) = \sum_{n\in\mathbb{Z}} \xi_{jn}(r)e^{\mathrm{i}n\theta}, \quad \hat{R} < r < R.$$

Meanwhile, we assume that

$$\boldsymbol{\xi}(r,\theta) = \sum_{n\in\mathbb{Z}} \left(\xi^r_n(r)\boldsymbol{e}_r + \xi^\theta_n(r)\boldsymbol{e}_\theta\right) e^{\mathrm{i}n\theta}. \tag{2.28}$$

Lemma 2.4.8 *The Fourier coefficients $\xi_{jn}, j=1,2$ satisfy the system*

$$\begin{cases} \xi'_{1n}(r) + \frac{\mathrm{i}n}{r}\xi_{2n}(r) = \xi^r_n(r), & r\in(\hat{R},R), \\ \frac{\mathrm{i}n}{r}\xi_{1n}(r) - \xi'_{2n}(r) = \xi^\theta_n(r), & r\in(\hat{R},R), \\ \xi_{1n}(R) = 0, \quad \xi_{2n}(R) = 0, & r = R, \end{cases} \tag{2.29}$$

which has a unique solution given by

$$\xi_{1n}(r) = \frac{\mathrm{i}}{2}\int_r^R \left[\left(\frac{r}{t}\right)^n - \left(\frac{t}{r}\right)^n\right]\xi_n^\theta(t)\mathrm{d}t - \frac{1}{2}\int_r^R \left[\left(\frac{r}{t}\right)^n + \left(\frac{t}{r}\right)^n\right]\xi_n^r(t)\mathrm{d}t \quad (2.30)$$

$$\xi_{2n}(r) = \frac{\mathrm{i}}{2}\int_r^R \left[\left(\frac{t}{r}\right)^n - \left(\frac{r}{t}\right)^n\right]\xi_n^r(t)\mathrm{d}t - \frac{1}{2}\int_r^R \left[\left(\frac{r}{t}\right)^n + \left(\frac{t}{r}\right)^n\right]\xi_n^\theta(t)\mathrm{d}t \quad (2.31)$$

Proof Following from the Fourier series expansions and the Helmholtz decomposition, we get

$$\begin{aligned}
\boldsymbol{\xi}(r,\theta) &= \sum_{n\in\mathbb{Z}}\left[\xi_n^r(r)\boldsymbol{e}_r + \xi_n^\theta(r)\boldsymbol{e}_\theta\right]e^{\mathrm{i}n\theta} = \nabla\xi_1 + \mathbf{curl}\xi_2 \\
&= \sum_{n\in\mathbb{Z}}\left[\xi_{1n}'(r)\boldsymbol{e}_r + \frac{\mathrm{i}n}{r}\xi_{1n}(r)\boldsymbol{e}_\theta + \frac{\mathrm{i}n}{r}\xi_{2n}(r)\boldsymbol{e}_r - \xi_{2n}'(r)\boldsymbol{e}_\theta\right]e^{\mathrm{i}n\theta} \\
&= \sum_{n\in\mathbb{Z}}\left[\Big(\xi_{1n}'(r) + \frac{\mathrm{i}n}{r}\xi_{2n}(r)\Big)\boldsymbol{e}_r + \Big(\frac{\mathrm{i}n}{r}\xi_{1n}(r) - \xi_{2n}'(r)\Big)\boldsymbol{e}_\theta\right]e^{\mathrm{i}n\theta},
\end{aligned}$$

which shows that $[\xi_n^{(1)}, \xi_n^{(2)}]$ satisfies

$$\xi_{1n}'(r) + \frac{\mathrm{i}n}{r}\xi_{2n}(r) = \xi_n^r(r), \quad \frac{\mathrm{i}n}{r}\xi_{1n}(r) - \xi_{2n}'(r) = \xi_n^\theta(r), \qquad r \in (\hat{R}, R).$$

Denote

$$A_n(r) = \begin{bmatrix} 0 & -\frac{\mathrm{i}n}{r} \\ \frac{\mathrm{i}n}{r} & 0 \end{bmatrix}.$$

By the standard theory of the first order differential system, the fundamental solution $\Phi_n(r)$ is

$$\begin{aligned}
\Phi_n(r) &= e^{\int_{\hat{R}}^r A_n(\tau)\mathrm{d}\tau} = \exp\left(\begin{bmatrix} 0 & -\mathrm{i}n\ln\frac{r}{\hat{R}} \\ \mathrm{i}n\ln\frac{r}{\hat{R}} & 0 \end{bmatrix}\right) \\
&= \begin{bmatrix} \frac{1}{\sqrt{2}} & \frac{\mathrm{i}}{\sqrt{2}} \\ \frac{\mathrm{i}}{\sqrt{2}} & \frac{1}{\sqrt{2}} \end{bmatrix}\begin{bmatrix} \left(\frac{r}{\hat{R}}\right)^n & 0 \\ 0 & \left(\frac{r}{\hat{R}}\right)^{-n} \end{bmatrix}\begin{bmatrix} \frac{1}{\sqrt{2}} & -\frac{\mathrm{i}}{\sqrt{2}} \\ -\frac{\mathrm{i}}{\sqrt{2}} & \frac{1}{\sqrt{2}} \end{bmatrix}.
\end{aligned}$$

The inverse of Φ_n is

$$\Phi_n^{-1}(r) = \begin{bmatrix} \frac{1}{\sqrt{2}} & \frac{\mathrm{i}}{\sqrt{2}} \\ \frac{\mathrm{i}}{\sqrt{2}} & \frac{1}{\sqrt{2}} \end{bmatrix}\begin{bmatrix} \left(\frac{r}{\hat{R}}\right)^{-n} & 0 \\ 0 & \left(\frac{r}{\hat{R}}\right)^{n} \end{bmatrix}\begin{bmatrix} \frac{1}{\sqrt{2}} & -\frac{\mathrm{i}}{\sqrt{2}} \\ -\frac{\mathrm{i}}{\sqrt{2}} & \frac{1}{\sqrt{2}} \end{bmatrix}.$$

Using the method of variation of parameters, we let

$$(\xi_{1n}(r), \xi_{2n}(r))^\top = \Phi_n(r) C_n(r),$$

where the unknown vector $C_n(r)$ satisfies

$$\begin{aligned} C_n'(r) &= \Phi_n^{-1}(r)(\xi_n^r(r), \xi_n^\theta(r))^\top \\ &= \frac{1}{2}\begin{bmatrix} \left[\left(\frac{r}{\hat{R}}\right)^{-n} + \left(\frac{r}{\hat{R}}\right)^{n}\right] \xi_n^r(r) + \mathrm{i}\left[\left(\frac{r}{\hat{R}}\right)^{n} - \left(\frac{r}{\hat{R}}\right)^{-n}\right] \xi_n^\theta(r) \\ \mathrm{i}\left[\left(\frac{r}{\hat{R}}\right)^{-n} - \left(\frac{r}{\hat{R}}\right)^{n}\right] \xi_n^r(r) + \left[\left(\frac{r}{\hat{R}}\right)^{n} + \left(\frac{r}{\hat{R}}\right)^{-n}\right] \xi_n^\theta(r) \end{bmatrix}. \end{aligned} \tag{2.32}$$

Using the boundary condition yields

$$(\xi_{1n}(R), \xi_{2n}(R))^\top = \Phi_n(R) C_n(R) = (0,0)^\top,$$

which implies that $C_n(R) = (0,0)^\top$. Then

$$C_n(r) = -\int_r^R C_n'(t)\mathrm{d}t. \tag{2.33}$$

Combining (2.32) and (2.33), we have

$$C_n(r) = -\frac{1}{2}\begin{bmatrix} \int_r^R \left[\left(\frac{t}{\hat{R}}\right)^{-n} + \left(\frac{t}{\hat{R}}\right)^{n}\right] \xi_n^r(t)\mathrm{d}t + \mathrm{i}\int_r^R \left[\left(\frac{t}{\hat{R}}\right)^{n} - \left(\frac{t}{\hat{R}}\right)^{-n}\right] \xi_n^\theta(t)\mathrm{d}t \\ \mathrm{i}\int_r^R \left[\left(\frac{t}{\hat{R}}\right)^{-n} - \left(\frac{t}{\hat{R}}\right)^{n}\right] \xi_n^r(t)\mathrm{d}t + \int_r^R \left[\left(\frac{t}{\hat{R}}\right)^{n} + \left(\frac{t}{\hat{R}}\right)^{-n}\right] \xi_n^\theta(t)\mathrm{d}t. \end{bmatrix}.$$

Substituting $C_n(r)$ into the general solution, we obtain

$$\begin{aligned} \xi_{1n}(r) &= -\frac{1}{2}\left(\frac{r}{\hat{R}}\right)^{n}\int_r^R \left(\frac{t}{\hat{R}}\right)^{-n} \xi_n^r(t)\mathrm{d}t + \frac{\mathrm{i}}{2}\left(\frac{r}{\hat{R}}\right)^{n}\int_r^R \left(\frac{t}{\hat{R}}\right)^{-n} \xi_n^\theta(t)\mathrm{d}t \\ &\quad -\frac{1}{2}\left(\frac{r}{\hat{R}}\right)^{-n}\int_r^R \left(\frac{t}{\hat{R}}\right)^{n} \xi_n^r(t)\mathrm{d}t - \frac{\mathrm{i}}{2}\left(\frac{r}{\hat{R}}\right)^{-n}\int_r^R \left(\frac{t}{\hat{R}}\right)^{n} \xi_n^\theta(t)\mathrm{d}t \\ \xi_{2n}(r) &= -\frac{\mathrm{i}}{2}\left(\frac{r}{\hat{R}}\right)^{n}\int_r^R \left(\frac{t}{\hat{R}}\right)^{-n} \xi_n^r(t)\mathrm{d}t + \frac{\mathrm{i}}{2}\left(\frac{r}{\hat{R}}\right)^{-n}\int_r^R \left(\frac{t}{\hat{R}}\right)^{n} \xi_n^r(t)\mathrm{d}t \\ &\quad -\frac{1}{2}\left(\frac{r}{\hat{R}}\right)^{n}\int_r^R \left(\frac{t}{\hat{R}}\right)^{-n} \xi_n^\theta(t)\mathrm{d}t - \frac{1}{2}\left(\frac{r}{\hat{R}}\right)^{-n}\int_r^R \left(\frac{t}{\hat{R}}\right)^{n} \xi_n^\theta(t)\mathrm{d}t, \end{aligned}$$

which completes the proof. ■

Let $\boldsymbol{p}$ be the solution of the dual problem (2.26). Then $\boldsymbol{p}$ satisfies the following boundary value problem in $B_R\backslash\overline{B}_{\hat{R}}$:

$$\begin{cases} \mu\Delta\boldsymbol{p} + (\lambda+\mu)\nabla\nabla\cdot\boldsymbol{p} + \omega^2\boldsymbol{p} = -\boldsymbol{\xi} & \text{in } B_R\backslash\overline{B_{\hat{R}}}, \\ \boldsymbol{p}(\hat{R},\theta) = \boldsymbol{p}(\hat{R},\theta) & \text{on } \partial B_{\hat{R}}, \\ \mathscr{B}\boldsymbol{p} = \mathscr{T}^*\boldsymbol{p} & \text{on } \partial B_R. \end{cases} \tag{2.34}$$

Introduce the Helmholtz decomposition for $\boldsymbol{p}$:

$$\boldsymbol{p} = \nabla q_1 + \mathbf{curl} q_2, \tag{2.35}$$

where $q_j, j = 1, 2$ admits the Fourier series expansion

$$q_j(r,\theta) = \sum_{n\in\mathbb{Z}} q_{jn}(r)e^{\mathrm{i}n\theta}.$$

Let $\xi_{jn}, j = 1, 2$ be the solution of the system (2.29). Consider the second order system for $q_{jn}, j = 1, 2$:

$$\begin{cases} q_{jn}''(r) + \frac{1}{r}q_{jn}'(r) + \left(\kappa_j^2 - \left(\frac{n}{R}\right)^2\right)q_{jn}(r) = c_j\xi_{jn}(r), & r \in (\hat{R}, R), \\ q_{jn}(\hat{R}) = q_{jn}(\hat{R}), & r = \hat{R}, \\ q_{jn}'(R) = \overline{\alpha_{jn}}q_{jn}(R), & r = R, \end{cases} \tag{2.36}$$

where $c_1 = -1/(\lambda+2\mu), c_2 = -1/\mu$, and α_{jn} is given in (2.58). The boundary condition $q_{jn}'(R) = \overline{\alpha_{jn}}q_{jn}(R)$ comes from (2.55), i.e., q_j satisfies the boundary condition

$$\partial_r q_j = \mathscr{T}_j^* q_j := \sum_{n\in\mathbb{Z}} \overline{\alpha_{jn}}q_{jn}(R)e^{\mathrm{i}n\theta} \quad \text{on } \partial B_R,$$

where $\mathscr{T}_j^*$ is the adjoint operator to the DtN operator $\mathscr{T}_j$.

Lemma 2.4.9 *The boundary value problem* (2.34) *and the second order system* (2.36) *are equivalent under the Helmholtz decomposition* (2.35).

Proof It suffices to show if the Fourier coefficients q_{jn} satisfy the second order system (2.36), then $\boldsymbol{p} = \nabla q_1 + \mathbf{curl} q_2$ is the solution of (2.34).

In the polar coordinates, we let

$$\boldsymbol{p}(r,\theta)=\sum_{n\in\mathbb{Z}}(p_n^r(r)\boldsymbol{e}_r+p_n^\theta(r)\boldsymbol{e}_\theta)e^{\mathrm{i}n\theta},\quad r\in(\hat{R},R). \tag{2.37}$$

It follows from the Helmholtz decomposition that

$$p_n^r(r)=q_{1n}'(r)+\frac{\mathrm{i}n}{r}q_{2n}(r),\quad p_n^\theta(r)=\frac{\mathrm{i}n}{r}q_{1n}(r)-q_{2n}'(r). \tag{2.38}$$

Using (2.37)–(2.38), we have from a straightforward calculation that

$$\begin{aligned}
\mathscr{B}\boldsymbol{p} &= \big(\mu\partial_r\boldsymbol{p}+(\lambda+\mu)\nabla\cdot\boldsymbol{p}\boldsymbol{e}_r\big)|_{r=R}\\
&= \sum_{n\in\mathbb{Z}}\Big[(\lambda+2\mu)q_{1n}''(R)+(\lambda+\mu)\frac{1}{R}q_{1n}'(R)-(\lambda+\mu)\frac{n^2}{R^2}q_{1n}(R)\Big]e^{\mathrm{i}n\theta}\boldsymbol{e}_r\\
&\quad+\sum_{n\in\mathbb{Z}}\Big[\mu\frac{\mathrm{i}n}{R}q_{1n}'(R)-\mu\frac{\mathrm{i}n}{R^2}q_{1n}(R)\Big]e^{\mathrm{i}n\theta}\boldsymbol{e}_\theta+\sum_{n\in\mathbb{Z}}\Big[\mu\frac{\mathrm{i}n}{R}q_{2n}'(R)-\mu\frac{\mathrm{i}n}{R^2}q_{2n}(R)\Big]e^{\mathrm{i}n\theta}\boldsymbol{e}_r\\
&\quad+\sum_{n\in\mathbb{Z}}-\mu q_{2n}''(R)e^{\mathrm{i}n\theta}\boldsymbol{e}_\theta.
\end{aligned}$$

On the other hand, it is easy to verify that

$$\begin{aligned}
\mathscr{T}^*\boldsymbol{p} &= \sum_{n\in\mathbb{Z}}\Big\{\Big[\overline{M_{11}^{(n)}}p_n^r(R)+\overline{M_{21}^{(n)}}p_n^\theta(R)\Big]\boldsymbol{e}_r+\Big[\overline{M_{12}^{(n)}}p_n^r(R)+\overline{M_{22}^{(n)}}p_n^\theta(R)\Big]\boldsymbol{e}_\theta\Big\}\,e^{\mathrm{i}n\theta}\\
&= \sum_{n\in\mathbb{Z}}\left\{\overline{M_{11}^{(n)}}\Big[q_{1n}'(R)+\frac{\mathrm{i}n}{R}q_{2n}(R)\Big]+\overline{M_{21}^{(n)}}\Big[\frac{\mathrm{i}n}{R}q_{1n}(R)-q_{2n}'(R)\Big]\right\}\boldsymbol{e}_re^{\mathrm{i}n\theta}\\
&\quad+\sum_{n\in\mathbb{Z}}\left\{\overline{M_{12}^{(n)}}\Big[q_{1n}'(R)+\frac{\mathrm{i}n}{R}q_{2n}(R)\Big]+\overline{M_{22}^{(n)}}\Big[\frac{\mathrm{i}n}{R}q_{1n}(R)-q_{2n}'(R)\Big]\right\}\boldsymbol{e}_\theta e^{\mathrm{i}n\theta},
\end{aligned}$$

where $M_{ij}^{(n)},i,j=1,2$ are given in (2.57).

Using the boundary condition $q_{jn}'(R)=\overline{\alpha_{jn}}q_{jn}(R)$, we get

$$\begin{aligned}
&\left(\mu\frac{\mathrm{i}n}{R}-\overline{M_{12}^{(n)}}\right)q_{1n}'(R)-\left(\overline{M_{22}^{(n)}}\frac{\mathrm{i}n}{R}+\mu\frac{\mathrm{i}n}{R^2}\right)q_{1n}(R)\\
=&\left(\mu\frac{\mathrm{i}n}{R}-\mathrm{i}n\frac{\mu}{R}+\omega^2\frac{\mathrm{i}n}{R}\frac{1}{\overline{\Lambda_n(R)}}\right)q_{1n}'(R)-\left(-\frac{\mu}{R}\frac{\mathrm{i}n}{R}+\omega^2\frac{\mathrm{i}n}{R}\frac{\overline{\alpha_{1n}}}{\overline{\Lambda_n(R)}}+\mu\frac{\mathrm{i}n}{R^2}\right)q_{1n}(R)\\
=&\ \omega^2\frac{\mathrm{i}n}{R}\frac{1}{\overline{\Lambda_n(R)}}\left(q_{1n}'(R)-\overline{\alpha_{1n}}q_{1n}(R)\right)=0
\end{aligned}$$

and

$$\begin{aligned}
&\left(\mu\frac{\mathrm{i}n}{R}+\overline{M_{21}^{(n)}}\right)q_{2n}'(R)-\left(\overline{M_{11}^{(n)}}\frac{\mathrm{i}n}{R}+\mu\frac{\mathrm{i}n}{R^2}\right)q_{2n}(R)\\
=&\left(\mu\frac{\mathrm{i}n}{R}-\mathrm{i}n\frac{\mu}{R}+\mathrm{i}n\frac{\omega^2}{R}\frac{1}{\overline{\Lambda_n(R)}}\right)q_{2n}'(R)-\left(\mu\frac{\mathrm{i}n}{R^2}-\frac{\mu}{R}\frac{\mathrm{i}n}{R}+\omega^2\frac{\mathrm{i}n}{R}\frac{\overline{\alpha_{2n}}}{\overline{\Lambda_n(R)}}\right)q_{2n}(R)\\
=&\ \mathrm{i}n\frac{\omega^2}{R}\frac{1}{\overline{\Lambda_n(R)}}\left(q_{2n}'(R)-\overline{\alpha_{2n}}q_{2n}(R)\right)=0.
\end{aligned}$$

Since q_{2n} satisfies the second order equation

$$q_{2n}''(r)+\frac{1}{r}q_{2n}'(r)+\left(\kappa_2^2-\left(\frac{n}{R}\right)^2\right)q_{2n}(r)=-\frac{1}{\mu}\xi_{2n},\quad r\in(\hat{R},R),$$

we obtain from the boundary condition $\xi_{2n}(R)=0$ that

$$\begin{aligned}
&-\mu q_{2n}''(R)-\left(\overline{M_{12}^{(n)}}\frac{\mathrm{i}n}{R}q_{2n}(R)-\overline{M_{22}^{(n)}}q_{2n}'(R)\right)\\
&\quad=-\mu q_{2n}''(R)-\frac{\mathrm{i}n}{R}\left(\mathrm{i}n\frac{\mu}{R}-\omega^2\frac{\mathrm{i}n}{R}\frac{1}{\overline{\Lambda_n(R)}}\right)q_{2n}(R)+\left(-\frac{\mu}{R}+\omega^2\frac{\overline{\alpha_{1n}}}{\overline{\Lambda_n(R)}}\right)q_{2n}'(R)\\
&\quad=\xi_{2n}(R)+\mu\kappa_2^2q_{2n}(R)+\omega^2\left(\frac{\mathrm{i}n}{R}\right)^2\frac{1}{\overline{\Lambda_n(R)}}q_{2n}(R)+\omega^2\frac{\overline{\alpha_{1n}}}{\overline{\Lambda_n(R)}}q_{2n}'(R)\\
&\quad=\xi_{2n}(R)+\frac{\omega^2}{\overline{\Lambda_n(R)}}\left(\left(\frac{n}{R}\right)^2q_{2n}(R)-\overline{\alpha_{1n}\alpha_{2n}}q_{2n}(R)-\left(\frac{n}{R}\right)^2q_{2n}(R)+\overline{\alpha_{1n}}q_{2n}'(R)\right)\\
&\quad=\xi_{2n}(R)+\omega^2\frac{\overline{\alpha_{1n}}}{\overline{\Lambda_n(R)}}\left(-\overline{\alpha_{2n}}q_{2n}(R)+q_{2n}'(R)\right)=0.
\end{aligned}$$

Similarly, combining the equation

$$q_{1n}''(r)+\frac{1}{r}q_{1n}'(r)+\left(\kappa_1^2-\left(\frac{n}{r}\right)^2\right)q_{1n}(r)=-\frac{1}{\lambda+2\mu}\xi_{1n}(r),\quad r\in(\hat{R},R)$$

and the boundary condition $\xi_{1n}(R) = 0$, we have

$$\begin{aligned}
&(\lambda+2\mu)q_{1n}''(R) + (\lambda+\mu)\frac{1}{R}q_{1n}'(r) - (\lambda+\mu)\frac{n^2}{R^2}q_{1n}(R) - \overline{M_{11}^{(n)}}q_{1n}'(R) - \frac{\mathrm{i}n}{R}\overline{M_{21}^{(n)}}q_{1n}(R)\\
= \;& (\lambda+2\mu)\left[-\frac{1}{\lambda+2\mu}\xi_{1n}(R) - \frac{1}{R}q_{1n}'(R) - \left(\kappa_1^2 - \left(\frac{n}{R}\right)^2\right)q_{1n}(R)\right]\\
&+\left(\frac{\lambda+2\mu}{R} - \omega^2\frac{\overline{\alpha_{2n}}}{\overline{\Lambda_n(R)}}\right)q_{1n}'(R) + \left(-(\lambda+2\mu)\left(\frac{n}{R}\right)^2 + \omega^2\frac{1}{\overline{\Lambda_n(R)}}\left(\frac{n}{R}\right)^2\right)q_{1n}(R)\\
= \;& -\xi_{1n}(R) - \omega^2\frac{\overline{\alpha_{2n}}}{\overline{\Lambda_n(R)}}q_{1n}'(R) + \left(-\omega^2 + \omega^2\frac{1}{\overline{\Lambda_n(R)}}\left(\frac{n}{R}\right)^2\right)q_{1n}(R)\\
= \;& -\xi_{1n}(R) - \frac{\omega^2}{\overline{\Lambda_n(R)}}\left(\overline{\alpha_{2n}}q_{1n}'(R) + \left(\frac{n}{R}\right)^2 q_{1n}(R) - \overline{\alpha_{1n}\alpha_{2n}}q_{1n}(R) - \left(\frac{n}{R}\right)^2 q_{1n}(R)\right)\\
= \;& -\xi_{1n}(R) - \frac{\omega^2}{\overline{\Lambda_n(R)}}\overline{\alpha_{2n}}\left[q_{1n}'(R) - \overline{\alpha_{1n}}q_{1n}(R)\right] = 0.
\end{aligned}$$

Hence we prove that $\mathscr{B}\boldsymbol{p} = \mathscr{T}^*\boldsymbol{p}$ on ∂B_R.

Moreover, we get from the Helmholtz decomposition that

$$\begin{aligned}
&\mu\Delta\boldsymbol{p} + (\lambda+\mu)\nabla\nabla\cdot\boldsymbol{p} + \omega^2\boldsymbol{p}\\
= \;& \nabla\left((\lambda+2\mu)\Delta q_1 + \omega^2 q_1\right) + \mathbf{curl}\left(\mu\Delta q_2 + \omega^2 q_2\right)\\
= \;& -\nabla\xi_1 - \mathbf{curl}\xi_2 = -\boldsymbol{\xi},
\end{aligned}$$

which completes the proof. ■

Based on Lemma 2.4.8 and Lemma 2.4.9, we have the asymptotic properties of the solution to the dual problem (2.34) for large $|n|$.

Theorem 2.4.10 *Let $\boldsymbol{p}$ be the solution of* (2.34) *and amdit the Fourier series expansion*

$$\boldsymbol{p}(r,\theta) = \sum_{n\in Z}\left(p_n^r(r)\boldsymbol{e}_r + p_n^\theta(r)\boldsymbol{e}_\theta\right)e^{\mathrm{i}\,n\theta}.$$

For sufficient large $|n|$, the Fourier coefficients p_n^r, p_n^θ satisfy the estimate

$$\begin{aligned}
|p_n^r(R)|^2 + |p_n^\theta(R)|^2 \;\lesssim\; & n^2\left(\frac{\hat{R}}{R}\right)^{2|n|+2}\left(|p_n^r(\hat{R})|^2 + |p_n^\theta(\hat{R})|^2\right)\\
&+\frac{1}{|n|^2}\left(\|\xi_n^r\|^2_{L^\infty([\hat{R},R])} + \|\xi_n^\theta\|^2_{L^\infty([\hat{R},R])}\right),
\end{aligned}$$

where ξ_n^r, ξ_n^θ are the Fourier coefficients of $\boldsymbol{\xi}$ in the polar coordinates and are given in (2.28).

Proof It is shown in [61] that the second order systems (2.36) have a unique solution given by

$$\begin{aligned} q_{1n}(r) &= \beta_{1n}(r)q_{1n}(\hat{R}) + \frac{\mathrm{i}\pi}{4}\int_{\hat{R}}^{r} tW_{1n}(r,t)\xi_{1n}(t)\mathrm{d}t \\ &\quad + \frac{\mathrm{i}\pi}{4}\int_{\hat{R}}^{R} t\beta_{1n}(t)W_{1n}(\hat{R},r)\xi_{1n}(t)\mathrm{d}t, \qquad (2.39) \\ q_{2n}(r) &= \beta_{2n}(r)q_{2n}(\hat{R}) + \frac{\mathrm{i}\pi}{4}\int_{\hat{R}}^{r} tW_{2n}(r,t)\xi_{2n}(t)\mathrm{d}t \\ &\quad + \frac{\mathrm{i}\pi}{4}\int_{\hat{R}}^{R} t\beta_{2n}(t)W_{2n}(\hat{R},r)\xi_{2n}(t)\mathrm{d}t, \qquad (2.40) \end{aligned}$$

where

$$\beta_{jn}(r) = \frac{H_n^{(2)}(\kappa_j r)}{H_n^{(2)}(\kappa_j \hat{R})}, \quad W_{jn}(r,t) = H_n^{(1)}(\kappa_j r)H_n^{(2)}(\kappa_j t) - H_n^{(1)}(\kappa_j t)H_n^{(2)}(\kappa_j r).$$

Taking the derivative of (2.39)–(2.40) respective to r gives

$$\begin{aligned} q_{1n}'(r) &= \beta_{1n}'(r)q_{1n}(\hat{R}) + \frac{\mathrm{i}\pi}{4}\int_{\hat{R}}^{r} t\partial_r W_{1n}(r,t)\xi_{1n}(t)\mathrm{d}t \\ &\quad + \frac{\mathrm{i}\pi}{4}\int_{\hat{R}}^{R} t\beta_{1n}(t)\partial_t W_{1n}(\hat{R},r)\xi_{1n}(t)\mathrm{d}t, \qquad (2.41) \end{aligned}$$

$$\begin{aligned} q_{2n}'(r) &= \beta_{2n}'(r)q_{2n}(\hat{R}) + \frac{\mathrm{i}\pi}{4}\int_{\hat{R}}^{r} t\partial_r W_{2n}(r,t)\xi_{2n}(t)\mathrm{d}t \\ &\quad + \frac{\mathrm{i}\pi}{4}\int_{\hat{R}}^{R} t\beta_{2n}(t)\partial_t W_{2n}(\hat{R},r)\xi_{2n}(t)\mathrm{d}t. \qquad (2.42) \end{aligned}$$

Evaluating (2.39)–(2.40) and (2.41)–(2.42) at $r = R$ and $r = \hat{R}$, respectively, we may verify that

$$\begin{aligned} q_{1n}(R) &= \beta_{1n}(R)q_{1n}(\hat{R}) + \frac{\mathrm{i}\pi}{4}\int_{\hat{R}}^{R} t\beta_{1n}(R)W_{1n}(\hat{R},t)\xi_{1n}(t)\mathrm{d}t, \\ q_{2n}(R) &= \beta_{2n}(R)q_{2n}(\hat{R}) + \frac{\mathrm{i}\pi}{4}\int_{\hat{R}}^{R} t\beta_{2n}(R)W_{2n}(\hat{R},t)\xi_{2n}(t)\mathrm{d}t, \\ q_{1n}'(\hat{R}) &= \beta_{1n}'(\hat{R})q_{1n}(\hat{R}) + \frac{1}{\hat{R}}\int_{\hat{R}}^{R} t\beta_{1n}(t)\xi_{1n}(t)\mathrm{d}t, \\ q_{2n}'(\hat{R}) &= \beta_{2n}'(\hat{R})q_{2n}(\hat{R}) + \frac{1}{\hat{R}}\int_{\hat{R}}^{R} t\beta_{2n}(t)\xi_{2n}(t)\mathrm{d}t. \end{aligned}$$

It follows from the Helmholtz decomposition that

$$p_n^r(r) = q_{1n}'(r) + \frac{\mathrm{i}n}{r} q_{2n}(r), \quad p_n^\theta(r) = \frac{\mathrm{i}n}{r} q_{1n}(r) - q_{2n}'(r). \tag{2.43}$$

Evaluating (2.43) at $r = R$, noting $\beta_{jn}'(R) = \overline{\alpha_{jn}(R)}$ and $q_{jn}'(R) = \overline{\alpha_{jn}(R)} q_{jn}(R)$, we obtain

$$\begin{bmatrix} p_n^r(R) \\ p_n^\theta(R) \end{bmatrix} = U_n(R) \begin{bmatrix} q_{1n}(\hat{R}) \\ q_{2n}(\hat{R}) \end{bmatrix} + \frac{\mathrm{i}\pi}{4} U_n(R) \begin{bmatrix} \int_{\hat{R}}^R t W_{1n}(\hat{R}, t) \xi_{1n}(t) \mathrm{d}t \\ \int_{\hat{R}}^R t W_{2n}(\hat{R}, t) \xi_{2n}(t) \mathrm{d}t \end{bmatrix}, \tag{2.44}$$

where

$$U_n(R) = \begin{bmatrix} \overline{\alpha_{1n}(R)} & \frac{\mathrm{i}n}{R} \\ \frac{\mathrm{i}n}{R} & -\overline{\alpha_{2n}(R)} \end{bmatrix} \begin{bmatrix} \beta_{1n}(R) & 0 \\ 0 & \beta_{2n}(R) \end{bmatrix}.$$

Similarly, evaluating (2.43) at $r = \hat{R}$ and noting $\beta_{jn}'(\hat{R}) = \overline{\alpha_{jn}(\hat{R})}$ yield that

$$\begin{bmatrix} p_n^r(\hat{R}) \\ p_n^\theta(\hat{R}) \end{bmatrix} = K_n(\hat{R}) \begin{bmatrix} q_{1n}(\hat{R}) \\ q_{2n}(\hat{R}) \end{bmatrix} + \begin{bmatrix} \eta_1 \\ \eta_2 \end{bmatrix}, \tag{2.45}$$

where

$$K_n(\hat{R}) = \begin{bmatrix} \overline{\alpha_{1n}(\hat{R})} & \frac{\mathrm{i}n}{\hat{R}} \\ \frac{\mathrm{i}n}{\hat{R}} & -\overline{\alpha_{2n}(\hat{R})} \end{bmatrix},$$

and

$$\eta_{1n} = \frac{1}{\hat{R}} \int_{\hat{R}}^R t \beta_{1n}(t) \xi_{1n}(t) \mathrm{d}t, \quad \eta_{2n} = -\frac{1}{\hat{R}} \int_{\hat{R}}^R t \beta_{2n}(t) \xi_{2n}(t) \mathrm{d}t.$$

Solving (2.45) for $q_{1n}(\hat{R}), q_{2n}(\hat{R})$ in terms of $p_n^r(\hat{R}), p_n^r(\hat{R})$ gives

$$\begin{bmatrix} q_{1n}(\hat{R}) \\ q_{2n}(\hat{R}) \end{bmatrix} = \frac{V_n(\hat{R})}{\overline{\Lambda_n(\hat{R})}} \begin{bmatrix} p_n^r(\hat{R}) - \eta_{1n} \\ p_n^\theta(\hat{R}) - \eta_{2n} \end{bmatrix}, \tag{2.46}$$

where

$$\Lambda_n(\hat{R}) = \left(\frac{n}{\hat{R}}\right)^2 - \alpha_{1n}(\hat{R}) \alpha_{2n}(\hat{R}), \quad V_n(\hat{R}) = \begin{bmatrix} -\overline{\alpha_{2n}(\hat{R})} & -\frac{\mathrm{i}n}{\hat{R}} \\ -\frac{\mathrm{i}n}{\hat{R}} & \overline{\alpha_{1n}(\hat{R})} \end{bmatrix}.$$

Substituting (2.46) into (2.44) yields

$$\begin{bmatrix} p_n^r(R) \\ p_n^\theta(R) \end{bmatrix} = \frac{U_n(R)V_n(\hat{R})}{\overline{\Lambda_n(\hat{R})}} \begin{bmatrix} p_n^r(R_1) \\ p_n^\theta(R_1) \end{bmatrix} + \frac{\mathrm{i}\pi}{4} U_n(R) \begin{bmatrix} \int_{\hat{R}}^R tW_{1n}(\hat{R},t)\xi_{1n}(t)\mathrm{d}t \\ \int_{\hat{R}}^R tW_{2n}(\hat{R},t)\xi_{2n}(t)\mathrm{d}t \end{bmatrix} - \frac{U_n(R)V_n(\hat{R})}{\overline{\Lambda_n(\hat{R})}} \begin{bmatrix} \eta_{1n} \\ \eta_{2n} \end{bmatrix}. \tag{2.47}$$

Following proofs in Lemmas 2.4.6 and 2.7.1, we may similarly show that for sufficiently large $|n|$

$$\left| \frac{U_n(R)V_n(\hat{R})}{\overline{\Lambda_n(\hat{R})}} \right| \lesssim |n| \left(\frac{\hat{R}}{R} \right)^{|n|}.$$

For fixed t and sufficiently large $|n|$, using (2.30) and (2.31), we may easily show that

$$|\xi_{1n}(t)| \lesssim \left(\|\xi_n^r\|_{L^\infty([\hat{R},R])} + \|\xi_n^\theta\|_{L^\infty([\hat{R},R])} \right) \int_t^R \left(\frac{r}{t} \right)^{|n|} \mathrm{d}r, \tag{2.48}$$

$$|\xi_{2n}(t)| \lesssim \left(\|\xi_n^r\|_{L^\infty([\hat{R},R])} + \|\xi_n^\theta\|_{L^\infty([\hat{R},R])} \right) \int_t^R \left(\frac{r}{t} \right)^{|n|} \mathrm{d}r. \tag{2.49}$$

By (2.48)–(2.49) and

$$W_{jn}(\hat{R},t) \sim -\frac{2\mathrm{i}}{\pi|n|} \left[\left(\frac{t}{\hat{R}} \right)^{|n|} - \left(\frac{\hat{R}}{t} \right)^{|n|} \right], \quad \beta_{jn}(t) \sim \left(\frac{\hat{R}}{t} \right)^{|n|},$$

we get

$$\begin{aligned} \left| \int_{\hat{R}}^R tW_{jn}(\hat{R},t)\xi_{jn}(t)\mathrm{d}t \right| &\lesssim \left(\|\xi_n^r\|_{L^\infty([\hat{R},R])} + \|\xi_n^\theta\|_{L^\infty([\hat{R},R])} \right) \frac{1}{|n|} \int_{\hat{R}}^R t \left(\frac{t}{\hat{R}} \right)^{|n|} \int_t^R \left(\frac{r}{t} \right)^{|n|} \mathrm{d}r\mathrm{d}t \\ &\lesssim \left(\|\xi_n^r\|_{L^\infty([\hat{R},R])} + \|\xi_n^\theta\|_{L^\infty([\hat{R},R])} \right) \frac{1}{|n|^2} \left(\frac{R}{\hat{R}} \right)^{|n|}, \end{aligned}$$

$$\begin{aligned} \left| \frac{1}{\hat{R}} \int_{\hat{R}}^R t\beta_{jn}(t)\xi_{jn}(t)\mathrm{d}t \right| &\lesssim \left(\|\xi_n^r\|_{L^\infty([\hat{R},R])} + \|\xi_n^\theta\|_{L^\infty([\hat{R},R])} \right) \left| \int_{\hat{R}}^R t \left(\frac{\hat{R}}{t} \right)^{|n|} \int_t^R \left(\frac{r}{t} \right)^{|n|} \mathrm{d}r\mathrm{d}t \right| \\ &\lesssim \left(\|\xi_n^r\|_{L^\infty([\hat{R},R])} + \|\xi_n^\theta\|_{L^\infty([\hat{R},R])} \right) \frac{1}{|n|^2} \left(\frac{R}{\hat{R}} \right)^{|n|}. \end{aligned}$$

Substituting the above estimates into (2.47), we obtain

$$\begin{aligned} |p_n^r(R)|^2 + |p_n^\theta(R)|^2 &\lesssim n^2 \left(\frac{\hat{R}}{R} \right)^{2|n|+2} \left(|p_n^r(\hat{R})|^2 + |p_n^\theta(\hat{R})|^2 \right) \\ &\quad + \frac{1}{|n|^2} \left(\|\xi_n^r\|_{L^\infty([\hat{R},R])}^2 + \|\xi_n^\theta\|_{L^\infty([\hat{R},R])}^2 \right), \end{aligned}$$

which completes the proof. ■

Using Theorem 2.4.10, we may estimate the last term in (2.27).

Lemma 2.4.11 *Let $\boldsymbol{p}$ be the solution of the dual problem* (2.34). *For sufficiently large N, the following estimate holds*

$$\left|\int_{\partial B_R}(\mathscr{T}-\mathscr{T}_N)\,\boldsymbol{\xi}\cdot\overline{\boldsymbol{p}}\mathrm{d}s\right|\lesssim\frac{1}{N}\|\boldsymbol{\xi}\|^2_{\boldsymbol{H}^1(\Omega)}.$$

Proof Using the definitions of the DtN operators $\mathscr{T}$ and $\mathscr{T}_N$ and Lemma 2.4.4, we have

$$\begin{aligned}
&\left|\int_{\partial B_R}(\mathscr{T}-\mathscr{T}_N)\,\boldsymbol{\xi}\cdot\overline{\boldsymbol{p}}\mathrm{d}s\right|\leqslant 2\pi R\sum_{|n|>N}|(M_n\boldsymbol{\xi}_n(R))\cdot\overline{\boldsymbol{p}}_n(R)|\\
&\lesssim 2\pi R\sum_{|n|>N}|n|\left(|\xi_n^r(R)|+|\xi_n^\theta(R)|\right)\left(|p_n^r(R)|+|p_n^\theta(R)|\right)\\
&\lesssim\sum_{|n|>N}\left((1+n^2)^{1/2}|n|\right)^{-1/2}\left[\sum_{|n|>N}(1+n^2)^{1/2}\left(|\xi_n^r(R)|+|\xi_n^\theta(R)|\right)^2\right]^{1/2}\\
&\qquad\times\left[\sum_{|n|>N}|n|^3\left(|p_n^r(R)|+|p_n^\theta(R)|\right)^2\right]^{1/2}\\
&\lesssim N^{-1}\|\boldsymbol{\xi}\|_{H^{1/2}(\partial B_R)}\left[\sum_{|n|>N}|n|^3\left(|p_n^r(R)|^2+|p_n^\theta(R)|^2\right)\right]^{1/2}\\
&\lesssim N^{-1}\|\boldsymbol{\xi}\|_{H^1(\Omega)}\left[\sum_{|n|>N}|n|^3\left(|p_n^r(R)|^2+|p_n^\theta(R)|^2\right)\right]^{1/2}. \qquad (2.50)
\end{aligned}$$

Following [61], we let $t\in[\hat{R},R]$ and assume, without loss of generality, that t is closer to the left endpoint $\hat{R}$ than the right endpoint R. Denote $\zeta=R-\hat{R}$. Then we have $R-t\geqslant\frac{\zeta}{2}$. Thus

$$\begin{aligned}
|\xi_n^{(r,\theta)}(t)|^2 &= \frac{1}{R-t}\int_R^t\left((R-s)|\xi_n^{(r,\theta)}(s)|^2\right)'\mathrm{d}s\\
&= \frac{1}{R-t}\int_R^t\left(-|\xi_n^{(r,\theta)}(s)|^2+2\,(R-s)\,\Re\big(\xi_n^{(r,\theta)\prime}(s)\overline{\xi_n^{(r,\theta)}(s)}\big)\right)\mathrm{d}s\\
&\leqslant \frac{1}{R-t}\int_t^R|\xi_n^{(r,\theta)}(s)|^2\mathrm{d}s+2\int_{\hat{R}}^R|\xi_n^{(r,\theta)}(s)||\xi_n^{(r,\theta)\prime}(s)|\mathrm{d}s,
\end{aligned}$$

which implies that

$$\begin{aligned}\|\xi_n^{(r,\theta)}\|^2_{L^\infty([\hat{R},R])} &\leqslant \frac{2}{\zeta}\|\xi_n^{(r,\theta)}\|^2_{L^2([\hat{R},R])} + 2\|\xi_n^{(r,\theta)}\|_{L^2([\hat{R},R])}\|\xi_n^{(r,\theta)\prime}\|_{L^2([\hat{R},R])} \\ &\leqslant \left(\frac{2}{\zeta}+|n|\right)\|\xi_n^{(r,\theta)}\|^2_{L^2([\hat{R},R])} + |n|^{-1}\|\xi_n^{(r,\theta)\prime}\|^2_{L^2([\hat{R},R])}.\end{aligned}$$

Using Lemma 2.4.10 and the Cauchy–Schwarz inequality, we get

$$\begin{aligned}&\sum_{|n|>N}|n|^3\left(|p_n^r(R)|^2+|p_n^\theta(R)|^2\right) \\ &\lesssim \sum_{|n|>N}|n|^3\left\{n^2\left(\frac{\hat{R}}{R}\right)^{2|n|+2}\left(|p_n^r(\hat{R})|^2+|p_n^\theta(\hat{R})|^2\right)+\frac{1}{|n|^2}\left(\|\xi_n^r\|^2_{L^\infty([\hat{R},R])}+\|\xi_n^\theta\|^2_{L^\infty([\hat{R},R])}\right)\right\} \\ &\lesssim \sum_{|n|>N}|n|^5\left(\frac{\hat{R}}{R}\right)^{|2n|}\left(|p_n^r(\hat{R})|^2+|p_n^\theta(\hat{R})|^2\right)+\sum_{|n|>N}|n|\left(\|\xi_n^r\|^2_{L^\infty([\hat{R},R])}+\|\xi_n^\theta\|^2_{L^\infty([\hat{R},R])}\right) \\ &:= I_1+I_2.\end{aligned}$$

Noting that the function t^4e^{-2t} is bounded on $(0,+\infty)$, we have

$$I_1 \lesssim \max_{|n|>N}\left(n^4\left(\frac{\hat{R}}{R}\right)^{|2n|}\right)\sum_{|n|>N}|n|\left(|p_n^r(\hat{R})|^2+|p_n^\theta(\hat{R})|^2\right) \lesssim \|\boldsymbol{p}\|^2_{H^{1/2}(\partial B_{\hat{R}})} \lesssim \|\boldsymbol{\xi}\|^2_{H^1(\Omega)},$$

where the last inequality uses the stability of the dual problem (2.34). For I_2, we can show that

$$\begin{aligned}I_2 &\lesssim \sum_{|n|>N}\left[|n|\left(\frac{2}{\zeta}+|n|\right)\left(\|\xi_n^r\|^2_{L^2([\hat{R},R])}+\|\xi_n^\theta\|^2_{L^2([\hat{R},R])}\right)+\left(\|\xi_n^{r\prime}\|^2_{L^2([\hat{R},R])}+\|\xi_n^{\theta\prime}\|^2_{L^2([\hat{R},R])}\right)\right] \\ &\leqslant \sum_{|n|>N}\left[\left(\frac{2}{\zeta}|n|+n^2\right)\|\boldsymbol{\xi}_n\|^2_{L^2([\hat{R},R])}+\|\boldsymbol{\xi}_n'\|^2_{L^2([\hat{R},R])}\right].\end{aligned}$$

On the other hand, a simple calculation yields

$$\begin{aligned}\|\xi_n^{(r,\theta)}\|^2_{H^1(B_R\setminus B_{\hat{R}})} &= 2\pi\sum_{n\in\mathbb{Z}}\int_{\hat{R}}^R\left[\left(r+\frac{n^2}{r}\right)|\xi_n^{(r,\theta)}(r)|^2+r|\xi_n^{(r,\theta)\prime}(r)|^2\right]\mathrm{d}r \\ &\geqslant 2\pi\sum_{n\in\mathbb{Z}}\int_{\hat{R}}^R\left[\left(\hat{R}+\frac{n^2}{R}\right)|\xi_n^{(r,\theta)}(r)|^2+\hat{R}|\xi_n^{(r,\theta)\prime}(r)|^2\right]\mathrm{d}r.\end{aligned}$$

It is easy to note that

$$\frac{2}{\zeta}|n|+n^2 \lesssim \hat{R}+\frac{n^2}{R}.$$

Combining the above estimates, we obtain

$$I_2 \lesssim \|\boldsymbol{\xi}\|^2_{H^1(B_R\setminus B_{R_1})} \leqslant \|\boldsymbol{\xi}\|^2_{H^1(\Omega)},$$

which gives

$$\sum_{|n|>N} |n|^3 \left(|p_n^r(R)| + |p_n^\theta(R)|\right)^2 \lesssim \|\boldsymbol{\xi}\|^2_{H^1(\Omega)}.$$

Substituting the above inequality into (2.50), we get

$$\left|\int_{\partial B_R} (\mathscr{T} - \mathscr{T}_N)\, \boldsymbol{\xi} \cdot \overline{\boldsymbol{p}} \mathrm{d}s\right| \lesssim \frac{1}{N} \|\boldsymbol{\xi}\|^2_{\boldsymbol{H}^1(\Omega)}, \tag{2.51}$$

which completes the proof. ■

Now, we prove the main result of this chapter.

Proof By Lemma 2.18, Lemma 2.4.3, Lemma 2.4.6, and Lemma 2.4.7, we obtain

$$\begin{aligned}
\|\!|\boldsymbol{\xi}|\!\|^2_{\boldsymbol{H}^1(\Omega)} &= \Re b(\xi,\xi) + \Re \int_{\partial B_R} (\mathscr{T} - \mathscr{T}_N)\, \boldsymbol{\xi} \cdot \overline{\boldsymbol{\xi}} \mathrm{d}s + 2\omega^2 \int_\Omega \boldsymbol{\xi} \cdot \overline{\boldsymbol{\xi}} \mathrm{d}\boldsymbol{x} + \Re \int_{\partial B_R} \mathscr{T}_N \boldsymbol{\xi} \cdot \overline{\boldsymbol{\xi}} \mathrm{d}s \\
&\leqslant C_1 \left[\left(\sum_{K\in\mathcal{M}_h} \eta_K^2 \right)^{1/2} + \max_{|n|>N} |n| \left(\frac{\hat{R}}{R}\right)^{|n|} \|\boldsymbol{u}^{\mathrm{inc}}\|_{\boldsymbol{H}^1(\Omega)} \right] \|\boldsymbol{\xi}\|_{\boldsymbol{H}^1(\Omega)} \\
&\quad + \left(C_2 + C(\delta)\right) \|\boldsymbol{\xi}\|^2_{\boldsymbol{L}^2(\Omega)} + \frac{R}{\hat{R}} \delta \|\boldsymbol{\xi}\|^2_{\boldsymbol{H}^1(\Omega)}.
\end{aligned}$$

Using (2.17) and choosing δ such that $\frac{R}{\hat{R}} \frac{\delta}{\min(\mu,\omega^2)} < \frac{1}{2}$, we get

$$\begin{aligned}
\|\!|\boldsymbol{\xi}|\!\|^2_{\boldsymbol{H}^1(\Omega)} &\leqslant 2C_1 \left[\left(\sum_{K\in\mathcal{M}_h} \eta_K^2 \right)^{1/2} + \max_{|n|>N} |n| \left(\frac{\hat{R}}{R}\right)^{|n|} \|\boldsymbol{u}^{\mathrm{inc}}\|_{\boldsymbol{H}^1(\Omega)} \right] \|\boldsymbol{\xi}\|_{\boldsymbol{H}^1(\Omega)} \\
&\quad + 2\left(C_2 + C(\delta)\right) \|\boldsymbol{\xi}\|^2_{\boldsymbol{L}^2(\Omega)}.
\end{aligned} \tag{2.52}$$

It follows from (2.27), (2.51), and (2.17) that we have

$$\begin{aligned}
\|\!|\boldsymbol{\xi}|\!\|^2_{\boldsymbol{L}^2(\Omega)} &= b(\boldsymbol{\xi},\boldsymbol{p}) + \int_{\partial B_R} (\mathscr{T} - \mathscr{T}_N)\, \boldsymbol{\xi} \cdot \overline{\boldsymbol{p}} \mathrm{d}s - \int_{\partial B_R} (\mathscr{T} - \mathscr{T}_N)\, \boldsymbol{\xi} \cdot \overline{\boldsymbol{p}} \mathrm{d}s \\
&\lesssim \left[\left(\sum_{K\in\mathcal{M}_h} \eta_K^2 \right)^{1/2} + \max_{|n|>N} |n| \left(\frac{\hat{R}}{R}\right)^{|n|} \|\boldsymbol{u}^{\mathrm{inc}}\|_{\boldsymbol{H}^1(\Omega)} \right] \|\boldsymbol{\xi}\|_{H^1(\Omega)} + \frac{1}{N} \|\boldsymbol{\xi}\|^2_{H^1(\Omega)}.
\end{aligned}$$

Substituting the above estimate intro (2.52) and taking sufficiently large N such that

$$\frac{2\left(C_2 + C(\delta)\right)}{N} \frac{1}{\min(\mu, \omega^2)} < 1,$$

By the equivalence of weighted norm $|||\cdot|||_{\boldsymbol{H}^1(\Omega)}$ with the standard norm $\|\cdot\|_{\boldsymbol{H}^1(\Omega)}$, we obtain

$$\|\boldsymbol{u} - \boldsymbol{u}_N^h\|_{\boldsymbol{H}^1(\Omega)} \lesssim \left(\sum_{K\in\mathcal{M}_h} \eta_K^2\right)^{1/2} + \max_{|n|>N} \left(|n| \left(\frac{\hat{R}}{R}\right)^{|n|}\right) \|\boldsymbol{u}^{\text{inc}}\|_{\boldsymbol{H}^1(\Omega)}.$$

which completes the proof of theorem. ■

2.5 Implementation and Numerical Experiments

In this section, we discuss the algorithmic implementation of the adaptive finite element DtN method and present two numerical examples to demonstrate the effectiveness of the proposed method.

2.5.1 Adaptive Algorithm

Based on the a posteriori error estimate from Theorem 2.4.1, we use the FreeFem [50] to implement the adaptive algorithm of the linear finite element formulation. It is shown in Theorem 2.4.1 that the a posteriori error estimator consists two parts: the finite element discretization error ϵ_h and the DtN truncation error ϵ_N which dependents on the truncation number N. Explicitly

$$\epsilon_h = \left(\sum_{T\in\mathcal{M}_h} \eta_T^2\right)^{1/2}, \quad \epsilon_N = \max_{|n|\geqslant N} \left(|n| \left(\frac{\hat{R}}{R}\right)^{|n|}\right) \|\boldsymbol{u}^{\text{inc}}\|_{\boldsymbol{H}^1(\Omega)}. \tag{2.53}$$

In the implementation, we choose $\hat{R}, R$, and N based on (2.53) to make sure that the finite element discretization error is not polluted by the DtN truncation error, i.e., ϵ_N is required to be very small compared to ϵ_h, for example, $\epsilon_N \leqslant 10^{-8}$. For simplicity, in the following numerical experiments, $\hat{R}$ is chosen such that the obstacle is exactly contained in the disk $B_{\hat{R}}$, and N is taken to be the smallest positive integer

Table 2.1.
The adaptive finite element DtN method for the elastic wave scattering problem.

---

1. Given the tolerance $\epsilon > 0, \theta \in (0,1)$;

2. Fix the computational domain $\Omega = B_R \backslash \overline{D}$ by choosing the radius R;

3. Choose $\hat{R}$ and N such that $\epsilon_N \leqslant 10^{-8}$;

4. Construct an initial triangulation $\mathcal{M}_h$ over Ω and compute error estimators;

5. While $\epsilon_h > \epsilon$ do

6. Refine the mesh $\mathcal{M}_h$ according to the strategy:

$$\text{if } \eta_{\hat{T}} > \theta \max_{T \in \mathcal{M}_h} \eta_T, \text{ then refine the element } \hat{T} \in M_h;$$

7. Denote refined mesh still by $\mathcal{M}_h$, solve the discrete problem (2.12) on the new mesh $\mathcal{M}_h$;

8. Compute the corresponding error estimators;

9. End while.

---

such that $\epsilon_N \leqslant 10^{-8}$. The algorithm is shown in Table 1 for the adaptive finite element DtN method for solving the elastic wave scattering problem.

2.5.2 Numerical Experiments

We report two examples to demonstrate the performance of the proposed method. The first example is a disk and has an analytical solution; the second example is a U-shaped obstacle which is commonly used to test numerical solutions for the wave scattering problems. In each example, we plot the magnitude of the numerical solution to give an intuition where the mesh should be refined, and also plot the

actual mesh obtained by our algorithm to show the agreement. The a posteriori error is plotted against the number of nodal points to show the convergence rate. In the first example, we compare the numerical results by using the uniform and adaptive meshes to illustrate the effectiveness of the adaptive algorithm.

Example 1. This example is constructed such that it has an exact solution. Let the obstacle $D = B_{0.5}$ be a disk with radius 0.5 and take $\Omega = B_1 \backslash \overline{B}_{0.5}$, i.e., $\hat{R} = 0.5, R = 1$. If we choose the incident wave as

$$\boldsymbol{u}^{\text{inc}}(\boldsymbol{x}) = -\frac{\kappa_1 H_0^{(1)'}(\kappa_1 r)}{r} \begin{pmatrix} x \\ y \end{pmatrix} - \frac{\kappa_2 H_0^{(1)'}(\kappa_2 r)}{r} \begin{pmatrix} y \\ -x \end{pmatrix}, \quad r = (x^2 + y^2)^{1/2},$$

then it is easy to check that the exact solution is

$$\boldsymbol{u}(\boldsymbol{x}) = \frac{\kappa_1 H_0^{(1)'}(\kappa_1 r)}{r} \begin{pmatrix} x \\ y \end{pmatrix} + \frac{\kappa_2 H_0^{(1)'}(\kappa_2 r)}{r} \begin{pmatrix} y \\ -x \end{pmatrix},$$

where κ_1 and κ_2 are the compressional wave number and shear wave number, respectively.

In Table 2, numerical results are shown for the adaptive mesh refinement and the uniform mesh refinement, where DoF_h stands for the degree of freedom or the number of nodal points of the mesh $\mathcal{M}_h$, ϵ_h is the a posteriori error estimate, and $e_h = \|\boldsymbol{u} - \boldsymbol{u}_N^h\|_{\boldsymbol{H}^1(\Omega)}$ is the a priori error. It can be seen that the adaptive mesh refinement requires fewer DoF_h than the uniform mesh refinement to reach the same level of accuracy, which shows the advantage of using the adaptive mesh refinement. Figure 2.2 displays the curves of $\log e_h$ and $\log \epsilon_h$ versus $\log \text{DoF}_h$ for the uniform and adaptive mesh refinements with $\omega = \pi, \lambda = 2, \mu = 1$, i.e., $\kappa_1 = \pi/2, \kappa_2 = \pi$. It indicates that the meshes and the associated numerical complexity are quasi-optimal, i.e., $\|\boldsymbol{u} - \boldsymbol{u}_N^h\|_{\boldsymbol{H}^1(\Omega)} = O\big(\text{DoF}_h^{-1/2}\big)$ holds asymptotically. Figure 2.3 plots the magnitude of the numerical solution and an adaptively refined mesh with 15407 elements. We can see that the solution oscillates on the edge of the obstacle but it is smooth away from the obstacle. This feature is caught by the algorithm. The mesh is adaptively refined around the obstacle and is coarse away from the obstacle.

Table 2.2.
Comparison of numerical results using adaptive mesh and uniform mesh refinements for Example 1.

Adaptive mesh			Uniform mesh		
DoF_h	e_h	ϵ_h	DoF_h	e_h	ϵ_h
1745	0.4632	3.9693	1745	0.4632	3.9693
2984	0.3256	2.6723	2667	0.3717	3.2365
5559	0.2253	1.9293	5857	0.2494	2.0625
9030	0.1778	1.5054	10630	0.1851	1.5856
15407	0.1384	1.1686	20224	0.1330	1.1257

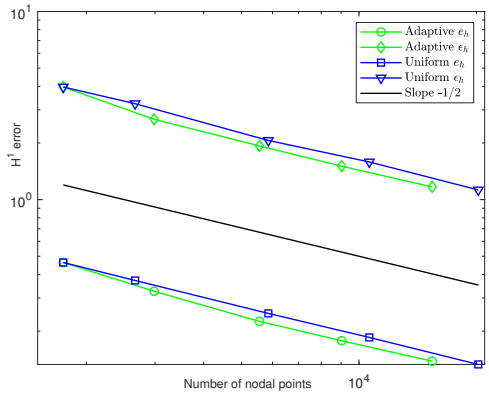

Figure 2.2. Quasi-optimality of the a priori and a posteriori error estimates for Example 1.

Example 2. This example does not have an analytical solution. We consider a compressional plane incident wave $\boldsymbol{u}^{\mathrm{inc}}(\boldsymbol{x}) = \boldsymbol{d}e^{\mathrm{i}\kappa_1 \boldsymbol{x}\cdot\boldsymbol{d}}$ with the incident direction $\boldsymbol{d} = (1,0)^\top$. The obstacle is U-shaped and is contained in the rectangular domain $\{\boldsymbol{x} \in \mathbb{R}^2 : -2 < x < 2.2, -0.7 < y < 0.7\}$. Due to the problem geometry, the solution contains singularity around the corners of the obstacle. We take $R = 3, \hat{R} = 2.31$. Figure 2.4 shows the curve of $\log \epsilon_h$ versus $\log \mathrm{DoF}_h$ at different frequencies $\omega = 1, \pi, 2\pi$.

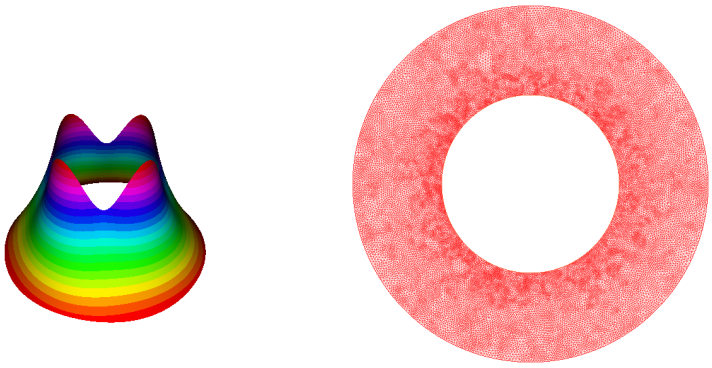

Figure 2.3. The numerical solution of Example 1. (left) the magnitude of the numerical solution; (left) an adaptively refined mesh with 15407 elements.

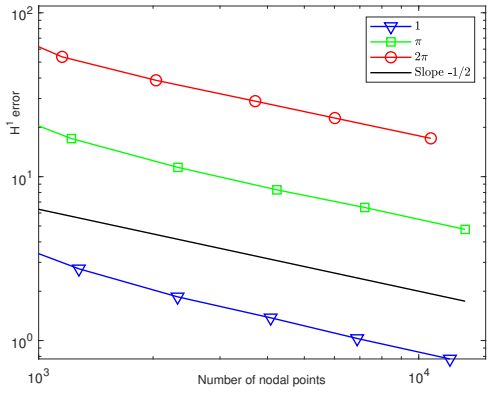

Figure 2.4. Quasi-optimality of the a posteriori error estimates with different frequencies for Example 2.

It demonstrates that the decay of the a posteriori error estimates are $O\big(\mathrm{DoF}_h^{-1/2}\big)$. Figure 2.5 plots the contour of the magnitude of the numerical solution and its corresponding mesh by using the parameters $\omega = \pi, \lambda = 2, \mu = 1$. Again, the algorithm does capture the solution feature and adaptively refines the mesh around the corners of the obstacle where the solution displays singularity.

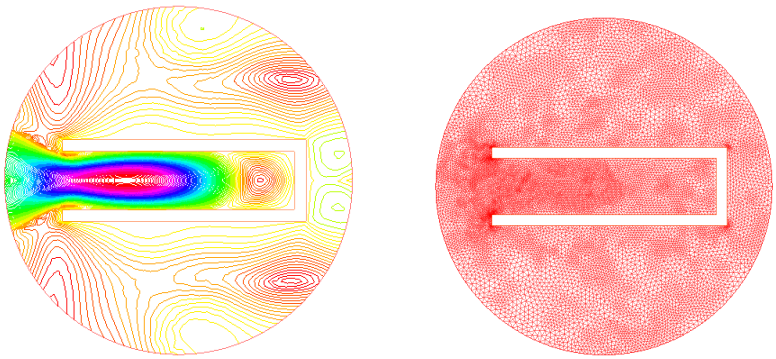

Figure 2.5. The numerical solution of Example 2. (left) The contour plot of the magnitude of the solution; (right) an adaptively refined mesh with 12329 elements

2.6 Conclusion

In this chapter, we present an adaptive finite element DtN method for the elastic obstacle scattering problem. Based on the Helmholtz decomposition, a new duality argument is developed to obtain the a posteriori error estimate. It not only takes into account of the finite element discretization error but also includes the truncation error of the DtN operator. We show that the truncation error decays exponentially with respect to the truncation parameter. The posteriori error estimate for the solution of the discrete problem serves as a basis for the adaptive finite element approximation. Numerical results show that the proposed method is accurate and effective. This work provides a viable alternative to the adaptive finite element PML method to solve the elastic obstacle scattering problem.

2.7 Appendix: Transparent Boundary Conditions

In this section, we show the transparent boundary conditions for the scalar potential functions ϕ, ψ and the displacement of the scattered field $\boldsymbol{u}$ on ∂B_R.

In the exterior domain $\mathbb{R}^2\backslash\overline{B}_R$, the solutions of the Helmholtz equations (2.5) have the Fourier series expansions in the polar coordinates:

$$\phi(r,\theta)=\sum_{n\in\mathbb{Z}}\frac{H_n^{(1)}(\kappa_1 r)}{H_n^{(1)}(\kappa_1 R)}\phi_n(R)e^{\mathrm{i}n\theta},\quad \psi(r,\theta)=\sum_{n\in\mathbb{Z}}\frac{H_n^{(1)}(\kappa_2 r)}{H_n^{(1)}(\kappa_2 R)}\psi_n(R)e^{\mathrm{i}n\theta},\tag{2.54}$$

where $H_n^{(1)}$ is the Hankel function of the first kind with order n. Taking the normal derivative of (2.54), we obtain the transparent boundary condition for the scalar potentials ϕ,ψ on ∂B_R:

$$\mathscr{T}_1\phi:=\sum_{n\in\mathbb{Z}}\frac{\kappa_1 H_n^{(1)'}(\kappa_1 R)}{H_n^{(1)}(\kappa_1 R)}\phi_n(R)e^{\mathrm{i}n\theta},\qquad \mathscr{T}_2\psi:=\sum_{n\in\mathbb{Z}}\frac{\kappa_2 H_n^{(1)'}(\kappa_2 R)}{H_n^{(1)}(\kappa_2 R)}\psi_n(R)e^{\mathrm{i}n\theta}.\tag{2.55}$$

The polar coordinates (r,θ) are related to the Cartesian coordinates $\boldsymbol{x}=(x,y)$ by $x=r\cos\theta, y=r\sin\theta$ with the local orthonormal basis $\{\boldsymbol{e}_r,\boldsymbol{e}_\theta\}$, where $\boldsymbol{e}_r=(\cos\theta,\sin\theta)^\top, \boldsymbol{e}_\theta=(-\sin\theta,\cos\theta)^\top$. Given a scalar function u and a vector function $\boldsymbol{u}=u_r\boldsymbol{e}_r+u_\theta\boldsymbol{e}_\theta$, introduce the differential operators in the polar coordinates:

$$\begin{aligned}\nabla u&=\partial_r u\boldsymbol{e}_r+\frac{1}{r}\partial_\theta u\boldsymbol{e}_\theta,\\ \mathbf{curl}u&=\frac{1}{r}\partial_\theta u\boldsymbol{e}_r-\partial_r u\boldsymbol{e}_\theta,\\ \nabla\cdot\boldsymbol{u}&=\partial_r u_r+\frac{1}{r}u_r+\frac{1}{r}\partial_\theta u_\theta.\end{aligned}$$

Define a boundary operator for the displacement of the scattered wave

$$\mathscr{B}\boldsymbol{u}=\mu\partial_r\boldsymbol{u}+(\lambda+\mu)(\nabla\cdot\boldsymbol{u})\boldsymbol{e}_r\quad\text{on }\partial B_R.$$

Based on the Helmholtz decomposition (2.5) and the transparent boundary condition (2.55), it is shown in [75] that the scattered field $\boldsymbol{u}$ satisfies the transparent boundary condition

$$\mathscr{B}\boldsymbol{u}=(\mathscr{T}\boldsymbol{u})(R,\theta):=\sum_{n\in\mathbb{Z}}M_n\boldsymbol{u}_n(R)e^{\mathrm{i}n\theta}\quad\text{on }\partial B_R,\tag{2.56}$$

where

$$\boldsymbol{u}(R,\theta)=\sum_{n\in\mathbb{Z}}\boldsymbol{u}_n(R)e^{\mathrm{i}n\theta}=\sum_{n\in\mathbb{Z}}\big(u_n^r(R)\boldsymbol{e}_r+u_n^\theta(R)\boldsymbol{e}_\theta\big)e^{\mathrm{i}n\theta}$$

and M_n is a 2×2 matrix defined by

$$M_n = \begin{bmatrix} M_{11}^{(n)} & M_{12}^{(n)} \\ M_{21}^{(n)} & M_{22}^{(n)} \end{bmatrix} = \frac{1}{\Lambda_n(R)} \begin{bmatrix} N_{11}^{(n)} & N_{12}^{(n)} \\ N_{21}^{(n)} & N_{22}^{(n)} \end{bmatrix}. \tag{2.57}$$

Here

$$\Lambda_n(R) = \Big(\frac{n}{R}\Big)^2 - \alpha_{1n}(R)\alpha_{2n}(R), \quad \alpha_{jn}(R) = \frac{\kappa_j H_n^{(1)'}(\kappa_j R)}{H_n^{(1)}(\kappa_j R)}, \tag{2.58}$$

and

$$\begin{aligned}
N_{11}^{(n)} =& \mu \Big(\frac{n}{R}\Big)^2 \Big(\alpha_{2n}(R) - \frac{1}{R}\Big) - \alpha_{2n}(R)\Big[(\lambda+2\mu)\frac{\kappa_1^2 H_n^{(1)''}(\kappa_1 R)}{H_n^{(1)}(\kappa_1 R))} \\
&+ (\lambda+\mu)\Big(\frac{1}{R}\alpha_{1n}(R) - \Big(\frac{n}{R}\Big)^2\Big)\Big], \\
N_{12}^{(n)} =& \mu \frac{\mathrm{i}n}{R}\alpha_{1n}(R)\Big(\alpha_{2n}(R) - \frac{1}{R}\Big) - \frac{\mathrm{i}n}{R}\Big[(\lambda+2\mu)\frac{\kappa_1^2 H_n^{(1)''}(\kappa_1 R)}{H_n^{(1)}(\kappa_1 R))} \\
&+ (\lambda+\mu)\Big(\frac{1}{R}\alpha_{1n}(R) - \Big(\frac{n}{R}\Big)^2\Big)\Big], \\
N_{21}^{(n)} =& -\mu \frac{\mathrm{i}n}{R}\alpha_{2n}(R)\Big(\alpha_{1n}(R) - \frac{1}{R}\Big) + \mu \frac{\mathrm{i}n}{R}\frac{\kappa_2^2 H_n^{(1)''}(\kappa_2 R)}{H_n^{(1)}(\kappa_2 R)}, \\
N_{22}^{(n)} =& \mu \Big(\frac{n}{R}\Big)^2 \Big(\alpha_{1n}(R) - \frac{1}{R}\Big) - \mu\alpha_{1n}(R)\frac{\kappa_2^2 H_n^{(1)''}(\kappa_2 R)}{H_n^{(1)}(\kappa_2 R)}.
\end{aligned}$$

The matrix entries $N_{ij}^{(n)}, i, j = 1, 2$ can be further simplied. Recall that the Hankel function $H_n^{(1)}(z)$ satisfies the Bessel differential equation

$$z^2 H_n^{(1)''}(z) + z H_n^{(1)'}(z) + (z^2 - n^2) H_n^{(1)}(z) = 0.$$

We have from straighforward calculations that

$$
\begin{aligned}
N_{11}^{(n)} &= -\alpha_{2n}(R)\Bigg[(\lambda+2\mu)\Bigg[-\frac{1}{R^2}\Big(\kappa_j R\frac{H_n^{(1)'}(\kappa_j R)}{H_n^{(1)}(\kappa_j R)}+\big((\kappa_j R)^2-n^2\big)\Big)\Bigg] \\
&\qquad +(\lambda+\mu)\left(\frac{1}{R}\alpha_{1n}(R)-\left(\frac{n}{R}\right)^2\right)\Bigg]+\mu\left(\frac{n}{R}\right)^2\left(\alpha_{2n}(R)-\frac{1}{R}\right) \\
&= -\alpha_{2n}(R)\Bigg[-\left(\frac{\lambda+2\mu}{R}\right)\alpha_{1n}(R)-(\lambda+2\mu)\kappa_1^2+(\lambda+2\mu)\left(\frac{n}{R}\right)^2+\left(\frac{\lambda+\mu}{R}\right)\alpha_{1n}(R) \\
&\qquad -(\lambda+\mu)\left(\frac{n}{R}\right)^2\Bigg]+\mu\left(\frac{n}{R}\right)^2\left(\alpha_{2n}(R)-\frac{1}{R}\right) \\
&= -\frac{\mu}{R}\left[\left(\frac{n}{R}\right)^2-\alpha_{1n}(R)\alpha_{2n}(R)\right]+\alpha_{2n}(R)\omega^2 \\
&= -\frac{\mu}{R}\Lambda_n(R)+\alpha_{2n}(R)\omega^2,
\end{aligned}
$$

$$
\begin{aligned}
N_{12}^{(n)} &= -\frac{\mathrm{i}n}{R}\Bigg[(\lambda+2\mu)\Bigg[-\frac{1}{R^2}\Big(\kappa_j R\frac{H_n^{(1)'}(\kappa_j R)}{H_n^{(1)}(\kappa_j R)}+\big((\kappa_j R)^2-n^2\big)\Big)\Bigg] \\
&\qquad +(\lambda+\mu)\left(\frac{1}{R}\alpha_{1n}(R)-\left(\frac{n}{R}\right)^2\right)\Bigg]+\frac{\mathrm{i}n\mu}{R}\alpha_{1n}(R)\alpha_{2n}(R)-\mu\frac{\mathrm{i}n}{R^2}\alpha_{1n}(R) \\
&= -\frac{\mathrm{i}n}{R}\left[-\frac{\mu}{R}\alpha_{1n}(R)+\mu\left(\frac{n}{R}\right)^2-(\lambda+2\mu)\kappa_1^2\right]+\frac{\mathrm{i}n\mu}{R}\alpha_{1n}(R)\alpha_{2n}(R)-\frac{\mathrm{i}n}{R^2}\mu\alpha_{1n}(R) \\
&= -\frac{\mathrm{i}n\mu}{R}\Lambda_n(R)+\frac{\mathrm{i}n}{R}\omega^2,
\end{aligned}
$$

$$
\begin{aligned}
N_{21}^{(n)} &= -\mu\frac{\mathrm{i}n}{R}\alpha_{2n}(R)\alpha_{1n}(R)+\frac{\mathrm{i}n\mu}{R^2}\alpha_{2n}(R)+\mu\frac{\mathrm{i}n}{R}\left(\frac{-1}{R^2}\right)\left(R\alpha_{2n}(R)+(\kappa_2 R)^2-n^2\right) \\
&= -\mu\frac{\mathrm{i}n}{R}\alpha_{1n}(R)\alpha_{2n}(R)+\frac{\mathrm{i}n\mu}{R^2}\alpha_{2n}(R)-\mu\frac{\mathrm{i}n}{R^2}\alpha_{2n}(R)-\frac{\mathrm{i}n\mu}{R}\kappa_2^2+\mathrm{i}\mu\left(\frac{n}{R}\right)^3 \\
&= \frac{\mathrm{i}\mu n}{R}\Lambda_n(R)-\frac{\mathrm{i}n}{R}\omega^2,
\end{aligned}
$$

$$
\begin{aligned}
N_{22}^{(n)} &= \mu\left(\frac{n}{R}\right)^2\alpha_{1n}(R)-\frac{\mu}{R}\left(\frac{n}{R}\right)^2-\mu\alpha_{1n}(R)\frac{-1}{R^2}\left(R\alpha_{2n}(R)+(\kappa_2 R)^2-n^2\right) \\
&= \mu\left(\frac{n}{R}\right)^2\alpha_{1n}(R)-\frac{\mu}{R}\left(\frac{n}{R}\right)^2+\frac{\mu}{R}\alpha_{1n}(R)\alpha_{2n}(R)+\alpha_{1n}(R)\mu\kappa_2^2-\mu\left(\frac{n}{R}\right)^2\alpha_{1n}(R) \\
&= -\frac{\mu}{R}\left(\left(\frac{n}{R}\right)^2-\alpha_{1n}(R)\alpha_{2n}(R)\right)+\alpha_{1n}(R)\omega^2 \\
&= -\frac{\mu}{R}\Lambda_n(R)+\alpha_{1n}(R)\omega^2.
\end{aligned}
$$

Substituting the above into (2.56), we obtain

$$\begin{aligned}\mathscr{B}\boldsymbol{u} = \mathscr{T}\boldsymbol{u} = \sum_{n\in\mathbb{Z}} \frac{1}{\Lambda_n}\Big\{\Big[\Big(-\frac{\mu}{R}\Lambda_n(R) + \alpha_{2n}(R)\omega^2\Big)u_n^r(R) \\ + \Big(-\frac{\mathrm{i}n\mu}{R}\Lambda_n(R) + \frac{\mathrm{i}n}{R}\omega^2\Big)u_n^\theta(R)\Big]\boldsymbol{e}_r + \Big[\Big(\frac{\mathrm{i}\mu n}{R}\Lambda_n(R) - \frac{\mathrm{i}n}{R}\omega^2\Big)u_n^r(R) \\ + \Big(-\frac{\mu}{R}\Lambda_n(R) + \alpha_{1n}(R)\omega^2\Big)u_n^\theta(R)\Big]\boldsymbol{e}_\theta\Big\}e^{\mathrm{i}n\theta}. \qquad (2.59)\end{aligned}$$

Lemma 2.7.1 *Let $z > 0$. For sufficiently large $|n|$, $\Lambda_n(z)$ admits the following asymptotic property*

$$\Lambda_n(z) = \frac{1}{2}(\kappa_1^2 + \kappa_2^2) + \mathcal{O}\Big(\frac{1}{|n|}\Big).$$

Proof Using the asymptotic expansions of the Hankel functions [95]

$$\frac{H_n^{(1)'}(z)}{H_n^{(1)}(z)} = -\frac{|n|}{z} + \frac{z}{2|n|} + \mathcal{O}\Big(\frac{1}{|n|^2}\Big),$$

we have

$$\alpha_{jn}(z) = \frac{\kappa_j H_n^{(1)'}(\kappa_j z)}{H_n^{(1)}(\kappa_j z)} = -\frac{|n|}{z} + \frac{\kappa_j^2 z}{2|n|} + \mathcal{O}\Big(\frac{1}{|n|^2}\Big).$$

A simple calcuation yields that

$$\Lambda_n(z) = \Big(\frac{n}{z}\Big)^2 - \alpha_{1n}(z)\alpha_{2n}(z) = \frac{1}{2}(\kappa_1^2 + \kappa_2^2) + \mathcal{O}\Big(\frac{1}{|n|}\Big),$$

which completes the proof. ■

3. THE DIRECT ELASTIC SURFACE SCATTERING PROBLEM

3.1 Introduction

The scattering theory in periodic structures, which are known as gratings in optics, has many significant applications in micro-optics including the design and fabrication of optical elements such as corrective lenses, anti-reflective interfaces, beam splitters, and sensors [8, 86]. Driven by the optical industry applications, the time-harmonic scattering problems have been extensively studied for acoustic and electromagnetic waves in periodic structures. We refer to [10, 27] and the references cited therein for the mathematical results on well-posedness of the solutions for the diffraction grating problems. Computationally, various numerical methods have been developed, such as boundary integral equation method [83, 96], finite element method [5, 6], boundary perturbation method [23]. Recently, the scattering problems for elastic waves have received much attention due to the important applications in seismology and geophysics [1, 2, 72]. This chapter concerns the scattering of a time-harmonic elastic plane wave by a periodic surface. Compared with acoustic and electromagnetic wave equations, the elastic wave equation is less studied due to the complexity of the coexistence of compressional and shear waves with different wavenumbers. In addition, there are two challenges for the scattering problem: the solution may have singularity due to a possible nonsmooth surface; the problem is imposed in an open domain. In this chapter, we intend to address both issues.

In this chapter, we present an adaptive finite element DtN method for the elastic wave scattering problem in periodic structures. The goal is threefold: (1) prove the exponential convergence of the truncated DtN operator; (2) give a complete a posteriori error estimate; (3) develop an effective adaptive finite element algorithm. This

chapter significantly extends the work on the acoustic scattering problem [94], where the Helmholtz equation was considered. Apparently, the techniques differ greatly from the existing work because of the complicated transparent boundary condition associated with the elastic wave equation. A related work can be found in [77] for an adaptive finite element DtN method for solving the obstacle scattering problem of elastic waves.

Specifically, we consider the scattering of an elastic plane wave by a one-dimensional rigid periodic surface, where the wave motion is governed by the two-dimensional Navier equation. The open space above the surface is assumed to be filled with a homogeneous and isotropic elastic medium. The Helmholtz decomposition is utilized to reduce the elastic wave equation equivalently into a coupled boundary value problem of the Helmholtz equation. By combining the quasi-periodic boundary condition and a DtN operator, an exact TBC is introduced to reduce the original scattering problem into a boundary value problem of the elastic wave equation in a bounded domain. The discrete problem is studied by using the finite element method with the truncated DtN operator. Based on the Helmholtz decomposition, a new duality argument is developed to obtain an a posteriori error estimate between the solution of the original scattering problem and the discrete problem. The a posteriori error estimate contains the finite element approximation error and the DtN operator truncation error, which is shown to decay exponentially with respect to the truncation parameter. The estimate is used to design the adaptive finite element algorithm to choose elements for refinements and to determine the truncation parameter N. Due to the exponential convergence of the truncated DtN operator, the choice of the truncation parameter N is not sensitive to the given tolerance. Numerical experiments are presented to demonstrate the effectiveness of the proposed method.

The outline of the chapter is as follows. In Section 3.2, the model equation is introduced for the scattering problem. In Section 3.3, the boundary value problem is formulated by using the TBC and the corresponding weak formulation is studied. In Section 3.4, the discrete problem is considered by using the finite element method with

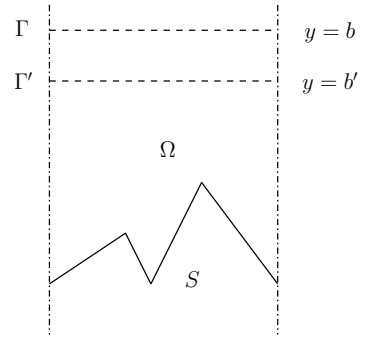

Figure 3.1. Schematic of the elastic wave scattering by a periodic structure.

the truncated DtN operator. Section 3.5 is devoted to the a posterior error estimate. In Section 3.6, we discuss the numerical implementation of the adaptive algorithm and present two examples to illustrate the performance of the proposed method. The chapter is concluded with some general remarks and directions for future work in Section 3.7.

3.2 Problem Formulation

Consider the scattering of a time-harmonic plane wave by an elastically rigid surface, which is assumed to be invariant in the z-axis and periodic in the x-axis with period Λ. Due to the periodic structure, the problem can be restricted into a single periodic cell where $x \in (0, \Lambda)$. Let $\boldsymbol{x} = (x, y) \in \mathbb{R}^2$. Denote the surface by $S = \{\boldsymbol{x} \in \mathbb{R}^2 : y = f(x),\, x \in (0, \Lambda)\}$, where f is a Lipschitz continuous function. Let ν and τ be the unit normal and tangent vectors on S, respectively. Above S, the open space is assumed to be filled with a homogeneous and isotropic elastic medium with unit mass density. Denote $\Omega_f^+ = \{\boldsymbol{x} \in \mathbb{R}^2 : y > f(x),\, x \in (0, \Lambda)\}$. Let $\Gamma = \{\boldsymbol{x} \in \mathbb{R}^2 : y = b,\, x \in (0, \Lambda)\}$ and $\Gamma' = \{\boldsymbol{x} \in \mathbb{R}^2 : y = b',\, x \in (0, \Lambda)\}$, where b and b' are constants satisfying $b > b' > \max_{x\in(0,\Lambda)} f(x)$. Denote $\Omega = \{\boldsymbol{x} \in \mathbb{R}^2 : f(x) < y < b,\, x \in (0, \Lambda)\}$. The problem geometry is shown in Figure 3.1.

The incident wave $\boldsymbol{u}^{\text{inc}}$ satisfies the two-dimensional elastic wave equation

$$\mu\Delta\boldsymbol{u}^{\text{inc}} + (\lambda+\mu)\nabla\nabla\cdot\boldsymbol{u}^{\text{inc}} + \omega^2\boldsymbol{u}^{\text{inc}} = 0 \quad \text{in } \Omega_f^+,$$

where $\omega > 0$ is the angular frequency and μ, λ are the Lamé parameters satisfying $\mu > 0, \lambda + \mu > 0$. Specifically, the incident wave can be the compressional plane wave $\boldsymbol{u}^{\text{inc}}(\boldsymbol{x}) = \boldsymbol{d}e^{\mathrm{i}\kappa_1\boldsymbol{x}\cdot\boldsymbol{d}}$ or the shear plane wave $\boldsymbol{u}^{\text{inc}}(\boldsymbol{x}) = \boldsymbol{d}^{\perp}e^{\mathrm{i}\kappa_2\boldsymbol{x}\cdot\boldsymbol{d}}$, where $\boldsymbol{d} = (\sin\theta, -\cos\theta)^{\top}, \boldsymbol{d}^{\perp} = (\cos\theta, \sin\theta)^{\top}, \theta = (-\pi/2, \pi/2)$ is the incident angle, $\kappa_1 = \omega/(\lambda+2\mu)^{1/2}$ and $\kappa_2 = \omega/\mu^{1/2}$ are known as the compressional and shear wavenumbers, respectively. For clarity, we shall take the compressional plane wave as the incident field. The results will be similar if the incident field is the shear plane wave.

Due to the interaction between the incident wave and the surface, the scattered wave is generated and satisfies

$$\mu\Delta\boldsymbol{u} + (\lambda+\mu)\nabla\nabla\cdot\boldsymbol{u} + \omega^2\boldsymbol{u} = 0 \quad \text{in } \Omega_f^+. \tag{3.1}$$

Since the surface S is elastically rigid, the displacement of the total field vanishes and the scattered field satisfies

$$\boldsymbol{u} = -\boldsymbol{u}^{\text{inc}} \quad \text{on } S. \tag{3.2}$$

For any solution $\boldsymbol{u}$ of (3.1), it has the Helmholtz decomposition

$$\boldsymbol{u} = \nabla\phi_1 + \mathbf{curl}\phi_2, \tag{3.3}$$

where $\phi_j, j = 1, 2$ are scalar potential functions and $\mathbf{curl}\phi_2 = (\partial_y\phi_2, -\partial_x\phi_2)^{\top}$. Substituting (3.3) into (3.1), we may verify that ϕ_j satisfies the Helmholtz equation

$$\Delta\phi_j + \kappa_j^2\phi_j = 0 \quad \text{in } \Omega_f^+. \tag{3.4}$$

Taking the dot product of (3.2) with ν and τ, respectively, yields that

$$\partial_\nu\phi_1 - \partial_\tau\phi_2 = \boldsymbol{u}^{\text{inc}}\cdot\nu, \quad \partial_\nu\phi_2 + \partial_\tau\phi_1 = -\boldsymbol{u}^{\text{inc}}\cdot\tau \quad \text{on } S.$$

Let $\alpha = \kappa_{\text{p}}\sin\theta$. It is clear to note that $\boldsymbol{u}^{\text{inc}}$ is a quasi-periodic function with respect to x, i.e., $\boldsymbol{u}^{\text{inc}}(x, y)e^{-\mathrm{i}\alpha x}$ is a periodic function with respect to x. Motivated

by uniqueness of the solution, we require that the solution $\boldsymbol{u}$ of (3.1)–(3.2) is also a quasi-periodic function of x with period Λ.

We introduce some notations and functional spaces. Let $H^1(\Omega)$ be the standard Sobolev space. Denote a quasi-periodic functional space

$$H^1_{\rm qp}(\Omega) = \{u \in H^1(\Omega) : u(\Lambda, y) = u(0, y)e^{{\rm i}\alpha\Lambda}\}.$$

Let $H^1_{S,{\rm qp}}(\Omega) = \{u \in H^1_{\rm qp}(\Omega) : u = 0 \text{ on } S\}$. Clearly, $H^1_{\rm qp}(\Omega)$ and $H^1_{S,{\rm qp}}(\Omega)$ are subspaces of $H^1(\Omega)$ with the standard H^1-norm. For any function $u \in H^1_{\rm qp}(\Omega)$, it admits the Fourier expansion on Γ:

$$u(x, b) = \sum_{n\in\mathbb{Z}} u^{(n)}(b)e^{{\rm i}\alpha_n x}, \quad u^{(n)}(b) = \frac{1}{\Lambda}\int_0^\Lambda u(x, b)e^{-{\rm i}\alpha_n x}{\rm d}x, \quad \alpha_n = \alpha + n\left(\frac{2\pi}{\Lambda}\right).$$

The trace functional space $H^s(\Gamma), s \in \mathbb{R}$ is defined by

$$H^s(\Gamma) = \left\{u \in L^2(\Gamma) : \|u\|_{H^s(\Gamma)} < \infty\right\},$$

where the norm is given by

$$\|u\|_{H^s(\Gamma)} = \left(\Lambda \sum_{n\in\mathbb{Z}} \left(1 + \alpha_n^2\right)^s |u^{(n)}(b)|^2\right)^{1/2}.$$

Let $\boldsymbol{H}^1_{\rm qp}(\Omega), \boldsymbol{H}^1_{S,{\rm qp}}(\Omega), \boldsymbol{H}^s(\Gamma)$ be the Cartesian product spaces equipped with the corresponding 2-norms of $H^1_{\rm qp}(\Omega), H^1_{S,{\rm qp}}(\Omega), H^s(\Gamma)$, respectively. Throughout the chapter, the notation $a \lesssim b$ stands for $a \leqslant Cb$, where C is a positive constant whose value is not required but should be clear from the context.

3.3 The Boundary Value Problem

The scattering problem (3.1)–(3.2) is formulated in the open domain Ω_f^+, which needs to be truncated into the bounded domain Ω. An appropriate boundary condition is required on Γ to avoid artificial wave reflection.

Let ϕ_j be the solution of the Helmholtz equation (3.4) along with the bounded outgoing wave condition. It is shown in [72] that ϕ_j is a quasi-periodic function and admits the Fourier series expansion

$$\phi_j(x,y) = \sum_{n\in\mathbb{Z}} \phi_j^{(n)}(b) e^{\mathrm{i}\left(\alpha_n x + \beta_j^{(n)}(y-b)\right)}, \quad y > b, \tag{3.5}$$

where

$$\beta_j^{(n)} = \begin{cases} \left(\kappa_j^2 - \alpha_n^2\right)^{1/2}, & |\alpha_n| < \kappa_j, \\ \mathrm{i}\left(\alpha_n^2 - \kappa_j^2\right)^{1/2}, & |\alpha_n| > \kappa_j. \end{cases} \tag{3.6}$$

We assume that $\kappa_j \neq |\alpha_n|$ for $n \in \mathbb{Z}$ to exclude possible resonance. Taking the normal derivative of (3.5) on Γ yields

$$\partial_y \phi_j(x,b) = \sum_{n\in\mathbb{Z}} \mathrm{i}\beta_j^{(n)} \phi_j^{(n)}(b) e^{\mathrm{i}\alpha_n x}.$$

As a quasi-periodic function, the solution $\boldsymbol{u}(x,y) = (u_1(x,y), u_2(x,y))^\top$ admits the Fourier expansion

$$\boldsymbol{u}(x,y) = \sum_{n\in\mathbb{Z}} (u_1^{(n)}(y), u_2^{(n)}(y))^\top e^{\mathrm{i}\alpha_n x}, \quad y > b,$$

where $u_j^{(n)}$ is the Fourier coefficient of u_j. Define a boundary operator

$$\mathscr{B}\boldsymbol{u} = \mu \partial_y \boldsymbol{u} + (\lambda+\mu)(0,1)^\top \nabla \cdot \boldsymbol{u} \quad \text{on } \Gamma.$$

It is shown in [60] that the solution of (3.1) satisfies the transparent boundary condition

$$\mathscr{B}\boldsymbol{u} = \mathscr{T}\boldsymbol{u} := \sum_{n\in\mathbb{Z}} M^{(n)} (u_1^{(n)}(b), u_2^{(n)}(b))^\top e^{\mathrm{i}\alpha_n x} \quad \text{on } \Gamma, \tag{3.7}$$

where $\mathscr{T}$ is called the Dirichlet-to-Neumann (DtN) operator and $M^{(n)}$ is a 2×2 matrix given by

$$M^{(n)} = \frac{\mathrm{i}}{\chi_n} \begin{bmatrix} \omega^2 \beta_1^{(n)} & \mu\alpha_n\chi_n - \omega^2\alpha_n \\ \omega^2\alpha_n - \mu\alpha_n\chi_n & \omega^2\beta_2^{(n)} \end{bmatrix}. \tag{3.8}$$

Here $\chi_n = \alpha_n^2 + \beta_1^{(n)}\beta_2^{(n)}$.

By the transparent boundary condition (3.7), the variational problem of (3.1)–(3.2) is to find $\boldsymbol{u} \in \boldsymbol{H}^1_{\rm qp}(\Omega)$ with $\boldsymbol{u} = -\boldsymbol{u}^{\rm inc}$ on S such that

$$a(\boldsymbol{u}, \boldsymbol{v}) = 0, \quad \forall \boldsymbol{v} \in \boldsymbol{H}^1_{S,\rm qp}(\Omega), \tag{3.9}$$

where the sesquilinear form $a : \boldsymbol{H}^1_{\rm qp}(\Omega) \times \boldsymbol{H}^1_{\rm qp}(\Omega) \to \mathbb{C}$ is defined as

$$\begin{aligned} a(\boldsymbol{u}, \boldsymbol{v}) = \mu \int_\Omega \nabla \boldsymbol{u} : \nabla \overline{\boldsymbol{v}} {\rm d}\boldsymbol{x} + (\lambda + \mu) \int_\Omega (\nabla \cdot \boldsymbol{u}) (\nabla \cdot \overline{\boldsymbol{v}}) \, {\rm d}\boldsymbol{x} \\ -\omega^2 \int_\Omega \boldsymbol{u} \cdot \overline{\boldsymbol{v}} {\rm d}\boldsymbol{x} - \int_\Gamma \mathscr{T} \boldsymbol{u} \cdot \overline{\boldsymbol{v}} {\rm d}s. \end{aligned}$$

Here $A : B = {\rm tr}(AB^\top)$ is the Frobenius inner product of two square matrices A and B.

The well-posedness of the variational problem (3.9) was discussed in [41]. It was shown that the variational problem (3.9) has a unique solution for all frequencies if the surface S is Lipschitz continuous. Hence we may assume that the variational problem (3.9) admits a unique solution and the solution satisfies the estimate

$$\|\boldsymbol{u}\|_{\boldsymbol{H}^1(\Omega)} \lesssim \|\boldsymbol{u}^{\rm inc}\|_{\boldsymbol{H}^{1/2}(S)} \lesssim \|\boldsymbol{u}^{\rm inc}\|_{\boldsymbol{H}^1(\Omega)}. \tag{3.10}$$

By the general theory of Babuska and Aziz [3], there exists $\gamma > 0$ such that the following inf-sup condition holds

$$\sup_{0 \neq \boldsymbol{v} \in \boldsymbol{H}^1_{\rm qp}(\Omega)} \frac{|a(\boldsymbol{u}, \boldsymbol{v})|}{\|\boldsymbol{v}\|_{\boldsymbol{H}^1(\Omega)}} \geqslant \gamma \|\boldsymbol{u}\|_{\boldsymbol{H}^1(\Omega)}, \quad \forall \boldsymbol{u} \in \boldsymbol{H}^1_{\rm qp}(\Omega).$$

3.4 The Discrete Problem

We consider the discrete problem of (3.9) by using the finite element approximation. Let $\mathcal{M}_h$ be a regular triangulation of Ω, where h denotes the maximum diameter of all the elements in $\mathcal{M}_h$. Since our focus is on the a posteriori error estimate, for simplicity, we assume that S is polygonal and ignore the approximation error of the boundary S. Thus any edge $e \in \mathcal{M}_h$ is a subset of $\partial\Omega$ if it has two boundary vertices. Moreover, we require that if $(0, y)$ is a node on the left boundary, then (Λ, y) is also

a node on the right boundary and vice versa, which allows to define a finite element space whose functions are quasi-periodic respect to x.

Let $\boldsymbol{V}_h \subset \boldsymbol{H}^1_{\rm qp}(\Omega)$ be a conforming finite element space, i.e.,

$$\boldsymbol{V}_h := \left\{\boldsymbol{v} \in C(\overline{\Omega})^2 : \boldsymbol{v}|_K \in P_m(K)^2 \text{ for any } K \in \mathcal{M}_h,\ \boldsymbol{v}(0,y) = e^{-\mathrm{i}\alpha\Lambda}\boldsymbol{v}(\Lambda,y)\right\},$$

where m is a positive integer and $P_m(K)$ denotes the set of all polynomials of degree no more than m. The finite element approximation to the variational problem (3.9) is to find $\boldsymbol{u}^h \in \boldsymbol{V}_h$ with $\boldsymbol{u}^h = -\boldsymbol{u}^{\rm inc}$ on S such that

$$a(\boldsymbol{u}^h, \boldsymbol{v}^h) = 0, \quad \forall \boldsymbol{v}^h \in \boldsymbol{V}_{h,S}, \tag{3.11}$$

where $\boldsymbol{V}_{h,S} = \{\boldsymbol{v} \in \boldsymbol{V}_h : \boldsymbol{v} = 0 \text{ on } S\}$.

In the variational problem (3.11), the boundary operator $\mathscr{T}$ is defined as an infinite series, in practice, it must be truncated to a sum of finitely many terms as follows

$$\mathscr{T}_N\boldsymbol{u} = \sum_{|n|\leqslant N} M^{(n)}(u_1^{(n)}(b), u_2^{(n)}(b))^\top e^{\mathrm{i}\alpha_n x}, \tag{3.12}$$

where $N > 0$ is a sufficiently large constant. Using the truncated boundary operator, we arrive at the truncated finite element approximation: Find $\boldsymbol{u}_N^h \in \boldsymbol{V}_h$ such that it satisfies $\boldsymbol{u}_N^h = -\boldsymbol{u}^{\rm inc}$ on S and the variational problem

$$a_N(\boldsymbol{u}_N^h, \boldsymbol{v}^h) = 0, \quad \forall \boldsymbol{v}^h \in \boldsymbol{V}_{h,S}, \tag{3.13}$$

where the sesquilinear form $a_N : \boldsymbol{V}_h \times \boldsymbol{V}_h \to \mathbb{C}$ is defined as

$$\begin{aligned} a_N(\boldsymbol{u}, \boldsymbol{v}) = \mu \int_\Omega \nabla\boldsymbol{u} : \nabla\overline{\boldsymbol{v}}\mathrm{d}\boldsymbol{x} + (\lambda+\mu)\int_\Omega (\nabla\cdot\boldsymbol{u})(\nabla\cdot\overline{\boldsymbol{v}})\mathrm{d}\boldsymbol{x} \\ -\omega^2\int_\Omega \boldsymbol{u}\cdot\overline{\boldsymbol{v}}\mathrm{d}\boldsymbol{x} - \int_\Gamma \mathscr{T}_N\boldsymbol{u}\cdot\overline{\boldsymbol{v}}\mathrm{d}s. \end{aligned}$$

It follows from [90] that the discrete inf-sup condition of the sesquilinear form a_N can be established for sufficient large N and small enough h. Based on the general theory in [3], it can be shown that the discreted variational problem (3.13) has a unique solution $\boldsymbol{u}_N^h \in \boldsymbol{V}_h$. The details are omitted for brevity.

3.5 The a Posteriori Error Analysis

For any triangular element $K \in \mathcal{M}_h$, denoted by h_K its diameter. Let $\mathcal{B}_h$ denote the set of all the edges of K. For any $e \in \mathcal{B}_h$, denoted by h_e its length. For any interior edge e which is the common side of K_1 and $K_2 \in \mathcal{M}_h$, we define the jump residual across e as

$$J_e = \mu \nabla \boldsymbol{u}_N^h|_{K_1} \cdot \boldsymbol{\nu}_1 + (\lambda+\mu)(\nabla \cdot \boldsymbol{u}_N^h|_{K_1})\boldsymbol{\nu}_1 + \mu \nabla \boldsymbol{u}_N^h|_{K_2} \cdot \boldsymbol{\nu}_2 + (\lambda+\mu)(\nabla \cdot \boldsymbol{u}_N^h|_{K_2})\boldsymbol{\nu}_2,$$

where $\boldsymbol{\nu}_j$ is the unit outward normal vector on the boundary of $K_j, j = 1, 2$. For any boundary edge $e \subset \Gamma$, we define the jump residual

$$J_e = 2(\mathscr{T}_N \boldsymbol{u}_N^h - \mathscr{B}\boldsymbol{u}_N^h).$$

For any boundary edge on the left line segment of $\partial\Omega$, i.e., $e \in \{x = 0\} \cap \partial K_1$ for some $K_1 \in \mathcal{M}_h$, and its corresponding edge on the right line segment of $\partial\Omega$, i.e., $e' \in \{x = \Lambda\} \cap \partial K_2$ for some $K_2 \in \mathcal{M}_h$, the jump residual is

$$\begin{aligned} J_e &= \left[\mu \partial_x \boldsymbol{u}_N^h|_{K_1} + (\lambda+\mu)(1,0)^\top \nabla \cdot \boldsymbol{u}_N^h|_{K_1}\right] - e^{-\mathrm{i}\alpha\Lambda}\left[\mu \partial_x \boldsymbol{u}_N^h|_{K_2} + (\lambda+\mu)(1,0)^\top \nabla \cdot \boldsymbol{u}_N^h|_{K_2}\right], \\ J_{e'} &= e^{\mathrm{i}\alpha\Lambda}\left[\mu \partial_x \boldsymbol{u}_N^h|_{K_1} + (\lambda+\mu)(1,0)^\top \nabla \cdot \boldsymbol{u}_N^h|_{K_1}\right] - \left[\mu \partial_x \boldsymbol{u}_N^h|_{K_2} + (\lambda+\mu)(1,0)^\top \nabla \cdot \boldsymbol{u}_N^h|_{K_2}\right]. \end{aligned}$$

For any triangular element $K \in \mathcal{M}_h$, denote by η_K the local error estimator which is given by

$$\eta_K = h_K \|\mathscr{R}\boldsymbol{u}_N^h\|_{\boldsymbol{L}^2(K)} + \left(\frac{1}{2}\sum_{e \in \partial K} h_e \|J_e\|^2_{\boldsymbol{L}^2(e)}\right)^{1/2},$$

where $\mathscr{R}$ is the residual operator defined by

$$\mathscr{R}\boldsymbol{u} = \mu\Delta\boldsymbol{u} + (\lambda+\mu)\nabla(\nabla \cdot \boldsymbol{u}) + \omega^2 \boldsymbol{u}.$$

For convenience, we introduce a weighted norm of $\boldsymbol{H}^1(\Omega)$ as

$$|||\boldsymbol{u}|||^2_{\boldsymbol{H}^1(\Omega)} = \mu \int_\Omega |\nabla \boldsymbol{u}|^2 \mathrm{d}\boldsymbol{x} + (\lambda+\mu)\int_\Omega |\nabla \cdot \boldsymbol{u}|^2 \mathrm{d}\boldsymbol{x} + \omega^2 \int_\Omega |\boldsymbol{u}|^2 \mathrm{d}\boldsymbol{x}.$$

It is easy to check that

$$\min\left(\mu, \omega^2\right)\|\boldsymbol{u}\|^2_{\boldsymbol{H}^1(\Omega)} \leqslant |||\boldsymbol{u}|||^2_{\boldsymbol{H}^1(\Omega)} \leqslant \max\left(2\lambda+3\mu, \omega^2\right)\|\boldsymbol{u}\|^2_{\boldsymbol{H}^1(\Omega)}, \quad \forall \boldsymbol{u} \in \boldsymbol{H}^1(\Omega). \tag{3.14}$$

which implies that the weighted norm is equivalent to standard $\boldsymbol{H}^1(\Omega)$ norm.

Now we state the main result of this chapter.

Theorem 3.5.1 *Let $\boldsymbol{u}$ and $\boldsymbol{u}_N^h$ be the solutions of the variational problem* (3.9) *and* (3.13)*, respectively. Then for sufficient large N, the following a posteriori error estimate holds*

$$\|\boldsymbol{u}-\boldsymbol{u}_N^h\|_{\boldsymbol{H}^1(\Omega)} \lesssim \left(\sum_{K\in\mathcal{M}_h}\eta_K^2\right)^{1/2} + \max_{|n|>N}\left(|n|e^{-|\beta_2^{(n)}|(b-b')}\right)\|\boldsymbol{u}^{\mathrm{inc}}\|_{\boldsymbol{H}^1(\Omega)}.$$

It is easy to note that the a posteriori error consists of two parts: the finite element discretization error and the truncation error of the DtN operator. We point out that the latter is almost exponentially decaying since $b > b'$ and $|\beta_2^{(n)}| > 0$. In practice, the DtN truncated error can be controlled to be small enough such that it does not contaminate the finite element discretization error.

In the rest of the chapter, we shall prove the a posteriori error estimate in Theorem 3.5.1. First, let's state the trace regularity for functions in $H^1_{\mathrm{qp}}(\Omega)$. The proof can be found in [29].

Lemma 3.5.2 *For any $u \in H^1_{\mathrm{qp}}(\Omega)$, the following estimates hold*

$$\|u\|_{H^{1/2}(\Gamma_b)} \lesssim \|u\|_{H^1(\Omega)}, \quad \|u\|_{H^{1/2}(\Gamma_{b'})} \lesssim \|u\|_{H^1(\Omega)}.$$

Denote by $\boldsymbol{\xi} = \boldsymbol{u} - \boldsymbol{u}_N^h$ the error between the solutions of (3.9) and (3.13). It can be verified that

$$\begin{aligned}
|||\boldsymbol{\xi}|||^2_{\boldsymbol{H}^1(\Omega)} &= \mu\int_\Omega \nabla\boldsymbol{\xi} : \nabla\overline{\boldsymbol{\xi}}\mathrm{d}\boldsymbol{x} + (\lambda+\mu)\int_\Omega (\nabla\cdot\boldsymbol{\xi})\left(\nabla\cdot\overline{\boldsymbol{\xi}}\right)\mathrm{d}\boldsymbol{x} + \omega^2\int_\Omega \boldsymbol{\xi}\cdot\overline{\boldsymbol{\xi}}\mathrm{d}\boldsymbol{x} \\
&= \Re a(\boldsymbol{\xi},\boldsymbol{\xi}) + 2\omega^2\int_\Omega \boldsymbol{\xi}\cdot\overline{\boldsymbol{\xi}}\mathrm{d}\boldsymbol{x} + \Re\int_\Gamma \mathscr{T}\boldsymbol{\xi}\cdot\overline{\boldsymbol{\xi}}\mathrm{d}s \qquad (3.15)\\
&= \Re a(\boldsymbol{\xi},\boldsymbol{\xi}) + \Re\int_\Gamma (\mathscr{T}-\mathscr{T}_N)\boldsymbol{\xi}\cdot\overline{\boldsymbol{\xi}}\mathrm{d}s + 2\omega^2\int_\Omega \boldsymbol{\xi}\cdot\overline{\boldsymbol{\xi}}\mathrm{d}\boldsymbol{x} + \Re\int_\Gamma \mathscr{T}_N\boldsymbol{\xi}\cdot\overline{\boldsymbol{\xi}}\mathrm{d}s.
\end{aligned}$$

In the following, we shall discuss the four terms in the right hand side of (3.15). Lemma 3.5.3 gives the error estimate of the truncated DtN operator. Lemma 3.5.4 presents the a posteriori error estimate for the finite element approximation and the truncated DtN operator.

Lemma 3.5.3 *Let $\boldsymbol{u} \in \boldsymbol{H}^1_{\rm qp}(\Omega)$ be the solution of the variational problem* (3.9)*. For any $\boldsymbol{v} \in \boldsymbol{H}^1_{\rm qp}(\Omega)$, the following estimate holds:*

$$\left| \int_\Gamma (\mathscr{T} - \mathscr{T}_N)\, \boldsymbol{u} \cdot \overline{\boldsymbol{v}}\, \mathrm{d}s \right| \leqslant C \max_{|n|>N} \left(|n| e^{\mathrm{i}\beta_2^n (b-b')} \right) \|\boldsymbol{u}^{\rm inc}\|_{\boldsymbol{H}^1(\Omega)} \|\boldsymbol{v}\|_{\boldsymbol{H}^1(\Omega)},$$

where $C > 0$ is a constant independent of N.

Proof Using (3.3) and (3.5) yields

$$\phi_j^{(n)}(b) = \phi_j^{(n)}(b') e^{\mathrm{i}\beta_j^{(n)}(b-b')}.$$

It follows from the straightforward calculations that we obtain

$$\begin{aligned} \begin{bmatrix} u_1^{(n)}(b) \\ u_2^{(n)}(b) \end{bmatrix} &= \frac{1}{\chi_n} \begin{bmatrix} \mathrm{i}\alpha_n & \mathrm{i}\beta_2^{(n)} \\ \mathrm{i}\beta_1^{(n)} & -\mathrm{i}\alpha_n \end{bmatrix} \begin{bmatrix} e^{\mathrm{i}\beta_1^{(n)}(b-b')} & 0 \\ 0 & e^{\mathrm{i}\beta_2^{(n)}(b-b')} \end{bmatrix} \begin{bmatrix} -\mathrm{i}\alpha_n & -\mathrm{i}\beta_2^{(n)} \\ -\mathrm{i}\beta_1^{(n)} & \mathrm{i}\alpha_n \end{bmatrix} \begin{bmatrix} u_1^{(n)}(b') \\ u_2^{(n)}(b') \end{bmatrix} \\ &:= P^{(n)} \begin{bmatrix} u_1^{(n)}(b') \\ u_2^{(n)}(b') \end{bmatrix}, \end{aligned} \tag{3.16}$$

where

$$\begin{aligned} P_{11}^{(n)} &= \frac{1}{\chi_n} \left(\alpha_n^2 e^{\mathrm{i}\beta_1^{(n)}(b-b')} + \beta_1^{(n)} \beta_2^{(n)} e^{\mathrm{i}\beta_2^{(n)}(b-b')} \right), \\ P_{12}^{(n)} &= \frac{\alpha_n \beta_2^{(n)}}{\chi_n} \left(e^{\mathrm{i}\beta_1^{(n)}(b-b')} - e^{\mathrm{i}\beta_2^{(n)}(b-b')} \right), \\ P_{21}^{(n)} &= \frac{\alpha_n \beta_1^{(n)}}{\chi_n} \left(e^{\mathrm{i}\beta_1^{(n)}(b-b')} - e^{\mathrm{i}\beta_2^{(n)}(b-b')} \right), \\ P_{22}^{(n)} &= \frac{1}{\chi_n} \left(\alpha_n^2 e^{\mathrm{i}\beta_2^{(n)}(b-b')} + \beta_1^{(n)} \beta_2^{(n)} e^{\mathrm{i}\beta_1^{(n)}(b-b')} \right). \end{aligned}$$

It is clear to note from (3.6) that $\beta_j^{(n)}$ is purely imaginary for sufficiently large $|n|$. By the mean value theorem, for sufficiently large $|n|$, there exists $\tau \in (\mathrm{i}\beta_1^{(n)}, \mathrm{i}\beta_2^{(n)})$ such that

$$\begin{aligned} \chi_n P_{11}^{(n)} &= \left(\alpha_n^2 + \beta_1^{(n)} \beta_2^{(n)} \right) e^{\mathrm{i}\beta_1^{(n)}(b-b')} + \beta_1^{(n)} \beta_2^{(n)} \left(e^{\mathrm{i}\beta_2^{(n)}(b-b')} - e^{\mathrm{i}\beta_1^{(n)}(b-b')} \right), \\ &= \left(\alpha_n^2 + \beta_1^{(n)} \beta_2^{(n)} \right) e^{\mathrm{i}\beta_1^{(n)}(b-b')} + \beta_1^{(n)} \beta_2^{(n)} (b-b') \mathrm{i}(\beta_2^{(n)} - \beta_1^{(n)}) e^{\tau(b-b')}. \end{aligned}$$

A simple calculation yields

$$\begin{aligned}\alpha_n^2+\beta_1^{(n)}\beta_2^{(n)} &= \alpha_n^2-(\alpha_n^2-\kappa_1^2)^{1/2}(\alpha_n^2-\kappa_2^2)^{1/2}\\ &= \frac{\alpha_n^2\left(\kappa_1^2+\kappa_2^2\right)-\kappa_1^2\kappa_2^2}{\alpha_n^2+(\alpha_n^2-\kappa_1^2)^{1/2}(\alpha_n^2-\kappa_2^2)^{1/2}}<\kappa_1^2+\kappa_2^2\end{aligned}$$

and

$$\begin{aligned}\mathrm{i}\beta_2^{(n)}-\mathrm{i}\beta_1^{(n)} &= (\alpha_n^2-\kappa_1^2)^{1/2}-(\alpha_n^2-\kappa_2^2)^{1/2}\\ &= \frac{\kappa_2^2-\kappa_1^2}{(\alpha_n^2-\kappa_1^2)^{1/2}+(\alpha_n^2-\kappa_2^2)^{1/2}}<\frac{\kappa_2^2-\kappa_1^2}{2(\alpha_n^2-\kappa_2^2)^{1/2}}.\end{aligned}$$

which give

$$|P_{11}^{(n)}|\lesssim e^{\mathrm{i}\beta_1^{(n)}(b-b')}+|n|e^{\tau(b-b')}\lesssim |n|e^{\mathrm{i}\beta_2^{(n)}(b-b')}. \tag{3.17}$$

Similarly, we may show that

$$|P_{ij}^{(n)}|\lesssim |n|e^{\mathrm{i}\beta_2^{(n)}(b-b')},\quad i,j=1,2.$$

Combining the above estimates lead to

$$|u_1^{(n)}(b)|^2+|u_2^{(n)}(b)|^2\lesssim n^2e^{2\mathrm{i}\beta_2^{(n)}(b-b')}\left(|u_1^{(n)}(b')|^2+|u_2^{(n)}(b')|^2\right).$$

By (3.7) and (3.12), we have from Lemma 3.5.2 that

$$\begin{aligned}&\left|\int_\Gamma(\mathscr{T}-\mathscr{T}_N)\,\boldsymbol{u}\cdot\overline{\boldsymbol{v}}\mathrm{d}s\right|=\left|\Lambda\sum_{|n|>N}(M^{(n)}\boldsymbol{u}^{(n)}(b))\cdot\overline{\boldsymbol{v}^{(n)}(b)}\right|\\ &\lesssim\sum_{|n|>N}\left|\left(|n|^{\frac12}\boldsymbol{u}^{(n)}(b)\right)\cdot\left(|n|^{\frac12}\overline{\boldsymbol{v}^{(n)}(b)}\right)\right|\\ &\lesssim\left(\sum_{|n|>N}|n|\left(|u_1^{(n)}(b)|^2+|u_2^{(n)}(b)|^2\right)\right)^{1/2}\left(\sum_{|n|>N}|n|\left(|v_1^{(n)}(b)|^2+|v_2^{(n)}(b)|^2\right)\right)^{1/2}\\ &\lesssim\left(\sum_{|n|>N}|n|^3e^{2\mathrm{i}\beta_2^{(n)}(b-b')}\left(|u_1^{(n)}(b')|^2+|u_2^{(n)}(b')|^2\right)\right)^{1/2}\|\boldsymbol{v}\|_{\boldsymbol{H}^{1/2}(\Gamma)}\\ &\lesssim\max_{|n|>N}\left(|n|e^{\mathrm{i}\beta_2^{(n)}(b-b')}\right)\|\boldsymbol{u}\|_{\boldsymbol{H}^{1/2}(\Gamma_{b'})}\|\boldsymbol{v}\|_{\boldsymbol{H}^{1/2}(\Gamma)}\\ &\lesssim\max_{|n|>N}\left(|n|e^{\mathrm{i}\beta_2^{(n)}(b-b')}\right)\|\boldsymbol{u}\|_{\boldsymbol{H}^1(\Omega)}\|\boldsymbol{v}\|_{\boldsymbol{H}^1(\Omega)}.\end{aligned}$$

Using (3.10), we get

$$\left|\int_\Gamma (\mathscr{T}-\mathscr{T}_N)\,\boldsymbol{u}\cdot\overline{\boldsymbol{v}}\mathrm{d}s\right| \lesssim \max_{|n|>N}\left(|n|e^{\mathrm{i}\beta_2^{(n)}(b-b')}\right)\|\boldsymbol{u}^{\mathrm{inc}}\|_{\boldsymbol{H}^1(\Omega)}\|\boldsymbol{v}\|_{\boldsymbol{H}^1(\Omega)},$$

which completes the proof. ■

In the following lemmas, the first two terms in (3.15) are estimated.

Lemma 3.5.4 *Let $\boldsymbol{v}$ be any function in $\boldsymbol{H}^1_{S,\mathrm{qp}}(\Omega)$, the following estimate holds*

$$\left|a(\boldsymbol{\xi},\boldsymbol{v})+\int_\Gamma (\mathscr{T}-\mathscr{T}_N)\,\boldsymbol{\xi}\cdot\overline{\boldsymbol{v}}\mathrm{d}s\right| \lesssim \left(\left(\sum_{K\in\mathcal{M}_n}\eta_K^2\right)^{1/2}+\max_{|n|>N}\left(|n|e^{\mathrm{i}\beta_2^{(n)}(b-b')}\right)\|\boldsymbol{u}^{\mathrm{inc}}\|_{\boldsymbol{H}^1(\Omega)}\right)\|\boldsymbol{v}\|_{\boldsymbol{H}^1(\Omega)}.$$

Proof For any function $\boldsymbol{v}\in H^1_{S,\mathrm{qp}}(\Omega)$, we have

$$\begin{aligned}
a(\boldsymbol{\xi},\boldsymbol{v})+\int_\Gamma (\mathscr{T}-\mathscr{T}_N)\,\boldsymbol{\xi}\cdot\overline{\boldsymbol{v}}\mathrm{d}s &= a(\boldsymbol{u},\boldsymbol{v})-a(\boldsymbol{u}_N^h,\boldsymbol{v})+\int_\Gamma (\mathscr{T}-\mathscr{T}_N)\,\boldsymbol{\xi}\cdot\overline{\boldsymbol{v}}\mathrm{d}s\\
&= a(\boldsymbol{u},\boldsymbol{v})-a_N^h(\boldsymbol{u}_N^h,\boldsymbol{v})+a_N^h(\boldsymbol{u}_N^h,\boldsymbol{v})-a(\boldsymbol{u}_N^h,\boldsymbol{v})+\int_\Gamma (\mathscr{T}-\mathscr{T}_N)\,\boldsymbol{\xi}\cdot\overline{\boldsymbol{v}}\mathrm{d}s\\
&= a(\boldsymbol{u},\boldsymbol{v})-a_N^h(\boldsymbol{u}_N^h,\boldsymbol{v}^h)-a_N^h(\boldsymbol{u}_N^h,\boldsymbol{v}-\boldsymbol{v}^h)+\int_\Gamma (\mathscr{T}-\mathscr{T}_N)\,\boldsymbol{u}_N^h\cdot\overline{\boldsymbol{v}}\mathrm{d}s\\
&\quad+\int_\Gamma (\mathscr{T}-\mathscr{T}_N)\,\boldsymbol{\xi}\cdot\overline{\boldsymbol{v}}\mathrm{d}s\\
&= -a_N^h(\boldsymbol{u}_N^h,\boldsymbol{v}-\boldsymbol{v}^h)+\int_\Gamma (\mathscr{T}-\mathscr{T}_N)\,\boldsymbol{u}\cdot\overline{\boldsymbol{v}}\mathrm{d}s.
\end{aligned}$$

For any function $\boldsymbol{v}\in\boldsymbol{H}^1_{S,\mathrm{qp}}(\Omega)$ and $\boldsymbol{v}^h\in\boldsymbol{V}_{h,S}$, it follows from the integration by parts that

$$\begin{aligned}
&-a_N^h(\boldsymbol{u}_N^h,\boldsymbol{v}-\boldsymbol{v}^h)\\
=\;& -\sum_{K\in\mathcal{M}_h}\left\{\mu\int_K\nabla\boldsymbol{u}_N^h:\nabla\big(\overline{\boldsymbol{v}}-\overline{\boldsymbol{v}^h}\big)\mathrm{d}\boldsymbol{x}+(\lambda+\mu)\int_K(\nabla\cdot\boldsymbol{u}_N^h)\nabla\cdot\big(\overline{\boldsymbol{v}}-\overline{\boldsymbol{v}^h}\big)\mathrm{d}\boldsymbol{x}\right\}\\
&-\sum_{K\in\mathcal{M}_h}\left\{-\omega^2\int_K\boldsymbol{u}_N^h\cdot\big(\overline{\boldsymbol{v}}-\overline{\boldsymbol{v}^h}\big)\mathrm{d}\boldsymbol{x}-\int_{\Gamma\cap\partial K}\mathscr{T}\boldsymbol{u}_N^h\cdot\big(\overline{\boldsymbol{v}}-\overline{\boldsymbol{v}^h}\big)\mathrm{d}s\right\}\\
=\;& \sum_{K\in\mathcal{M}_h}\left\{-\int_{\partial K}\big[\mu\nabla\boldsymbol{u}_N^h\cdot\boldsymbol{\nu}+(\lambda+\mu)(\nabla\cdot\boldsymbol{u}_N^h)\boldsymbol{\nu}\big]\cdot\big(\overline{\boldsymbol{v}}-\overline{\boldsymbol{v}^h}\big)\mathrm{d}\boldsymbol{x}+\int_{\Gamma\cap\partial K}\mathscr{T}\boldsymbol{u}_N^h\cdot\big(\overline{\boldsymbol{v}}-\overline{\boldsymbol{v}^h}\big)\mathrm{d}s\right\}\\
&+\sum_{K\in\mathcal{M}_h}\int_K\big[\mu\Delta\boldsymbol{u}_N^h+(\lambda+\mu)\nabla\nabla\cdot\boldsymbol{u}_N^h+\omega^2\boldsymbol{u}_N^h\big]\cdot\big(\overline{\boldsymbol{v}}-\overline{\boldsymbol{v}^h}\big)\mathrm{d}\boldsymbol{x}\\
=\;& \sum_{K\in\mathcal{M}_h}\left[\int_K\mathscr{R}\boldsymbol{u}_N^h\cdot\big(\overline{\boldsymbol{v}}-\overline{\boldsymbol{v}^h}\big)\mathrm{d}\boldsymbol{x}+\sum_{e\in\partial K}\frac{1}{2}\int_e J_e\cdot\big(\overline{\boldsymbol{v}}-\overline{\boldsymbol{v}^h}\big)\mathrm{d}s\right].
\end{aligned}\tag{3.18}$$

We take $\boldsymbol{v}^h = \Pi_h \boldsymbol{v} \in \boldsymbol{V}_{h,S}$, where Π_h is the Scott–Zhang interpolation operator and has the following interpolation estimates

$$\|\boldsymbol{v} - \Pi_h \boldsymbol{v}\|_{\boldsymbol{L}^2(K)} \lesssim h_K \|\nabla \boldsymbol{v}\|_{\boldsymbol{L}^2(\tilde{K})}, \quad \|\boldsymbol{v} - \Pi_h \boldsymbol{v}\|_{\boldsymbol{L}^2(e)} \lesssim h_e^{1/2} \|\boldsymbol{v}\|_{\boldsymbol{H}^1(\tilde{K}_e)}.$$

Here $\tilde{K}$ and $\tilde{K}_e$ are the unions of all the triangular elements in $\mathcal{M}_h$, which have nonempty intersection with the element K and the side e, respectively. By the Hölder equality, we get from (3.18) that

$$|a_N^h(\boldsymbol{u}_N^h, \boldsymbol{v} - \boldsymbol{v}^h)| \lesssim \left(\sum_{K \in \mathcal{M}_h} \eta_K^2 \right)^{1/2} \|\boldsymbol{v}\|_{\boldsymbol{H}^1(\Omega)},$$

which completes the proof. ■

Lemma 3.5.5 *Let $\hat{M}^{(n)} = -\frac{1}{2}(M^{(n)} + (M^{(n)})^*)$, where $M^{(n)}$ is defined in* (3.8)*. Then $\hat{M}^{(n)}$ is positive definite for sufficiently large $|n|$.*

Proof It follows from (3.6) that $\beta_j^{(n)}$ is purely imaginary for sufficiently large $|n|$. By (3.8), we have

$$\hat{M}^{(n)} = -\frac{1}{\chi_n} \begin{bmatrix} \mathrm{i}\omega^2 \beta_1^{(n)} & \mathrm{i}\left(\mu \alpha_n \chi_n - \omega^2 \alpha_n\right) \\ \mathrm{i}\left(\omega^2 \alpha_n - \mu \alpha_n \chi_n\right) & \mathrm{i}\omega^2 \beta_2^{(n)} \end{bmatrix}.$$

Since $\chi_n = \alpha_n^2 - (\alpha_n^2 - \kappa_1^2)^{1/2}(\alpha_n^2 - \kappa_2^2)^{1/2} > 0$, we get

$$\hat{M}_{11}^{(n)} = -\frac{\mathrm{i}}{\chi_n} \omega^2 \beta_1^{(n)} = \frac{\omega^2}{\chi_n} (\alpha_n^2 - \kappa_1^2)^{1/2} > 0.$$

A simple calculation yields that

$$\begin{aligned} \chi_n^2 \det \hat{M}^{(n)} &= -\omega^4 \beta_1^{(n)} \beta_2^{(n)} - \left(\mu \alpha_n \chi_n - \omega^2 \alpha_n\right)^2 \\ &= -\mu^2 \kappa_2^4 \left(\chi_n - \alpha_n^2\right) - \mu^2 \alpha_n^2 \left(\chi_n - \kappa_2^2\right)^2 \\ &= \mu^2 \chi_n \left(-\kappa_2^4 - \alpha_n^2 \chi_n + 2\alpha_n^2 \kappa_2^2\right). \end{aligned}$$

Since $\kappa_2 > \kappa_1$ and α_n^2 has an order of n^2 for sufficiently large $|n|$, we obtain

$$\begin{aligned} 2\kappa_2^2 - \chi_n &= 2\kappa_2^2 - \alpha_n^2 + (\alpha_n^2 - \kappa_2^2)^{1/2}(\alpha_n^2 - \kappa_1^2)^{1/2} \\ &= \kappa_2^2 + (\alpha_n^2 - \kappa_2^2)^{1/2}\left((\alpha_n^2 - \kappa_1^2)^{1/2} - (\alpha_n^2 - \kappa_2^2)^{1/2}\right) > 0, \end{aligned}$$

which gives that $\det \hat{M}^{(n)} > 0$ and completes the proof. ■

Lemma 3.5.6 *Let $\Omega' = \{\boldsymbol{x} \in \mathbb{R}^2 : b' < y < b,\ 0 < x < \Lambda\}$. Then for any $\delta > 0$, there exists a positive constant $C(\delta)$ independent of N such that*

$$\Re \int_\Gamma \mathscr{T}_N \boldsymbol{\xi} \cdot \overline{\boldsymbol{\xi}} \mathrm{d}s \leqslant C(\delta) \|\boldsymbol{\xi}\|^2_{\boldsymbol{L}^2(\Omega')} + \delta \|\boldsymbol{\xi}\|^2_{\boldsymbol{H}^1(\Omega')}.$$

Proof Using (3.12), we get from a simple calculation that

$$\Re \int_\Gamma \mathscr{T}_N \boldsymbol{\xi} \cdot \overline{\boldsymbol{\xi}} \mathrm{d}s = \Lambda \sum_{|n| \leqslant N} \Re \left(M^{(n)} \boldsymbol{\xi}^{(n)} \right) \cdot \overline{\boldsymbol{\xi}^{(n)}} = -\Lambda \sum_{|n| \leqslant N} \left(\hat{M}^{(n)} \boldsymbol{\xi}^{(n)} \right) \cdot \overline{\boldsymbol{\xi}^{(n)}}.$$

By Lemma 3.5.5, $\hat{M}^{(n)}$ is positive definite for sufficiently large $|n|$. Hence, for fixed ω, λ, μ, there exists N^* such that $-\left(\hat{M}^{(n)} \boldsymbol{\xi}^{(n)} \right) \cdot \overline{\boldsymbol{\xi}^{(n)}} \leqslant 0$ for $n > N^*$. Correspondingly, we split $\Re \int_\Gamma \mathscr{T}_N \boldsymbol{\xi} \cdot \overline{\boldsymbol{\xi}} \mathrm{d}s$ into two parts:

$$\Re \int_\Gamma \mathscr{T}_N \boldsymbol{\xi} \cdot \overline{\boldsymbol{\xi}} \mathrm{d}s = -\Lambda \sum_{|n| \leqslant \min(N^*, N)} \left(\hat{M}^{(n)} \boldsymbol{\xi}_n \right) \cdot \overline{\boldsymbol{\xi}_n} - \Lambda \sum_{N > |n| > \min(N^*, N)} \left(\hat{M}^{(n)} \boldsymbol{\xi}_n \right) \cdot \overline{\boldsymbol{\xi}_n}, \tag{3.19}$$

where $\sum_{N > |n| > \min(N^*, N)} \left(\hat{M}^{(n)} \boldsymbol{\xi}_n \right) \cdot \overline{\boldsymbol{\xi}_n} = 0$ if $N > N^*$. Since the second part in the right hand side of (3.19) is non-positive, we only need to estimate the first part in the right hand side of (3.19), which has finitely many terms. Hence there exists a constant C depending only on ω, μ, λ such that $\left| \left(\hat{M}^{(n)} \boldsymbol{\xi}^{(n)} \right) \cdot \overline{\boldsymbol{\xi}^{(n)}} \right| \leqslant C |\boldsymbol{\xi}^{(n)}|^2$ for all $|n| \leqslant \min(N^*, N)$.

For any $\delta > 0$, it follows from Yong's inequality that

$$\begin{aligned}
(b - b') \left| \phi(b) \right|^2 &= \int_{b'}^b |\phi(y)|^2 \mathrm{d}y + \int_{b'}^b \int_y^b \left(|\phi(s)|^2 \right)' \mathrm{d}s \mathrm{d}y \\
&\leqslant \int_{b'}^b |\phi(y)|^2 \mathrm{d}y + (b - b') \int_{b'}^b 2 |\phi(y)| |\phi'(y)| \mathrm{d}y \\
&= \int_{b'}^b |\phi(y)|^2 \mathrm{d}y + (b - b') \int_{b'}^b 2 \frac{|\phi(y)|}{\sqrt{\delta}} \sqrt{\delta} |\phi'(y)| \mathrm{d}y \\
&\leqslant \int_{b'}^b |\phi(y)|^2 \mathrm{d}y + \frac{b - b'}{\delta} \int_{b'}^b |\phi(y)|^2 \mathrm{d}y + \delta (b - b') \int_{b'}^b |\phi'(y)|^2 \mathrm{d}y,
\end{aligned}$$

which gives

$$|\phi(b)|^2 \leqslant \left[\frac{1}{\delta} + (b - b')^{-1} \right] \int_{b'}^b |\phi(y)|^2 \mathrm{d}y + \delta \int_{b'}^b |\phi'(y)|^2 \mathrm{d}y.$$

Let $\phi(x,y)=\sum\limits_{n\in\mathbb{Z}}\phi_n(y)e^{\mathrm{i}\alpha_n x}$. A simple calculation yields that

$$\begin{aligned}\|\nabla\phi\|^2_{\boldsymbol{L}^2(\Omega')} &= \Lambda\sum_{n\in\mathbb{Z}}\int_{b'}^{b}\left(|\phi_n'(y)|^2+\alpha_n^2|\phi_n(y)|^2\right)\mathrm{d}y,\\ \|\phi\|^2_{L^2(\Omega')} &= \Lambda\sum_{n\in\mathbb{Z}}\int_{b'}^{b}|\phi_n(y)|^2\mathrm{d}y.\end{aligned}$$

Using the above estimates, we have for any $\phi\in H^1(\Omega')$ that

$$\begin{aligned}&\|\phi\|^2_{L^2(\Gamma)}=\Lambda\sum_{n\in\mathbb{Z}}|\phi_n(b)|^2\\ &\leqslant\Lambda\left[\frac{1}{\delta}+(b-b')^{-1}\right]\sum_{n\in\mathbb{Z}}\int_{b'}^{b}|\phi_n(y)|^2\mathrm{d}y+\Lambda\delta\sum_{n\in\mathbb{Z}}\int_{b'}^{b}|\phi'(y)|^2\mathrm{d}y\\ &\leqslant\Lambda\left[\frac{1}{\delta}+(b-b')^{-1}\right]\sum_{n\in\mathbb{Z}}\int_{b'}^{b}|\phi_n(y)|^2\mathrm{d}y+\Lambda\delta\sum_{n\in\mathbb{Z}}\int_{b'}^{b}\left(|\phi_n'(y)|^2+\alpha_n^2|\phi_n(y)|^2\right)\mathrm{d}y\\ &\leqslant\left[\frac{1}{\delta}+(b-b')^{-1}\right]\|\phi\|^2_{L^2(\Omega')}+\delta\|\nabla\phi\|^2_{L^2(\Omega)}\\ &\leqslant C(\delta)\|\phi\|^2_{L^2(\Omega')}+\delta\|\nabla\phi\|^2_{L^2(\Omega')}.\end{aligned}$$

Combining the above estimates, we obtain

$$\begin{aligned}\mathrm{Re}\int_\Gamma\mathscr{T}_N\boldsymbol{\xi}\cdot\overline{\boldsymbol{\xi}}\mathrm{d}s &\leqslant C\|\boldsymbol{\xi}\|^2_{\boldsymbol{L}^2(\Gamma)}\leqslant C(\delta)\|\boldsymbol{\xi}\|^2_{\boldsymbol{L}^2(\Omega')}+\delta\int_{\Omega'}|\nabla\boldsymbol{\xi}|^2\mathrm{d}\boldsymbol{x}\\ &\leqslant C(\delta)\|\boldsymbol{\xi}\|^2_{\boldsymbol{L}^2(\Omega')}+\delta\|\boldsymbol{\xi}\|^2_{\boldsymbol{H}^1(\Omega')},\end{aligned}$$

which completes the proof. ■

To estimate $\int_\Omega|\boldsymbol{\xi}|^2\mathrm{d}\boldsymbol{x}$ in (3.15) , we introduce the dual problem

$$a(\boldsymbol{v},\boldsymbol{p})=\int_\Omega\boldsymbol{v}\cdot\overline{\boldsymbol{\xi}}\mathrm{d}\boldsymbol{x},\quad\forall\boldsymbol{v}\in\boldsymbol{H}^1_{S,\mathrm{qp}}(\Omega).\tag{3.20}$$

It can be verified that $\boldsymbol{p}$ is the weak solution of the boundary value problem

$$\begin{cases}\mu\Delta\boldsymbol{p}+(\lambda+\mu)\nabla\nabla\cdot\boldsymbol{p}+\omega^2\boldsymbol{p}=-\boldsymbol{\xi} & \text{in}\,\Omega,\\ \boldsymbol{p}=0 & \text{on}\,S,\\ \mathscr{B}\boldsymbol{p}=\mathscr{T}^*\boldsymbol{p} & \text{on}\,\Gamma,\end{cases}\tag{3.21}$$

where $\mathscr{T}^*$ is the adjoint operator to the DtN operator $\mathscr{T}$.

It requires to explicitly solve the boundary value problem (3.21). We consider the Helmholtz decomposition and let

$$\boldsymbol{\xi} = \nabla\zeta_1 + \mathbf{curl}\zeta_2, \tag{3.22}$$

where $\zeta_j, j = 1, 2$ has the Fourier series expansion

$$\zeta_j(x, y) = \sum_{n\in\mathbb{Z}} \zeta_j^{(n)}(y)e^{\mathrm{i}\alpha_n x}, \quad b' < y < b.$$

Consider the following coupled first order ordinary different equations

$$\begin{cases} \xi_1^{(n)}(y) = \mathrm{i}\,\alpha_n\zeta_1^{(n)}(y) + \zeta_2^{(n)\prime}(y), \\ \xi_2^{(n)}(y) = \zeta_1^{(n)\prime}(y) - \mathrm{i}\alpha_n\zeta_2^{(n)}(y), \\ \zeta_1^{(n)}(b) = 0, \quad \zeta_2^{(n)}(b) = 0. \end{cases}$$

It follows from straightforward calculations that the solution is

$$\begin{aligned} \zeta_1^{(n)}(y) &= -\frac{\mathrm{i}}{2}e^{\alpha_n(y-b)}\int_y^b e^{-\alpha_n(t-b)}\xi_n^{(1)}(t)\mathrm{d}t + \frac{\mathrm{i}}{2}e^{-\alpha_n(y-b)}\int_y^b e^{\alpha_n(t-b)}\xi_n^{(1)}(t)\mathrm{d}t \\ &\quad -\frac{1}{2}e^{\alpha_n(y-b)}\int_y^b e^{-\alpha_n(t-b)}\xi_n^{(2)}(t)\mathrm{d}t - \frac{1}{2}e^{-\alpha_n(y-b)}\int_y^b e^{\alpha_n(t-b)}\xi_n^{(2)}(t)\mathrm{d}t, \\ \zeta_2^{(n)}(y) &= -\frac{1}{2}e^{\alpha_n(y-b)}\int_y^b e^{-\alpha_n(t-b)}\xi_n^{(1)}(t)\mathrm{d}t - \frac{1}{2}e^{-\alpha_n(y-b)}\int_y^b e^{\alpha_n(t-b)}\xi_n^{(1)}(t)\mathrm{d}t \\ &\quad +\frac{\mathrm{i}}{2}e^{\alpha_n(y-b)}\int_y^b e^{-\alpha_n(t-b)}\xi_n^{(2)}(t)\mathrm{d}t - \frac{\mathrm{i}}{2}e^{-\alpha_n(y-b)}\int_y^b e^{\alpha_n(t-b)}\xi_n^{(2)}(t)\mathrm{d}t. \end{aligned}$$

It is easy to verify the following estimate

$$\left|\zeta_j^{(n)}(y)\right| \lesssim \left(\|\xi_1^{(n)}\|_{L^\infty(b',b)} + \|\xi_2^{(n)}\|_{L^\infty(b',b)}\right)\frac{1}{|\alpha_n|}e^{|\alpha_n|(b-y)}, \quad j = 1, 2.$$

Let $\boldsymbol{p}$ be the solution of the dual problem (3.21). Then it satisfies the following boundary value problem

$$\begin{cases} \mu\Delta\boldsymbol{p} + (\lambda+\mu)\nabla\nabla\cdot\boldsymbol{p} + \omega^2\boldsymbol{p} = -\boldsymbol{\xi} & \text{in } \Omega', \\ \boldsymbol{p}(x, b') = \boldsymbol{p}(x, b') & \text{on } \Gamma' \\ \mathscr{B}\boldsymbol{p} = \mathscr{T}^*\boldsymbol{p} & \text{on } \Gamma. \end{cases} \tag{3.23}$$

Let function $q_j, j = 1, 2$ have the Fourier expansion in Ω':

$$q_j(x, y) = \sum_{n\in\mathbb{Z}} q_j^{(n)}(y) e^{\mathrm{i}\alpha_n x}.$$

The Fourier coefficients $q_j^{(n)}$ are required to satisfy the two point boundary value problem

$$\begin{cases} q_j^{(n)''}(y) + (\kappa_j^2 - \alpha_n^2) q_j^{(n)}(y) = -c_j \zeta_j^{(n)}(y), \\ q_j^{(n)}(b') = q_j^{(n)}(b'), \\ q_j^{(n)'}(b) = -\mathrm{i}\overline{\beta_j^{(n)}} q_j^{(n)}(b), \end{cases} \tag{3.24}$$

where $c_1 = (\lambda + 2\mu)^{-1}$ and $c_2 = \mu^{-1}$, $\zeta_j^{(n)}$ are the Fourier coefficients of the potential functions ζ_j for the Helmholtz decomposition of $\boldsymbol{\xi}$ in (3.22).

Lemma 3.5.7 *Let* $\boldsymbol{p} = \nabla q_1 + \mathbf{curl} q_2$. *Then* $\boldsymbol{p}$ *satisfies* (3.23).

Proof If (3.24) holds, then it is easy to check that

$$(\lambda + 2\mu)\left(\Delta q_1 + \kappa_1^2 q_1\right) = -\zeta_1, \quad \mu\left(\Delta q_2 + \kappa_2^2 q_2\right) = -\zeta_2.$$

Noting $\boldsymbol{p} = \nabla q_1 + \mathbf{curl} q_2$, we obtain

$$\begin{aligned} &\mu\Delta\boldsymbol{p} + (\lambda + \mu)\nabla\nabla\cdot\boldsymbol{p} + \omega^2\boldsymbol{p} \\ &= \mu\nabla\left(\Delta q_1\right) + \mu\mathbf{curl}\Delta q_2 + (\lambda + \mu)\nabla\Delta q_1 + \omega^2\nabla q_1 + \omega^2\mathbf{curl} q_2 \\ &= (\lambda + 2\mu)\nabla\left(\Delta q_1 + \kappa_1^2 q_1\right) + \mu\mathbf{curl}\left(\Delta q_2 + \kappa_2^2 q_2\right) \\ &= -\nabla\zeta_1 - \mathbf{curl}\zeta_2 = -\boldsymbol{\xi}. \end{aligned}$$

Next is to verify that the boundary condition on $y = b$. Assume that $\boldsymbol{p}$ admits the Fourier expansion $\boldsymbol{p} = \sum_{n\in\mathbb{Z}} (p_1^{(n)}(y), p_2^{(n)}(y))^\top e^{\mathrm{i}\alpha_n x}$. It follows from the Helmholtz decomposition that

$$\begin{bmatrix} p_1^{(n)}(y) \\ p_2^{(n)}(y) \end{bmatrix} = \begin{bmatrix} \mathrm{i}\alpha_n q_1^{(n)}(y) + q_2^{(n)'}(y) \\ q_1^{(n)'}(y) - \mathrm{i}\alpha_n q_2^{(n)}(y) \end{bmatrix},$$

which gives

$$\begin{bmatrix} p_1^{(n)'}(y) \\ p_2^{(n)'}(y) \end{bmatrix} = \begin{bmatrix} \mathrm{i}\alpha_n q_1^{(n)'}(y) + q_2^{(n)''}(y) \\ q_1^{(n)''}(y) - \mathrm{i}\alpha_n q_2^{(n)'}(y) \end{bmatrix}.$$

A straightforward calculation yields that

$$\begin{aligned} \mathscr{B}\boldsymbol{p} &= \mu\partial_y \boldsymbol{p} + (\lambda+\mu)(0,1)^\top \nabla\cdot\boldsymbol{p} \\ &= \sum_{n\in\mathbb{Z}} \begin{bmatrix} \mu\left(\mathrm{i}\alpha_n q_1^{(n)'}(y) + q_2^{(n)''}(y)\right) \\ (\lambda+\mu)\mathrm{i}\alpha_n\left(\mathrm{i}\alpha_n q_1^{(n)}(y) + q_2^{(n)'}(y)\right) + (\lambda+2\mu)\left(q_1^{(n)''}(y) - \mathrm{i}\alpha_n q_2^{(n)'}(y)\right) \end{bmatrix} e^{\mathrm{i}\alpha_n x} \\ &= \sum_{n\in\mathbb{Z}} \begin{bmatrix} \mu\left(\mathrm{i}\alpha_n q_1^{(n)'}(y) + q_2^{(n)''}(y)\right) \\ (\lambda+2\mu)q_1^{(n)''}(y) - (\lambda+\mu)\alpha_n^2 q_1^{(n)}(y) - \mathrm{i}\mu\alpha_n q_2^{(n)'}(y) \end{bmatrix} e^{\mathrm{i}\alpha_n x}. \end{aligned}$$

Evaluating the above equations at $y = b$, we get

$$\mathscr{B}\boldsymbol{p}|_{y=b} = \sum_{n\in\mathbb{Z}} \begin{bmatrix} \mathrm{i}\mu\alpha_n q_1^{(n)'}(b) + \mu q_2^{(n)''}(b) \\ (\lambda+2\mu)q_1^{(n)''}(b) - (\lambda+\mu)\alpha_n^2 q_1^{(n)}(b) - \mathrm{i}\mu\alpha_n q_2^{(n)'}(b) \end{bmatrix} e^{\mathrm{i}\alpha_n x}.$$

Noting $\zeta_j^{(n)}(b) = 0$, we have from (3.24) that $q_j^{(n)''}(b) = -(\kappa_j^2 - \alpha_n^2)q_j^{(n)}(b)$. Hence

$$\mathscr{B}\boldsymbol{p}|_{y=b} = \sum_{n\in\mathbb{Z}} \begin{bmatrix} \mu\alpha_n\overline{\beta_1^{(n)}} & -\omega^2 + \mu\alpha_n^2 \\ \mu\alpha_n^2 - \omega^2 & -\mu\alpha_n\overline{\beta_2^{(n)}} \end{bmatrix} \begin{bmatrix} q_1^{(n)}(b) \\ q_2^{(n)}(b) \end{bmatrix} e^{\mathrm{i}\alpha_n x}.$$

On the other hand, we have

$$\begin{aligned} \mathscr{T}^*\boldsymbol{p} &= \sum_{n\in\mathbb{Z}} (M^{(n)})^* \boldsymbol{p}^{(n)}(b) e^{\mathrm{i}\alpha_n x} \\ &= \sum_{n\in\mathbb{Z}} -\frac{\mathrm{i}}{\overline{\chi}_n} \begin{bmatrix} \omega^2\overline{\beta_1^{(n)}} & \omega^2\alpha_n - \mu\alpha_n\overline{\chi}_n \\ \mu\alpha_n\overline{\chi}_n - \omega^2\alpha_n & \omega^2\overline{\beta_2^{(n)}} \end{bmatrix} \boldsymbol{p}^{(n)}(b) e^{\mathrm{i}\alpha_n x} \\ &= \sum_{n\in\mathbb{Z}} -\frac{\mathrm{i}}{\overline{\chi}_n} \begin{bmatrix} \omega^2\overline{\beta_1^{(n)}} & \omega^2\alpha_n - \mu\alpha_n\overline{\chi}_n \\ \mu\alpha_n\overline{\chi}_n - \omega^2\alpha_n & \omega^2\overline{\beta_2^{(n)}} \end{bmatrix} \begin{bmatrix} \mathrm{i}\alpha_n & -\mathrm{i}\overline{\beta_2^{(n)}} \\ -\mathrm{i}\overline{\beta_1^{(n)}} & -\mathrm{i}\alpha_n \end{bmatrix} \begin{bmatrix} q_1^{(n)}(b) \\ q_2^{(n)}(b) \end{bmatrix} e^{\mathrm{i}\alpha_n x} \\ &= \sum_{n\in\mathbb{Z}} \begin{bmatrix} \mu\alpha_n\overline{\beta_1^{(n)}} & -\omega^2 + \mu\alpha_n^2 \\ \mu\alpha_n^2 - \omega^2 & -\mu\alpha_n\overline{\beta_2^{(n)}} \end{bmatrix} \begin{bmatrix} q_1^{(n)}(b) \\ q_2^{(n)}(b) \end{bmatrix} e^{\mathrm{i}\alpha_n x}, \end{aligned}$$

which shows $\mathscr{B}\boldsymbol{p} = \mathscr{T}^*\boldsymbol{p}$ and completes the proof. ■

It follows from the classic theory of second order differential equations that the solution of the system

$$\begin{cases} q_j^{(n)''}(y) - |\beta_j^{(n)}|^2 q_j^{(n)}(y) = -c_j \zeta_j^{(n)}(y), \\ q_j^{(n)}(b') = q_j^{(n)}(b'), \\ q_j^{(n)'}(b) = -|\beta_j^{(n)}| q_j^{(n)}(b) \end{cases}$$

is

$$q_j^{(n)}(y) = \frac{1}{2|\beta_j^{(n)}|} \Bigg\{ - c_j \int_b^y e^{|\beta_j^{(n)}|(y-s)} \zeta_j^{(n)}(s) \mathrm{d}s + c_j \int_{b'}^y e^{|\beta_j^{(n)}|(s-y)} \zeta_j^{(n)}(s) \mathrm{d}s$$
$$- c_j \int_{b'}^b e^{|\beta_j^{(n)}|(2b'-y-s)} \zeta_j^{(n)}(s) \mathrm{d}s + 2|\beta_j^{(n)}| e^{|\beta_j^{(n)}|(b'-y)} q_j^{(n)}(b') \Bigg\}. \quad (3.25)$$

Lemma 3.5.8 *Let $\boldsymbol{p} = (p_1, p_2)^\top$ be the solution of the dual problem problem* (3.20)*. For sufficiently large $|n|$, the following estimate hold*

$$\left| p_j^{(n)}(b) \right| \lesssim |n| e^{|\beta_2^{(n)}|(b'-b)} \left(|p_1^{(n)}(b')| + |p_2^{(n)}(b')| \right) + \frac{1}{|n|} \left(\|\xi_1^{(n)}\|_{L^\infty(b',b)} + \|\xi_2^{(n)}\|_{L^\infty(b',b)} \right),$$

where $p_j^{(n)}$ is the Fourier coefficient of $p_j, j = 1, 2$.

Proof Evaluating (3.25) at $y = b$ yields

$$q_j^{(n)}(b) = \frac{1}{2|\beta_j^{(n)}|} \Bigg\{ c_j \int_{b'}^b e^{|\beta_j^{(n)}|(s-b)} \zeta_j^{(n)}(s) \mathrm{d}s - c_j \int_{b'}^b e^{|\beta_j^{(n)}|(2b'-b-s)} \zeta_j^{(n)}(s) \mathrm{d}s$$
$$+ 2|\beta_j^{(n)}| e^{|\beta_j^{(n)}|(b'-b)} q_j^{(n)}(b') \Bigg\}. \quad (3.26)$$

Taking the derivative of $q_j^{(n)}$ with respect to y in (3.25) and then evaluating at $y = b'$, we have

$$q_j^{(n)'}(b') = c_j \int_{b'}^b e^{|\beta_j^{(n)}|(b'-s)} \zeta_j^{(n)}(s) \mathrm{d}s - |\beta_j^{(n)}| q_1^{(n)}(b'), \quad j = 1, 2,$$

which is equivalent to

$$\begin{bmatrix} q_1^{(n)'}(b') \\ q_2^{(n)'}(b') \end{bmatrix} = \begin{bmatrix} -|\beta_1^{(n)}| & 0 \\ 0 & -|\beta_2^{(n)}| \end{bmatrix} \begin{bmatrix} q_1^{(n)}(b') \\ q_2^{(n)}(b') \end{bmatrix} + \begin{bmatrix} \hat{\zeta}_1^{(n)} \\ \hat{\zeta}_2^{(n)} \end{bmatrix},$$

where

$$\hat{\zeta}_j^{(n)} = c_j \int_{b'}^{b} e^{|\beta_j^{(n)}|(b'-s)} \zeta_j^{(n)}(s)\mathrm{d}s.$$

It follows from Lemma 3.5.7 and the Helmholtz decomposition $\boldsymbol{p} = \nabla q_1 + \mathbf{curl} q_2$ that

$$\begin{bmatrix} p_1^{(n)}(b') \\ p_2^{(n)}(b') \end{bmatrix} = \begin{bmatrix} \mathrm{i}\alpha_n q_1^{(n)}(b') + q_2^{(n)'}(b') \\ q_1^{(n)'}(b') - \mathrm{i}\alpha_n q_2^{(n)}(b') \end{bmatrix} = \begin{bmatrix} \mathrm{i}\alpha_n & -|\beta_2^{(n)}| \\ -|\beta_1^{(n)}| & -\mathrm{i}\alpha_n \end{bmatrix} \begin{bmatrix} q_1^{(n)}(b') \\ q_2^{(n)}(b') \end{bmatrix} + \begin{bmatrix} \hat{\zeta}_2^{(n)} \\ \hat{\zeta}_1^{(n)} \end{bmatrix},$$

which gives

$$\begin{bmatrix} q_1^{(n)}(b') \\ q_2^{(n)}(b') \end{bmatrix} = \frac{1}{\chi_n} \begin{bmatrix} -\mathrm{i}\alpha_n & |\beta_2^{(n)}| \\ |\beta_1^{(n)}| & \mathrm{i}\alpha_n \end{bmatrix} \begin{bmatrix} p_1^{(n)}(b') \\ p_2^{(n)}(b') \end{bmatrix} - \frac{1}{\chi_n} \begin{bmatrix} -\mathrm{i}\alpha_n & |\beta_2^{(n)}| \\ |\beta_1^{(n)}| & \mathrm{i}\alpha_n \end{bmatrix} \begin{bmatrix} \hat{\zeta}_2^{(n)} \\ \hat{\zeta}_1^{(n)} \end{bmatrix}.$$

Substituting the boundary condition

$$\begin{bmatrix} q_1^{(n)'}(b) \\ q_2^{(n)'}(b) \end{bmatrix} = \begin{bmatrix} -|\beta_1^{(n)}| & 0 \\ 0 & -|\beta_2^{(n)}| \end{bmatrix} \begin{bmatrix} q_1^{(n)}(b) \\ q_2^{(n)}(b) \end{bmatrix}$$

into the Helmholtz decomposition $\boldsymbol{p} = \nabla q_1 + \mathbf{curl} q_2$, i.e.,

$$\begin{bmatrix} p_1^{(n)}(b) \\ p_2^{(n)}(b) \end{bmatrix} = \begin{bmatrix} \mathrm{i}\alpha_n q_1^{(n)}(b) + q_2^{(n)'}(b) \\ q_1^{(n)'}(b) - \mathrm{i}\alpha_n q_2^{(n)}(b) \end{bmatrix},$$

we obtain

$$\begin{bmatrix} p_1^{(n)}(b) \\ p_2^{(n)}(b) \end{bmatrix} = \begin{bmatrix} \mathrm{i}\alpha_n & -|\beta_2^{(n)}| \\ -|\beta_1^{(n)}| & -\mathrm{i}\alpha_n \end{bmatrix} \begin{bmatrix} q_1^{(n)}(b) \\ q_2^{(n)}(b) \end{bmatrix}.$$

By (3.26),

$$\begin{bmatrix} q_1^{(n)}(b) \\ q_2^{(n)}(b) \end{bmatrix} = \begin{bmatrix} e^{|\beta_1^{(n)}|(b'-b)} & 0 \\ 0 & e^{|\beta_2^{(n)}|(b'-b)} \end{bmatrix} \begin{bmatrix} q_1^{(n)}(b') \\ q_2^{(n)}(b') \end{bmatrix} + \begin{bmatrix} \eta_1^{(n)} \\ \eta_2^{(n)} \end{bmatrix},$$

where

$$\eta_j^{(n)} = \frac{c_j}{2|\beta_j^{(n)}|} \int_{b'}^{b} \left(e^{|\beta_j^{(n)}|(s-b)} - e^{|\beta_j^{(n)}|(2b'-b-s)} \right) \zeta_j^{(n)}(s)\mathrm{d}s.$$

Combining the above equations leads to

$$\begin{aligned}\begin{bmatrix} p_1^{(n)}(b) \\ p_2^{(n)}(b) \end{bmatrix} &= \begin{bmatrix} \mathrm{i}\alpha_n & -|\beta_2^{(n)}| \\ -|\beta_1^{(n)}| & -\mathrm{i}\alpha_n \end{bmatrix} \begin{bmatrix} e^{|\beta_1^{(n)}|(b'-b)} & 0 \\ 0 & e^{|\beta_2^{(n)}|(b'-b)} \end{bmatrix} \begin{bmatrix} q_1^{(n)}(b') \\ q_2^{(n)}(b') \end{bmatrix} \\ &\quad + \begin{bmatrix} \mathrm{i}\alpha_n & -|\beta_2^{(n)}| \\ -|\beta_1^{(n)}| & -\mathrm{i}\alpha_n \end{bmatrix} \begin{bmatrix} \eta_1^{(n)} \\ \eta_2^{(n)} \end{bmatrix} \\ &= P^{(n)} \begin{bmatrix} p_1^{(n)}(b') \\ p_2^{(n)}(b') \end{bmatrix} - P^{(n)} \begin{bmatrix} \hat{\zeta}_2^{(n)} \\ \hat{\zeta}_1^{(n)} \end{bmatrix} + \begin{bmatrix} \mathrm{i}\alpha_n & -|\beta_2^{(n)}| \\ -|\beta_1^{(n)}| & -\mathrm{i}\alpha_n \end{bmatrix} \begin{bmatrix} \eta_1^{(n)} \\ \eta_2^{(n)} \end{bmatrix},\end{aligned}$$

where $P^{(n)}$ is defined in (3.16).

Recall that

$$|\zeta_j^{(n)}(s)| \lesssim \frac{1}{|\alpha_n|}\left(\|\xi_1^{(n)}\|_{L^\infty(b',b)} + \|\xi_2^{(n)}\|_{L^\infty(b',b)}\right) e^{|\alpha_n|(b-s)}.$$

Since $s-b \geqslant 2b'-b-s$ and $|\alpha_n| \sim |n|, |\beta_j^{(n)}| \sim |n|$ for sufficiently large $|n|$, we have from (3.17) and the mean-value theorem that

$$\begin{aligned}|\eta_j^{(n)}| &\lesssim \left(\|\xi_1^{(n)}\|_{L^\infty(b',b)} + \|\xi_2^{(n)}\|_{L^\infty(b',b)}\right) \frac{1}{|\beta_j^{(n)}|} \left| \int_{b'}^{b} e^{|\beta_j^{(n)}|(s-b)} \frac{1}{|\alpha_n|} e^{|\alpha_n|(b-s)} \mathrm{d}s \right| \\ &= \left(\|\xi_1^{(n)}\|_{L^\infty(b',b)} + \|\xi_2^{(n)}\|_{L^\infty(b',b)}\right) \frac{1}{|\alpha_n||\beta_j^{(n)}|} \frac{-1}{|\alpha_n| - |\beta_j^{(n)}|} \left(1 - e^{\left(|\alpha_n| - |\beta_j^{(n)}|\right)(b-b')}\right) \\ &\lesssim \frac{1}{n^2}\left(\|\xi_1^{(n)}\|_{L^\infty(b',b)} + \|\xi_2^{(n)}\|_{L^\infty(b',b)}\right).\end{aligned}$$

Combining the above estimates yields

$$\left|\mathrm{i}\,\alpha_n \eta_1^{(n)} - |\beta_2^{(n)}|\eta_2^{(n)}\right|, \quad \left|-|\beta_1^{(n)}|\eta_1^{(n)} - \mathrm{i}\,\alpha_n \eta_2^{(n)}\right| \lesssim \frac{1}{|n|}\left(\|\xi_1^{(n)}\|_{L^\infty(b',b)} + \|\xi_2^{(n)}\|_{L^\infty(b',b)}\right).$$

Following the similar steps of the estimate for $\eta_j^{(n)}$, we can show that

$$\begin{aligned}|\hat{\zeta}_j^{(n)}| &\lesssim \left(\|\xi_1^{(n)}\|_{L^\infty(b',b)} + \|\xi_2^{(n)}\|_{L^\infty(b',b)}\right) \int_{b'}^{b} e^{|\beta_j^{(n)}|(b'-s)} e^{|\alpha_n|(b-s)} \frac{1}{|\alpha_n|} \mathrm{d}s \\ &\lesssim \frac{1}{|\alpha_n|(|\alpha_n| + |\beta_j^{(n)}|)} \left(\|\xi_1^{(n)}\|_{L^\infty(b',b)} + \|\xi_2^{(n)}\|_{L^\infty(b',b)}\right) \left| e^{|\beta_j^{(n)}|(b'-b)} - e^{|\alpha_n|(b-b')} \right| \\ &\lesssim \frac{1}{n^2}\left(\|\xi_1^{(n)}\|_{L^\infty(b',b)} + \|\xi_2^{(n)}\|_{L^\infty(b',b)}\right) e^{|\alpha_n|(b-b')},\end{aligned}$$

which gives

$$\begin{aligned}\left|P^{(n)}\begin{bmatrix}\hat{\zeta}_1^{(n)}\\ \hat{\zeta}_2^{(n)}\end{bmatrix}\right| &\lesssim |n|e^{-|\beta_2^{(n)}|(b-b')}\frac{1}{n^2}\left(\|\xi_1^{(n)}\|_{L^\infty(b',b)}+\|\xi_2^{(n)}\|_{L^\infty(b',b)}\right)e^{|\alpha_n|(b-b')}\\ &\lesssim \frac{1}{|n|}e^{\left(|\alpha_n|-|\beta_2^{(n)}|\right)(b-b')}\left(\|\xi_1^{(n)}\|_{L^\infty(b',b)}+\|\xi_2^{(n)}\|_{L^\infty(b',b)}\right).\end{aligned}$$

Since for sufficiently large $|n|$, we have

$$|\alpha_n|-|\beta_2^{(n)}| = |\alpha_n|-\left(\alpha_n^2-\kappa_2^2\right)^{1/2} = \frac{\kappa_2^2}{|\alpha_n|+\left(\alpha_n^2-\kappa_2^2\right)^{1/2}} \sim \frac{1}{|n|}.$$

Hence

$$\left|P^{(n)}\begin{bmatrix}\hat{\zeta}_1^{(n)}\\ \hat{\zeta}_2^{(n)}\end{bmatrix}\right| \lesssim \frac{1}{|n|}\left(\|\xi_1^{(n)}\|_{L^\infty(b',b)}+\|\xi_2^{(n)}\|_{L^\infty(b',b)}\right),$$

which proves

$$\left|p_j^{(n)}(b)\right| \lesssim |n|e^{|\beta_2^{(n)}|(b'-b)}\left(|p_1^{(n)}(b')|+|p_2^{(n)}(b')|\right)+\frac{1}{|n|}\left(\|\xi_1^{(n)}\|_{L^\infty(b',b)}+\|\xi_2^{(n)}\|_{L^\infty(b',b)}\right).$$

The proof is completed. ■

Taking $\boldsymbol{v}=\boldsymbol{\xi}$ in (3.20), we have

$$\|\boldsymbol{\xi}\|^2_{\boldsymbol{L}^2(\Omega)} = a(\boldsymbol{\xi},\boldsymbol{p})-\int_\Gamma(\mathscr{T}-\mathscr{T}_N)\,\boldsymbol{\xi}\cdot\overline{\boldsymbol{p}}\,\mathrm{d}s+\int_\Gamma(\mathscr{T}-\mathscr{T}_N)\,\boldsymbol{\xi}\cdot\overline{\boldsymbol{p}}\,\mathrm{d}s. \tag{3.27}$$

By Lemma 3.5.8, we obtain

$$\begin{aligned}&\left|\int_\Gamma(\mathscr{T}-\mathscr{T}_N)\,\boldsymbol{\xi}\cdot\overline{\boldsymbol{p}}\,\mathrm{d}s\right| \leqslant \Lambda\sum_{|n|>N}\left|\left(M^{(n)}\boldsymbol{\xi}_n(b)\right)\cdot\overline{\boldsymbol{p}}_n(b)\right|\\ &\lesssim \Lambda\sum_{|n|>N}|n|\left(|\xi_1^{(n)}(b)|+|\xi_2^{(n)}(b)|\right)\left(|p_1^{(n)}(b)|+|p_2^{(n)}(b)|\right)\\ &\lesssim N^{-1}\left[\sum_{|n|>N}(1+n^2)^{1/2}\left(|\xi_1^{(n)}(b)|+|\xi_2^{(n)}(b)|\right)^2\right]^{1/2}\left[\sum_{|n|>N}|n|^3\left(|p_1^{(n)}(b)|+|p_2^{(n)}(b)|\right)^2\right]^{1/2}\\ &\lesssim N^{-1}\|\boldsymbol{\xi}\|_{\boldsymbol{H}^{1/2}(\Gamma)}\left[\sum_{|n|>N}|n|^3\left(|p_1^{(n)}(b)|^2+|p_2^{(n)}(b)|^2\right)\right]^{1/2}\\ &\lesssim N^{-1}\|\boldsymbol{\xi}\|_{\boldsymbol{H}^{1}(\Omega)}\left[\sum_{|n|>N}|n|^3\left(|p_1^{(n)}(b)|^2+|p_2^{(n)}(b)|^2\right)\right]^{1/2}.\end{aligned} \tag{3.28}$$

Following the similar proof in [61, eq. (30)], we may show that

$$\|\xi_j^{(n)}\|^2_{L^\infty(b',b)} \leqslant \left(\frac{2}{\delta}+|n|\right)\|\xi_j^{(n)}(t)\|^2_{L^2(b',b)} + |n|^{-1}\|\xi_j^{(n)\prime}(t)\|^2_{L^2(b',b)}. \tag{3.29}$$

It follows from the Cauchy–Schwarz inequality that

$$\begin{aligned}
&\sum_{|n|>N}|n|^3\left(|p_1^{(n)}(b)|^2+|p_2^{(n)}(b)|^2\right)\\
&\lesssim \sum_{|n|>N}|n|^3\left\{n^2e^{2|\beta_2^{(n)}|(b'-b)}\left(|p_1^{(n)}(b')|^2+|p_2^{(n)}(b')|^2\right)+\frac{1}{|n|^2}\left(\|\xi_1^{(n)}\|^2_{L^\infty(b',b)}+\|\xi_2^{(n)}\|^2_{L^\infty(b',b)}\right)\right\}\\
&\lesssim \sum_{|n|>N}|n|^5e^{2|\beta_2^{(n)}|(b'-b)}\left(|p_1^{(n)}(b')|^2+|p_2^{(n)}(b')|^2\right)+\sum_{|n|>N}|n|\left(\|\xi_1^{(n)}\|^2_{L^\infty(b',b)}+\|\xi_2^{(n)}\|^2_{L^\infty(b',b)}\right)\\
&:= I_1+I_2.
\end{aligned}$$

Noting that the function t^4e^{-2t} is bounded on $(0,+\infty)$, we have

$$I_1 \lesssim \max_{|n|>N}\left(n^4e^{2|\beta_2^{(n)}|(b'-b)}\right)\sum_{|n|>N}|n|\left(|p_1^{(n)}(b')|^2+|p_2^{(n)}(b')|^2\right)\lesssim \|\boldsymbol{p}\|^2_{\boldsymbol{H}^{1/2}(\Gamma')}\lesssim\|\boldsymbol{\xi}\|^2_{\boldsymbol{H}^1(\Omega)}.$$

Substituting (3.29) into I_2, we get

$$\begin{aligned}
I_2 &\lesssim \sum_{|n|>N}\left[|n|\left(\frac{2}{\delta}+|n|\right)\left(\|\xi_1^{(n)}\|^2_{L^2(b',b)}+\|\xi_2^{(n)}\|^2_{L^2(b',b)}\right)+\left(\|\xi_1^{(n)\prime}\|^2_{L^2(b',b)}+\|\xi_2^{(n)\prime}\|^2_{L^2(b',b)}\right)\right]\\
&\leqslant \sum_{|n|>N}\left[\left(\frac{2}{\delta}|n|+n^2\right)\|\boldsymbol{\xi}_n\|^2_{\boldsymbol{L}^2(b',b)}+\|\boldsymbol{\xi}_n'\|^2_{\boldsymbol{L}^2(b',b)}\right].
\end{aligned}$$

A simple calculation yields

$$\|\xi_j^{(n)}\|^2_{H^1(\Omega')} = \Lambda\sum_{n\in\mathbb{Z}}\int_{b'}^{b}\left[\left(1+\alpha_n^2\right)|\xi_j^{(n)}(y)|^2+|\xi_j^{(n)\prime}(y)|^2\right]\mathrm{d}y.$$

It is easy to note that

$$\frac{2}{\delta}|n|+n^2\lesssim 1+\alpha_n^2.$$

Then

$$I_2\lesssim\|\boldsymbol{\xi}\|^2_{\boldsymbol{H}^1(\Omega')}\leqslant\|\boldsymbol{\xi}\|^2_{\boldsymbol{H}^1(\Omega)}.$$

Therefore,

$$\sum_{|n|>N}|n|^3\left(|p_1^{(n)}(b)|+|p_2^{(n)}(b)|\right)^2\lesssim\|\boldsymbol{\xi}\|^2_{\boldsymbol{H}^1(\Omega)}. \tag{3.30}$$

Plugging (3.30) to (3.28), we obtain

$$|\int_\Gamma (\mathscr{T}-\mathscr{T}_N)\,\boldsymbol{\xi}\cdot\overline{\boldsymbol{p}}\,\mathrm{d}s| \lesssim \frac{1}{N}\|\boldsymbol{\xi}\|^2_{\boldsymbol{H}^1(\Omega)}. \tag{3.31}$$

Now, we prove Theorem 3.5.1.

Proof By Lemma 3.5.3, Lemma 3.5.4, and Lemma 3.5.6, we have

$$\begin{aligned}
|||\boldsymbol{\xi}|||^2_{\boldsymbol{H}^1(\Omega)} &= \Re a(\boldsymbol{\xi},\boldsymbol{\xi}) + \Re\int_\Gamma (\mathscr{T}-\mathscr{T}_N)\,\boldsymbol{\xi}\cdot\overline{\boldsymbol{\xi}}\mathrm{d}s + 2\omega^2\int_\Omega \boldsymbol{\xi}\cdot\overline{\boldsymbol{\xi}}\mathrm{d}\boldsymbol{x} + \Re\int_\Gamma \mathscr{T}_N\boldsymbol{\xi}\cdot\overline{\boldsymbol{\xi}}\mathrm{d}s\\
&\leqslant C_1\left[\left(\sum_{T\in M_h}\eta_T^2\right)^{1/2} + \max_{|n|>N}\left(|n|e^{|\beta_2^{(n)}|(b'-b)}\right)\|\boldsymbol{u}^{\mathrm{inc}}\|_{\boldsymbol{H}^1(\Omega)}\right]\|\boldsymbol{\xi}\|_{\boldsymbol{H}^1(\Omega)}\\
&\quad + (C_2+C(\delta))\,\|\boldsymbol{\xi}\|^2_{\boldsymbol{L}^2(\Omega)} + \delta\|\boldsymbol{\xi}\|^2_{\boldsymbol{H}^1(\Omega)},
\end{aligned}$$

where $C_1, C_2, C(\delta)$ are positive constants. From (3.14), by choosing δ such that $\frac{\delta}{\min(\mu,\omega^2)} < \frac{1}{2}$, we get

$$\begin{aligned}
|||\boldsymbol{\xi}|||^2_{\boldsymbol{H}^1(\Omega)} \leqslant 2C_1&\left[\left(\sum_{T\in M_h}\eta_T^2\right)^{1/2} + \max_{|n|>N}\left(|n|e^{|\beta_2^{(n)}|(b'-b)}\right)\|\boldsymbol{u}^{\mathrm{inc}}\|_{\boldsymbol{H}^1(\Omega)}\right]\|\boldsymbol{\xi}\|_{\boldsymbol{H}^1(\Omega)}\\
&+2\,(C_2+C(\delta))\,\|\boldsymbol{\xi}\|^2_{\boldsymbol{L}^2(\Omega)}.
\end{aligned} \tag{3.32}$$

It follows from (3.27) and (3.31) that

$$\begin{aligned}
\|\boldsymbol{\xi}\|^2_{\boldsymbol{L}^2(\Omega)} &= b(\boldsymbol{\xi},\boldsymbol{p}) + \int_\Gamma (\mathscr{T}-\mathscr{T}_N)\,\boldsymbol{\xi}\cdot\overline{\boldsymbol{p}}\,\mathrm{d}s - \int_\Gamma (\mathscr{T}-\mathscr{T}_N)\,\boldsymbol{\xi}\cdot\overline{\boldsymbol{p}}\,\mathrm{d}s\\
&\lesssim \left[\left(\sum_{T\in M_h}\eta_T^2\right)^{1/2} + \max_{|n|>N}\left(|n|e^{|\beta_2^{(n)}|(b'-b)}\right)\|\boldsymbol{u}^{\mathrm{inc}}\|_{\boldsymbol{H}^1(\Omega)}\right]\|\boldsymbol{\xi}\|_{\boldsymbol{H}^1(\Omega)} + N^{-1}\|\boldsymbol{\xi}\|^2_{\boldsymbol{H}^1(\Omega)}
\end{aligned} \tag{3.33}$$

Taking sufficiently large N such that $\frac{2(C_2+C(\delta))}{N}\frac{1}{\min(\mu,\omega^2)} < 1$ and substituting (3.33) into (3.32), we obtain

$$|||\boldsymbol{u}-\boldsymbol{u}_N^h|||_{\boldsymbol{H}^1(\Omega)} \lesssim \left(\sum_{T\in M_h}\eta_T^2\right)^{1/2} + \max_{|n|>N}\left(|n|e^{|\beta_2^{(n)}|(b'-b)}\right)\|\boldsymbol{u}^{\mathrm{inc}}\|_{\boldsymbol{H}^1(\Omega)}.$$

The proof is completed by noting the equivalence of the norms $|||\cdot|||_{\boldsymbol{H}^1(\Omega)}$ and $\|\cdot\|_{\boldsymbol{H}^1(\Omega)}$.

■

3.6 Numerical Experiments

In this section, we introduce the algorithmic implementation of the adaptive finite element DtN method and present two numerical examples to demonstrate the effectiveness of the proposed method.

3.6.1 Adaptive Algorithm

Our implementation is based on the FreeFem [50]. The first-order linear element is used to solve the problem. It is shown in Theorem 3.5.1 that the a posteriori error consists of two parts: the finite element discretization error ϵ_h and the DtN operator truncation error ϵ_N, where

$$\epsilon_h = \left(\sum_{K \in \mathcal{M}_h} \eta_K^2 \right)^{1/2}, \quad \epsilon_N = \max_{|n|>N} \left(|n| e^{-|\beta_2^{(n)}|(b-b')} \right) \|\boldsymbol{u}^{\text{inc}}\|_{\boldsymbol{H}^1(\Omega)}. \tag{3.34}$$

In the implementation, we choose the parameters b, b' and N based on (3.34) to make sure that the DtN operator truncation error is smaller than the finite element discretization error. In the following numerical experiments, b' is chosen such that $b' = \max_{x \in (0,\Lambda)} f(x)$ and N is the smallest positive integer that makes $\epsilon_N \leqslant 10^{-8}$. The adaptive finite element algorithm is shown in Table 1.

3.6.2 Numerical Experiments

We report two examples to illustrate the numerical performance of the proposed method. The first example concerns the scattering by a flat surface and has an exact solution; the second example is constructed such that the solution has corner singularity.

Example 1. We consider the simplest periodic structure, a straight line, where the exact solution is available. Let $S = \{y = 0\}$ and take the artificial boundary $\Gamma = \{y = 0.25\}$. The space above the flat surface is filled with a homogenenous and isotropic elastic medium, which is characterized by the Lamé constants $\lambda = 2$,

Table 3.1.
The adaptive finite element DtN method.

---

1. Given the tolerance $\epsilon > 0$ and the parameter $\tau \in (0, 1)$.

2. Fix the computational domain Ω by choosing b.

3. Choose b' and N such that $\epsilon_N \leqslant 10^{-8}$.

4. Construct an initial triangulation $\mathcal{M}_h$ over Ω and compute error estimators.

5. While $\epsilon_h > \epsilon$ do

6. refine mesh $\mathcal{M}_h$ according to the strategy that

$$\text{if } \eta_{\hat{K}} > \tau \max_{K \in \mathcal{M}_h} \eta_K, \text{ refine the element } \hat{K} \in \mathcal{M}_h,$$

7. denote refined mesh still by $\mathcal{M}_h$, solve the discrete problem (3.13) on the new mesh $\mathcal{M}_h$,

8. compute the corresponding error estimators.

9. End while.

$\mu = 1$. The rigid surface is impinged by the compressional plane wave $\boldsymbol{u}^{\text{inc}} = \boldsymbol{d}e^{\mathrm{i}\kappa_1 \boldsymbol{x}\cdot\boldsymbol{d}}$, where the incident angle is $\theta = \pi/3$. The compressional and shear wavenumbers are $\kappa_1 = \omega/2$ and $\kappa_2 = \omega$, respectively, where ω is the angular frequency. It can be verified that the exact solution is

$$u(\boldsymbol{x}) = \frac{1}{\kappa_1}\begin{bmatrix}\alpha\\ -\beta\end{bmatrix} e^{\mathrm{i}(\alpha x - \beta y)} - \frac{1}{\kappa_1}\left(\frac{\alpha^2 - \beta\gamma}{\alpha^2 + \beta\gamma}\right)\begin{bmatrix}\alpha\\ \beta\end{bmatrix} e^{\mathrm{i}(\alpha x + \beta y)} - \frac{1}{\kappa_1}\left(\frac{2\alpha\beta}{\alpha^2 + \beta\gamma}\right)\begin{bmatrix}\gamma\\ -\alpha\end{bmatrix} e^{\mathrm{i}(\alpha x + \gamma y)},$$

where $\alpha = \kappa_1 \sin\theta, \beta = \kappa_1 \cos\theta, \gamma = (\kappa_2^2 - \alpha^2)^{1/2}$. The period $\Lambda = 0.5$. Figure 3.2 shows the curves of $\log e_h$ versus $\log \mathrm{DoF}_h$ with different angular frequencies, where $e_h = \|\boldsymbol{u} - \boldsymbol{u}_N^h\|_{\boldsymbol{H}^1(\Omega)}$ is the a priori error and DoF_h stands for the degree of freedom or

the number of nodal points. It indicates that the meshes and the associated numerical complexity are quasi-optimal, i.e., $e_h = \mathcal{O}(\mathrm{DoF}_h^{-1/2})$ holds asymptotically.

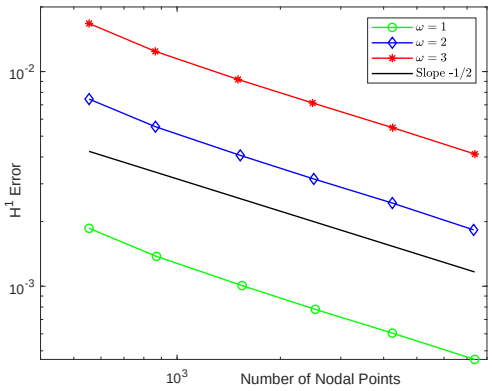

Figure 3.2. Quasi-optimality of the a priori error estimates for Example 1.

Example 2. This example concerns the scattering of the compressional plane wave by a piecewise linear surface, which has multiple sharp angles. The incident wave $\boldsymbol{u}^{\mathrm{inc}}$ and the parameters are chosen the same as Example 1, i.e., $b = 0.25, \Lambda = 0.5, \theta = \pi/3, \lambda = 1, \mu = 2$. Clearly, the solution has singularity around the corners of the surface. Since there is no exact solution for this example, we plot in Figure 3.3 the curves of $\log \epsilon_h$ versus $\log \mathrm{DoF}_h$ at different angular frequencies, where ϵ_h is the a posteriori error. Again, it indicates that the meshes and the associated numerical complexity are quasi-optimal, i.e., $\epsilon_h = \mathcal{O}(\mathrm{DoF}_h^{-1/2})$. Figure 3.4 plots the contour of the magnitude of the numerical solution and its corresponding mesh at the angular frequency $\omega = 2$. It is clear to note that the algorithm does capture the solution feature and adaptively refines the mesh around the corners where solution displays singularity.

3.7 Conclusion

In this chapter, we have presented an adaptive finite element DtN method for the elastic scattering problem in periodic structures. Based on the Helmholtz decomposi-

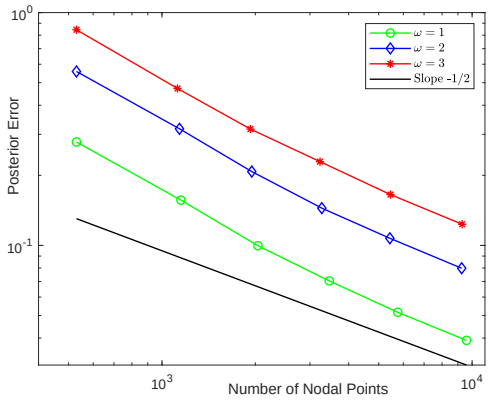

Figure 3.3. Quasi-optimality of the a posteriori error estimates for Example 2.

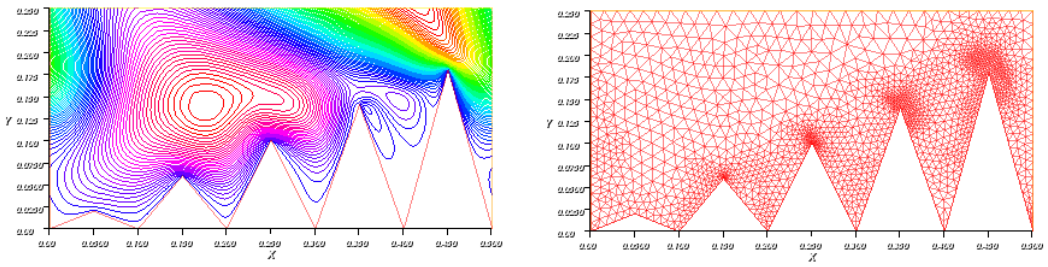

Figure 3.4. The numerical solution of Example 2. (left) The contour plot of the magnitude of the solution; (right) The corresponding adaptively refined mesh.

tion, a new duality argument is developed to obtain the a posteriori error estimate. It contains both the finite element discretization error and the DtN operator truncation error, which is shown to decay exponentially with respect to the truncation parameter. Numerical results show that the proposed method is effective and accurate. This work provides a viable alternative to the adaptive finite element PML method for solving the elastic surface scattering problem. It also enriches the range of choices available for solving wave propagation problems imposed in unbounded domains. One possible future work is to extend our analysis to the adaptive finite element DtN method for solving the three-dimensional elastic surface scattering problem, where a more complicated TBC needs to be considered.

4. THE INVERSE ELASTIC OBSTACLE SCATTERING PROBLEM

4.1 Introduction

In this chapter, we consider the direct and inverse obstacle scattering problems for elastic waves in three dimensions. The goal is fourfold: (1) develop a transparent boundary condition to reduce the scattering problem into a boundary value problem; (2) establish the well-posedness of the solution for the direct problem by studying its variational formulation; (3) characterize the domain derivative of the wave field with respect to the variation of the obstacle's surface; (4) propose a frequency continuation method to reconstruct the obstacle's surface. This chapter significantly extends the two-dimensional work [75]. We need to consider more complicated Maxwell's equation and associated spherical harmonics when studying the transparent boundary condition (TBC). Computationally, it is also more intensive.

The obstacle is assumed to be embedded in an open space filled with a homogeneous and isotropic elastic medium. The scattering problem is reduced into a boundary value problem by introducing a transparent boundary condition on a sphere enclosing the obstacle. The non-reflecting boundary conditions can also be found in [45, 46] for the two- and three-dimensional elastic wave equation. We show that the direct problem has a unique weak solution by examining its variational formulation. The proofs are based on asymptotic analysis of the boundary operators, the Helmholtz decomposition, and the Fredholm alternative theorem.

The calculation of domain derivatives, which characterize the variation of the wave field with respect to the perturbation of the boundary of an medium, is an essential step for inverse scattering problems. The domain derivatives have been discussed by many authors for the inverse acoustic and electromagnetic obstacle scattering

problems [47, 64, 87]. Recently, the domain derivative is studied in [68] for the elastic wave by using boundary integral equations. Here we present a variational approach to show that it is the unique weak solution of some boundary value problem. We propose a frequency continuation method to solve the inverse problem. The method requires multi-frequency data and proceed with respect to the frequency. At each frequency, we apply the descent method with the starting point given by the output from the previous step, and create an approximation to the surface filtered at a higher frequency. Numerical experiments are presented to demonstrate the effectiveness of the proposed method. A topic review can be found in [15] for solving inverse scattering problems with multi-frequencies to increase the resolution and stability of reconstructions.

The chapter is organized as follows. Section 2 introduces the formulation of the obstacle scattering problem for elastic waves. The direct problem is discussed in section 3 where well-posedness of the solution is established. Section 4 is devoted to the inverse problem. The domain derivative is studied and a frequency continuation method is introduced for the inverse problem. Numerical experiments are presented in section 5. The chapter is concluded in section 6. To avoid distraction from the main results, we collect in the appendices some necessary notation and useful results on the spherical harmonics, functional spaces, and transparent boundary conditions.

4.2 Problem Formulation

Consider a three-dimensional elastically rigid obstacle D with a Lipschitz continuous boundary ∂D. Denote by $\boldsymbol{\nu} = (\nu_1, \nu_2, \nu_3)$ the unit normal vector on ∂D pointing towards the exterior of D. We assume that the open exterior domain $\mathbb{R}^3 \backslash \bar{D}$ is filled with a homogeneous and isotropic elastic medium with a unit mass density. Let $B_R = \{\boldsymbol{x} \in \mathbb{R}^3 : |\boldsymbol{x}| < R\}$ be a ball with radius $R > 0$ such that $\bar{D} \subset B_R$. Denote by $\Gamma_R = \{\boldsymbol{x} \in \mathbb{R}^3 : |\boldsymbol{x}| = R\}$ boundary of B_R. Let $\Omega = B_R \backslash \bar{D}$ be the bounded domain which is enclosed by ∂D and Γ_R.

Let the obstacle be illuminated by a time-harmonic plane wave

$$\boldsymbol{u}^{\rm inc} = \boldsymbol{d} e^{{\rm i}\kappa_{\rm p}\boldsymbol{x}\cdot\boldsymbol{d}} \quad \text{or} \quad \boldsymbol{u}^{\rm inc} = \boldsymbol{d}^{\perp} e^{{\rm i}\kappa_{\rm s}\boldsymbol{x}\cdot\boldsymbol{d}}, \tag{4.1}$$

where $\boldsymbol{d}$ is the unit incident direction vector and $\boldsymbol{d}^{\perp}$ is the unit polarization vector satisfying $\boldsymbol{d}\cdot\boldsymbol{d}^{\perp}$=0. In (4.1), the former is called the compressional plane wave while the latter is called the shear plane wave. Here

$$\kappa_{\rm p} = \frac{\omega}{(\lambda+2\mu)^{1/2}} \quad \text{and} \quad \kappa_{\rm s} = \frac{\omega}{\mu^{1/2}} \tag{4.2}$$

are known the compressional wavenumber and the shear wavenumber, respectively, where $\omega > 0$ is the angular frequency, μ and λ are the Lamé parameters satisfying $\mu > 0$ and $\lambda + \mu > 0$. It is easy to verify that both the compressional plane wave and the shear plane wave in (4.1) satisfy the three-dimensional Navier equation:

$$\mu\Delta\boldsymbol{u}^{\rm inc} + (\lambda+\mu)\nabla\nabla\cdot\boldsymbol{u}^{\rm inc} + \omega^2\boldsymbol{u}^{\rm inc} = 0 \quad \text{in } \mathbb{R}^3\backslash\bar{D}. \tag{4.3}$$

The displacement of the total wave field $\boldsymbol{u}$ also satisfies

$$\mu\Delta\boldsymbol{u} + (\lambda+\mu)\nabla\nabla\cdot\boldsymbol{u} + \omega^2\boldsymbol{u} = 0 \quad \text{in } \mathbb{R}^3\backslash\bar{D}. \tag{4.4}$$

Since the obstacle is elastically rigid, the total wave field vanishes on ∂D:

$$\boldsymbol{u} = 0 \quad \text{on } \partial D. \tag{4.5}$$

The total wave field $\boldsymbol{u}$ can be decomposed into the incident wave $\boldsymbol{u}^{\rm inc}$ and the scattered wave $\boldsymbol{v}$:

$$\boldsymbol{u} = \boldsymbol{u}^{\rm inc} + \boldsymbol{v}.$$

Subtracting (4.3) from (4.4) yields the Navier equation for the scattered wave $\boldsymbol{v}$:

$$\mu\Delta\boldsymbol{v} + (\lambda+\mu)\nabla\nabla\cdot\boldsymbol{v} + \omega^2\boldsymbol{v} = 0 \quad \text{in } \mathbb{R}^3\backslash\bar{D}. \tag{4.6}$$

An appropriate radiation condition is needed for the exterior scattering problem. For any solution $\boldsymbol{v}$ of (4.6), we introduce the Helmholtz decomposition:

$$\boldsymbol{v} = \nabla\phi + \nabla\times\boldsymbol{\psi}, \quad \nabla\cdot\boldsymbol{\psi} = 0, \tag{4.7}$$

where ϕ and $\boldsymbol{\psi}$ is called the scalar potential function and the vector potential function, respectively. Substituting (4.7) into (4.6) yields

$$\nabla\left[(\lambda+2\mu)\Delta\phi+\omega^2\phi\right]+\nabla\times(\mu\Delta\boldsymbol{\psi}+\omega^2\boldsymbol{\psi})=0,$$

which is fulfilled if ϕ and $\boldsymbol{\psi}$ satisfy the Helmholtz equation:

$$\Delta\phi+\kappa_{\mathrm{p}}^2\phi=0,\quad \Delta\boldsymbol{\psi}+\kappa_{\mathrm{s}}^2\boldsymbol{\psi}=0. \tag{4.8}$$

where κ_{p} and κ_{s} are defined in (4.2). Hence, we request that ϕ and $\boldsymbol{\psi}$ satisfy the Sommerfeld radiation condition:

$$\lim_{r\to\infty} r\left(\partial_r\phi-\mathrm{i}\kappa_{\mathrm{p}}\phi\right)=0,\quad \lim_{r\to\infty} r\left(\partial_r\boldsymbol{\psi}-\mathrm{i}\kappa_{\mathrm{s}}\boldsymbol{\psi}\right)=0,\quad r=|\boldsymbol{x}|. \tag{4.9}$$

Using the identity

$$\nabla\times(\nabla\times\boldsymbol{\psi})=-\Delta\boldsymbol{\psi}+\nabla(\nabla\cdot\boldsymbol{\psi}),$$

we have from the Helmholtz equation (4.8) that $\boldsymbol{\psi}$ satisfies the Maxwell system:

$$\nabla\times(\nabla\times\boldsymbol{\psi})-\kappa_{\mathrm{s}}^2\boldsymbol{\psi}=0. \tag{4.10}$$

As is known, the Silver–Müller radition condition is commonly imposed as an appropriate radiation condition for Maxwell's equations. It is shown (cf. [38, Theorem 6.8]) that the Sommerfeld radiation for $\boldsymbol{\psi}$ in (4.9) is equivalent to the Silver–Müller radiation condition:

$$\lim_{r\to\infty}\left((\nabla\times\boldsymbol{\psi})\times\boldsymbol{x}-\mathrm{i}\kappa_{\mathrm{s}}r\boldsymbol{\psi}\right)=0,\quad r=|\boldsymbol{x}|. \tag{4.11}$$

Given the incident field $\boldsymbol{u}^{\mathrm{inc}}$, the direct problem is to determine the displacement of the total field $\boldsymbol{u}$ for the known obstacle D; the inverse problem is to determine the obstacle's surface ∂D from the boundary measurement of the displacement $\boldsymbol{u}$ on Γ_R. The purpose of this chapter is to study the well-posedness of the direct problem and develop a continuation method for the inverse problem. Hereafter, we take the notation of $a\lesssim b$ or $a\gtrsim b$ to stand for $a\leqslant Cb$ or $a\geqslant Cb$, where C is a positive constant. Some commonly used functional spaces, such as $\boldsymbol{H}^1_{\partial D}(\Omega)$, $\boldsymbol{H}^s(\Gamma_R)$, and $\boldsymbol{H}(\mathrm{curl},\Omega)$, are list in appendix 4.7.2.

4.3 Direct Scattering Problem

In this section, we study the variational formulation for the direct problem and show that it admits a unique weak solution.

4.3.1 Transparent Boundary Condition

We derive a transparent boundary condition on Γ_R to reformulate the problem from the open domain $\mathbb{R}^3\backslash\bar{D}$ into the bounded domain Ω.

Given $\boldsymbol{v} \in \boldsymbol{L}^2(\Gamma_R)$, it follows from Appendix 4.7.1 that $\boldsymbol{v}$ has the Fourier expansion

$$\boldsymbol{v}(R,\theta,\varphi) = \sum_{n=0}^{\infty}\sum_{m=-n}^{n} v_{1n}^m \boldsymbol{T}_n^m(\theta,\varphi) + v_{2n}^m \boldsymbol{V}_n^m(\theta,\varphi) + v_{3n}^m \boldsymbol{W}_n^m(\theta,\varphi),$$

where the Fourier coefficients

$$\begin{aligned} v_{1n}^m &= \int_{\Gamma_R} \boldsymbol{v}(R,\theta,\varphi)\cdot\bar{\boldsymbol{T}}_n^m(\theta,\varphi)\mathrm{d}\gamma, \\ v_{2n}^m &= \int_{\Gamma_R} \boldsymbol{v}(R,\theta,\varphi)\cdot\bar{\boldsymbol{V}}_n^m(\theta,\varphi)\mathrm{d}\gamma, \\ v_{3n}^m &= \int_{\Gamma_R} \boldsymbol{v}(R,\theta,\varphi)\cdot\bar{\boldsymbol{W}}_n^m(\theta,\varphi)\mathrm{d}\gamma. \end{aligned}$$

Define a boundary operator

$$\mathscr{B}\boldsymbol{v} = \mu\partial_r\boldsymbol{v} + (\lambda+\mu)(\nabla\cdot\boldsymbol{v})\boldsymbol{e}_r \quad \text{on } \Gamma_R, \tag{4.12}$$

which is assumed to have the Fourier expansion:

$$(\mathscr{B}\boldsymbol{v})(R,\theta,\varphi) = \sum_{n=0}^{\infty}\sum_{m=-n}^{n} w_{1n}^m \boldsymbol{T}_n^m(\theta,\varphi) + w_{2n}^m \boldsymbol{V}_n^m(\theta,\varphi) + w_{3n}^m \boldsymbol{W}_n^m(\theta,\varphi). \tag{4.13}$$

Taking ∂_r of $\boldsymbol{v}$ in (4.60), evaluating it at $r = R$, and using the spherical Bessel differential equations [95], we get

$$\begin{aligned} \partial_r\boldsymbol{v}(R,\theta,\varphi) = \sum_{n=0}^{\infty}\sum_{m=-n}^{n} \Bigg[&\frac{\sqrt{n(n+1)}\phi_n^m}{R^2}(z_n(\kappa_{\mathrm{p}}R)-1) - \frac{\psi_{2n}^m}{R^2}\Big(1 + z_n(\kappa_{\mathrm{s}}R) \\ &+ (R\kappa_{\mathrm{s}})^2 - n(n+1)\Big)\Bigg]\boldsymbol{T}_n^m + \left[\frac{\kappa_{\mathrm{s}}^2\psi_{3n}^m}{\sqrt{n(n+1)}}z_n(\kappa_{\mathrm{s}}R)\right]\boldsymbol{V}_n^m + \Bigg[\frac{\phi_n^m}{R^2}\big(n(n+1) \\ &- (R\kappa_{\mathrm{p}})^2 - 2z_n(\kappa_{\mathrm{p}}R)\big) + \frac{\sqrt{n(n+1)}\psi_{2n}^m}{R^2}(z_n(\kappa_{\mathrm{s}}R)-1)\Bigg]\boldsymbol{W}_n^m, \end{aligned} \tag{4.14}$$

where $z_n(t) = th_n^{(1)'}(t)/h_n^{(1)}(t), h_n^{(1)}$ is the spherical Hankel function of the first kind with order n, ϕ_n^m and ψ_{jn}^m are the Fourier coefficients for ϕ and $\boldsymbol{\psi}$ on Γ_R, respectively.

Noting (4.60) and using $\nabla \cdot \boldsymbol{v} = \Delta\phi = \frac{2}{r}\partial_r\phi + \partial_r^2\phi + \frac{1}{r}\Delta_{\Gamma_R}\phi$, we have

$$\nabla \cdot \boldsymbol{v}(r,\theta,\varphi) = \sum_{n=0}^{\infty}\sum_{m=-n}^{n} \frac{\phi_n^m}{h_n^{(1)}(\kappa_{\mathrm{p}}R)}\bigg[\frac{2}{r}\frac{\mathrm{d}}{\mathrm{d}r}h_n^{(1)}(\kappa_{\mathrm{p}}r) + \frac{\mathrm{d}^2}{\mathrm{d}r^2}h_n^{(1)}(\kappa_{\mathrm{p}}r) - \frac{n(n+1)}{r^2}h_n^{(1)}(\kappa_{\mathrm{p}}r)\bigg]X_n^m, \tag{4.15}$$

where Δ_{Γ_R} is the Laplace–Beltrami operator on Γ_R.

Combining (4.12) and (4.14)–(4.15), we obtain

$$\begin{aligned}\mathscr{B}\boldsymbol{v} = \sum_{n=0}^{\infty}\sum_{m=-n}^{n} \frac{\mu}{R^2}\Big[&\sqrt{n(n+1)}(z_n(\kappa_{\mathrm{p}}R)-1)\phi_n^m - \big(1 + z_n(\kappa_{\mathrm{s}}R) + (R\kappa_{\mathrm{s}})^2 \\ &- n(n+1)\big)\psi_{2n}^m\Big]\boldsymbol{T}_n^m + \frac{\mu\kappa_{\mathrm{s}}^2}{\sqrt{n(n+1)}}z_n(\kappa_{\mathrm{s}}R)\psi_{3n}^m\boldsymbol{V}_n^m + \frac{1}{R^2}\Big[\mu\big(n(n+1) - (R\kappa_{\mathrm{p}})^2 \\ &- 2z_n(\kappa_{\mathrm{p}}R)\big)\phi_n^m + \mu\sqrt{n(n+1)}(z_n(\kappa_{\mathrm{s}}R)-1)\psi_{2n}^m - (\lambda+\mu)(\kappa_{\mathrm{p}}R)^2\phi_n^m\Big]\boldsymbol{W}_n^m. \end{aligned}\tag{4.16}$$

Comparing (4.13) with (4.16), we have

$$(w_{1n}^m, w_{2n}^m, w_{3n}^m)^\top = \frac{1}{R^2}G_n(\phi_n^m, \psi_{2n}^m, \psi_{3n}^m)^\top, \tag{4.17}$$

where the matrix

$$G_n = \begin{bmatrix} 0 & 0 & G_{13}^{(n)} \\ G_{21}^{(n)} & G_{22}^{(n)} & 0 \\ G_{31}^{(n)} & G_{32}^{(n)} & 0 \end{bmatrix}.$$

Here

$$\begin{aligned} G_{13}^{(n)} &= \frac{\mu(\kappa_{\mathrm{s}}R)^2 z_n(\kappa_{\mathrm{s}}R)}{\sqrt{n(n+1)}}, \quad G_{21}^{(n)} = \mu\sqrt{n(n+1)}(z_n(\kappa_{\mathrm{p}}R)-1), \\ G_{22}^{(n)} &= \mu\left(n(n+1) - (\kappa_{\mathrm{s}}R)^2 - 1 - z_n(\kappa_{\mathrm{s}}R)\right), \\ G_{31}^{(n)} &= \mu\left(n(n+1) - (\kappa_{\mathrm{p}}R)^2 - 2z_n(\kappa_{\mathrm{p}}R)\right) - (\lambda+\mu)(\kappa_{\mathrm{p}}R)^2, \\ G_{32}^{(n)} &= \mu\sqrt{n(n+1)}(z_n(\kappa_{\mathrm{s}}R)-1). \end{aligned}$$

Let $\boldsymbol{v}_n^m = (v_{1n}^m, v_{2n}^m, v_{3n}^m)^\top$, $\quad M_n \boldsymbol{v}_n^m = \boldsymbol{b}_n^m = (b_{1n}^m, b_{2n}^m, b_{3n}^m)^\top$, where the matrix

$$M_n = \begin{bmatrix} M_{11}^{(n)} & 0 & 0 \\ 0 & M_{22}^{(n)} & M_{23}^{(n)} \\ 0 & M_{32}^{(n)} & M_{33}^{(n)} \end{bmatrix}.$$

Here

$$M_{11}^{(n)} = \left(\frac{\mu}{R}\right) z_n(\kappa_{\rm s} R), \quad M_{22}^{(n)} = -\left(\frac{\mu}{R}\right)\left(1 + \frac{(\kappa_{\rm s}R)^2 z_n(\kappa_{\rm p}R)}{\Lambda_n}\right),$$

$$M_{23}^{(n)} = \sqrt{n(n+1)}\left(\frac{\mu}{R}\right)\left(1 + \frac{(\kappa_{\rm s}R)^2}{\Lambda_n}\right),$$

$$M_{32}^{(n)} = \sqrt{n(n+1)}\left(\frac{\mu}{R} + \frac{(\lambda+2\mu)}{R}\frac{(\kappa_{\rm p}R)^2}{\Lambda_n}\right),$$

$$M_{33}^{(n)} = -\frac{(\lambda+2\mu)}{R}\frac{(\kappa_{\rm p}R)^2}{\Lambda_n}(1 + z_n(\kappa_{\rm s}R)) - 2\left(\frac{\mu}{R}\right),$$

where $\Lambda_n = z_n(\kappa_{\rm p}R)(1 + z_n(\kappa_{\rm s}R)) - n(n+1)$.

Using the above notation and combining (4.17) and (4.64), we derive the transparent boundary condition:

$$\mathscr{B}\boldsymbol{v} = \mathscr{T}\boldsymbol{v} := \sum_{n=0}^{\infty}\sum_{m=-n}^{n} b_{1n}^m \boldsymbol{T}_n^m + b_{2n}^m \boldsymbol{V}_n^m + b_{3n}^m \boldsymbol{W}_n^m \quad \text{on } \Gamma_R. \tag{4.18}$$

Lemma 4.3.1 *The matrix $\hat{M}_n = -\frac{1}{2}(M_n + M_n^*)$ is positive definite for sufficiently large n.*

Proof Using the asymptotic expansions of the spherical Bessel functions [95], we may verify that

$$z_n(t) = -(n+1) + \frac{1}{16n}t^4 + \frac{1}{2n}t^2 + O\left(\frac{1}{n^2}\right),$$

$$\Lambda_n(t) = -\frac{1}{16}(\kappa_{\rm p}t)^4 - \frac{1}{16}(\kappa_{\rm s}t)^4 - \frac{1}{2}(\kappa_{\rm p}t)^2 - \frac{1}{2}(\kappa_{\rm s}t)^2 + O\left(\frac{1}{n}\right).$$

It follows from straightforward calculations that

$$\hat{M}_n = \begin{bmatrix} \hat{M}_{11}^{(n)} & 0 & 0 \\ 0 & \hat{M}_{22}^{(n)} & \hat{M}_{23}^{(n)} \\ 0 & \hat{M}_{32}^{(n)} & \hat{M}_{33}^{(n)} \end{bmatrix},$$

where

$$\hat{M}_{11}^{(n)} = \left(\frac{\mu}{R}\right)(n+1) + O\left(\frac{1}{n}\right), \quad \hat{M}_{22}^{(n)} = -\left(\frac{\omega^2 R}{\Lambda_n}\right)(n+1) + O(1),$$
$$\hat{M}_{23}^{(n)} = -\left(\frac{\mu}{R} + \frac{\omega^2 R}{\Lambda_n}\right)\sqrt{n(n+1)} + O(1),$$
$$\hat{M}_{32}^{(n)} = -\left(\frac{\mu}{R} + \frac{\omega^2 R}{\Lambda_n}\right)\sqrt{n(n+1)} + O(1),$$
$$\hat{M}_{33}^{(n)} = \frac{2\mu}{R} + \frac{\omega^2 R}{\Lambda_n}(1 + z_n(\kappa_s R)) = -\left(\frac{\omega^2 R}{\Lambda_n}\right)n + O(1).$$

For sufficiently large n, we have

$$\hat{M}_{11}^{(n)} > 0 \quad \text{and} \quad \hat{M}_{22}^{(n)} > 0,$$

which gives

$$\det[(\hat{M}_n)_{(1:2,1:2)}] = \hat{M}_{11}^{(n)}\hat{M}_{22}^{(n)} > 0.$$

Since $\Lambda_n < 0$ for sufficiently large n, we have

$$\hat{M}_{22}^{(n)}\hat{M}_{33}^{(n)} - \left(\hat{M}_{23}^{(n)}\right)^2 = n(n+1)\left[\left(\frac{\omega^2 R}{\Lambda_n}\right)^2 - \left(\frac{\mu}{R} + \frac{\omega^2 R}{\Lambda_n}\right)^2\right] + O(n) > 0.$$

A simple calculation yields

$$\det[\hat{M}_n] = \hat{M}_{11}^{(n)}\left(\hat{M}_{22}^{(n)}\hat{M}_{33}^{(n)} - \left(\hat{M}_{23}^{(n)}\right)^2\right) > 0,$$

which completes the proof by applying Sylvester's criterion. ■

Lemma 4.3.2 *The boundary operator* $\mathscr{T} : \boldsymbol{H}^{1/2}(\Gamma_R) \to \boldsymbol{H}^{-1/2}(\Gamma_R)$ *is continuous, i.e.,*

$$\|\mathscr{T}\boldsymbol{u}\|_{\boldsymbol{H}^{-1/2}(\Gamma_R)} \lesssim \|\boldsymbol{u}\|_{\boldsymbol{H}^{1/2}(\Gamma_R)}, \quad \forall\, \boldsymbol{u} \in \boldsymbol{H}^{1/2}(\Gamma_R).$$

Proof For any given $\boldsymbol{u} \in \boldsymbol{H}^{1/2}(\Gamma_R)$, it has the Fourier expansion

$$\boldsymbol{u}(R,\theta,\varphi) = \sum_{n=0}^{\infty}\sum_{m=-n}^{n} u_{1n}^m \boldsymbol{T}_n^m(\theta,\varphi) + u_{2n}^m \boldsymbol{V}_n^m(\theta,\varphi) + u_{3n}^m \boldsymbol{W}_n^m(\theta,\varphi).$$

Let $\boldsymbol{u}_n^m = (u_{1n}^m, u_{2n}^m, u_{3n}^m)^\top$. It is easy to verify from the definition of M_n and the asymptotic expansion of $z_n(t)$ that

$$|M_{i,j}^{(n)}| \lesssim (1 + n(n+1))^{1/2}.$$

Hence we have

$$\begin{aligned}\|\mathscr{T}\boldsymbol{u}\|^2_{\boldsymbol{H}^{1/2}(\Gamma_R)} &= \sum_{n=0}^{\infty}\sum_{m=-n}^{n}\left(1+n(n+1)\right)^{-1/2}|M_n\boldsymbol{u}_n^m|^2\\ &\lesssim \sum_{n=0}^{\infty}\sum_{m=-n}^{n}\left(1+n(n+1)\right)^{1/2}|\boldsymbol{u}_n^m|^2 = \|\boldsymbol{u}\|^2_{\boldsymbol{H}^{1/2}(\Gamma_R)},\end{aligned}$$

which completes the proof. ■

4.3.2 Uniqueness

It follows from the Dirichlet boundary condition (4.5) and the Helmholtz decomposition (4.7) that

$$\boldsymbol{v} = \nabla\phi + \nabla\times\boldsymbol{\psi} = -\boldsymbol{u}^{\mathrm{inc}} \quad \text{on } \partial D. \tag{4.19}$$

Taking the dot product and the cross product of (4.19) with the unit normal vector $\boldsymbol{\nu}$ on ∂D, respectively, we get

$$\partial_{\boldsymbol{\nu}}\phi + (\nabla\times\boldsymbol{\psi})\cdot\boldsymbol{\nu} = -u_1, \quad (\nabla\times\boldsymbol{\psi})\times\boldsymbol{\nu} + \nabla\phi\times\boldsymbol{\nu} = -\boldsymbol{u}_2,$$

where

$$u_1 = \boldsymbol{u}^{\mathrm{inc}}\cdot\boldsymbol{\nu}, \quad \boldsymbol{u}_2 = \boldsymbol{u}^{\mathrm{inc}}\times\boldsymbol{\nu}.$$

We obtain a coupled boundary value problem for the potential functions ϕ and $\boldsymbol{\psi}$:

$$\begin{cases}\Delta\phi + \kappa_{\mathrm{p}}^2\phi = 0, \quad \nabla\times(\nabla\times\boldsymbol{\psi}) - \kappa_{\mathrm{s}}^2\boldsymbol{\psi} = 0, & \text{in } \Omega,\\ \partial_{\boldsymbol{\nu}}\phi + (\nabla\times\boldsymbol{\psi})\cdot\boldsymbol{\nu} = -u_1, \quad (\nabla\times\boldsymbol{\psi})\times\boldsymbol{\nu} + \nabla\phi\times\boldsymbol{\nu} = -\boldsymbol{u}_2 & \text{on } \partial D,\\ \partial_r\phi - \mathscr{T}_1\phi = 0, \quad (\nabla\times\boldsymbol{\psi})\times\boldsymbol{e}_r - \mathrm{i}\kappa_{\mathrm{s}}\mathscr{T}_2\boldsymbol{\psi}_{\Gamma_R} = 0 & \text{on } \Gamma_R.\end{cases} \tag{4.20}$$

where $\mathscr{T}_1$ and $\mathscr{T}_2$ are the transparent boundary operators given in (4.46) and (4.54), respectively.

Multiplying test functions $(p,\boldsymbol{q}) \in H^1(\Omega)\times\boldsymbol{H}(\mathrm{curl},\Omega)$, we arrive at the weak formulation of (4.20): To find $(\phi,\boldsymbol{\psi}) \in H^1(\Omega)\times\boldsymbol{H}(\mathrm{curl},\Omega)$ such that

$$a(\phi,\boldsymbol{\psi};p,\boldsymbol{q}) = \langle u_1, p\rangle_{\partial D} + \langle \boldsymbol{u_2}, \boldsymbol{q}\rangle_{\partial D}, \quad \forall\,(p,\boldsymbol{q}) \in H^1(\Omega)\times\boldsymbol{H}(\mathrm{curl},\Omega), \tag{4.21}$$

where the sesquilinear form

$$a(\phi,\boldsymbol{\psi};p,\boldsymbol{q}) = (\nabla\phi,\nabla p) + (\nabla\times\boldsymbol{\psi},\nabla\times\boldsymbol{q}) - \kappa_{\rm p}^2(\phi,p) - \kappa_{\rm s}^2(\boldsymbol{\psi},\boldsymbol{q})$$
$$- \langle(\nabla\times\boldsymbol{\psi})\cdot\boldsymbol{\nu},p\rangle_{\partial D} - \langle\nabla\phi\times\boldsymbol{\nu},\boldsymbol{q}\rangle_{\partial D} - \langle\mathscr{T}_1\phi,p\rangle_{\Gamma_R} - {\rm i}\kappa_{\rm s}\langle\mathscr{T}_2\boldsymbol{\psi}_{\Gamma_R},\boldsymbol{q}_{\Gamma_R}\rangle_{\Gamma_R}.$$

Theorem 4.3.3 *The variational problem* (4.21) *has at most one solution.*

Proof It suffices to show that $\phi=0,\boldsymbol{\psi}=0$ in Ω if $u_1=0,\boldsymbol{u_2}=0$ on ∂D. If $(\phi,\boldsymbol{\psi})$ satisfy the homogeneous variational problem (4.21), then we have

$$(\nabla\phi,\nabla\phi) + (\nabla\times\boldsymbol{\psi},\nabla\times\boldsymbol{\psi}) - \kappa_{\rm p}^2(\phi,\phi) - \kappa_{\rm s}^2(\boldsymbol{\psi},\boldsymbol{\psi}) - \langle(\nabla\times\boldsymbol{\psi})\cdot\boldsymbol{\nu},\phi\rangle_{\partial D}$$
$$-\langle\nabla\phi\times\boldsymbol{\nu},\boldsymbol{\psi}\rangle_{\partial D} - \langle\mathscr{T}_1\phi,\phi\rangle_{\Gamma_R} - {\rm i}\kappa_{\rm s}\langle\mathscr{T}_2\boldsymbol{\psi}_{\Gamma_R},\boldsymbol{\psi}_{\Gamma_R}\rangle_{\Gamma_R} = 0. \tag{4.22}$$

Using the integration by parts, we may verify that

$$\langle(\nabla\times\boldsymbol{\psi})\cdot\boldsymbol{\nu},\phi\rangle_{\partial D} = -\langle\boldsymbol{\psi},\boldsymbol{\nu}\times\nabla\phi\rangle_{\partial D} = \langle\boldsymbol{\psi},\nabla\phi\times\boldsymbol{\nu}\rangle_{\partial D},$$

which gives

$$\langle(\nabla\times\boldsymbol{\psi})\cdot\boldsymbol{\nu},\phi\rangle_{\partial D} + \langle\nabla\phi\times\boldsymbol{\nu},\boldsymbol{\psi}\rangle_{\partial D} = 2{\rm Re}\langle\nabla\phi\times\boldsymbol{\nu},\boldsymbol{\psi}\rangle_{\partial D}. \tag{4.23}$$

Taking the imaginary part of (4.22) and using (4.23), we obtain

$${\rm Im}\langle\mathscr{T}_1\phi,\phi\rangle_{\Gamma_R} + \kappa_{\rm s}{\rm Re}\langle\mathscr{T}_2\boldsymbol{\psi}_{\Gamma_R},\boldsymbol{\psi}_{\Gamma_R}\rangle_{\Gamma_R} = 0,$$

which gives $\phi=0,\boldsymbol{\psi}=0$ on Γ_R, due to Lemma 4.7.1 and Lemma 4.7.2. Using (4.46) and (4.54), we have $\partial_r\phi=0,(\nabla\times\boldsymbol{\psi})\times\boldsymbol{e}_r=0$ on Γ_R. By the Holmgren uniqueness theorem, we have $\phi=0,\boldsymbol{\psi}=0$ in $\mathbb{R}^3\backslash\bar{B}$. A unique continuation result concludes that $\phi=0,\boldsymbol{\psi}=0$ in Ω. ■

4.3.3 Well-posedness

Using the transparent boundary condition (4.18), we obtain a boundary value problem for $\boldsymbol{u}$:

$$\begin{cases} \mu\Delta\boldsymbol{u} + (\lambda+\mu)\nabla\nabla\cdot\boldsymbol{u} + \omega^2\boldsymbol{u} = 0 & \text{in } \Omega, \\ \boldsymbol{u} = 0 & \text{on } \partial D, \\ \mathscr{B}\boldsymbol{u} = \mathscr{T}\boldsymbol{u} + \boldsymbol{g} & \text{on } \Gamma_R, \end{cases} \tag{4.24}$$

where $\boldsymbol{g} = (\mathscr{B} - \mathscr{T})\boldsymbol{u}^{\mathrm{inc}}$. The variational problem of (4.24) is to find $\boldsymbol{u} \in \boldsymbol{H}^1_{\partial D}(\Omega)$ such that

$$b(\boldsymbol{u}, \boldsymbol{v}) = \langle \boldsymbol{g}, \boldsymbol{v} \rangle_{\Gamma_R}, \quad \forall\, \boldsymbol{v} \in \boldsymbol{H}^1_{\partial D}(\Omega), \tag{4.25}$$

where the sesquilinear form $b : \boldsymbol{H}^1_{\partial D}(\Omega) \times \boldsymbol{H}^1_{\partial D}(\Omega) \to \mathbb{C}$ is defined by

$$\begin{aligned} b(\boldsymbol{u}, \boldsymbol{v}) = \mu \int_\Omega \nabla \boldsymbol{u} : \nabla \bar{\boldsymbol{v}} \, \mathrm{d}\boldsymbol{x} + (\lambda + \mu) \int_\Omega (\nabla \cdot \boldsymbol{u})(\nabla \cdot \bar{\boldsymbol{v}}) \, \mathrm{d}\boldsymbol{x} \\ -\omega^2 \int_\Omega \boldsymbol{u} \cdot \bar{\boldsymbol{v}} \, \mathrm{d}\boldsymbol{x} - \langle \mathscr{T} \boldsymbol{u}, \boldsymbol{v} \rangle_{\Gamma_R}. \end{aligned}$$

Here $A : B = \mathrm{tr}(AB^\top)$ is the Frobenius inner product of square matrices A and B.

The following result follows from the standard trace theorem of the Sobolev spaces. The proof is omitted for brevity.

Lemma 4.3.4 *It holds the estimate*

$$\|\boldsymbol{u}\|_{\boldsymbol{H}^{1/2}(\Gamma_R)} \lesssim \|\boldsymbol{u}\|_{\boldsymbol{H}^1(\Omega)}, \quad \forall\, \boldsymbol{u} \in \boldsymbol{H}^1_{\partial D}(\Omega).$$

Lemma 4.3.5 *For any $\varepsilon > 0$, there exists a positive constant $C(\varepsilon)$ such that*

$$\|\boldsymbol{u}\|_{\boldsymbol{L}^2(\Gamma_R)} \leqslant \varepsilon \|\boldsymbol{u}\|_{\boldsymbol{H}^1(\Omega)} + C(\varepsilon) \|\boldsymbol{u}\|_{\boldsymbol{L}^2(\Omega)}, \quad \forall\, \boldsymbol{u} \in \boldsymbol{H}^1_{\partial D}(\Omega).$$

Proof Let B' be the ball with radius $R' > 0$ such that $\bar{B}' \subset D$. Denote $\tilde{\Omega} = B \backslash \bar{B}'$. Given $\boldsymbol{u} \in \boldsymbol{H}^1_{\partial D}(\Omega)$, let $\tilde{\boldsymbol{u}}$ be the zero extension of $\boldsymbol{u}$ from Ω to $\tilde{\Omega}$, i.e.,

$$\tilde{\boldsymbol{u}}(\boldsymbol{x}) = \begin{cases} \boldsymbol{u}(\boldsymbol{x}), & \boldsymbol{x} \in \Omega, \\ 0, & \boldsymbol{x} \in \tilde{\Omega} \backslash \bar{\Omega}. \end{cases}$$

The extension of $\tilde{\boldsymbol{u}}$ has the Fourier expansion

$$\tilde{\boldsymbol{u}}(r, \theta, \varphi) = \sum_{n=0}^{\infty} \sum_{m=-n}^{n} \tilde{u}^m_{1n}(r) \boldsymbol{T}^m_n(\theta, \varphi) + \tilde{u}^m_{2n}(r) \boldsymbol{V}^m_n(\theta, \varphi) + \tilde{u}^m_{3n}(r) \boldsymbol{W}^m_n(\theta, \varphi).$$

A simple calculation yields

$$\|\tilde{\boldsymbol{u}}\|^2_{\boldsymbol{L}^2(\Gamma_R)} = \sum_{n=0}^{\infty} \sum_{m=-n}^{n} |\tilde{u}^m_{1n}(R)|^2 + |\tilde{u}^m_{2n}(R)|^2 + |\tilde{u}^m_{3n}(R)|^2.$$

Since $\tilde{\boldsymbol{u}}(R',\theta,\varphi)=0$, we have $\tilde{u}_{jn}^m(R')=0$. For any given $\varepsilon>0$, it follows from Young's inequality that

$$\begin{aligned}|\tilde{u}_{jn}^m(R)|^2 &= \int_{R'}^R \frac{\mathrm{d}}{\mathrm{d}r}|\tilde{u}_{jn}^m(r)|^2\mathrm{d}r \leqslant \int_{R'}^R 2|\tilde{u}_{jn}^m(r)|\left|\frac{\mathrm{d}}{\mathrm{d}r}\tilde{u}_{jn}^m(r)\right|\mathrm{d}r\\ &\leqslant (R'\varepsilon)^{-2}\int_{R'}^R |\tilde{u}_{jn}^m(r)|^2\mathrm{d}r + (R'\varepsilon)^2\int_{R'}^R\left|\frac{\mathrm{d}}{\mathrm{d}r}\tilde{u}_{jn}^m(r)\right|^2\mathrm{d}r,\end{aligned}$$

which gives

$$|\tilde{u}_{jn}^m(R)|^2 \leqslant C(\varepsilon)\int_{R'}^R |\tilde{u}_{jn}^m(r)|^2 r^2\mathrm{d}r + \varepsilon^2\int_{R'}^R\left|\frac{\mathrm{d}}{\mathrm{d}r}\tilde{u}_{jn}^m(r)\right|^2 r^2\mathrm{d}r.$$

The proof is completed by noting that

$$\|\tilde{\boldsymbol{u}}\|_{\boldsymbol{L}^2(\Gamma_R)} = \|\boldsymbol{u}\|_{\boldsymbol{L}^2(\Gamma_R)},\quad \|\tilde{\boldsymbol{u}}\|_{\boldsymbol{L}^2(\tilde{\Omega})} = \|\boldsymbol{u}\|_{\boldsymbol{L}^2(\Omega)},\quad \|\tilde{\boldsymbol{u}}\|_{\boldsymbol{H}^1(\tilde{\Omega})} = \|\boldsymbol{u}\|_{\boldsymbol{H}^1(\Omega)}.$$

■

Lemma 4.3.6 *It holds the estimate*

$$\|\boldsymbol{u}\|_{\boldsymbol{H}^1(\Omega)} \lesssim \|\nabla\boldsymbol{u}\|_{\boldsymbol{L}^2(\Omega)},\quad \forall\,\boldsymbol{u}\in\boldsymbol{H}^1_{\partial D}(\Omega).$$

Proof As is defined in the proof of Lemma 4.3.5, let $\tilde{\boldsymbol{u}}$ be the zero extension of $\boldsymbol{u}$ from Ω to $\tilde{\Omega}$. It follows from the Cauchy–Schwarz inequality that

$$|\tilde{\boldsymbol{u}}(r,\theta,\varphi)|^2 = \left|\int_{R'}^r \partial_r\tilde{\boldsymbol{u}}(r,\theta,\varphi)\mathrm{d}r\right|^2 \lesssim \int_{R'}^R |\partial_r\tilde{\boldsymbol{u}}(r,\theta,\varphi)|^2\,\mathrm{d}r.$$

Hence we have

$$\begin{aligned}\|\tilde{\boldsymbol{u}}\|^2_{\boldsymbol{L}^2(\tilde{\Omega})} &= \int_{R'}^R\int_0^{2\pi}\int_0^{\pi}|\tilde{\boldsymbol{u}}(r,\theta,\varphi)|^2 r^2\mathrm{d}r\mathrm{d}\theta\mathrm{d}\varphi\\ &\lesssim \int_{R'}^R\int_0^{2\pi}\int_0^{\pi}\int_{R'}^R|\partial_r\tilde{\boldsymbol{u}}(r,\theta,\varphi)|^2\mathrm{d}r\mathrm{d}\theta\mathrm{d}\varphi\mathrm{d}r\\ &\lesssim \int_{R'}^R\int_0^{2\pi}\int_0^{\pi}|\partial_r\tilde{\boldsymbol{u}}(r,\theta,\varphi)|^2\mathrm{d}r\mathrm{d}\theta\mathrm{d}\varphi \lesssim \|\nabla\tilde{\boldsymbol{u}}\|^2_{\boldsymbol{L}^2(\tilde{\Omega})}.\end{aligned}$$

The proof is completed by noting that

$$\begin{aligned}&\|\boldsymbol{u}\|_{\boldsymbol{L}^2(\Omega)} = \|\tilde{\boldsymbol{u}}\|_{\boldsymbol{L}^2(\tilde{\Omega})},\quad \|\nabla\boldsymbol{u}\|_{\boldsymbol{L}^2(\Omega)} = \|\nabla\tilde{\boldsymbol{u}}\|_{\boldsymbol{L}^2(\tilde{\Omega})},\\ &\|\boldsymbol{u}\|^2_{\boldsymbol{H}^1(\Omega)} = \|\boldsymbol{u}\|^2_{\boldsymbol{L}^2(\Omega)} + \|\nabla\boldsymbol{u}\|^2_{\boldsymbol{L}^2(\Omega)}.\end{aligned}$$

■

Theorem 4.3.7 *The variational problem* (4.25) *admits a unique weak solution* $\boldsymbol{u} \in \boldsymbol{H}^1_{\partial D}(\Omega)$.

Proof Using the Cauchy–Schwarz inequality, Lemma 4.3.2, and Lemma 4.3.4, we have

$$\begin{aligned}|b(\boldsymbol{u},\boldsymbol{v})| \leqslant& \mu\|\nabla\boldsymbol{u}\|_{\boldsymbol{L}^2(\Omega)}\|\nabla\boldsymbol{v}\|_{\boldsymbol{L}^2(\Omega)} + (\lambda+\mu)\|\nabla\cdot\boldsymbol{u}\|_{0,\Omega}\|\nabla\cdot\boldsymbol{v}\|_{\boldsymbol{L}^2(\Omega)}\\ &+ \omega^2\|\boldsymbol{u}\|_{\boldsymbol{L}^2(\Omega)}\|\boldsymbol{v}\|_{\boldsymbol{L}^2(\Omega)} + \|\mathscr{T}\boldsymbol{u}\|_{\boldsymbol{H}^{-1/2}(\Gamma_R)}\|\boldsymbol{v}\|_{\boldsymbol{H}^{1/2}(\Gamma_R)}\\ \lesssim& \|\boldsymbol{u}\|_{\boldsymbol{H}^1(\Omega)}\|\boldsymbol{v}\|_{\boldsymbol{H}^1(\Omega)},\end{aligned}$$

which shows that the sesquilinear form $b(\cdot,\cdot)$ is bounded.

It follows from Lemma 4.3.1 that there exists an $N_0 \in \mathbb{N}$ such that $\hat{M}_n$ is positive definite for $n > N_0$. The sesquilinear form b can be written as

$$\begin{aligned}b(\boldsymbol{u},\boldsymbol{v}) =& \mu\int_\Omega (\nabla\boldsymbol{u} : \nabla\bar{\boldsymbol{v}})\,\mathrm{d}\boldsymbol{x} + (\lambda+\mu)\int_\Omega (\nabla\cdot\boldsymbol{u})(\nabla\cdot\bar{\boldsymbol{v}})\,\mathrm{d}\boldsymbol{x} - \omega^2\int_\Omega \boldsymbol{u}\cdot\bar{\boldsymbol{v}}\,\mathrm{d}\boldsymbol{x}\\ &- \sum_{|n|>N_0}\sum_{m=-n}^{n}\langle M_n\boldsymbol{u}_n^m, \boldsymbol{v}_n^m\rangle - \sum_{|n|\leqslant N_0}\sum_{m=-n}^{n}\langle M_n\boldsymbol{u}_n^m, \boldsymbol{v}_n^m\rangle.\end{aligned}$$

Taking the real part of b, and using Lemma 4.3.1, Lemma 4.3.6, Lemma 4.3.5, we obtain

$$\begin{aligned}\operatorname{Re} b(\boldsymbol{u},\boldsymbol{u}) =& \mu\|\nabla\boldsymbol{u}\|^2_{\boldsymbol{L}^2(\Omega)} + (\lambda+\mu)\|\nabla\cdot\boldsymbol{u}\|^2_{\boldsymbol{L}^2(\Omega)} + \sum_{|n|>N_0}\sum_{m=-n}^{n}\langle\hat{M}_n\boldsymbol{u}_n^m, \boldsymbol{u}_n^m\rangle\\ &- \omega^2\|\boldsymbol{u}\|_{\boldsymbol{L}^2(\Omega)} + \sum_{|n|\leqslant N_0}\sum_{m=-n}^{n}\langle\hat{M}_n\boldsymbol{u}_n^m, \boldsymbol{u}_n^m\rangle\\ \geqslant& C_1\|\boldsymbol{u}\|_{\boldsymbol{H}^1(\Omega)} - \omega^2\|\boldsymbol{u}\|_{\boldsymbol{L}^2(\Omega)} - C_2\|\boldsymbol{u}\|_{\boldsymbol{L}^2(\Gamma_R)}\\ \geqslant& C_1\|\boldsymbol{u}\|_{\boldsymbol{H}^1(\Omega)} - \omega^2\|\boldsymbol{u}\|_{\boldsymbol{L}^2(\Omega)} - C_2\varepsilon\|\boldsymbol{u}\|_{\boldsymbol{H}^1(\Omega)} - C(\varepsilon)\|\boldsymbol{u}\|_{\boldsymbol{L}^2(\Omega)}\\ =& (C_1 - C_2\varepsilon)\|\boldsymbol{u}\|_{\boldsymbol{H}^1(\Omega)} - C_3\|\boldsymbol{u}\|_{\boldsymbol{L}^2(\Omega)}.\end{aligned}$$

Letting $\varepsilon > 0$ to be sufficiently small, we have $C_1 - C_2\varepsilon > 0$ and thus Gårding's inequality. Since the injection of $\boldsymbol{H}^1_{\partial D}(\Omega)$ into $\boldsymbol{L}^2(\Omega)$ is compact, the proof is completed by using the Fredholm alternative (cf. [82, Theorem 5.4.5]) and the uniqueness result in Theorem 4.3.3. ∎

4.4 Inverse Scattering

In this section, we study a domain derivative of the scattering problem and present a continuation method to reconstruct the surface.

4.4.1 Domain Derivative

We assume that the obstacle has a C^2 boundary, i.e., $\partial D \in C^2$. Given a sufficiently small number $h > 0$, define a perturbed domain Ω_h which is surrounded by ∂D_h and Γ_R, where

$$\partial D_h = \{\boldsymbol{x} + h\boldsymbol{p}(\boldsymbol{x}) : \boldsymbol{x} \in \partial D\}.$$

Here the function $\boldsymbol{p} \in \boldsymbol{C}^2(\partial D)$.

Consider the variational formulation for the direct problem in the perturbed domain Ω_h: To find $\boldsymbol{u}_h \in \boldsymbol{H}^1_{\partial D_h}(\Omega_h)$ such that

$$b^h(\boldsymbol{u}_h, \boldsymbol{v}_h) = \langle \boldsymbol{g}, \boldsymbol{v}_h \rangle_{\Gamma_R}, \quad \forall\, \boldsymbol{v}_h \in \boldsymbol{H}^1_{\partial D_h}(\Omega_h), \tag{4.26}$$

where the sesquilinear form $b^h : \boldsymbol{H}^1_{\partial D_h}(\Omega_h) \times \boldsymbol{H}^1_{\partial D_h}(\Omega_h) \to \mathbb{C}$ is defined by

$$\begin{aligned} b^h(\boldsymbol{u}_h, \boldsymbol{v}_h) = \mu \int_{\Omega_h} \nabla \boldsymbol{u}_h : \nabla \bar{\boldsymbol{v}}_h \, \mathrm{d}\boldsymbol{y} + (\lambda + \mu) \int_{\Omega_h} (\nabla \cdot \boldsymbol{u}_h)(\nabla \cdot \bar{\boldsymbol{v}}_h) \, \mathrm{d}\boldsymbol{y} \\ -\omega^2 \int_{\Omega_h} \boldsymbol{u}_h \cdot \bar{\boldsymbol{v}}_h \, \mathrm{d}\boldsymbol{y} - \langle \mathscr{T} \boldsymbol{u}_h, \boldsymbol{v}_h \rangle \Gamma_R. \end{aligned} \tag{4.27}$$

Similarly, we may follow the proof of Theorem 4.3.7 to show that the variational problem (4.26) has a unique weak solution $\boldsymbol{u}_h \in \boldsymbol{H}^1_{\partial D_h}(\Omega_h)$ for any $h > 0$.

Since the variational problem (4.3.7) is well-posed, we introduce a nonlinear scattering operator:

$$\mathscr{S} : \partial D_h \to \boldsymbol{u}_h|_{\Gamma_R},$$

which maps the obstacle's surface to the displacement of the wave field on Γ_R. Let $\boldsymbol{u}_h$ and $\boldsymbol{u}$ be the solution of the direct problem in the domain Ω_h and Ω, respectively. Define the domain derivative of the scattering operator $\mathscr{S}$ on ∂D along the direction $\boldsymbol{p}$ as

$$\mathscr{S}'(\partial D; \boldsymbol{p}) := \lim_{h \to 0} \frac{\mathscr{S}(\partial D_h) - \mathscr{S}(\partial D)}{h} = \lim_{h \to =0} \frac{\boldsymbol{u}_h|_{\Gamma_R} - \boldsymbol{u}|_{\Gamma_R}}{h}.$$

For a given $\boldsymbol{p} \in \boldsymbol{C}^2(\partial D)$, we extend its domain to $\bar{\Omega}$ by requiring that $\boldsymbol{p} \in \boldsymbol{C}^2(\Omega) \cap \boldsymbol{C}(\bar{\Omega}), \boldsymbol{p} = 0$ on Γ_R, and $\boldsymbol{y} = \boldsymbol{\xi}^h(\boldsymbol{x}) = \boldsymbol{x} + h\boldsymbol{p}(\boldsymbol{x})$ maps Ω to Ω_h. It is clear to note that $\boldsymbol{\xi}^h$ is a diffeomorphism from Ω to Ω_h for sufficiently small h. Denote by $\boldsymbol{\eta}^h(\boldsymbol{y}) : \Omega_h \to \Omega$ the inverse map of $\boldsymbol{\xi}^h$.

Define $\breve{\boldsymbol{u}}(\boldsymbol{x}) = (\breve{u}_1, \breve{u}_2, \breve{u}_3) := (\boldsymbol{u}_h \circ \boldsymbol{\xi}^h)(\boldsymbol{x})$. Using the change of variable $\boldsymbol{y} = \xi^h(\boldsymbol{x})$, we have from straightforward calculations that

$$\begin{aligned}
\int_{\Omega_h} (\nabla \boldsymbol{u}_h : \nabla \overline{\boldsymbol{v}}_h)\, \mathrm{d}\boldsymbol{y} &= \sum_{j=1}^{3} \int_{\Omega} \nabla \breve{u}_j J_{\boldsymbol{\eta}^h} J_{\boldsymbol{\eta}^h}^{\top} \nabla \bar{\breve{v}}_j \det(J_{\boldsymbol{\xi}^h})\, \mathrm{d}\boldsymbol{x}, \\
\int_{\Omega_h} (\nabla \cdot \boldsymbol{u}_h)(\nabla \cdot \bar{\boldsymbol{v}}_h)\, \mathrm{d}\boldsymbol{y} &= \int_{\Omega} (\nabla \breve{\boldsymbol{u}} : J_{\boldsymbol{\eta}^h}^{\top})(\nabla \bar{\breve{\boldsymbol{v}}} : J_{\boldsymbol{\eta}^h}^{\top}) \det(J_{\boldsymbol{\xi}^h})\, \mathrm{d}\boldsymbol{x}, \\
\int_{\Omega_h} \boldsymbol{u}_h \cdot \bar{\boldsymbol{v}}_h\, \mathrm{d}\boldsymbol{y} &= \int_{\Omega} \breve{\boldsymbol{u}} \cdot \bar{\breve{\boldsymbol{v}}} \det(J_{\boldsymbol{\xi}^h})\, \mathrm{d}\boldsymbol{x},
\end{aligned}$$

where $\breve{\boldsymbol{v}}(\boldsymbol{x}) = (\breve{v}_1, \breve{v}_2, \breve{v}_3) := (\boldsymbol{v}_h \circ \boldsymbol{\xi}^h)(\boldsymbol{x})$, $J_{\boldsymbol{\eta}^h}$ and $J_{\boldsymbol{\xi}^h}$ are the Jacobian matrices of the transforms $\boldsymbol{\eta}^h$ and $\boldsymbol{\xi}^h$, respectively.

For a test function $\boldsymbol{v}_h$ in the domain Ω_h, it follows from the transform that $\breve{\boldsymbol{v}}$ is a test function in the domain Ω. Therefore, the sesquilinear form b^h in (4.27) becomes

$$\begin{aligned}
b^h(\breve{\boldsymbol{u}}, \boldsymbol{v}) = \sum_{j=1}^{3} \mu \int_{\Omega} \nabla \breve{u}_j J_{\boldsymbol{\eta}^h} J_{\boldsymbol{\eta}^h}^{\top} \nabla \bar{v}_j \det(J_{\boldsymbol{\xi}^h})\, \mathrm{d}\boldsymbol{x} + (\lambda + \mu) \int_{\Omega} (\nabla \breve{\boldsymbol{u}} : J_{\boldsymbol{\eta}^h}^{\top})(\nabla \bar{\boldsymbol{v}} : J_{\boldsymbol{\eta}^h}^{\top}) \\
\times \det(J_{\boldsymbol{\xi}^h})\, \mathrm{d}\boldsymbol{x} - \omega^2 \int_{\Omega} \breve{\boldsymbol{u}} \cdot \bar{\boldsymbol{v}} \det(J_{\boldsymbol{\xi}^h})\, \mathrm{d}\boldsymbol{x} - \langle \mathscr{T} \breve{\boldsymbol{u}}, \boldsymbol{v} \rangle_{\Gamma_R},
\end{aligned}$$

which gives an equivalent variational formulation of (4.26):

$$b^h(\breve{\boldsymbol{u}}, \boldsymbol{v}) = \langle \boldsymbol{g}, \boldsymbol{v} \rangle_{\Gamma_R}, \quad \forall\, \boldsymbol{v} \in \boldsymbol{H}^1_{\partial D}(\Omega).$$

A simple calculation yields

$$b(\breve{\boldsymbol{u}} - \boldsymbol{u}, \boldsymbol{v}) = b(\breve{\boldsymbol{u}}, \boldsymbol{v}) - \langle \boldsymbol{g}, \boldsymbol{v} \rangle_{\Gamma_R} = b(\breve{\boldsymbol{u}}, \boldsymbol{v}) - b^h(\breve{\boldsymbol{u}}, \boldsymbol{v}) = b_1 + b_2 + b_3,$$

where

$$b_1 = \sum_{j=1}^{3} \mu \int_{\Omega} \nabla \breve{u}_j \left(I - J_{\boldsymbol{\eta}^h} J_{\boldsymbol{\eta}^h}^{\top} \det(J_{\boldsymbol{\xi}^h}) \right) \nabla \bar{v}_j\, \mathrm{d}\boldsymbol{x}, \tag{4.28}$$

$$b_2 = (\lambda + \mu) \int_{\Omega} (\nabla \cdot \breve{\boldsymbol{u}})(\nabla \cdot \bar{\boldsymbol{v}}) - (\nabla \breve{\boldsymbol{u}} : J_{\boldsymbol{\eta}^h}^{\top})(\nabla \bar{\boldsymbol{v}} : J_{\boldsymbol{\eta}^h}^{\top}) \det(J_{\boldsymbol{\xi}^h})\, \mathrm{d}\boldsymbol{x}, \tag{4.29}$$

$$b_3 = \omega^2 \int_{\Omega} \breve{\boldsymbol{u}} \cdot \bar{\boldsymbol{v}} \left(\det(J_{\boldsymbol{\xi}^h}) - 1 \right) \mathrm{d}\boldsymbol{x}. \tag{4.30}$$

Here I is the identity matrix. Following the definitions of the Jacobian matrices, we may easily verify that

$$\begin{aligned}
\det(J_{\boldsymbol{\xi}^h}) &= 1 + h\nabla\cdot\boldsymbol{p} + O(h^2),\\
J_{\boldsymbol{\eta}^h} &= J^{-1}_{\boldsymbol{\xi}^h}\circ\boldsymbol{\eta}^h = I - hJ_{\boldsymbol{p}} + O(h^2),\\
J_{\boldsymbol{\eta}^h}J^{\top}_{\boldsymbol{\eta}^h}\det(J_{\boldsymbol{\xi}^h}) &= I - h(J_{\boldsymbol{p}} + J^{\top}_{\boldsymbol{p}}) + h(\nabla\cdot\boldsymbol{p})I + O(h^2),
\end{aligned}$$

where the matrix $J_{\boldsymbol{p}} = \nabla\boldsymbol{p}$.

Substituting the above estimates into (4.28)–(4.30), we obtain

$$\begin{aligned}
b_1 &= \sum_{j=1}^{3}\mu\int_\Omega \nabla\breve{u}_j\left(h(J_{\boldsymbol{p}} + J^{\top}_{\boldsymbol{p}}) - h(\nabla\cdot\boldsymbol{p})I + O(h^2)\right)\nabla\bar{v}_j\,\mathrm{d}\boldsymbol{x},\\
b_2 &= (\lambda+\mu)\int_\Omega h(\nabla\cdot\breve{\boldsymbol{u}})(\nabla\bar{\boldsymbol{v}} : J^{\top}_{\boldsymbol{p}}) + h(\nabla\cdot\bar{\boldsymbol{v}})(\nabla\breve{\boldsymbol{u}} : J^{\top}_{\boldsymbol{p}})\\
&\qquad - h(\nabla\cdot\boldsymbol{p})(\nabla\cdot\breve{\boldsymbol{u}})(\nabla\cdot\bar{\boldsymbol{v}}) + O(h^2)\,\mathrm{d}\boldsymbol{x},\\
b_3 &= \omega^2\int_\Omega \breve{\boldsymbol{u}}\cdot\bar{\boldsymbol{v}}\,\left(h\nabla\cdot\boldsymbol{p} + O(h^2)\right)\,\mathrm{d}\boldsymbol{x}.
\end{aligned}$$

Hence we have

$$b\left(\frac{\breve{\boldsymbol{u}}-\boldsymbol{u}}{h},\boldsymbol{v}\right) = g_1(\boldsymbol{p})(\breve{\boldsymbol{u}},\boldsymbol{v}) + g_2(\boldsymbol{p})(\breve{\boldsymbol{u}},\boldsymbol{v}) + g_3(\boldsymbol{p})(\breve{\boldsymbol{u}},\boldsymbol{v}) + O(h), \tag{4.31}$$

where

$$\begin{aligned}
g_1 &= \sum_{j=1}^{3}\mu\int_\Omega \nabla\breve{u}_j\left((J_{\boldsymbol{p}} + J^{\top}_{\boldsymbol{p}}) - (\nabla\cdot\boldsymbol{p})I\right)\nabla\bar{v}_j\,\mathrm{d}\boldsymbol{x},\\
g_2 &= (\lambda+\mu)\int_\Omega (\nabla\cdot\breve{\boldsymbol{u}})(\nabla\bar{\boldsymbol{v}} : J^{\top}_{\boldsymbol{p}}) + (\nabla\cdot\bar{\boldsymbol{v}})(\nabla\breve{\boldsymbol{u}} : J^{\top}_{\boldsymbol{p}}) - (\nabla\cdot\boldsymbol{p})(\nabla\cdot\breve{\boldsymbol{u}})(\nabla\cdot\bar{\boldsymbol{v}})\,\mathrm{d}\boldsymbol{x},\\
g_3 &= \omega^2\int_\Omega (\nabla\cdot\boldsymbol{p})\breve{\boldsymbol{u}}\cdot\bar{\boldsymbol{v}}\,\mathrm{d}\boldsymbol{x}.
\end{aligned}$$

Theorem 4.4.1 *Given $\boldsymbol{p}\in\boldsymbol{C}^2(\partial D)$, the domain derivative of the scattering operator $\mathscr{S}$ is $\mathscr{S}'(\partial D;\boldsymbol{p}) = \boldsymbol{u}'|_{\Gamma_R}$, where $\boldsymbol{u}'$ is the unique weak solution of the boundary value problem:*

$$\begin{cases}
\mu\Delta\boldsymbol{u}' + (\lambda+\mu)\nabla\nabla\cdot\boldsymbol{u}' + \omega^2\boldsymbol{u}' = 0 & \text{in } \Omega,\\
\boldsymbol{u}' = -(\boldsymbol{p}\cdot\boldsymbol{\nu})\partial_{\boldsymbol{\nu}}\boldsymbol{u} & \text{on } \partial D,\\
\mathscr{B}\boldsymbol{u}' = \mathscr{T}\boldsymbol{u}' & \text{on } \Gamma_R,
\end{cases} \tag{4.32}$$

and $\boldsymbol{u}$ *is the solution of the variational problem* (4.25) *corresponding to the domain* Ω*.*

Proof Given $\boldsymbol{p} \in \boldsymbol{C}^2(\partial D)$, we extend its definition to the domain $\bar{\Omega}$ as before. It follows from the well-posedness of the variational problem (4.25) that $\breve{\boldsymbol{u}} \to \boldsymbol{u}$ in $\boldsymbol{H}^1_{\partial D}(\Omega)$ as $h \to 0$. Taking the limit $h \to 0$ in (4.31) gives

$$b\left(\lim_{h\to 0} \frac{\breve{\boldsymbol{u}} - \boldsymbol{u}}{h}, \boldsymbol{v}\right) = g_1(\boldsymbol{p})(\boldsymbol{u}, \boldsymbol{v}) + g_2(\boldsymbol{p})(\boldsymbol{u}, \boldsymbol{v}) + g_3(\boldsymbol{p})(\boldsymbol{u}, \boldsymbol{v}), \tag{4.33}$$

which shows that $(\breve{\boldsymbol{u}} - \boldsymbol{u})/h$ is convergent in $\boldsymbol{H}^1_{\partial D}(\Omega)$ as $h \to 0$. Denote the limit by $\dot{\boldsymbol{u}}$ and rewrite (4.33) as

$$b(\dot{\boldsymbol{u}}, \boldsymbol{v}) = g_1(\boldsymbol{p})(\boldsymbol{u}, \boldsymbol{v}) + g_2(\boldsymbol{p})(\boldsymbol{u}, \boldsymbol{v}) + g_3(\boldsymbol{p})(\boldsymbol{u}, \boldsymbol{v}). \tag{4.34}$$

First we compute $g_1(\boldsymbol{p})(\boldsymbol{u}, \boldsymbol{v})$. Noting $\boldsymbol{p} = 0$ on ∂B and using the identity

$$\begin{aligned}\nabla u \left((J_{\boldsymbol{p}} + J_{\boldsymbol{p}}^\top) - (\nabla \cdot \boldsymbol{p})I\right) \nabla \bar{v} =& \nabla \cdot [(\boldsymbol{p} \cdot \nabla u)\nabla \bar{v} + (\boldsymbol{p} \cdot \nabla \bar{v})\nabla u - (\nabla u \cdot \nabla \bar{v})\boldsymbol{p}] \\ & - (\boldsymbol{p} \cdot \nabla u)\Delta \bar{v} - (\boldsymbol{p} \cdot \nabla \bar{v})\Delta u,\end{aligned}$$

we obtain from the divergence theorem that

$$\begin{aligned} g_1(\boldsymbol{p})(\boldsymbol{u}, \boldsymbol{v}) =& -\sum_{j=1}^{3} \mu \int_{\partial D} (\boldsymbol{p} \cdot \nabla u_j)(\boldsymbol{\nu} \cdot \nabla \bar{v}_j) + (\boldsymbol{p} \cdot \nabla \bar{v}_j)(\boldsymbol{\nu} \cdot \nabla u_j)\, \mathrm{d}\gamma \\ & + \sum_{j=1}^{3} \mu \int_{\partial D} (\boldsymbol{p} \cdot \boldsymbol{\nu})(\nabla u_j \cdot \nabla \bar{v}_j)\, \mathrm{d}\gamma \\ & - \sum_{j=1}^{3} \mu \int_{\Omega} (\boldsymbol{p} \cdot \nabla u_j)\Delta \bar{v}_j + (\boldsymbol{p} \cdot \nabla \bar{v}_j)\Delta u_j\, \mathrm{d}\boldsymbol{x} \\ =& -\mu \int_{\partial D} (\boldsymbol{p} \cdot \nabla \boldsymbol{u}) \cdot (\boldsymbol{\nu} \cdot \nabla \bar{\boldsymbol{v}}) + (\boldsymbol{p} \cdot \nabla \bar{\boldsymbol{v}}) \cdot (\boldsymbol{\nu} \cdot \nabla \boldsymbol{u}) \\ & + \mu \int_{\partial D} (\boldsymbol{p} \cdot \boldsymbol{\nu})(\nabla \boldsymbol{u} : \nabla \bar{\boldsymbol{v}})\, \mathrm{d}\gamma \\ & - \mu \int_{\Omega} (\boldsymbol{p} \cdot \nabla \boldsymbol{u}) \cdot \Delta \bar{\boldsymbol{v}} + (\boldsymbol{p} \cdot \nabla \bar{\boldsymbol{v}}) \cdot \Delta \boldsymbol{u}\, \mathrm{d}\boldsymbol{x}. \end{aligned}$$

Noting

$$\mu \Delta \boldsymbol{u} + (\lambda + \mu)\nabla \nabla \cdot \boldsymbol{u} + \omega^2 \boldsymbol{u} = 0 \quad \text{in } \Omega,$$

we have from the integration by parts that

$$\mu \int_\Omega (\boldsymbol{p}\cdot\nabla\bar{\boldsymbol{v}})\cdot\Delta\boldsymbol{u}\,\mathrm{d}\boldsymbol{x} = -(\lambda+\mu)\int_\Omega (\boldsymbol{p}\cdot\nabla\bar{\boldsymbol{v}})\cdot(\nabla\nabla\cdot\boldsymbol{u})\,\mathrm{d}\boldsymbol{x} - \omega^2\int_\Omega (\boldsymbol{p}\cdot\nabla\bar{\boldsymbol{v}})\cdot\boldsymbol{u}\,\mathrm{d}\boldsymbol{x}$$
$$= (\lambda+\mu)\int_\Omega (\nabla\cdot\boldsymbol{u})\nabla\cdot(\boldsymbol{p}\cdot\nabla\bar{\boldsymbol{v}})\,\mathrm{d}\boldsymbol{x} + (\lambda+\mu)\int_{\partial D}(\nabla\cdot\boldsymbol{u})(\boldsymbol{\nu}\cdot(\boldsymbol{p}\cdot\nabla\bar{\boldsymbol{v}}))\,\mathrm{d}\gamma$$
$$-\omega^2\int_\Omega (\boldsymbol{p}\cdot\nabla\bar{\boldsymbol{v}})\cdot\boldsymbol{u}\,\mathrm{d}\boldsymbol{x}.$$

Using the integration by parts again yields

$$\mu\int_\Omega (\boldsymbol{p}\cdot\nabla\boldsymbol{u})\cdot\Delta\bar{\boldsymbol{v}}\,\mathrm{d}\boldsymbol{x} = -\mu\int_\Omega \nabla(\boldsymbol{p}\cdot\nabla\boldsymbol{u}):\nabla\bar{\boldsymbol{v}}\,\mathrm{d}\boldsymbol{x} + \mu\int_{\partial D}(\boldsymbol{p}\cdot\nabla\boldsymbol{u})\cdot(\boldsymbol{\nu}\cdot\nabla\bar{\boldsymbol{v}})\,\mathrm{d}\gamma.$$

Let $\boldsymbol{\tau}_1(\boldsymbol{x}), \boldsymbol{\tau}_2(\boldsymbol{x})$ be any two linearly independent unit tangent vectors on ∂D. Since $\boldsymbol{u} = \boldsymbol{v} = 0$ on ∂D, we have

$$\partial_{\boldsymbol{\tau}_1} u_j = \partial_{\boldsymbol{\tau}_2} u_j = \partial_{\boldsymbol{\tau}_1} v_j = \partial_{\boldsymbol{\tau}_2} v_j = 0.$$

Using the identities

$$\nabla u_j = \boldsymbol{\tau}_1\partial_{\boldsymbol{\tau}_1}u_j + \boldsymbol{\tau}_2\partial_{\boldsymbol{\tau}_2}u_j + \boldsymbol{\nu}\partial_{\boldsymbol{\nu}}u_j = \boldsymbol{\nu}\partial_{\boldsymbol{\nu}}u_j,$$
$$\nabla v_j = \boldsymbol{\tau}_1\partial_{\boldsymbol{\tau}_1}v_j + \boldsymbol{\tau}_2\partial_{\boldsymbol{\tau}_2}v_j + \boldsymbol{\nu}\partial_{\boldsymbol{\nu}}v_j = \boldsymbol{\nu}\partial_{\boldsymbol{\nu}}v_j,$$

we have

$$(\boldsymbol{p}\cdot\nabla\bar{v}_j)(\boldsymbol{\nu}\cdot\nabla u_j) = (\boldsymbol{p}\cdot\boldsymbol{\nu}\partial_{\boldsymbol{\nu}}\bar{v}_j)(\boldsymbol{\nu}\cdot\boldsymbol{\nu}\partial_{\boldsymbol{\nu}}u_j) = (\boldsymbol{p}\cdot\boldsymbol{\nu})(\partial_{\boldsymbol{\nu}}\bar{v}_j\partial_{\boldsymbol{\nu}}u_j),$$

which gives

$$\int_{\partial D}(\boldsymbol{p}\cdot\nabla\bar{\boldsymbol{v}})\cdot(\boldsymbol{\nu}\cdot\nabla\boldsymbol{u}) - (\boldsymbol{p}\cdot\boldsymbol{\nu})(\nabla\boldsymbol{u}:\nabla\bar{\boldsymbol{v}})\,\mathrm{d}\gamma = 0.$$

Noting $\boldsymbol{v} = 0$ on ∂D and

$$(\nabla\cdot\boldsymbol{p})(\boldsymbol{u}\cdot\bar{\boldsymbol{v}}) + (\boldsymbol{p}\cdot\nabla\bar{\boldsymbol{v}})\cdot\boldsymbol{u} = \nabla\cdot((\boldsymbol{u}\cdot\bar{\boldsymbol{v}})\boldsymbol{p}) - (\boldsymbol{p}\cdot\nabla\boldsymbol{u})\cdot\bar{\boldsymbol{v}},$$

we obtain by the divergence theorem that

$$\int_\Omega (\nabla\cdot\boldsymbol{p})(\boldsymbol{u}\cdot\bar{\boldsymbol{v}}) + (\boldsymbol{p}\cdot\nabla\bar{\boldsymbol{v}})\cdot\boldsymbol{u}\,\mathrm{d}\boldsymbol{x} = -\int_\Omega (\boldsymbol{p}\cdot\nabla\boldsymbol{u})\cdot\bar{\boldsymbol{v}}\,\mathrm{d}\boldsymbol{x}.$$

Combining the above identities, we conclude that

$$\begin{aligned} & g_1(\boldsymbol{p})(\boldsymbol{u},\boldsymbol{v}) + g_3(\boldsymbol{p})(\boldsymbol{u},\boldsymbol{v}) \\ &= \mu \int_\Omega \nabla(\boldsymbol{p}\cdot\nabla\boldsymbol{u}) : \nabla\bar{\boldsymbol{v}}\,\mathrm{d}\boldsymbol{x} - (\lambda+\mu)\int_\Omega (\nabla\cdot\boldsymbol{u})\nabla\cdot(\boldsymbol{p}\cdot\nabla\bar{\boldsymbol{v}})\,\mathrm{d}\boldsymbol{x} \\ &\quad - \omega^2\int_\Omega (\boldsymbol{p}\cdot\nabla\boldsymbol{u})\cdot\bar{\boldsymbol{v}}\,\mathrm{d}\boldsymbol{x} + (\lambda+\mu)\int_{\partial D}(\nabla\cdot\boldsymbol{u})(\boldsymbol{\nu}\cdot(\boldsymbol{p}\cdot\nabla\bar{\boldsymbol{v}}))\,\mathrm{d}\gamma. \end{aligned} \tag{4.35}$$

Next we compute $g_2(\boldsymbol{p})(\boldsymbol{u},\boldsymbol{v})$. It is easy to verify that

$$\begin{aligned} \int_\Omega (\nabla\cdot\boldsymbol{u})(\nabla\bar{\boldsymbol{v}} : J_{\boldsymbol{p}}^\top) + (\nabla\cdot\bar{\boldsymbol{v}})(\nabla\boldsymbol{u} : J_{\boldsymbol{p}}^\top)\,\mathrm{d}\boldsymbol{x} &= \int_\Omega (\nabla\cdot\boldsymbol{u})\nabla\cdot(\boldsymbol{p}\cdot\nabla\bar{\boldsymbol{v}})\,\mathrm{d}\boldsymbol{x} \\ - \int_\Omega (\nabla\cdot\boldsymbol{u})(\boldsymbol{p}\cdot(\nabla\cdot(\nabla\bar{\boldsymbol{v}})^\top))\,\mathrm{d}\boldsymbol{x} &+ \int_\Omega (\nabla\cdot\bar{\boldsymbol{v}})\nabla\cdot(\boldsymbol{p}\cdot\nabla\boldsymbol{u})\,\mathrm{d}\boldsymbol{x} \\ - \int_\Omega (\nabla\cdot\bar{\boldsymbol{v}})(\boldsymbol{p}\cdot(\nabla\cdot(\nabla\boldsymbol{u})^\top))\,\mathrm{d}\boldsymbol{x}. & \end{aligned}$$

Using the integration by parts, we obtain

$$\begin{aligned} \int_\Omega (\nabla\cdot\boldsymbol{p})(\nabla\cdot\boldsymbol{u})(\nabla\cdot\bar{\boldsymbol{v}})\,\mathrm{d}\boldsymbol{x} &= -\int_\Omega \boldsymbol{p}\cdot\nabla((\nabla\cdot\boldsymbol{u})(\nabla\cdot\bar{\boldsymbol{v}}))\,\mathrm{d}\boldsymbol{x} \\ &\quad - \int_{\partial D}(\nabla\cdot\boldsymbol{u})(\nabla\cdot\bar{\boldsymbol{v}})(\boldsymbol{\nu}\cdot\boldsymbol{p})\,\mathrm{d}\gamma \\ = -\int_\Omega (\nabla\cdot\bar{\boldsymbol{v}})(\boldsymbol{p}\cdot(\nabla\cdot(\nabla\boldsymbol{u})^\top))\,\mathrm{d}\boldsymbol{x} &- \int_\Omega (\nabla\cdot\boldsymbol{u})(\boldsymbol{p}\cdot(\nabla\cdot(\nabla\boldsymbol{v})^\top))\,\mathrm{d}\boldsymbol{x} \\ &\quad - \int_{\partial D}(\nabla\cdot\boldsymbol{u})(\nabla\cdot\bar{\boldsymbol{v}})(\boldsymbol{\nu}\cdot\boldsymbol{p})\,\mathrm{d}\gamma. \end{aligned}$$

Let $\boldsymbol{\tau}_1 = (-\nu_3, 0, \nu_1)^\top, \boldsymbol{\tau}_2 = (0, -\nu_3, \nu_2)^\top, \boldsymbol{\tau}_3 = (-\nu_2, \nu_1, 0)^\top$. It follows from $\boldsymbol{\tau}_j\cdot\boldsymbol{\nu} = 0$ that $\boldsymbol{\tau}_j$ are tangent vectors on ∂D. Since $\boldsymbol{v} = 0$ on ∂D, we have $\partial_{\boldsymbol{\tau}_j}\boldsymbol{v} = 0$, which yields that

$$\begin{aligned} &\nu_1\partial_{x_3}v_1 = \nu_3\partial_{x_1}v_1, \quad \nu_1\partial_{x_3}v_2 = \nu_3\partial_{x_1}v_2, \quad \nu_1\partial_{x_2}v_1 = \nu_2\partial_{x_1}v_1, \\ &\nu_1\partial_{x_3}v_3 = \nu_3\partial_{x_1}v_3, \quad \nu_1\partial_{x_2}v_2 = \nu_2\partial_{x_1}v_2, \quad \nu_1\partial_{x_2}v_3 = \nu_2\partial_{x_1}v_3, \\ &\nu_2\partial_{x_3}v_1 = \nu_3\partial_{x_2}v_1, \quad \nu_2\partial_{x_3}v_2 = \nu_3\partial_{x_2}v_2, \quad \nu_2\partial_{x_3}v_3 = \nu_3\partial_{x_2}v_3. \end{aligned}$$

Hence we get

$$\int_{\partial D}(\nabla\cdot\boldsymbol{u})(\nabla\cdot\bar{\boldsymbol{v}})(\boldsymbol{\nu}\cdot\boldsymbol{p})\,\mathrm{d}\gamma = \int_{\partial D}(\nabla\cdot\boldsymbol{u})(\boldsymbol{\nu}\cdot(\boldsymbol{p}\cdot\nabla\bar{\boldsymbol{v}}))\,\mathrm{d}\gamma.$$

Combining the above identities gives

$$g_2(\boldsymbol{p})(\boldsymbol{u},\boldsymbol{v}) = (\lambda+\mu)\int_\Omega (\nabla\cdot\boldsymbol{u})\nabla\cdot(\boldsymbol{p}\cdot\nabla\bar{\boldsymbol{v}})\,\mathrm{d}\boldsymbol{x} + (\lambda+\mu)\int_\Omega \nabla\cdot(\boldsymbol{p}\cdot\nabla\boldsymbol{u})(\nabla\cdot\bar{\boldsymbol{v}})\,\mathrm{d}\boldsymbol{x} - (\lambda+\mu)\int_{\partial D}(\nabla\cdot\boldsymbol{u})(\nu\cdot(\boldsymbol{p}\cdot\nabla\bar{\boldsymbol{v}}))\,\mathrm{d}\gamma. \tag{4.36}$$

Noting (4.34), adding (4.35) and (4.36), we obtain

$$b(\dot{\boldsymbol{u}},\boldsymbol{v}) = \mu\int_\Omega \nabla(\boldsymbol{p}\cdot\nabla\boldsymbol{u}):\nabla\bar{\boldsymbol{v}}\,\mathrm{d}\boldsymbol{x} + (\lambda+\mu)\int_\Omega \nabla\cdot(\boldsymbol{p}\cdot\nabla\boldsymbol{u})(\nabla\cdot\bar{\boldsymbol{v}})\,\mathrm{d}\boldsymbol{x} - \omega^2\int_\Omega(\boldsymbol{p}\cdot\nabla\boldsymbol{u})\cdot\bar{\boldsymbol{v}}\,\mathrm{d}\boldsymbol{x}.$$

Define $\boldsymbol{u}' = \dot{\boldsymbol{u}} - \boldsymbol{p}\cdot\nabla\boldsymbol{u}$. It is clear to note that $\boldsymbol{p}\cdot\nabla\boldsymbol{u} = 0$ on Γ_R since $\boldsymbol{p} = 0$ on Γ_R. Hence, we have

$$b(\boldsymbol{u}',\boldsymbol{v}) = 0, \quad \forall\,\boldsymbol{v}\in\boldsymbol{H}^1_{\partial D}(\Omega), \tag{4.37}$$

which shows that $\boldsymbol{u}'$ is the weak solution of the boundary value problem (4.32). To verify the boundary condition of $\boldsymbol{u}'$ on ∂D, we recall the definition of $\boldsymbol{u}'$ and have from $\breve{\boldsymbol{u}} = \boldsymbol{u} = 0$ on ∂D that

$$\boldsymbol{u}' = \lim_{h\to 0}\frac{\breve{\boldsymbol{u}}-\boldsymbol{u}}{h} - \boldsymbol{p}\cdot\nabla\boldsymbol{u} = -\boldsymbol{p}\cdot\nabla\boldsymbol{u} \quad \text{on } \partial D.$$

Noting $\boldsymbol{u} = 0$ on ∂D, we have

$$\boldsymbol{p}\cdot\nabla\boldsymbol{u} = (\boldsymbol{p}\cdot\boldsymbol{\nu})\partial_{\boldsymbol{\nu}}\boldsymbol{u}, \tag{4.38}$$

which completes the proof by combining (4.37) and (4.38). ■

4.4.2 Reconstruction Method

Consider a parametric equation for the surface:

$$\partial D = \{\boldsymbol{r}(\theta,\varphi) = (r_1(\theta,\varphi), r_2(\theta,\varphi), r_3(\theta,\varphi))^\top,\ \theta\in(0,\pi),\ \varphi\in(0,2\pi)\},$$

where r_j are biperiodic functions of (θ,φ) and have the Fourier series expansions:

$$r_j(\theta,\phi) = \sum_{n=0}^{\infty}\sum_{m=-n}^{n} a_{jn}^m \mathrm{Re}Y_n^m(\theta,\varphi) + b_{jn}^m \mathrm{Im}Y_n^m(\theta,\varphi),$$

where Y_n^m are the spherical harmonics of order n. It suffices to determine a_{jn}^m, b_{jn}^m in order to reconstruct the surface. In practice, a cut-off approximation is needed:

$$r_{j,N}(\theta,\varphi) = \sum_{n=0}^{N}\sum_{m=-n}^{n} a_{jn}^m \mathrm{Re}Y_n^m(\theta,\varphi) + b_{jn}^m \mathrm{Im}Y_n^m(\theta,\varphi).$$

Denote by D_N the approximated obstacle with boundary ∂D_N, which has the parametric equation

$$\partial D_N = \{\boldsymbol{r}_N(\theta,\varphi) = (r_{1,N}(\theta,\varphi), r_{2,N}(\theta,\varphi), r_{3,N}(\theta,\varphi))^\top,\ \theta\in(0,\pi),\ \phi\in(0,2\pi)\}.$$

Let $\Omega_N = B_R\backslash\bar{D}_N$ and

$$\boldsymbol{a}_j = (a_{j0}^0,\cdots,a_{jn}^m,\cdots,a_{jN}^N), \quad \boldsymbol{b}_j = (b_{j0}^0,\cdots,b_{jn}^m,\cdots,b_{jN}^N),$$

where $n = 0,1,\ldots,N,\ m = -n,\ldots,n$. Denote the vector of Fourier coefficients

$$\boldsymbol{C} = (\boldsymbol{a}_1,\boldsymbol{b}_1,\boldsymbol{a}_2,\boldsymbol{b}_2,\boldsymbol{a}_3,\boldsymbol{b}_3)^\top = (c_1,c_2,\ldots,c_{6(N+1)^2})^\top \in \mathbb{R}^{6(N+1)^2}$$

and a vector of scattering data

$$\boldsymbol{U} = (\boldsymbol{u}(\boldsymbol{x}_1),\ldots,\boldsymbol{u}(\boldsymbol{x}_K))^\top \in \mathbb{C}^{3K},$$

where $\boldsymbol{x}_k \in \Gamma_R, k = 1,\ldots,K$. Then the inverse problem can be formulated to solve an approximate nonlinear equation:

$$\mathscr{F}(\boldsymbol{C}) = \boldsymbol{U},$$

where the operator $\mathscr{F}$ maps a vector in $\mathbb{R}^{6(N+1)^2}$ into a vector in $\mathbb{C}^{3K}$.

Theorem 4.4.2 *Let $\boldsymbol{u}_N$ be the solution of (4.25) corresponding to the obstacle D_N. The operator $\mathscr{F}$ is differentiable and its derivatives are*

$$\frac{\partial \mathscr{F}_k(\boldsymbol{C})}{\partial c_i} = \boldsymbol{u}_i'(\boldsymbol{x}_k), \quad i = 1,\ldots,6(N+1)^2,\ k = 1,\ldots,K,$$

where $\boldsymbol{u}_i'$ is the unique weak solution of the boundary value problem

$$\begin{cases} \mu\Delta\boldsymbol{u}_i' + (\lambda+\mu)\nabla\nabla\cdot\boldsymbol{u}_i' + \omega^2\boldsymbol{u}_i' = 0 & \text{in } \Omega_N, \\ \boldsymbol{u}_i' = -q_i\partial_{\boldsymbol{\nu}_N}\boldsymbol{u}_N & \text{on } \partial D_N. \\ \mathscr{B}\boldsymbol{u}_i' = \mathscr{T}\boldsymbol{u}_i' & \text{on } \Gamma_R. \end{cases} \tag{4.39}$$

Here $\boldsymbol{\nu}_N = (\nu_{N1}, \nu_{N2}, \nu_{N3})^\top$ *is the unit normal vector on* ∂D_N *and*

$$q_i(\theta,\varphi) = \begin{cases} \nu_{N1}\mathrm{Re}Y_n^m(\theta,\varphi), & i = n^2+n+m+1, \\ \nu_{N1}\mathrm{Im}Y_n^m(\theta,\varphi), & i = (N+1)^2+n^2+n+m+1, \\ \nu_{N2}\mathrm{Re}Y_n^m(\theta,\varphi), & i = 2(N+1)^2+n^2+n+m+1, \\ \nu_{N2}\mathrm{Im}Y_n^m(\theta,\varphi), & i = 3(N+1)^2+n^2+n+m+1, \\ \nu_{N3}\mathrm{Re}Y_n^m(\theta,\varphi), & i = 4(N+1)^2+n^2+n+m+1, \\ \nu_{N3}\mathrm{Im}Y_n^m(\theta,\varphi), & i = 5(N+1)^2+n^2+n+m+1, \end{cases}$$

where $n = 0, 1, \ldots, N, m = -n, \ldots, n$.

Proof Fix $i \in \{1, \ldots, 6(N+1)^2\}$ and $k \in \{1, \ldots, K\}$, and let $\{\boldsymbol{e}_1, \ldots, \boldsymbol{e}_{6(N+1)^2}\}$ be the set of natural basis vectors in $\mathbb{R}^{6(N+1)^2}$. By definition, we have

$$\frac{\partial \mathscr{F}_k(\boldsymbol{C})}{\partial c_i} = \lim_{h\to 0} \frac{\mathscr{F}_k(\boldsymbol{C}+h\boldsymbol{e}_i) - \mathscr{F}_k(\boldsymbol{C})}{h}.$$

A direct application of Theorem 4.4.1 shows that the above limit exists and the limit is the unique weak solution of the boundary value problem (4.39). ■

Consider the objective function

$$f(\boldsymbol{C}) = \frac{1}{2}\|\mathscr{F}(\boldsymbol{C}) - \boldsymbol{U}\|^2 = \frac{1}{2}\sum_{k=1}^{K} |\mathscr{F}_k(\boldsymbol{C}) - \boldsymbol{u}(\boldsymbol{x}_k)|^2.$$

The inverse problem can be formulated as the minimization problem:

$$\min_{\boldsymbol{C}} f(\boldsymbol{C}), \quad \boldsymbol{C} \in \mathbb{R}^{6(N+1)^2}.$$

To apply the descend method, we compute the gradient of the objective function:

$$\nabla f(\boldsymbol{C}) = \left(\frac{\partial f(\boldsymbol{C})}{\partial c_1}, \ldots, \frac{f(\boldsymbol{C})}{\partial c_{6(N+1)^2}}\right)^\top.$$

We have from Theorem 4.4.2 that

$$\frac{\partial f(\boldsymbol{C})}{\partial c_i} = \mathrm{Re}\sum_{k=1}^{K} \boldsymbol{u}_i'(\boldsymbol{x}_k)\cdot(\bar{\mathscr{F}}_k(\boldsymbol{C}) - \bar{\boldsymbol{u}}(\boldsymbol{x}_k)).$$

We assume that the scattering data $\boldsymbol{U}$ is available over a range of frequencies $\omega \in [\omega_{\min}, \omega_{\max}]$, which may be divided into $\omega_{\min} = \omega_0 < \omega_1 < \cdots < \omega_J = \omega_{\max}$. We now propose an algorithm to reconstruct the Fourier coefficients $c_i, i = 1, \ldots, 6(N+1)^2$.

Algorithm: Frequency continuation algorithm for surface reconstruction.

1. **Initialization**: take an initial guess $c_2 = -c_4 = 1.44472R_0$ and $c_{3(N+1)^2+2} = c_{3(N+1)^2+4} = 1.44472R_0$, $c_{4(N+1)^2+3} = 2.0467R_0$ and $c_i = 0$ otherwise. The initial guess is a ball with radius R_0 under the spherical harmonic functions;

2. **First approximation**: begin with ω_0, let $k_0 = [\omega_0]$, seek an approximation to the functions $r_{j,N}$:

$$r_{j,k_0} = \sum_{n=0}^{k_0} \sum_{m=-n}^{n} a_{jn}^m \mathrm{Re}Y_n^m(\theta, \phi) + b_{jn}^m \mathrm{Im}Y_n^m(\theta, \phi).$$

   Denote $\boldsymbol{C}_{k_0}^{(1)} = (c_1, c_2, \ldots, c_{6(k_0+1)^2})^\top$ and consider the iteration:

$$\mathbf{C}_{k_0}^{(l+1)} = \mathbf{C}_{k_0}^{(l)} - \tau \nabla f(\mathbf{C}_{k_0}^{(l)}), \quad l = 1, \ldots, L, \tag{4.40}$$

   where $\tau > 0$ and $L > 0$ are the step size and the number of iterations for every fixed frequency, respectively.

3. **Continuation**: increase to ω_1, let $k_1 = [\omega_1]$, repeat Step 2 with the previous approximation to $r_{j,N}$ as the starting point. More precisely, approximate $r_{j,N}$ by

$$r_{j,k_1} = \sum_{n=0}^{k_1} \sum_{m=-n}^{n} a_{jn}^m \mathrm{Re}Y_n^m(\theta, \phi) + b_{jn}^m \mathrm{Im}Y_n^m(\theta, \phi),$$

   and determine the coefficients $\tilde{c}_i, i = 1, \ldots, 6(k_1+1)^2$ by using the descent method starting from the previous result.

4. **Iteration**: repeat Step 3 until a prescribed highest frequency ω_J is reached.

4.5 Numerical Experiments

We present two examples to show the effectiveness of the proposed method. The scattering data is obtained from solving the direct problem by using the finite element method with the perfectly matched layer (PML) technique, which is implemented via FreeFem++ [50]. The research on the PML technique has undergone a tremendous development since Berenger proposed a PML for solving the Maxwell equations [20]. The basic idea of the PML technique is to surround the domain of interest by a layer of finite thickness fictitious material which absorbs all the waves coming from inside the computational domain. When the waves reach the outer boundary of the PML region, their values are so small that the homogeneous Dirichlet boundary conditions can be imposed. However, the PML technique is much less studied for the elastic wave scattering problems, especially for the rigorous convergence analysis [22, 30, 60]. In contrast, the transparent boundary condition (TBC) is mathematically exact. It helps to reduce the scattering problem equivalently from an open domain into a boundary value problem in a bounded domain, which makes the analysis feasible. The finite element solution is interpolated uniformly on Γ_R. To test the stability, we add noise to the data:

$$\boldsymbol{u}^\delta(\boldsymbol{x}_k) = \boldsymbol{u}(\boldsymbol{x}_k)(1 + \delta\,\mathrm{rand}), \quad k = 1, \ldots, K,$$

where rand are uniformly distributed random numbers in $[-1,\ 1]$ and δ is the noise level, $\boldsymbol{x}_k$ are the data points. In our experiments, we pick 100 uniformly distributed points $\boldsymbol{x}_k$ on Γ_R, i.e., $K = 100$. We take $\lambda = 2, \mu = 1$, $R = 1$. The radius of the initial $R_0 = 0.5$. The noise level $\delta = 5\%$. The step size in (4.40) is $\tau = 0.005/k_i$ where $k_i = [\omega_i]$. The incident field is taken as a plane compressional wave.

Example 1. Consider a bean-shaped obstacle:

$$\boldsymbol{r}(\theta, \varphi) = (r_1(\theta, \varphi), r_2(\theta, \varphi), r_3(\theta, \varphi))^\top,\ \theta \in [0, \pi],\ \varphi \in [0, 2\pi],$$

where

$$r_1(\theta,\varphi) = 0.75\left((1-0.05\cos(\pi\cos\theta))\sin\theta\cos\varphi\right)^{1/2},$$
$$r_2(\theta,\varphi) = 0.75\left((1-0.005\cos(\pi\cos\theta))\sin\theta\sin\varphi + 0.35\cos(\pi\cos\theta)\right)^{1/2},$$
$$r_3(\theta,\varphi) = 0.75\cos\theta.$$

The exact surface is plotted in Figure 4.1(a). This obstacle is non-convex and is usually difficult to reconstruct the concave part of the obstacle. The obstacle is illuminated by the compressional wave sent from a single direction $\boldsymbol{d} = (0,1,0)^\top$; the frequency ranges from $\omega_{\min} = 1$ to $\omega_{\max} = 5$ with increment 1 at each continuation step, i.e., $\omega_i = i+1, i = 0,\ldots,4$; for any fixed frequency, repeat $L = 100$ times with previous result as starting points. The step size for the decent method is $0.005/\omega_i$. The number of recovered coefficients is $6(\omega_i+2)^2$ for corresponding frequency. Figure 4.1(b) shows the initial guess which is the ball with radius $R_0 = 0.5$; Figure 4.1(c) shows the final reconstructed surface; Figures 4.1(d)–(f) show the cross section of the exact surface along the plane $x_1 = 0, x_2 = 0, x_3 = 0$, respectively; Figures 4.1(g)–(i) show the corresponding cross section for the reconstructed surface along the plane $x_1 = 0, x_2 = 0, x_3 = 0$, respectively. As is seen, the algorithm effectively reconstructs the bean-shaped obstacle.

Example 2. Consider a cushion-shaped obstacle:

$$\boldsymbol{r}(\theta,\varphi) = r(\theta,\varphi)(\sin(\theta)\cos(\varphi),\sin(\theta)\sin(\varphi),\cos(\theta))^\top,\ \theta\in[0,\pi],\ \varphi\in[0,2\pi],$$

where

$$r(\theta,\varphi) = \left(0.75 + 0.45(\cos(2\varphi)-1)(\cos(4\theta)-1)\right)^{1/2}.$$

Figure 4.2(a) shows the exact surface. This example is much more complex than the bean-shaped obstacle due to its multiple concave parts. Multiple incident directions are needed in order to obtain a good result. In this example, the obstacle is illuminated by the compressional wave from 6 directions, which are the unit vectors pointing to the origin from the face centers of the cube. The multiple frequencies are the same as the first example, i.e., the frequency ranges from $\omega_{\min} = 1$ to $\omega_{\max} = 5$ with

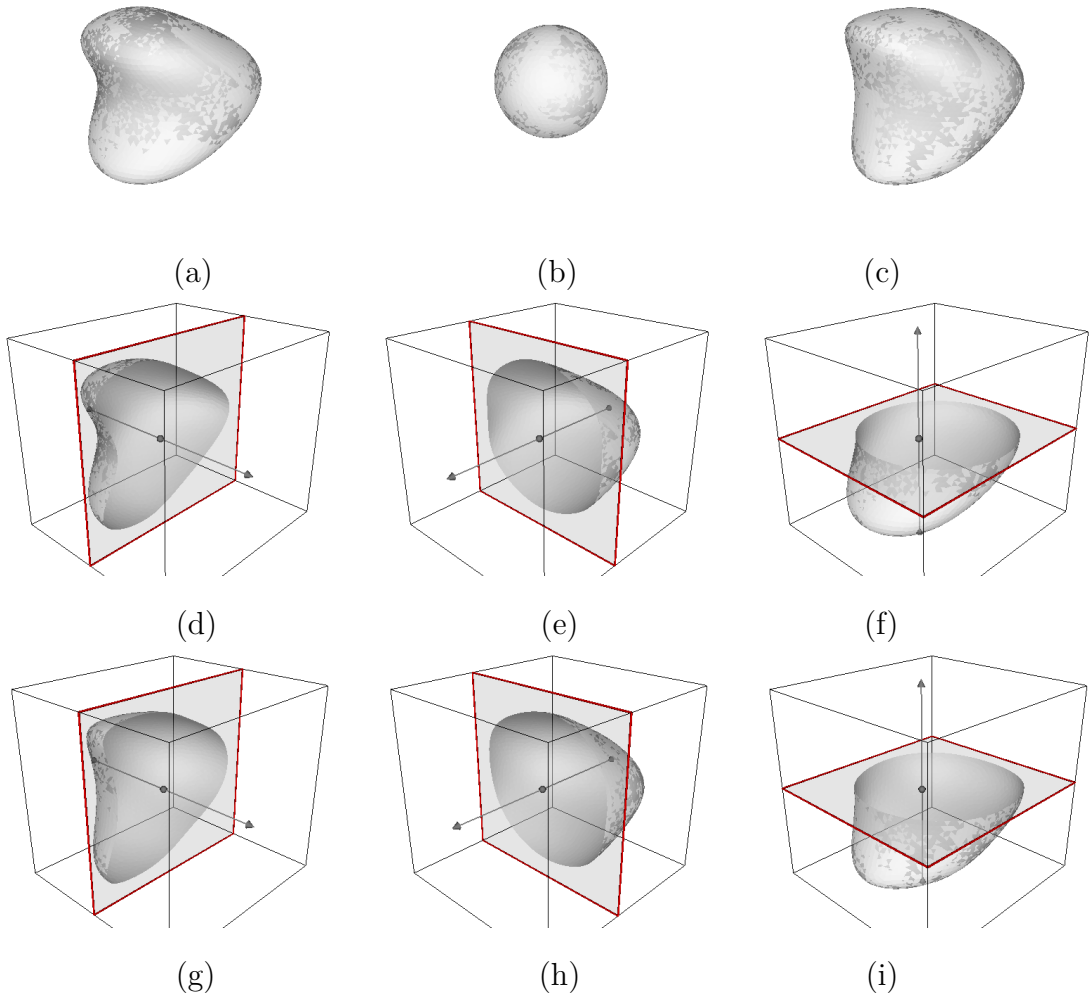

Figure 4.1. Example 1: A bean-shaped obstacle. (a) the exact surface; (b) the initial guess; (c) the reconstructed surface; (d)–(f) the corresponding cross section of the exact surface along plane $x_1 = 0, x_2 = 0, x_3 = 0$, respectively; (g)–(i) the corresponding cross section of the reconstructed surface along plane $x_1 = 0, x_2 = 0, x_3 = 0$, respectively.

$\omega_i = i+1, i = 0, \ldots, 4$. For each fixed frequency and incident direction, repeat $L = 50$ times with previous result as starting points. The step size for the decent method is $0.005/\omega_i$ and number of recovered coefficients is $6(\omega_i+2)^2$ for corresponding frequency. Figure 4.2(b) shows the initial guess ball with radius $R_0 = 0.5$; Figure 4.2(c) shows the final reconstructed surface; Figure 4.2(d)–(f) show the cross section of the exact

surface along the plane $x_1 = 0, x_2 = 0, x_3 = 0$, respectively; while Figure 4.2(g)–(i) show the corresponding cross section for the reconstructed surface along the plane $x_1 = 0, x_2 = 0, x_3 = 0$, respectively. It is clear to note that the algorithm can also reconstruct effectively the more complex cushion-shaped obstacle.

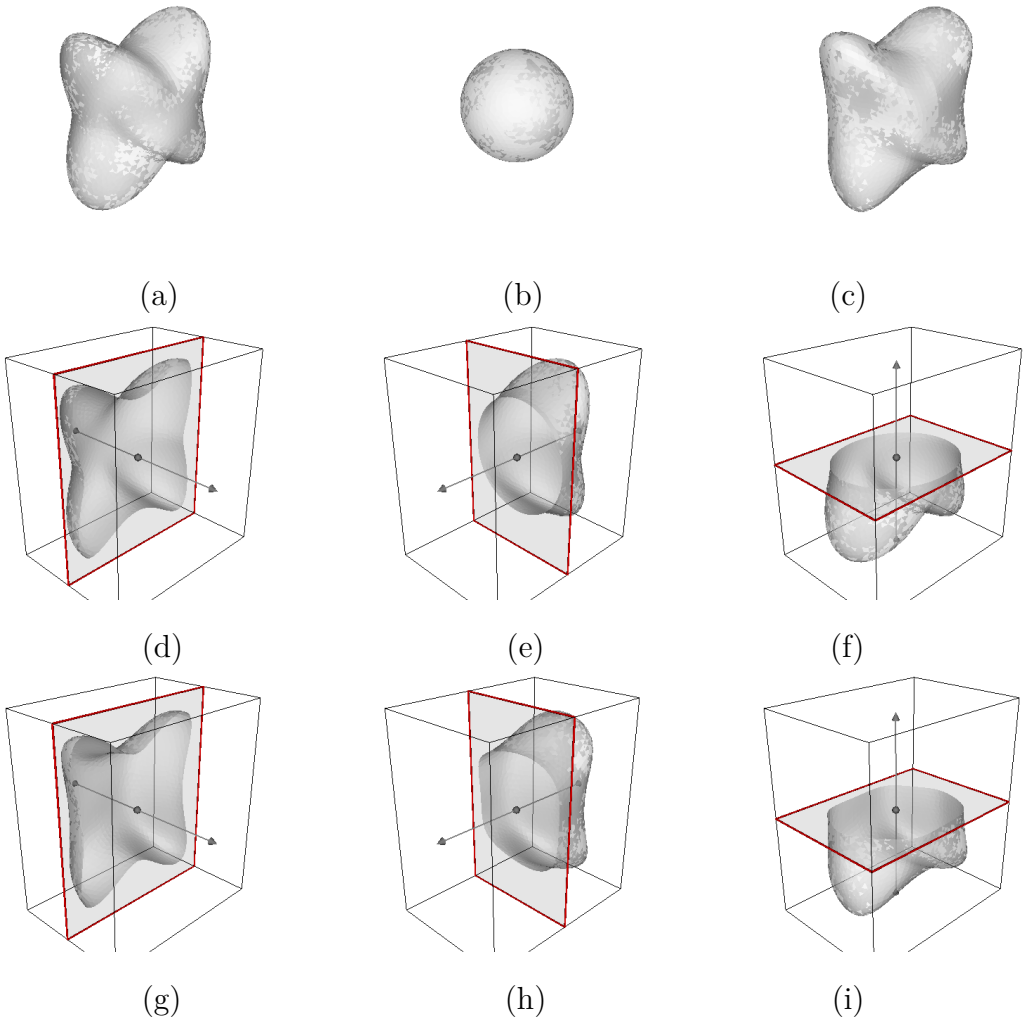

Figure 4.2. Example 2: A cushion-shaped obstacle. (a) the exact surface; (b) the initial guess; (c) the reconstructed surface; (d)–(f) the corresponding cross section of the exact surface along the plane $x_1 = 0, x_2 = 0, x_3 = 0$, respectively; (d)–(f) the corresponding cross section of the reconstructed surface along the plane $x_1 = 0, x_2 = 0, x_3 = 0$, respectively.

4.6 Conclusion

In this chapter, we study the direct and inverse obstacle scattering problems for elastic waves in three dimensions. An exact transparent boundary condition is developed. The direct problem is shown to have a unique weak solution. The domain derivative is derived for the total displacement. A frequency continuation method is proposed to solve the inverse problem. Numerical examples are presented to demonstrate the effectiveness of the proposed method. The results show that the method is stable and accurate to reconstruct surfaces with noise.

4.7 Appendix

4.7.1 Spherical Harmonics

The spherical coordinates (r, θ, φ) are related to the Cartesian coordinates $\boldsymbol{x} = (x_1, x_2, x_3)$ by $x_1 = r\sin\theta\cos\varphi, x_2 = r\sin\theta\sin\varphi, x_3 = r\cos\theta$. The local orthonormal basis is

$$\begin{aligned}
\boldsymbol{e}_r &= (\sin\theta\cos\varphi, \sin\theta\sin\varphi, \cos\theta),\\
\boldsymbol{e}_\theta &= (\cos\theta\cos\varphi, \cos\theta\sin\varphi, -\sin\theta),\\
\boldsymbol{e}_\varphi &= (-\sin\varphi, \cos\varphi, 0),
\end{aligned}$$

where θ and φ are the Euler angles. Note that $\boldsymbol{e}_r$ is also the unit outward normal vector on Γ_R.

Let $\{Y_n^m(\theta,\varphi) : n = 0, 1, 2, \ldots, m = -n, \ldots, n\}$ be the orthonormal sequence of spherical harmonics of order n on the unit sphere. Define rescaled spherical harmonics

$$X_n^m(\theta,\varphi) = \frac{1}{R} Y_n^m(\theta,\varphi).$$

It can be shown that $\{X_n^m(\theta,\varphi) : n = 0, 1, \ldots, m = -n, \ldots, n\}$ form a complete orthonormal system in $L^2(\Gamma_R)$, which is the space of square integrable functions on Γ_R.

For a smooth scalar function $u(R,\theta,\varphi)$ defined on Γ_R, let

$$\nabla_{\Gamma_R} u = \partial_\theta u\, \boldsymbol{e}_\theta + (\sin\theta)^{-1}\partial_\varphi u\, \boldsymbol{e}_\varphi$$

be the tangential gradient on Γ_R. The surface vector curl is defined by

$$\mathbf{curl}_{\Gamma_R} u = \nabla_{\Gamma_R} u \times \boldsymbol{e}_r.$$

Denote by div_{Γ_R} and curl_{Γ_R} the surface divergence and the surface scalar curl, respectively. For a smooth vector function $\boldsymbol{u}$ tangential to Γ_R, it can be represented by its coordinates in the local orthonormal basis:

$$\boldsymbol{u} = u_\theta \boldsymbol{e}_\theta + u_\varphi \boldsymbol{e}_\varphi,$$

where

$$u_\theta = \boldsymbol{u}\cdot\boldsymbol{e}_\theta, \quad u_\varphi = \boldsymbol{u}\cdot\boldsymbol{e}_\varphi.$$

The surface divergence and the surface scalar curl can be defined as

$$\begin{aligned}
\mathrm{div}_{\Gamma_R}\boldsymbol{u} &= (\sin\theta)^{-1}\left(\partial_\theta(u_\theta\sin\theta) + \partial_\varphi u_\varphi\right),\\
\mathrm{curl}_{\Gamma_R}\boldsymbol{u} &= (\sin\theta)^{-1}\left(\partial_\theta(u_\varphi\sin\theta) - \partial_\varphi u_\theta\right).
\end{aligned}$$

Define a sequence of vector spherical harmonics:

$$\begin{aligned}
\boldsymbol{T}_n^m(\theta,\varphi) &= \frac{1}{\sqrt{n(n+1)}}\nabla_{\Gamma_R} X_n^m(\theta,\varphi),\\
\boldsymbol{V}_n^m(\theta,\varphi) &= \boldsymbol{T}_n^m(\theta,\varphi)\times\boldsymbol{e}_r,\\
\boldsymbol{W}_n^m(\theta,\varphi) &= X_n^m(\theta,\varphi)\boldsymbol{e}_r,
\end{aligned}$$

where $n = 0,1,\ldots, m = -n,\ldots,n$. Using the orthogonality of the vector spherical harmonics, we can easily show that

1. $\{(\boldsymbol{T}_n^m, \boldsymbol{V}_n^m, \boldsymbol{W}_n^m) : n = 0,1,2,\ldots, m = -n,\ldots,n\}$ form a complete orthonormal system in $\boldsymbol{L}^2(\Gamma_R) = L^2(\Gamma_R)^3$;

2. $\{(\boldsymbol{T}_n^m, \boldsymbol{V}_n^m) : n = 0,1,2,\ldots, m = -n,\ldots,n\}$ form a complete orthonormal system in $\boldsymbol{L}_{\mathrm{t}}^2(\Gamma_R) = \{\boldsymbol{w}\in\boldsymbol{L}^2(\Gamma_R), \boldsymbol{w}\cdot\boldsymbol{e}_r = 0\}$.

4.7.2 Functional Spaces

Denote by $L^2(\Omega)$ the square integrable functions on Ω. Let $\boldsymbol{L}^2(\Omega) = L^2(\Omega)^3$ be equipped with the inner product and norm:

$$(\boldsymbol{u}, \boldsymbol{v}) = \int_\Omega \boldsymbol{u} \cdot \bar{\boldsymbol{v}} \, \mathrm{d}\boldsymbol{x}, \quad \|\boldsymbol{u}\|_{\boldsymbol{L}^2(\Omega)} = (\boldsymbol{u}, \boldsymbol{u})^{1/2}.$$

Denote by $H^1(\Omega)$ the standard Sobolev space with the norm given by

$$\|u\|_{H^1(\Omega)} = \left(\int_\Omega |u(\boldsymbol{x})|^2 + |\nabla u(\boldsymbol{x})|^2 \, \mathrm{d}\boldsymbol{x} \right)^{1/2}.$$

Let $\boldsymbol{H}^1_{\partial D}(\Omega) = H^1_{\partial D}(\Omega)^3$, where $H^1_{\partial D}(\Omega) := \{u \in H^1(\Omega) : u = 0 \text{ on } \partial D\}$. Introduce the Sobolev space

$$\boldsymbol{H}(\mathrm{curl}, \Omega) = \{\boldsymbol{u} \in \boldsymbol{L}^2(\Omega), \nabla \times \boldsymbol{u} \in \boldsymbol{L}^2(\Omega)\},$$

which is equipped with the norm

$$\|\boldsymbol{u}\|_{\boldsymbol{H}(\mathrm{curl},\Omega)} = \left(\|\boldsymbol{u}\|^2_{\boldsymbol{L}^2(\Omega)} + \|\nabla \times \boldsymbol{u}\|^2_{\boldsymbol{L}^2(\Omega)} \right)^{1/2}.$$

Denote by $H^s(\Gamma_R)$ the standard trace functional space which is equipped with the norm

$$\|u\|_{H^s(\Gamma_R)} = \left(\sum_{n=0}^{\infty} \sum_{m=-n}^{n} (1 + n(n+1))^s |u_n^m|^2 \right)^{1/2},$$

where

$$u(R, \theta, \varphi) = \sum_{n=0}^{\infty} \sum_{m=-n}^{n} u_n^m X_n^m(\theta, \varphi).$$

Let $\boldsymbol{H}^s(\Gamma_R) = H^s(\Gamma_R)^3$ which is equipped with the normal

$$\|\boldsymbol{u}\|_{\boldsymbol{H}^s(\Gamma_R)} = \left(\sum_{n=0}^{\infty} \sum_{m=-n}^{n} (1 + n(n+1))^s |\boldsymbol{u}_n^m|^2 \right)^{1/2},$$

where $\boldsymbol{u}_n^m = (u_{1n}^m, u_{2n}^m, u_{3n}^m)$ and

$$\boldsymbol{u}(R, \theta, \varphi) = \sum_{n=0}^{\infty} \sum_{m=-n}^{n} u_{1n}^m \boldsymbol{T}_n^m(\theta, \varphi) + u_{2n}^m \boldsymbol{V}_n^m(\theta, \varphi) + u_{3n}^m \boldsymbol{W}_n^m(\theta, \varphi).$$

It can be verified that $\boldsymbol{H}^{-s}(\Gamma_R)$ is the dual space of $\boldsymbol{H}^{s}(\Gamma_R)$ with respect to the inner product

$$\langle \boldsymbol{u}, \boldsymbol{v} \rangle_{\Gamma_R} = \int_{\Gamma_R} \boldsymbol{u} \cdot \bar{\boldsymbol{v}} \, \mathrm{d}\gamma = \sum_{n=0}^{\infty} \sum_{m=-n}^{n} u_{1n}^m \bar{v}_{1n}^m + u_{2n}^m \bar{v}_{2n}^m + u_{3n}^m \bar{v}_{3n}^m,$$

where

$$\boldsymbol{v}(R,\theta,\varphi) = \sum_{n=0}^{\infty} \sum_{m=-n}^{n} v_{1n}^m \boldsymbol{T}_n^m(\theta,\varphi) + v_{2n}^m \boldsymbol{V}_n^m(\theta,\varphi) + v_{3n}^m \boldsymbol{W}_n^m(\theta,\varphi).$$

Introduce three tangential trace spaces:

$$\begin{aligned}
\boldsymbol{H}_{\mathrm{t}}^{s}(\Gamma_R) &= \{\boldsymbol{u} \in \boldsymbol{H}^{s}(\Gamma_R),\ \boldsymbol{u} \cdot \boldsymbol{e}_r = 0\}, \\
\boldsymbol{H}^{-1/2}(\mathrm{curl}, \Gamma_R) &= \{\boldsymbol{u} \in \boldsymbol{H}_{\mathrm{t}}^{-1/2}(\Gamma_R),\ \mathrm{curl}_{\Gamma_R} \boldsymbol{u} \in H^{-1/2}(\Gamma_R)\}, \\
\boldsymbol{H}^{-1/2}(\mathrm{div}, \Gamma_R) &= \{\boldsymbol{u} \in \boldsymbol{H}_{\mathrm{t}}^{-1/2}(\Gamma_R),\ \mathrm{div}_{\Gamma_R} \boldsymbol{u} \in H^{-1/2}(\Gamma_R)\}.
\end{aligned}$$

For any tangential field $\boldsymbol{u} \in \boldsymbol{H}_{\mathrm{t}}^{s}(\Gamma_R)$, it can be represented in the series expansion

$$\boldsymbol{u}(R,\theta,\varphi) = \sum_{n=0}^{\infty} \sum_{m=-n}^{n} u_{1n}^m \boldsymbol{T}_n^m(\theta,\varphi) + u_{2n}^m \boldsymbol{V}_n^m(\theta,\varphi).$$

Using the series coefficients, the norm of the space $\boldsymbol{H}_{\mathrm{t}}^{s}(\Gamma_R)$ can be characterized by

$$\|\boldsymbol{u}\|^2_{\boldsymbol{H}_{\mathrm{t}}^{s}(\Gamma_R)} = \sum_{n=0}^{\infty} \sum_{m=-n}^{n} (1 + n(n+1))^s \left(|u_{1n}^m|^2 + |u_{2n}^m|^2 \right);$$

the norm of the space $\boldsymbol{H}^{-1/2}(\mathrm{curl}, \Gamma_R)$ can be characterized by

$$\|\boldsymbol{u}\|^2_{\boldsymbol{H}^{-1/2}(\mathrm{curl},\Gamma_R)} = \sum_{n=0}^{\infty} \sum_{m=-n}^{n} \frac{1}{\sqrt{1+n(n+1)}} |u_{1n}^m|^2 + \sqrt{1+n(n+1)} |u_{2n}^m|^2;$$

the norm of the space $\boldsymbol{H}^{-1/2}(\mathrm{div}, \Gamma_R)$ can be characterized by

$$\|\boldsymbol{u}\|^2_{\boldsymbol{H}^{-1/2}(\mathrm{div},\Gamma_R)} = \sum_{n=0}^{\infty} \sum_{m=-n}^{n} \sqrt{1+n(n+1)} |u_{1n}^m|^2 + \frac{1}{\sqrt{1+n(n+1)}} |u_{2n}^m|^2.$$

Given a vector field $\boldsymbol{u}$ on Γ_R, denote by

$$\boldsymbol{u}_{\Gamma_R} = -\boldsymbol{e}_r \times (\boldsymbol{e}_r \times \boldsymbol{u})$$

the tangential component of $\boldsymbol{u}$ on Γ_R. Define the inner product in $\mathbb{C}^3$:

$$\langle \boldsymbol{u}, \boldsymbol{v} \rangle = \boldsymbol{v}^* \boldsymbol{u}, \quad \forall\, \boldsymbol{u}, \boldsymbol{v} \in \mathbb{C}^3.$$

where $\boldsymbol{v}^*$ is the conjugate transpose of $\boldsymbol{v}$.

4.7.3 TBC for Potential Functions

It follows from the Helmholtz decomposition (4.7) that any solution of (4.6) can be written as

$$\boldsymbol{v} = \nabla\phi + \nabla \times \boldsymbol{\psi}, \quad \nabla \cdot \boldsymbol{\psi} = 0,$$

where the scalar potential function ϕ satisfies (4.8) and (4.9):

$$\begin{cases} \Delta\phi + \kappa_{\mathrm{p}}^2\phi = 0 & \text{in } \mathbb{R}^3\backslash\bar{D}, \\ \partial_r\phi - \mathrm{i}\kappa_{\mathrm{p}}\phi = o(r^{-1}) & \text{as } r \to \infty, \end{cases} \tag{4.41}$$

and the vector potential function $\boldsymbol{\psi}$ satisfies (4.10) and (4.11):

$$\begin{cases} \nabla \times (\nabla \times \boldsymbol{\psi}) - \kappa_{\mathrm{s}}^2\boldsymbol{\psi} = 0 & \text{in } \mathbb{R}^3\backslash\bar{D}, \\ (\nabla \times \boldsymbol{\psi}) \times \hat{\boldsymbol{x}} - \mathrm{i}\kappa_{\mathrm{s}}\boldsymbol{\psi} = o(r^{-1}) & \text{as } r \to \infty, \end{cases} \tag{4.42}$$

where $r = |\boldsymbol{x}|$ and $\hat{\boldsymbol{x}} = \boldsymbol{x}/r$.

In this section, we introduce the TBC for the scalar potential function ϕ and the vector potential function $\boldsymbol{\psi}$, respectively. The TBCs help to reduce (4.41) and (4.42) equivalently from the open domain $\mathbb{R}^3\backslash\bar{D}$ into the bounded domain Ω.

In the exterior domain $\mathbb{R}^3\backslash\bar{B}_R$, the solution ϕ of (4.41) has the following Fourier expansion in the spherical coordinates:

$$\phi(r,\theta,\varphi) = \sum_{n=0}^{\infty}\sum_{m=-n}^{n} \frac{h_n^{(1)}(\kappa_{\mathrm{p}} r)}{h_n^{(1)}(\kappa_{\mathrm{p}} R)}\phi_n^m X_n^m(\theta,\varphi), \tag{4.43}$$

where $h_n^{(1)}$ is the spherical Hankel function of the first kind with order n and the Fourier coefficient

$$\phi_n^m = \int_{\Gamma_R} \phi(R,\theta,\varphi)\bar{X}_n^m(\theta,\varphi)\mathrm{d}\gamma.$$

We define the boundary operator $\mathscr{T}_1$ such that

$$(\mathscr{T}_1\phi)(R,\theta,\varphi) = \frac{1}{R}\sum_{n=0}^{\infty}\sum_{m=-n}^{n} z_n(\kappa_{\mathrm{p}} R)\phi_n^m X_n^m(\theta,\varphi), \tag{4.44}$$

where

$$z_n(t) = \frac{t h_n^{(1)'}(t)}{h_n^{(1)}(t)}$$

satisfies (cf. [82, Theorem 2.6.1])

$$-(n+1) \leqslant \mathrm{Re} z_n(t) \leqslant -1, \quad 0 < \mathrm{Im} z_n(t) \leqslant t. \tag{4.45}$$

Evaluating the derivative of (4.43) with respect to r at $r = R$ and using (4.44), we get the transparent boundary condition for the scalar potential function ϕ:

$$\partial_r \phi = \mathscr{T}_1 \phi \quad \text{on } \Gamma_R. \tag{4.46}$$

The following result can be easily shown from (4.44)–(4.45).

Lemma 4.7.1 *The operator $\mathscr{T}_1$ is bounded from $H^{1/2}(\Gamma_R)$ to $H^{-1/2}(\Gamma_R)$. Moreover, it satisfies*

$$\mathrm{Re}\langle \mathscr{T}_1 u, u\rangle_{\Gamma_R} \leqslant 0, \quad \mathrm{Im}\langle \mathscr{T}_1 u, u\rangle_{\Gamma_R} \geqslant 0, \quad \forall u \in H^{1/2}(\Gamma_R).$$

If $\mathrm{Re}\langle \mathscr{T}_1 u, u\rangle_{\Gamma_R} = 0$ or $\mathrm{Im}\langle \mathscr{T}_1 u, u\rangle_{\Gamma_R} = 0$, then $u = 0$ on Γ_R.

Next is to derive the TBC for the vector potential function $\boldsymbol{\psi}$. Define an auxiliary function $\boldsymbol{\varphi} = (\mathrm{i}\kappa_{\mathrm{s}})^{-1}\nabla \times \boldsymbol{\psi}$. We have from (4.42) that

$$\nabla \times \boldsymbol{\psi} - \mathrm{i}\kappa_{\mathrm{s}} \boldsymbol{\varphi} = 0, \quad \nabla \times \boldsymbol{\varphi} + \mathrm{i}\kappa_{\mathrm{s}} \boldsymbol{\psi} = 0, \tag{4.47}$$

which are Maxwell's equations. Hence $\boldsymbol{\phi}$ and $\boldsymbol{\psi}$ plays the role of the electric field and the magnetic field, respectively.

Introduce the vector wave functions

$$\begin{cases} \boldsymbol{M}_n^m(r,\theta,\varphi) = \nabla \times (\boldsymbol{x} h_n^{(1)}(\kappa_{\mathrm{s}} r) X_n^m(\theta,\varphi)), \\ \boldsymbol{N}_n^m(r,\theta,\varphi) = (\mathrm{i}\kappa_{\mathrm{s}})^{-1}\nabla \times \boldsymbol{M}_n^m(r,\theta,\varphi), \end{cases} \tag{4.48}$$

which are the radiation solutions of (4.47) in $\mathbb{R}^3\backslash\{0\}$ (cf. [80, Theorem 9.16]):

$$\nabla \times \boldsymbol{M}_n^m(r,\theta,\varphi) - \mathrm{i}\kappa_{\mathrm{s}} \boldsymbol{N}_n^m(r,\theta,\varphi) = 0, \quad \nabla \times \boldsymbol{N}_n^m(r,\theta,\varphi) + \mathrm{i}\kappa_{\mathrm{s}} \boldsymbol{M}_n^m(r,\theta,\varphi) = 0.$$

Moreover, it can be verified from (4.48) that they satisfy

$$\boldsymbol{M}_n^m = h_n^{(1)}(\kappa_{\mathrm{s}} r) \nabla_{\Gamma_R} X_n^m \times \boldsymbol{e}_r \tag{4.49}$$

and

$$\boldsymbol{N}_n^m = \frac{\sqrt{n(n+1)}}{\mathrm{i}\kappa_{\mathrm{s}} r}(h_n^{(1)}(\kappa_{\mathrm{s}} r) + \kappa_{\mathrm{s}} r h_n^{(1)'}(\kappa_{\mathrm{s}} r))\boldsymbol{T}_n^m + \frac{n(n+1)}{\mathrm{i}\kappa_{\mathrm{s}} r} h_n^{(1)}(\kappa_{\mathrm{s}} r)\boldsymbol{W}_n^m. \quad (4.50)$$

In the domain $\mathbb{R}^3\backslash\bar{B}_R$, the solution of $\boldsymbol{\psi}$ in (4.47) can be written in the series

$$\boldsymbol{\psi} = \sum_{n=0}^{\infty}\sum_{m=-n}^{n} \alpha_n^m \boldsymbol{N}_n^m + \beta_n^m \boldsymbol{M}_n^m, \quad (4.51)$$

which is uniformly convergent on any compact subsets in $\mathbb{R}^3\backslash\bar{B}_R$. Correspondingly, the solution of $\boldsymbol{\varphi}$ in (4.47) is given by

$$\boldsymbol{\varphi} = (\mathrm{i}\kappa_{\mathrm{s}})^{-1}\nabla\times\boldsymbol{\psi} = \sum_{n=0}^{\infty}\sum_{m=-n}^{n} \beta_n^m \boldsymbol{N}_n^m - \alpha_n^m \boldsymbol{M}_n^m. \quad (4.52)$$

It follows from (4.49)–(4.50) that

$$\begin{aligned} -\boldsymbol{e}_r\times(\boldsymbol{e}_r\times\boldsymbol{M}_n^m) &= -\sqrt{n(n+1)}h_n^{(1)}(\kappa_{\mathrm{s}} r)\boldsymbol{V}_n^m, \\ -\boldsymbol{e}_r\times(\boldsymbol{e}_r\times\boldsymbol{N}_n^m) &= \frac{\sqrt{n(n+1)}}{\mathrm{i}\kappa_{\mathrm{s}} r}(h_n^{(1)}(\kappa_{\mathrm{s}} r) + \kappa_{\mathrm{s}} r h_n^{(1)'}(\kappa_{\mathrm{s}} r))\boldsymbol{T}_n^m \end{aligned}$$

and

$$\begin{aligned} \boldsymbol{e}_r\times\boldsymbol{M}_n^m &= \sqrt{n(n+1)}h_n^{(1)}(\kappa_{\mathrm{s}} r)\boldsymbol{T}_n^m, \\ \boldsymbol{e}_r\times\boldsymbol{N}_n^m &= \frac{\sqrt{n(n+1)}}{\mathrm{i}\kappa_{\mathrm{s}} r}(h_n^{(1)}(\kappa_{\mathrm{s}} r) + \kappa_{\mathrm{s}} r h_n^{(1)'}(\kappa_{\mathrm{s}} r))\boldsymbol{V}_n^m. \end{aligned}$$

Therefore, by (4.51), the tangential component of $\boldsymbol{\psi}$ on Γ_R is

$$\begin{aligned} \boldsymbol{\psi}_{\Gamma_R} = \sum_{n=0}^{\infty}\sum_{m=-n}^{n} &\frac{\sqrt{n(n+1)}}{\mathrm{i}\kappa_{\mathrm{s}} R}(h_n^{(1)}(\kappa_{\mathrm{s}} R) + \kappa_{\mathrm{s}} R h_n^{(1)'}(\kappa_{\mathrm{s}} R))\alpha_n^m \boldsymbol{T}_n^m \\ &+ \sqrt{n(n+1)}h_n^{(1)}(\kappa_{\mathrm{s}} R)\beta_n^m \boldsymbol{V}_n^m. \end{aligned}$$

Similarly, by (4.52), the tangential trace of $\boldsymbol{\varphi}$ on Γ_R is

$$\begin{aligned} \boldsymbol{\varphi}\times\boldsymbol{e}_r = \sum_{n=0}^{\infty}\sum_{m=-n}^{n} &\sqrt{n(n+1)}h_n^{(1)}(\kappa_{\mathrm{s}} R)\alpha_n^m \boldsymbol{T}_n^m \\ &- \frac{\sqrt{n(n+1)}}{\mathrm{i}\kappa_{\mathrm{s}} R}(h_n^{(1)}(\kappa_{\mathrm{s}} R) + \kappa_{\mathrm{s}} R h_n^{(1)'}(\kappa_{\mathrm{s}} R))\beta_n^m \boldsymbol{V}_n^m. \end{aligned}$$

Given any tangential component of the electric field on Γ_R with the expression

$$\boldsymbol{u} = \sum_{n=0}^{\infty} \sum_{m=-n}^{n} u_{1n}^m \boldsymbol{T}_n^m + u_{2n}^m \boldsymbol{V}_n^m,$$

where

$$u_{1n}^m = \int_{\Gamma_R} \boldsymbol{u}(R,\theta,\varphi) \cdot \bar{\boldsymbol{T}}_n^m(\theta,\varphi) \mathrm{d}\gamma, \quad u_{2n}^m = \int_{\Gamma_R} \boldsymbol{u}(R,\theta,\varphi) \cdot \bar{\boldsymbol{V}}_n^m(\theta,\varphi) \mathrm{d}\gamma,$$

we define

$$\mathscr{T}_2 \boldsymbol{u} = \sum_{n=0}^{\infty} \sum_{m=-n}^{n} \frac{\mathrm{i}\kappa_\mathrm{s} R}{1 + z_n(\kappa_\mathrm{s} R)} u_{1n}^m \boldsymbol{T}_n^m + \frac{1 + z_n(\kappa_\mathrm{s} R)}{\mathrm{i}\kappa_\mathrm{s} R} u_{2n}^m \boldsymbol{V}_n^m. \tag{4.53}$$

Using (4.53), we obtain the TBC for the vector potential $\boldsymbol{\psi}$:

$$(\nabla \times \boldsymbol{\psi}) \times \boldsymbol{e}_r = \mathrm{i}\kappa_\mathrm{s} \mathscr{T}_2 \boldsymbol{\psi}_{\Gamma_R} \quad \text{on } \Gamma_R. \tag{4.54}$$

The following result can also be easily shown from (4.45) and (4.53)

Lemma 4.7.2 *The operator $\mathscr{T}_2$ is bounded from $\boldsymbol{H}^{1/2}(\mathrm{curl}, \Gamma_R)$ to $\boldsymbol{H}^{-1/2}(\mathrm{div}, \Gamma_R)$. Moreover, it satisfies*

$$\mathrm{Re}\langle \mathscr{T}_2 \boldsymbol{u}, \boldsymbol{u} \rangle_{\Gamma_R} \geqslant 0, \quad \forall \boldsymbol{u} \in \boldsymbol{H}^{1/2}(\mathrm{curl}, \Gamma_R).$$

If $\mathrm{Re}\langle \mathscr{T}_2 \boldsymbol{u}, \boldsymbol{u} \rangle_{\Gamma_R} = 0$, then $\boldsymbol{u} = 0$ on Γ_R.

apt

4.7.4 Fourier Coefficients

Recalling the Helmholtz decomposition (4.7):

$$\boldsymbol{v} = \nabla\phi + \nabla \times \boldsymbol{\psi}, \quad \nabla \cdot \boldsymbol{\psi} = 0,$$

we derive the mutual representations of the Fourier coefficients between $\boldsymbol{v}$ and $(\phi, \boldsymbol{\psi})$.

First we have from (4.43) that

$$\phi(r,\theta,\varphi) = \sum_{n=0}^{\infty} \sum_{m=-n}^{n} \frac{h_n^{(1)}(\kappa_\mathrm{p} r)}{h_n^{(1)}(\kappa_\mathrm{p} R)} \phi_n^m X_n^m(\theta,\varphi). \tag{4.55}$$

Substituting (4.49)–(4.50) into (4.51) yields

$$\boldsymbol{\psi}(r,\theta,\varphi) = \sum_{n=0}^{\infty}\sum_{m=-n}^{n} \frac{\sqrt{n(n+1)}}{\mathrm{i}\kappa_{\mathrm{s}} r}(h_n^{(1)}(\kappa_{\mathrm{s}} r) + \kappa_{\mathrm{s}} r h_n^{(1)'}(\kappa_{\mathrm{s}} r))\alpha_n^m \boldsymbol{T}_n^m + \sqrt{n(n+1)}h_n^{(1)}(\kappa_{\mathrm{s}} r)\beta_n^m \boldsymbol{V}_n^m + \frac{n(n+1)}{\mathrm{i}\kappa_{\mathrm{s}} r}h_n^{(1)}(\kappa_{\mathrm{s}} r)\alpha_n^m \boldsymbol{W}_n^m. \tag{4.56}$$

Given $\boldsymbol{\psi}$ on Γ_R, it has the Fourier expansion:

$$\boldsymbol{\psi}(R,\theta,\varphi) = \sum_{n=0}^{\infty}\sum_{m=-n}^{n} \psi_{1n}^m \boldsymbol{T}_n^m(\theta,\varphi) + \psi_{2n}^m \boldsymbol{V}_n^m(\theta,\varphi) + \psi_{3n}^m \boldsymbol{W}_n^m(\theta,\varphi), \tag{4.57}$$

where the Fourier coefficients

$$\begin{aligned}
\psi_{1n}^m &= \int_{\Gamma_R} \boldsymbol{\psi}(R,\theta,\varphi)\cdot \bar{\boldsymbol{T}}_n^m(\theta,\varphi)\mathrm{d}\gamma,\\
\psi_{2n}^m &= \int_{\Gamma_R} \boldsymbol{\psi}(R,\theta,\varphi)\cdot \bar{\boldsymbol{V}}_n^m(\theta,\varphi)\mathrm{d}\gamma,\\
\psi_{3n}^m &= \int_{\Gamma_R} \boldsymbol{\psi}(R,\theta,\varphi)\cdot \bar{\boldsymbol{W}}_n^m(\theta,\varphi)\mathrm{d}\gamma.
\end{aligned}$$

Evaluating (4.56) at $r = R$ and then comparing it with (4.57), we get

$$\alpha_n^m = \frac{\mathrm{i}\kappa_{\mathrm{s}} R}{n(n+1)h_n^{(1)}(\kappa_{\mathrm{s}} R)}\psi_{3n}^m, \quad \beta_n^m = \frac{1}{\sqrt{n(n+1)}h_n^{(1)}(\kappa_{\mathrm{s}} R)}\psi_{2n}^m. \tag{4.58}$$

Plugging (4.58) back into (4.56) gives

$$\boldsymbol{\psi}(r,\theta,\varphi) = \sum_{n=0}^{\infty}\sum_{m=-n}^{n} \left(\frac{R}{r}\right)\left(\frac{h_n^{(1)}(\kappa_{\mathrm{s}} r) + \kappa_{\mathrm{s}} r h_n^{(1)'}(\kappa_{\mathrm{s}} r)}{\sqrt{n(n+1)}h_n^{(1)}(\kappa_{\mathrm{s}} R)}\right)\psi_{3n}^m \boldsymbol{T}_n^m + \left(\frac{h_n^{(1)}(\kappa_{\mathrm{s}} r)}{h_n^{(1)}(\kappa_{\mathrm{s}} R)}\right)\psi_{2n}^m \boldsymbol{V}_n^m + \left(\frac{R}{r}\right)\left(\frac{h_n^{(1)}(\kappa_{\mathrm{s}} r)}{h_n^{(1)}(\kappa_{\mathrm{s}} R)}\right)\psi_{3n}^m \boldsymbol{W}_n^m. \tag{4.59}$$

In the spherical coordinates, we have from (4.55) and (4.59) that

$$\begin{aligned}
\nabla\phi &= \partial_r\phi\, \boldsymbol{e}_r + \frac{1}{r}\nabla_{\Gamma_R}\phi\\
&= \sum_{n=0}^{\infty}\sum_{m=-n}^{n}\left(\frac{\kappa_{\mathrm{p}} h_n^{(1)'}(\kappa_{\mathrm{p}} r)}{h_n^{(1)}(\kappa_{\mathrm{p}} R)}\right)\phi_n^m X_n^m \boldsymbol{e}_r + \left(\frac{h_n^{(1)}(\kappa_{\mathrm{p}} r)}{r h_n^{(1)}(\kappa_{\mathrm{p}} R)}\right)\phi_n^m \nabla_{\Gamma_R} X_n^m\\
&= \sum_{n=0}^{\infty}\sum_{m=-n}^{n}\left(\frac{\kappa_{\mathrm{p}} h_n^{(1)'}(\kappa_{\mathrm{p}} r)}{h_n^{(1)}(\kappa_{\mathrm{p}} R)}\right)\phi_n^m \boldsymbol{W}_n^m + \left(\frac{\sqrt{n(n+1)}h_n^{(1)}(\kappa_{\mathrm{p}} r)}{r h_n^{(1)}(\kappa_{\mathrm{p}} R)}\right)\phi_n^m \boldsymbol{T}_n^m.
\end{aligned}$$

and

$$\nabla \times \boldsymbol{\psi} = \sum_{n=0}^{\infty} \sum_{m=-n}^{n} \boldsymbol{I}_{1n}^{m} + \boldsymbol{I}_{2n}^{m} + \boldsymbol{I}_{3n}^{m},$$

where

$$\begin{aligned}
\boldsymbol{I}_{1n}^{m} &= \nabla \times \left[\left(\frac{R}{r} \right) \left(\frac{h_n^{(1)}(\kappa_{\mathrm{s}} r) + \kappa_{\mathrm{s}} r h_n^{(1)'}(\kappa_{\mathrm{s}} r)}{\sqrt{n(n+1)} h_n^{(1)}(\kappa_{\mathrm{s}} R)} \right) \psi_{3n}^{m} \boldsymbol{T}_n^{m} \right] \\
&= \frac{R h_n^{(1)}(\kappa_{\mathrm{s}} r)}{\sqrt{n(n+1)} h_n^{(1)}(\kappa_{\mathrm{s}} R)} \left(\kappa_{\mathrm{s}}^2 - \frac{n(n+1)}{r^2} \right) \psi_{3n}^{m} \boldsymbol{V}_n^{m}, \\
\boldsymbol{I}_{2n}^{m} &= \nabla \times \left[\left(\frac{h_n^{(1)}(\kappa_{\mathrm{s}} r)}{h_n^{(1)}(\kappa_{\mathrm{s}} R)} \right) \psi_{2n}^{m} \boldsymbol{V}_n^{m} \right] \\
&= \left(\frac{h_n^{(1)}(\kappa_{\mathrm{s}} r) + \kappa_{\mathrm{s}} r h_n^{(1)'}(\kappa_{\mathrm{s}} r)}{r h_n^{(1)}(\kappa_{\mathrm{s}} R)} \right) \psi_{2n}^{m} \boldsymbol{T}_n^{m} + \frac{\sqrt{n(n+1)} h_n^{(1)}(\kappa_{\mathrm{s}} r)}{r h_n^{(1)}(\kappa_{\mathrm{s}} R)} \psi_{2n}^{m} \boldsymbol{W}_n^{m}, \\
\boldsymbol{I}_{3n}^{m} &= \nabla \times \left[\left(\frac{R}{r} \right) \left(\frac{h_n^{(1)}(\kappa_{\mathrm{s}} r)}{h_n^{(1)}(\kappa_{\mathrm{s}} R)} \right) \psi_{3n}^{m} \boldsymbol{W}_n^{m} \right] \\
&= \frac{R \sqrt{n(n+1)} h_n^{(1)}(\kappa_{\mathrm{s}} r)}{r^2 h_n^{(1)}(\kappa_{\mathrm{s}} R)} \psi_{3n}^{m} \boldsymbol{V}_n^{m}.
\end{aligned}$$

Combining the above equations, we obtain

$$\begin{aligned}
&\boldsymbol{v}(r,\theta,\varphi) = \nabla\phi(r,\theta,\varphi) + \nabla \times \boldsymbol{\psi}(r,\theta,\varphi) \\
&= \sum_{n=0}^{\infty} \sum_{m=-n}^{n} \left(\frac{\sqrt{n(n+1)} h_n^{(1)}(\kappa_{\mathrm{p}} r)}{r h_n^{(1)}(\kappa_{\mathrm{p}} R)} \phi_n^{m} + \frac{(h_n^{(1)}(\kappa_{\mathrm{s}} r) + \kappa_{\mathrm{s}} r h_n^{(1)'}(\kappa_{\mathrm{s}} r))}{r h_n^{(1)}(\kappa_{\mathrm{s}} R)} \psi_{2n}^{m} \right) \boldsymbol{T}_n^{m} \\
&\quad + \left(\frac{\kappa_{\mathrm{p}} h_n^{(1)'}(\kappa_{\mathrm{p}} r)}{h_n^{(1)}(\kappa_{\mathrm{p}} R)} \phi_n^{m} + \frac{\sqrt{n(n+1)} h_n^{(1)}(\kappa_{\mathrm{s}} r)}{r h_n^{(1)}(\kappa_{\mathrm{s}} R)} \psi_{2n}^{m} \right) \boldsymbol{W}_n^{m} \\
&\quad + \frac{\kappa_{\mathrm{s}}^2 R h_n^{(1)}(\kappa_{\mathrm{s}} r)}{\sqrt{n(n+1)} h_n^{(1)}(\kappa_{\mathrm{s}} R)} \psi_{3n}^{m} \boldsymbol{V}_n^{m},
\end{aligned} \tag{4.60}$$

which gives

$$\begin{aligned}
\boldsymbol{v}(R,\theta,\varphi) = \sum_{n=0}^{\infty} \sum_{m=-n}^{n} &\frac{1}{R} \left(\sqrt{n(n+1)} \phi_n^{m} + (1 + z_n(\kappa_{\mathrm{s}} R)) \psi_{2n}^{m} \right) \boldsymbol{T}_n^{m} \\
&+ \frac{\kappa_{\mathrm{s}}^2 R}{\sqrt{n(n+1)}} \psi_{3n}^{m} \boldsymbol{V}_n^{m} + \frac{1}{R} \left(z_n(\kappa_{\mathrm{p}} R) \phi_n^{m} + \sqrt{n(n+1)} \psi_{2n}^{m} \right) \boldsymbol{W}_n^{m}.
\end{aligned} \tag{4.61}$$

On the other hand, $\boldsymbol{v}$ has the Fourier expansion:

$$\boldsymbol{v}(R,\theta,\varphi)=\sum_{n=0}^{\infty}\sum_{m=-n}^{n} v_{1n}^m \boldsymbol{T}_n^m + v_{2n}^m \boldsymbol{V}_n^m + v_{3n}^m \boldsymbol{W}_n^m. \tag{4.62}$$

Comparing (4.61) with (4.62), we obtain

$$\begin{cases} v_{1n}^m = \dfrac{\sqrt{n(n+1)}}{R}\phi_n^m + \dfrac{(1+z_n(\kappa_{\mathrm{s}}R))}{R}\psi_{2n}^m, \\ v_{2n}^m = \dfrac{\kappa_{\mathrm{s}}^2 R}{\sqrt{n(n+1)}}\psi_{3n}^m, \\ v_{3n}^m = \dfrac{z_n(\kappa_{\mathrm{p}}R)}{R}\phi_n^m + \dfrac{\sqrt{n(n+1)}}{R}\psi_{2n}^m, \end{cases} \tag{4.63}$$

and

$$\begin{cases} \phi_n^m = \dfrac{R(1+z_n(\kappa_{\mathrm{s}}R))}{\Lambda_n}v_{3n}^m - \dfrac{R\sqrt{n(n+1)}}{\Lambda_n}v_{1n}^m, \\ \psi_{2n}^m = \dfrac{Rz_n(\kappa_{\mathrm{p}}R)}{\Lambda_n}v_{1n}^m - \dfrac{R\sqrt{n(n+1)}}{\Lambda_n}v_{3n}^m, \\ \psi_{3n}^m = \dfrac{\sqrt{n(n+1)}}{\kappa_{\mathrm{s}}^2 R}v_{2n}^m, \end{cases} \tag{4.64}$$

where

$$\Lambda_n = z_n(\kappa_{\mathrm{p}}R)(1+z_n(\kappa_{\mathrm{s}}R)) - n(n+1).$$

Noting (4.45), we have from a simple calculation that

$$\mathrm{Im}\Lambda_n = \mathrm{Re}z_n(\kappa_{\mathrm{p}}R)\mathrm{Im}z_n(\kappa_{\mathrm{s}}R) + (1+\mathrm{Re}z_n(\kappa_{\mathrm{s}}R))\mathrm{Im}z_n(\kappa_{\mathrm{p}}R) < 0,$$

which implies that $\Lambda_n \neq 0$ for $n = 0, 1, \ldots$.

5. THE INVERSE ELASTIC SURFACE SCATTERING PROBLEM

5.1 Introduction

In this chapter we focus on the inverse elastic scattering problem in periodic structures. The direct elastic scattering problem has been studied by many researchers [1, 2, 41, 43]. The uniqueness result of the inverse problem can be found in [25]. The numerical study can be found in [42] and [54] for the inverse problem by using an optimization method and the factorization method, respectively.

It is known that there is a resolution limit to the sharpness of the details which can be observed from conventional far-field optical microscopy, one half the wavelength, referred to as the Rayleigh criterion or the diffraction limit [39]. The loss of resolution is mainly due to the ignorance of the evanescent wave components. Near-field optical imaging is an effective approach to obtain images with subwavelength resolution. The inverse scattering problems via the near-field imaging for acoustic and electromagnetic waves have been undergoing extensive studies for impenetrable infinite rough surfaces [12], penetrable infinite rough surfaces [14], two- and three-dimensional diffraction gratings [9, 13, 31, 57], bounded obstacles [71], and interior cavities [70]. The two- and three-dimensional inverse elastic surface scattering problems have been investigated by using near-field data in [72–74]. However, there exits some difficulties of near-field optical imaging in practice, for example, it requires a sophisticated control of the probe when scanning samples to measure the near-field data. Recently, a rigorous mathematical model and an efficient numerical method are proposed in [17] to over the aforementioned obstacle in near-field imaging. The novel idea is to put a rectangular slab of larger index of refraction above the surfaces and allow more propagating wave modes to be able to propagate to the far-field regime. This work is devoted to the

inverse elastic surface scattering problem with far-field data. We point out that this is a nontrivial extension of the method from solving the inverse acoustic surface scattering problem to solving the inverse elastic surface scattering problem, because the latter involves the more complicated elastic wave equation due to the coexistence of compressional and shear waves propagating at different speeds.

In this chapter, we develop a rigorous mathematical model and an efficient numerical method for the inverse elastic surface scattering with far-field data. The scattering surface is assumed to be a small and smooth perturbation of an elastically rigid plane. A rectangular slab of homogeneous and isotropic elastic medium is placed above the scattering surface. The slab has a larger mass density than that of the free space, and has a wavelength comparable thickness. The measurement can be took on the top face of the slab, which is in the far-field regime. The method makes use of the Helmholtz decomposition to consider two coupled Helmholtz equations instead of the elastic wave equation. It consists of two steps. The first step is to do the far-to-near (FtN) field data conversion, which requires to solve a Cauchy problem of the Helmholtz equation in the slab. Using the Fourier analysis, we compute the analytic solution and find a formula connecting the wave fields on the top and bottom faces of the slab: a larger mass density of the slab allows more propagating wave modes to be converted stably from the far-field regime to the near-field regime. The second step is to solve an inverse surface scattering problem in the near-field zone by using the data obtained from the first step. Combining the Fourier analysis, we use the transformed field expansions to find an analytic solution for the direct problem. We refer to [23, 69, 78, 84] for the transformed field expansion and related boundary perturbation methods for solving direct surface scattering problems. A general account of theory on scattering by random rough surfaces can be found in [85]. Using the closed form of the analytic solution, we deduce expressions for the leading and linear terms of the power series solution. Dropping all higher order terms, we linearize the inverse problem and obtain explicit reconstruction formulas for the surface function. Moreover, a nonlinear correction scheme is also developed to improve the reconstruc-

tion. The method requires only a single illumination and is implemented efficiently by the fast Fourier transform (FFT). Numerical examples show it is effective and robust to reconstruct the scattering surfaces with subwavelength resolution.

The remaining part of the chapter is organized as follows. The mathematical model problem is formulated in Section 5.2. Sections 5.3 and 5.4 introduce the Helmholtz decomposition and the transparent boundary condition, respectively. In Section 5.5, we show how to convert the measured elastic wave data into the scattering data of the scalar potentials introduced from the Helmholtz decomposition. In Section 5.6, a reduced problem is modeled in the slab and the analytic solution is obtained to accomplish the FtN field data conversion. In Section 5.7, the transformed field expansion and corresponding recursive boundary value problems are presented. We give the reconstruction formulas for the inverse problem in Section 5.8. Numerical experiments are presented in Section 5.9 to demonstrate the effectiveness of the proposed method. Finally, we conclude some general remarks in Section 5.10.

5.2 Model Problem

Let us first introduce the problem geometry, which is shown in Figure 5.1. Consider an elastically rigid surface $\Gamma_f = \{\boldsymbol{x} = (x, y) \in \mathbb{R}^2 : y = f(x),\ 0 < x < \Lambda\}$, where f is a periodic Lipschitz continuous function with period Λ. The scattering surface function f is assumed to have the form

$$f(x) = \varepsilon g(x), \tag{5.1}$$

where $\varepsilon > 0$ is a sufficiently small constant and is called the surface deformation parameter, g is the surface profile function which is also periodic with the period Λ. Hence the surface Γ_f is a small perturbation of the planar surface $\Gamma_0 = \{\boldsymbol{x} \in \mathbb{R}^2 : y = 0, 0 < x < \Lambda\}$. Let a rectangular slab of homogeneous and isotropic elastic medium be placed above the scattering surface. The bottom face of the slab is $\Gamma_b = \{\boldsymbol{x} \in \mathbb{R}^2 : y = b,\ 0 < x < \Lambda\}$, where $b > \max_{x\in(0,\Lambda)} f(x)$ is a constant and stands for the separation distance between the scattering surface and the slab. The

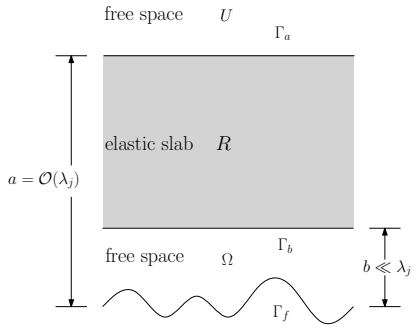

Figure 5.1. The problem geometry.

top face of the slab is $\Gamma_a = \{\boldsymbol{x} \in \mathbb{R}^2 : y = a,\, 0 < x < \Lambda\}$, where $a > b$ is a positive constant and stands for the measurement distance. Denote by Ω the bounded domain between Γ_f and Γ_b, i.e., $\Omega = \{\boldsymbol{x} \in \mathbb{R}^2 : f < y < b,\, 0 < x < \Lambda\}$. Let R be the domain of the slab, i.e., $R = \{\boldsymbol{x} \in \mathbb{R}^2 : b < y < a,\, 0 < x < \Lambda\}$. Finally, denote by U the open domain above Γ_a, i.e., $U = \{\boldsymbol{x} \in \mathbb{R}^2 : y > a,\, 0 < x < \Lambda\}$.

In this chapter, we assume for simplicity that the Lamé parameters μ, λ are constants satisfying $\mu > 0, \lambda + \mu > 0$; the mass density ρ is a piecewise constant, i.e.,

$$\rho(\boldsymbol{x}) = \begin{cases} \rho_0, & \boldsymbol{x} \in \Omega \cup U, \\ \rho_1, & \boldsymbol{x} \in R, \end{cases}$$

where ρ_0 and ρ_1 are the density of the free space and the elastic slab, respectively, and they satisfy $\rho_1 > \rho_0 > 0$. Define

$$\kappa_1 = \omega \left(\frac{\rho_0}{\lambda + 2\mu} \right)^{1/2}, \quad \kappa_2 = \omega \left(\frac{\rho_0}{\mu} \right)^{1/2},$$

which are known as the compressional wavenumber and the shear wavenumber in the free space, respectively. We comment that the method also works for the case where μ, λ take different values in the free space and the elastic slab. Let $\lambda_j = 2\pi/\kappa_j, j = 1, 2$ be the corresponding wavelength of the compressional and shear waves.

Let $\boldsymbol{u}^{\text{inc}}$ be a time-harmonic plane wave which is incident on the slab from above. The incident plane wave can be taken as either the compressional wave $\boldsymbol{u}^{\text{inc}}(\boldsymbol{x}) = \boldsymbol{d} e^{\mathrm{i}\kappa_1 \boldsymbol{x}\cdot\boldsymbol{d}}$ or the shear wave $\boldsymbol{u}^{\text{inc}} = \boldsymbol{d}^{\perp} e^{\mathrm{i}\kappa_2 \boldsymbol{x}\cdot\boldsymbol{d}}$, where $\boldsymbol{d} = (\sin\theta, -\cos\theta)^{\top}$ is the unit

incident direction vector, $\theta \in (-\pi/2, \pi/2)$ is the incident angle, and $\boldsymbol{d}^{\perp} = (\cos\theta, \sin\theta)^{\top}$ is an orthonormal vector to $\boldsymbol{d}$. In this work, we use the compressional incident plane wave as an example to present the results, which are similar and can be obtained with obvious modifications for the shear incident plane wave. Practically, the simplest configuration is the normal incidence for experiments, i.e., $\theta = 0$. Hence we focus on the normal incidence since our method requires only a single illumination. Under the normal incidence, the incident field reduces to

$$\boldsymbol{u}^{\mathrm{inc}}(\boldsymbol{x}) = (0, -1)^{\top} e^{-\mathrm{i}\kappa_1 y}. \tag{5.2}$$

It can be verified that the incident field $\boldsymbol{u}^{\mathrm{inc}}$ satisfies the elastic wave equation:

$$\mu\Delta\boldsymbol{u}^{\mathrm{inc}} + (\lambda+\mu)\nabla\nabla\cdot\boldsymbol{u}^{\mathrm{inc}} + \omega^2\rho_0\boldsymbol{u}^{\mathrm{inc}} = 0 \quad \text{in } U. \tag{5.3}$$

A transmission problem can be formulated due to the interaction between the elastic wave and the interfaces Γ_a and Γ_b. Let $\boldsymbol{u}, \boldsymbol{v}, \boldsymbol{w}$ be the displacements of the total field in the domains U, R, Ω, respectively. They satisfy the elastic wave equations:

$$\mu\Delta\boldsymbol{u} + (\lambda+\mu)\nabla\nabla\cdot\boldsymbol{u} + \omega^2\rho_0\boldsymbol{u} = 0 \quad \text{in } U, \tag{5.4a}$$

$$\mu\Delta\boldsymbol{v} + (\lambda+\mu)\nabla\nabla\cdot\boldsymbol{v} + \omega^2\rho_1\boldsymbol{v} = 0 \quad \text{in } R, \tag{5.4b}$$

$$\mu\Delta\boldsymbol{w} + (\lambda+\mu)\nabla\nabla\cdot\boldsymbol{w} + \omega^2\rho_0\boldsymbol{w} = 0 \quad \text{in } \Omega. \tag{5.4c}$$

In addition, the total fields are connected by the continuity conditions:

$$\boldsymbol{u} = \boldsymbol{v}, \quad \mu\partial_y\boldsymbol{u} + (\lambda+\mu)(0,1)^{\top}\nabla\cdot\boldsymbol{u} = \mu\partial_y\boldsymbol{v} + (\lambda+\mu)(0,1)^{\top}\nabla\cdot\boldsymbol{v} \quad \text{on } \Gamma_a, \tag{5.5a}$$

$$\boldsymbol{v} = \boldsymbol{w}, \quad \mu\partial_y\boldsymbol{v} + (\lambda+\mu)(0,1)^{\top}\nabla\cdot\boldsymbol{v} = \mu\partial_y\boldsymbol{w} + (\lambda+\mu)(0,1)^{\top}\nabla\cdot\boldsymbol{w} \quad \text{on } \Gamma_b. \tag{5.5b}$$

Since Γ_f is elastically rigid, we have the homogeneous Dirichlet boundary condition:

$$\boldsymbol{w} = 0 \quad \text{on } \Gamma_f. \tag{5.6}$$

In the open domain U, the total field $\boldsymbol{u}$ consists of the incident field $\boldsymbol{u}^{\mathrm{inc}}$ and the diffracted field $\boldsymbol{u}^{\mathrm{d}}$:

$$\boldsymbol{u} = \boldsymbol{u}^{\mathrm{inc}} + \boldsymbol{u}^{\mathrm{d}}, \tag{5.7}$$

where $\boldsymbol{u}^{\mathrm{d}}$ is required to satisfy the bounded outgoing wave condition.

Throughout, we assume that the measurement distance $a = \mathcal{O}(\lambda_j)$ and the separation distance $b \ll \lambda_j$, i.e., a is comparable with the wavelength and Γ_a is put in the far-field region; b is much smaller than the wavelength and Γ_b is put in the near-field region. Now we are ready to formulate the inverse problem: Given the incident field $\boldsymbol{u}^{\mathrm{inc}}$, the inverse problem is to determine the scattering surface f from the far-field measurement of the total field $\boldsymbol{u}$ on Γ_a.

5.3 The Helmholtz Decomposition

In this section, we introduce the Helmholtz decomposition for the total fields by using scalar potential functions, and deduce the continuity conditions for these scalar fields. Let $\boldsymbol{u} = (u_1, u_2)^\top$ and u be a vector and a scalar function, respectively. Introduce the scalar and vector curl operators:

$$\mathrm{curl}\boldsymbol{u} = \partial_x u_2 - \partial_y u_1, \quad \mathbf{curl}\, u = (\partial_y u, -\partial_x u)^\top.$$

For any solution $\boldsymbol{u} = (u_1, u_2)^\top$ of (5.4a), the Helmholtz decomposition reads

$$\boldsymbol{u} = \nabla\phi_1 + \mathbf{curl}\,\phi_2, \tag{5.8}$$

where $\phi_j, j = 1, 2$ are two scalar potential functions. Explicitly, we have

$$u_1 = \partial_x\phi_1 + \partial_y\phi_2, \quad u_2 = \partial_y\phi_1 - \partial_x\phi_2. \tag{5.9}$$

Substituting (5.8) into (5.4a) yields

$$\nabla\left((\lambda + 2\mu)\Delta\phi_1 + \omega^2\rho_0\phi_1\right) + \mathbf{curl}\left(\mu\Delta\phi_2 + \omega^2\rho_0\phi_2\right) = 0,$$

which is fulfilled if ϕ_j satisfies

$$\Delta\phi_j + \kappa_j^2\phi_j = 0 \quad \text{in } U. \tag{5.10}$$

Combining (5.10) and (5.8), we obtain

$$\phi_1 = -\frac{1}{\kappa_1^2}\nabla\cdot\boldsymbol{u}, \quad \phi_2 = \frac{1}{\kappa_2^2}\mathrm{curl}\boldsymbol{u},$$

which give

$$\partial_x u_1 + \partial_y u_2 = -\kappa_1^2 \phi_1, \quad \partial_x u_2 - \partial_y u_1 = \kappa_2^2 \phi_2. \tag{5.11}$$

For any solution $\boldsymbol{v} = (v_1, v_2)^\top$ of (5.4b), we introduce the Helmholtz decomposition by using scalar functions ψ_j:

$$\boldsymbol{v} = \nabla \psi_1 + \mathbf{curl} \psi_2, \tag{5.12}$$

which gives explicitly that

$$v_1 = \partial_x \psi_1 + \partial_y \psi_2, \quad v_2 = \partial_y \psi_1 - \partial_x \psi_2. \tag{5.13}$$

Plugging (5.12) into (5.4b), we may have

$$\Delta \psi_j + \eta_j^2 \psi_j = 0 \quad \text{in } R, \tag{5.14}$$

where η_1 and η_2 are the compressional and shear wavenumbers in the elastic slab, respectively, and are given by

$$\eta_1 = \omega \left(\frac{\rho_1}{\lambda + 2\mu} \right)^{1/2}, \quad \eta_2 = \omega \left(\frac{\rho_1}{\mu} \right)^{1/2}. \tag{5.15}$$

Combing (5.14) and (5.12), we get

$$\psi_1 = -\frac{1}{\eta_1^2} \nabla \cdot \boldsymbol{v}, \quad \psi_2 = \frac{1}{\eta_2^2} \mathrm{curl} \boldsymbol{v},$$

which give

$$\partial_x v_1 + \partial_y v_2 = -\eta_1^2 \psi_1, \quad \partial_x v_2 - \partial_y v_1 = \eta_2^2 \psi_2. \tag{5.16}$$

Since Γ_a is a horizontal line, it is easy to verify from the continuity condition (5.5a) that

$$u_j = v_j, \quad \partial_y u_j = \partial_y v_j. \tag{5.17}$$

Using (5.11), (5.16)–(5.17), we deduce the first continuity condition for the scalar potentials on Γ_a:

$$\kappa_j^2 \phi_j = \eta_j^2 \psi_j. \tag{5.18}$$

It follows from (5.9), (5.13), and (5.17) that we deduce the second continuity condition for the scalar potentials on Γ_a:

$$\partial_y\phi_1 - \partial_x\phi_2 = \partial_y\psi_1 - \partial_x\psi_2, \quad \partial_y\phi_2 + \partial_x\phi_1 = \partial_y\psi_2 + \partial_x\psi_1. \tag{5.19}$$

Similarly, for any solution $\boldsymbol{w} = (w_1, w_2)^\top$ of (5.4c), the Helmholtz decomposition is

$$\boldsymbol{w} = \nabla\varphi_1 + \mathbf{curl}\varphi_2. \tag{5.20}$$

Substituting (5.20) into (5.4c), we may get

$$\Delta\varphi_j + \kappa_j^2\varphi_j = 0 \quad \text{in } \Omega.$$

Noting (5.5b), we may repeat the same steps and obtain the continuity conditions on Γ_b:

$$\eta_j^2\psi_j = \kappa_j^2\varphi_j \tag{5.21}$$

and

$$\partial_y\psi_1 - \partial_x\psi_2 = \partial_y\varphi_1 - \partial_x\varphi_2, \quad \partial_y\psi_2 + \partial_x\psi_1 = \partial_y\varphi_2 + \partial_x\varphi_1. \tag{5.22}$$

Finally, it follows from the boundary condition (5.6) and the Helmholtz decomposition (5.20) that

$$\partial_x\varphi_1 + \partial_y\varphi_2 = 0, \quad \partial_y\varphi_1 - \partial_x\varphi_2 = 0 \quad \text{on } \Gamma_f. \tag{5.23}$$

5.4 Transparent Boundary Condition

It follows from (5.3), (5.4a), and (5.7) that the diffracted field $\boldsymbol{u}^{\mathrm{d}}$ also satisfies the elastic wave equation:

$$\mu\Delta\boldsymbol{u}^{\mathrm{d}} + (\lambda+\mu)\nabla\nabla\cdot\boldsymbol{u}^{\mathrm{d}} + \omega^2\rho_0\boldsymbol{u}^{\mathrm{d}} = 0 \quad \text{in } U. \tag{5.24}$$

Introduce the Helmholtz decomposition for the diffracted field $\boldsymbol{u}^{\mathrm{d}}$:

$$\boldsymbol{u}^{\mathrm{d}} = \nabla\phi_1^{\mathrm{d}} + \mathbf{curl}\phi_2^{\mathrm{d}}, \tag{5.25}$$

Substituting (5.25) into (5.24) may yield

$$\Delta\phi_j^{\mathrm{d}} + \kappa_j^2\phi_j^{\mathrm{d}} = 0 \quad \text{in } U. \tag{5.26}$$

It follows from the uniqueness of the solution for the direct problem that ϕ_j^{d} is a periodic function with period Λ and admits the Fourier series expansion:

$$\phi_j^{\mathrm{d}}(x,y) = \sum_{n\in\mathbb{Z}} \phi_{jn}^{\mathrm{d}}(y)e^{\mathrm{i}\alpha_n x}, \tag{5.27}$$

where $\alpha_n = 2n\pi/\Lambda$. Plugging (5.27) into (5.26) yields

$$\partial_{yy}^2\phi_{jn}^{\mathrm{d}}(y) + \beta_{jn}^2\phi_{jn}^{\mathrm{d}}(y) = 0, \quad y > a, \tag{5.28}$$

where

$$\beta_{jn} = \begin{cases} (\kappa_j^2 - \alpha_n^2)^{1/2}, & |\alpha_n| < \kappa_j, \\ \mathrm{i}(\alpha_n^2 - \kappa_j^2)^{1/2}, & |\alpha_n| > \kappa_j. \end{cases}$$

Here we assume that $\beta_{jn} \neq 0$ to exclude possible resonance.

Using the bounded outgoing wave condition, we may solve (5.28) analytically and obtain the solution of (5.26) explicitly:

$$\phi_j^{\mathrm{d}}(x,y) = \sum_{n\in\mathbb{Z}} \phi_{jn}^{\mathrm{d}}(a)e^{\mathrm{i}(\alpha_n x + \beta_{jn}(y-a))}, \tag{5.29}$$

which is called the Rayleigh expansion for the scalar potential function ϕ_j^{d}. Taking the normal derivative of (5.29) on Γ_a gives

$$\partial_y\phi_j^{\mathrm{d}}(x,a) = \sum_{n\in\mathbb{Z}} \mathrm{i}\beta_{jn}\phi_{jn}^{\mathrm{d}}(a)e^{\mathrm{i}\alpha_n x}. \tag{5.30}$$

For a given periodic function $u(x)$ with period Λ, it has the Fourier series expansion:

$$u(x) = \sum_{n\in\mathbb{Z}} u_n e^{\mathrm{i}\alpha_n x}, \quad u_n = \frac{1}{\Lambda}\int_0^\Lambda u(x)e^{-\mathrm{i}\alpha_n x}\mathrm{d}x.$$

We define the boundary operator:

$$(\mathscr{T}_j u)(x) = \sum_{n\in\mathbb{Z}} \mathrm{i}\beta_{jn}u_n e^{\mathrm{i}\alpha_n x}.$$

It is easy to verify from (5.30) that

$$\partial_y \phi_j^{\mathrm{d}} = \mathscr{T}_j \phi_j^{\mathrm{d}} \quad \text{on } \Gamma_a. \tag{5.31}$$

Recalling the incident field (5.2), we may also consider the Helmholtz decomposition for the incident field:

$$\boldsymbol{u}^{\mathrm{inc}} = \nabla \phi_1^{\mathrm{inc}} + \mathbf{curl} \phi_2^{\mathrm{inc}}, \tag{5.32}$$

which gives

$$\phi_1^{\mathrm{inc}} = -\frac{1}{\kappa_1^2} \nabla \cdot \boldsymbol{u}^{\mathrm{inc}} = -\frac{\mathrm{i}}{\kappa_1} e^{-\mathrm{i}\kappa_1 y}, \quad \phi_2^{\mathrm{inc}} = \frac{1}{\kappa_2^2} \mathrm{curl} \boldsymbol{u}^{\mathrm{inc}} = 0.$$

A simple calculation yields

$$\partial_y \phi_1^{\mathrm{inc}} = -e^{-\mathrm{i}\kappa_1 a}, \quad \mathscr{T}_1 \phi_1^{\mathrm{inc}} = e^{-\mathrm{i}\kappa_1 a},$$

which gives

$$\partial_y \phi_1^{\mathrm{inc}} = \mathscr{T}_1 \phi_1^{\mathrm{inc}} + g_1, \quad \partial_y \phi_2^{\mathrm{inc}} = \mathscr{T}_2 \phi_2^{\mathrm{inc}} + g_2. \tag{5.33}$$

Here $g_1 = -2e^{-\mathrm{i}\kappa_1 a}$ and $g_2 = 0$.

Letting $\phi_j = \phi_j^{\mathrm{inc}} + \phi_j^{\mathrm{d}}$ and recalling $\boldsymbol{u} = \boldsymbol{u}^{\mathrm{inc}} + \boldsymbol{u}^{\mathrm{d}}$, we get (5.8) by adding (5.32) and (5.25). Moreover, we obtain the transparent boundary condition for the total scalar potentials by combing (5.31) and (5.33):

$$\partial_y \phi_j = \mathscr{T}_j \phi_j + g_j \quad \text{on } \Gamma_a. \tag{5.34}$$

It follows from (5.18)–(5.19) that

$$\begin{aligned}
\partial_y \phi_1 &= \partial_y \psi_1 - \partial_x \psi_2 + \partial_x \phi_2 = \partial_y \psi_1 - \partial_x \psi_2 + \left(\frac{\eta_2^2}{\kappa_2^2} \right) \partial_x \psi_2 \\
&= \partial_y \psi_1 + \left(\frac{\eta_2^2 - \kappa_2^2}{\kappa_2^2} \right) \partial_x \psi_2, \\
\partial_y \phi_2 &= \partial_y \psi_2 + \partial_x \psi_1 - \partial_x \phi_1 = \partial_y \psi_2 + \partial_x \psi_1 - \left(\frac{\eta_1^2}{\kappa_1^2} \right) \partial_x \psi_1 \\
&= \partial_y \psi_2 - \left(\frac{\eta_1^2 - \kappa_1^2}{\kappa_1^2} \right) \partial_x \psi_1.
\end{aligned} \tag{5.35}$$

Combining (5.34)–(5.35) and (5.18) yields the boundary condition for ψ_j on Γ_a:

$$\begin{aligned}\partial_y\psi_1 + \left(\frac{\eta_2^2-\kappa_2^2}{\kappa_2^2}\right)\partial_x\psi_2 &= \left(\frac{\eta_1^2}{\kappa_1^2}\right)\mathscr{T}_1\psi_1 + g_1,\\ \partial_y\psi_2 - \left(\frac{\eta_1^2-\kappa_1^2}{\kappa_1^2}\right)\partial_x\psi_1 &= \left(\frac{\eta_2^2}{\kappa_2^2}\right)\mathscr{T}_2\psi_2 + g_2.\end{aligned} \tag{5.36}$$

Let $\boldsymbol{u}$ be a periodic function of x with period Λ. It admits the Fourier series expansion:

$$\boldsymbol{u}(x) = \sum_{n\in\mathbb{Z}} \boldsymbol{u}_n e^{\mathrm{i}\alpha_n x}, \quad \boldsymbol{u}_n = \frac{1}{\Lambda}\int_0^\Lambda \boldsymbol{u}(x)e^{-\mathrm{i}\alpha_n x}\mathrm{d}x.$$

Define the boundary operator on Γ_a:

$$(\mathscr{T}\boldsymbol{u})(x) = \sum_{n\in\mathbb{Z}} \mathrm{i}\begin{bmatrix} \frac{\omega^2\beta_{1n}}{\alpha_n^2+\beta_{1n}\beta_{2n}} & \mu\alpha_n - \frac{\omega^2\alpha_n^2}{\alpha_n^2+\beta_{1n}\beta_{2n}} \\ \frac{\omega^2\alpha_n^2}{\alpha_n^2+\beta_{1n}\beta_{2n}} - \mu\alpha_n & \frac{\omega^2\beta_{2n}}{\alpha_n^2+\beta_{1n}\beta_{2n}} \end{bmatrix}\boldsymbol{u}_n e^{\mathrm{i}\alpha_n x}.$$

It is shown in [72] that $\alpha_n^2 + \beta_{1n}\beta_{2n} \neq 0$ for $n \in \mathbb{Z}$ and the diffracted field $\boldsymbol{u}^{\mathrm{d}}$ satisfies the transparent boundary condition:

$$\mu\partial_y\boldsymbol{u}^{\mathrm{d}} + (\lambda+\mu)(0,1)^\top\nabla\cdot\boldsymbol{u}^{\mathrm{d}} = \mathscr{T}\boldsymbol{u}^{\mathrm{d}} \quad \text{on } \Gamma_a.$$

A simple calculation yields that

$$\mu\partial_y\boldsymbol{u}^{\mathrm{inc}} + (\lambda+\mu)(0,1)^\top\nabla\cdot\boldsymbol{u}^{\mathrm{inc}} = \mathrm{i}\kappa_1(\lambda+2\mu)(0,1)^\top e^{-\mathrm{i}\kappa_1 a}$$

and

$$\mathscr{T}\boldsymbol{u}^{\mathrm{inc}} = -\mathrm{i}\kappa_1(\lambda+2\mu)(0,1)^\top e^{-\mathrm{i}\kappa_1 a}.$$

Hence we obtain the boundary condition for the total displacement field $\boldsymbol{u}$:

$$\mu\partial_y\boldsymbol{u} + (\lambda+\mu)(0,1)^\top\nabla\cdot\boldsymbol{u} = \mathscr{T}\boldsymbol{u} + \boldsymbol{h} \quad \text{on } \Gamma_a,$$

where $\boldsymbol{h} = 2\mathrm{i}\kappa_1(\lambda+2\mu)(0,1)^\top e^{-\mathrm{i}\kappa_1 a}$. Noting the continuity condition (5.5a), we have

$$\mu\partial_y\boldsymbol{v} + (\lambda+\mu)(0,1)^\top\nabla\cdot\boldsymbol{v} = \mathscr{T}\boldsymbol{v} + \boldsymbol{h} \quad \text{on } \Gamma_a.$$

5.5 Scattering Data

We assume that the total field $\boldsymbol{u}$ is measured on Γ_a, i.e., $\boldsymbol{u}(x,a) = (u_1(x,a), u_2(x,a))^\top$ is available for $x \in (0,\Lambda)$. In this section, we show how to convert $\boldsymbol{u}(x,a)$ into the scattering data of the scalar potentials $\phi_j(x,a)$.

Evaluating (5.9) on Γ_a, we have

$$\partial_x\phi_1(x,a) + \partial_y\phi_2(x,a) = u_1(x,a), \quad \partial_y\phi_1(x,a) - \partial_x\phi_2(x,a) = u_2(x,a). \tag{5.37}$$

Let $\phi_j(x,a)$ admit the Fourier series expansion

$$\phi_j(x,a) = \sum_{n\in\mathbb{Z}} \phi_{jn} e^{\mathrm{i}\alpha_n x}. \tag{5.38}$$

It suffices to find all the Fourier coefficients of ϕ_{jn} in order to determine $\phi_j(x,a)$.

Taking the derivative of (5.38) with respect to x yields

$$\partial_x\phi_j(x,a) = \sum_{n\in\mathbb{Z}} \mathrm{i}\alpha_n\phi_{jn} e^{\mathrm{i}\alpha_n x}. \tag{5.39}$$

It follows from the transparent boundary condition (5.34) that

$$\partial_y\phi_j(x,a) = \sum_{n\in\mathbb{Z}} \mathrm{i}\beta_{jn}\phi_{jn} e^{\mathrm{i}\alpha_n x} + g_j. \tag{5.40}$$

Substituting (5.39) and (5.40) into (5.37), we obtain a linear system of equations for the Fourier coefficients ϕ_{jn}:

$$\mathrm{i}\begin{bmatrix} \alpha_n & \beta_{2n} \\ \beta_{1n} & -\alpha_n \end{bmatrix}\begin{bmatrix} \phi_{1n} \\ \phi_{2n} \end{bmatrix} = \begin{bmatrix} p_{1n} \\ p_{2n} \end{bmatrix}, \tag{5.41}$$

where $p_{1n} = u_{1n} - g_{2n}$, $p_{2n} = u_{2n} - g_{1n}$ and u_{jn} are the Fourier coefficients of u_j, i.e.,

$$u_{jn} = \frac{1}{\Lambda}\int_0^\Lambda u_j(x,a) e^{-\mathrm{i}\alpha_n x}\mathrm{d}x$$

and

$$g_{1n} = \begin{cases} -2e^{-\mathrm{i}\kappa_1 a} & \text{for } n = 0, \\ 0 & \text{for } n \neq 0, \end{cases} \qquad g_{2n} = 0 \text{ for } n \in \mathbb{Z}.$$

Using Cramer's rule, we obtain the unique solution of (5.41):

$$\phi_{1n} = -\mathrm{i}\left(\frac{\alpha_n p_{1n} + \beta_{2n} p_{2n}}{\alpha_n^2 + \beta_{1n}\beta_{2n}}\right), \quad \phi_{2n} = \mathrm{i}\left(\frac{\alpha_n p_{2n} - \beta_{1n} p_{1n}}{\alpha_n^2 + \beta_{1n}\beta_{2n}}\right). \tag{5.42}$$

Hence, we may assume that $\phi_j(x,a), j = 1,2$ are measured data. From now on, we shall only work on the potential functions.

5.6 Reduced Problem

Recall the continuity condition (5.18) and the boundary condition (5.36). Given the data ϕ_j on Γ_a, we consider the Cauchy problem for ψ_j:

$$\Delta\psi_j + \eta_j^2\psi_j = 0 \quad \text{in } R, \tag{5.43a}$$

$$\psi_j = \left(\frac{\kappa_j^2}{\eta_j^2}\right)\phi_j \quad \text{on } \Gamma_a, \tag{5.43b}$$

$$\partial_y\psi_1 + \left(\frac{\eta_2^2 - \kappa_2^2}{\kappa_2^2}\right)\partial_x\psi_2 = \left(\frac{\eta_1^2}{\kappa_1^2}\right)\mathscr{T}_1\psi_1 + g_1 \quad \text{on } \Gamma_a, \tag{5.43c}$$

$$\partial_y\psi_2 - \left(\frac{\eta_1^2 - \kappa_1^2}{\kappa_1^2}\right)\partial_x\psi_1 = \left(\frac{\eta_2^2}{\kappa_2^2}\right)\mathscr{T}_2\psi_2 + g_2 \quad \text{on } \Gamma_a. \tag{5.43d}$$

Since ψ_j is a periodic function of x, it has the Fourier series expansion

$$\psi_j(x,y) = \sum_{n\in\mathbb{Z}} \psi_{jn}(y)e^{\mathrm{i}\alpha_n x}. \tag{5.44}$$

Substituting (5.44) into (5.43), we obtain a final value problem for the second order equation in the frequency domain:

$$\partial_{yy}^2\psi_{jn}(y) + \gamma_{jn}^2\psi_{jn}(y) = 0, \quad b < y < a, \tag{5.45a}$$

$$\psi_{jn}(a) = \left(\frac{\kappa_j^2}{\eta_j^2}\right)\phi_{jn}, \quad y = a, \tag{5.45b}$$

$$\partial_y\psi_{1n}(a) + \mathrm{i}\alpha_n\left(\frac{\eta_2^2 - \kappa_2^2}{\kappa_2^2}\right)\psi_{2n}(a) = \mathrm{i}\beta_{1n}\left(\frac{\eta_1^2}{\kappa_1^2}\right)\psi_{1n}(a) + g_{1n}, \quad y = a, \tag{5.45c}$$

$$\partial_y\psi_{2n}(a) - \mathrm{i}\alpha_n\left(\frac{\eta_1^2 - \kappa_1^2}{\kappa_1^2}\right)\psi_{1n}(a) = \mathrm{i}\beta_{2n}\left(\frac{\eta_2^2}{\kappa_2^2}\right)\psi_{2n}(a) + g_{2n}, \quad y = a, \tag{5.45d}$$

where ϕ_{jn} is given in (5.42) and

$$\gamma_{jn} = \begin{cases} (\eta_j^2 - \alpha_n^2)^{1/2}, & |\alpha_n| < \eta_j, \\ \mathrm{i}(\alpha_n^2 - \eta_j^2)^{1/2}, & |\alpha_n| > \eta_j. \end{cases}$$

Again we assume that $\gamma_{jn} \neq 0$ to exclude possible resonance.

Using the continuity condition (5.18) again, we may further reduce (5.45) into the following final value problem:

$$\partial_{yy}^2 \psi_{jn}(y) + \gamma_{jn}^2 \psi_{jn}(y) = 0, \quad b < y < a, \tag{5.46a}$$

$$\psi_{jn} = \hat{\phi}_{jn}, \quad y = a, \tag{5.46b}$$

$$\partial_y \psi_{jn} - \mathrm{i}\hat{\beta}_{jn}\psi_{jn} = \hat{g}_{jn}, \quad y = a, \tag{5.46c}$$

where

$$\hat{\phi}_{jn} = \left(\frac{\kappa_j^2}{\eta_j^2}\right)\phi_{jn}, \quad \hat{\beta}_{jn} = \left(\frac{\eta_j^2}{\kappa_j^2}\right)\beta_{jn}$$

and

$$\hat{g}_{1n} = g_{1n} - \mathrm{i}\alpha_n \left(\frac{\eta_2^2 - \kappa_2^2}{\eta_2^2}\right)\phi_{2n},$$
$$\hat{g}_{2n} = g_{2n} + \mathrm{i}\alpha_n \left(\frac{\eta_1^2 - \kappa_1^2}{\eta_1^2}\right)\phi_{1n}.$$

It follows from Lemma (5.11.1) that the final value problem (5.46) has a unique solution which is

$$\begin{aligned}\psi_{jn}(y) =& (2\gamma_{jn}^{-1})\left((\gamma_{jn} + \hat{\beta}_{jn})\hat{\phi}_{jn} - \mathrm{i}\hat{g}_{jn}\right)e^{-\mathrm{i}\gamma_{jn}(a-y)} \\ &+ (2\gamma_{jn})^{-1}\left((\gamma_{jn} - \hat{\beta}_{jn})\hat{\phi}_{jn} + \mathrm{i}\hat{g}_{jn}\right)e^{\mathrm{i}\gamma_{jn}(a-y)}.\end{aligned} \tag{5.47}$$

Evaluating (5.47) at $y = b$ yields

$$\begin{aligned}\psi_{jn}(b) =& (2\gamma_{jn})^{-1}\left((\gamma_{jn} + \hat{\beta}_{jn})\hat{\phi}_{jn} - \mathrm{i}\hat{g}_{jn}\right)e^{-\mathrm{i}\gamma_{jn}(a-b)} \\ &+ (2\gamma_{jn})^{-1}\left((\gamma_{jn} - \hat{\beta}_{jn})\hat{\phi}_{jn} + \mathrm{i}\hat{g}_{jn}\right)e^{\mathrm{i}\gamma_{jn}(a-b)}.\end{aligned} \tag{5.48}$$

where $\psi_{jn}(b)$ are the Fourier coefficients of $\psi_j(x, b)$. Taking the partial derivative of (5.47) with respect to y and evaluating it at $y = b$, we obtain

$$\begin{aligned}\partial_y\psi_{jn}(b) =& \frac{\mathrm{i}}{2}\left((\gamma_{jn} + \hat{\beta}_{jn})\hat{\phi}_{jn} - \mathrm{i}\hat{g}_{jn}\right)e^{-\mathrm{i}\gamma_{jn}(a-b)} \\ &- \frac{\mathrm{i}}{2}\left((\gamma_{jn} - \hat{\beta}_{jn})\hat{\phi}_{jn} + \mathrm{i}\hat{g}_{jn}\right)e^{\mathrm{i}\gamma_{jn}(a-b)}.\end{aligned} \tag{5.49}$$

We point out that (5.48) gives the far-to-near (FtN) field data conversion formula. We observe from (5.48) that it is stable to convert the far-field data for the propagating wave components where the Fourier modes satisfy $|\alpha_n| < \eta_j$; it is exponentially unstable to convert the far-field for the evanescent wave components where the Fourier modes satisfy $|\alpha_n| > \eta_j$. Thus it is only reliable to make the near-field data by converting the low frequency far-field data ϕ_{jn} with $|\alpha_n| < \eta_j$. Noting $\rho_1 > \rho_0$ in the elastic slab, we are allowed to include more propagating wave modes to reconstruct the surface than the case without the slab, which contributes to a better resolution.

It follows from the continuity condition (5.21) that

$$\varphi_{jn}(b) = \left(\frac{\eta_j^2}{\kappa_j^2}\right)\psi_{jn}(b). \tag{5.50}$$

Using the continuity conditions (5.21)–(5.22) on Γ_b, we obtain

$$\begin{aligned}
\partial_y\varphi_1 &= \partial_y\psi_1 - \partial_x\psi_2 + \partial_x\varphi_2 = \partial_y\psi_1 - \partial_x\psi_2 + \left(\frac{\eta_2^2}{\kappa_2^2}\right)\partial_x\psi_2 \\
&= \partial_y\psi_1 + \left(\frac{\eta_2^2 - \kappa_2^2}{\kappa_2^2}\right)\partial_x\psi_2, \\
\partial_y\varphi_2 &= \partial_y\psi_2 + \partial_x\psi_1 - \partial_x\varphi_1 = \partial_y\psi_2 + \partial_x\psi_1 - \left(\frac{\eta_1^2}{\kappa_1^2}\right)\partial_x\psi_1 \\
&= \partial_y\psi_2 - \left(\frac{\eta_1^2 - \kappa_1^2}{\kappa_1^2}\right)\partial_x\psi_1,
\end{aligned}$$

which give in the frequency domain that

$$\begin{aligned}
\partial_y\varphi_{1n}(b) &= \partial_y\psi_{1n}(b) + \mathrm{i}\alpha_n\left(\frac{\eta_2^2 - \kappa_2^2}{\kappa_2^2}\right)\psi_{2n}(b), \\
\partial_y\varphi_{2n}(b) &= \partial_y\psi_{2n}(b) - \mathrm{i}\alpha_n\left(\frac{\eta_1^2 - \kappa_1^2}{\kappa_1^2}\right)\psi_{1n}(b).
\end{aligned} \tag{5.52}$$

Combining (5.50) and (5.52), we get

$$(\partial_y - \mathrm{i}\beta_{jn})\varphi_{jn} = \tau_{jn}, \tag{5.53}$$

where

$$\begin{aligned}
\tau_{1n} &= \partial_y\psi_{1n}(b) - \mathrm{i}\hat{\beta}_{1n}\psi_{1n}(b) + \mathrm{i}\alpha_n\left(\frac{\eta_2^2 - \kappa_2^2}{\kappa_2^2}\right)\psi_{2n}(b), \\
\tau_{2n} &= \partial_y\psi_{2n}(b) - \mathrm{i}\hat{\beta}_{2n}\psi_{2n}(b) - \mathrm{i}\alpha_n\left(\frac{\eta_1^2 - \kappa_1^2}{\kappa_1^2}\right)\psi_{1n}(b).
\end{aligned} \tag{5.54}$$

Here the Fourier coefficients $\psi_{jn}(b)$ and $\partial_y\psi_{jn}(b)$ are given in (5.48) and (5.49), respectively.

Using the boundary conditions (5.23) and (5.53), we may consider the following reduced boundary value problem for the scalar potential φ_j in Ω:

$$\Delta\varphi_j + \kappa_j^2\varphi_j = 0 \quad \text{in } \Omega, \tag{5.55a}$$

$$\partial_x\varphi_1 + \partial_y\varphi_2 = 0, \quad \partial_y\varphi_1 - \partial_x\varphi_2 = 0 \quad \text{on } \Gamma_f, \tag{5.55b}$$

$$\partial_y\varphi_j = \mathscr{T}_j\varphi_j + \tau_j \quad \text{on } \Gamma_b, \tag{5.55c}$$

where the Fourier coefficients of τ_j are given in (5.54). The inverse problem is reformulated to determine the periodic scattering surface function f from the Fourier coefficients $\varphi_{jn}(b)$ for $n \in M_j = \{n \in \mathbb{Z} : |\alpha_n| < \eta_j\}$.

5.7 Transformed Field Expansion

In this section, we introduce the transformed field expansion to derive an analytic solution to the boundary value problem (5.55).

5.7.1 Change of Variables

Consider the change of variables:

$$\tilde{x} = x, \quad \tilde{y} = b\left(\frac{y-f}{b-f}\right),$$

which maps Γ_f to Γ_0 but keeps Γ_b unchanged. Hence the domain Ω is mapped into the rectangular domain $D = \{(\tilde{x}, \tilde{y}) \in \mathbb{R}^2 : 0 < \tilde{x} < \Lambda,\, 0 < \tilde{y} < b\}$. It is easy to verify the differential rules:

$$\begin{aligned}
\partial_x =& \partial_{\tilde{x}} - f' \left(\frac{b - \tilde{y}}{b - f} \right) \partial_{\tilde{y}}, \\
\partial_y =& \left(\frac{b}{b - f} \right) \partial_{\tilde{y}}, \\
\partial_{xx}^2 =& \partial_{\tilde{x}\tilde{x}}^2 + (f')^2 \left(\frac{b - \tilde{y}}{b - f} \right)^2 \partial_{\tilde{y}\tilde{y}}^2 - 2f' \left(\frac{b - \tilde{y}}{b - f} \right) \partial_{\tilde{x}\tilde{y}}^2 \\
& - \left[f'' \left(\frac{b - \tilde{y}}{b - f} \right) + 2(f')^2 \frac{(b - \tilde{y})}{(b - f)^2} \right] \partial_{\tilde{y}}, \\
\partial_{yy}^2 =& \left(\frac{b}{b - f} \right)^2 \partial_{\tilde{y}\tilde{y}}^2.
\end{aligned}$$

We introduce a function $\tilde{\varphi}_j(\tilde{x}, \tilde{y})$ in order to reformulate the boundary value problem (5.55) using the new variables. Noting (5.55a), we have from the straightforward calculations that $\tilde{\varphi}$, upon dropping the tilde for simplicity of notation, satisfies

$$\left(c_1 \partial_{xx}^2 + c_2 \partial_{yy}^2 + c_3 \partial_{xy}^2 + c_4 \partial_y + c_1 \kappa_j^2 \right) \varphi_j = 0 \quad \text{in } D, \tag{5.56}$$

where

$$\begin{cases}
c_1 = (b - f)^2, \\
c_2 = \left[f'(b - y) \right]^2 + b^2, \\
c_3 = -2f'(b - y)(b - f), \\
c_4 = -(b - y) \left[f''(b - f) + 2(f')^2 \right].
\end{cases} \tag{5.57}$$

The boundary condition (5.55b) becomes

$$\left[\left(1 - b^{-1} f \right) \partial_x - f' \partial_y \right] \varphi_1 + \partial_y \varphi_2 = 0, \quad \partial_y \varphi_1 - \left[\left(1 - b^{-1} f \right) \partial_x - f' \partial_y \right] \varphi_2 = 0. \tag{5.58}$$

The boundary condition (5.55c) reduces to

$$\partial_y \varphi_j = \left(1 - b^{-1} f \right) (\mathscr{T}_j \varphi_j + \tau_j). \tag{5.59}$$

5.7.2 Power Series Expansion

Noting the surface function (5.1), we resort to the perturbation technique and consider formal power series expansion of φ_j in terms of ε:

$$\varphi_j(x,y;\varepsilon)=\sum_{k=0}^{\infty}\varphi_j^{(k)}(x,y)\varepsilon^k. \tag{5.60}$$

Substituting (5.1) into (5.57) and plugging (5.60) into (5.56), we may obtain the recurrence equations for $\varphi_j^{(k)}$ in D:

$$\Delta\varphi_j^{(k)}+\kappa_j^2\varphi_j^{(k)}=u_j^{(k)}, \tag{5.61}$$

where

$$u_j^{(k)}=\mathscr{D}_j^{(1)}\varphi_j^{(k-1)}+\mathscr{D}_j^{(2)}\varphi_j^{(k-2)}. \tag{5.62}$$

Here the differential operators are

$$\begin{aligned}\mathscr{D}_j^{(1)}=&b^{-1}\left[2g\partial_{xx}^2+2g'(b-y)\partial_{xy}^2+g''(b-y)\partial_y+2\kappa_j^2 g\right],\\ \mathscr{D}_j^{(2)}=&-b^{-2}\left\{g^2\partial_{xx}^2+(g')^2(b-y)^2\partial_{yy}^2+2gg'(b-y)\partial_{xy}^2\right.\\ &\left.-\left[2(g')^2-gg''\right](b-y)\partial_y+\kappa_j^2 g^2\right\}.\end{aligned}$$

Substituting (5.1) and (5.60) into (5.58), we obtain the recurrence equations for the boundary conditions on Γ_0:

$$\partial_x\varphi_1^{(k)}+\partial_y\varphi_2^{(k)}=p^{(k)},\quad \partial_y\varphi_1^{(k)}-\partial_x\varphi_2^{(k)}=q^{(k)},$$

where

$$p^{(k)}=\left(b^{-1}g\partial_x+g'\partial_y\right)\varphi_1^{(k-1)},\quad q^{(k)}=-\left(b^{-1}g\partial_x+g'\partial_y\right)\varphi_2^{(k-1)}. \tag{5.63}$$

Substituting (5.1) and (5.60) into (5.59), we derive the recurrence equations for the transparent boundary conditions on Γ_b:

$$\left(\partial_y-\mathscr{T}_j\right)\varphi_j^{(k)}=r_j^{(k)},$$

where

$$r_j^{(0)}=\tau_j,\quad r_j^{(1)}=-b^{-1}g(\mathscr{T}_j\varphi_j^{(0)}+\tau_j),\quad r_j^{(k)}=-b^{-1}g\mathscr{T}_j\varphi_j^{(k-1)}. \tag{5.64}$$

In all of the above recurrence equations, it is understood that $\varphi_j^{(k)}, u_j^{(k)}, p^{(k)}, q^{(k)}, r_j^{(k)}$ are zeros when $k < 0$. The boundary value problem (5.61)–(5.64) for the current terms $\varphi_j^{(k)}$ involve $u_j^{(k)}, p^{(k)}, q^{(k)}, r_j^{(k)}$, which depend only on previous two terms of $\varphi_j^{(k-1)}, \varphi_j^{(k-2)}$. Thus, the boundary value problem (5.61)–(5.64) can be recursively solved from $k = 0$.

5.7.3 Fourier Series Expansion

Since $\varphi_j^{(k)}$ are periodic functions of x with period Λ, they have the Fourier series expansions

$$\varphi_j^{(k)}(x, y) = \sum_{n\in\mathbb{Z}} \varphi_{jn}^{(k)}(y) e^{\mathrm{i}\alpha_n x}. \tag{5.65}$$

Substituting (5.65) into the boundary value problem (5.61)–(5.64), we obtain a coupled two-point boundary value problems:

$$\begin{aligned} \partial_{yy}^2 \varphi_{1n}^{(k)} + \beta_{1n}^2 \varphi_{1n}^{(k)} &= u_{1n}^{(k)}, \quad 0 < y < b, \\ \partial_y \varphi_{1n}^{(k)} &= q_n^{(k)} + \mathrm{i}\alpha_n \varphi_{2n}^{(k)}, \quad y = 0, \\ \partial_y \varphi_{1n}^{(k)} - \mathrm{i}\beta_{1n} \varphi_{1n}^{(k)} &= r_{1n}^{(k)}, \quad y = b \end{aligned} \tag{5.66}$$

and

$$\begin{aligned} \partial_{yy}^2 \varphi_{2n}^{(k)} + \beta_{2n}^2 \varphi_{2n}^{(k)} &= u_{2n}^{(k)}, \quad 0 < y < b, \\ \partial_y \varphi_{2n}^{(k)} &= p_n^{(k)} - \mathrm{i}\alpha_n \varphi_{1n}^{(k)}, \quad y = 0, \\ \partial_y \varphi_{2n}^{(k)} - \mathrm{i}\beta_{2n} \varphi_{2n}^{(k)} &= r_{2n}^{(k)}, \quad y = b, \end{aligned} \tag{5.67}$$

where $u_{jn}^{(k)}, p_n^{(k)}, q_n^{(k)}, r_{jn}^{(k)}$ are the Fourier coefficients of $u_j^{(k)}, p^{(k)}, q^{(k)}, r_j^{(k)}$, respectively.

It follows from Lemma 5.11.2 that the solutions of (5.66) and (5.67) are

$$\begin{aligned} \varphi_{1n}^{(k)}(y) =& K_1(y; \beta_{1n})(q_n^{(k)} + \mathrm{i}\alpha_n \varphi_{2n}^{(k)}(0)) \\ & - K_2(y; \beta_{1n}) r_{1n}^{(k)} + \int_0^b K_3(y, z; \beta_{1n}) u_{1n}^{(k)}(z) \mathrm{d}z, \end{aligned} \tag{5.68a}$$

$$\begin{aligned} \varphi_{2n}^{(k)}(y) =& K_1(y; \beta_{2n})(p_n^{(k)} - \mathrm{i}\alpha_n \varphi_{1n}^{(k)}(0)) \\ & - K_2(y; \beta_{2n}) r_{2n}^{(k)} + \int_0^b K_3(y, z; \beta_{2n}) u_{2n}^{(k)}(z) \mathrm{d}z, \end{aligned} \tag{5.68b}$$

where $\varphi_{jn}^{(k)}(0)$ are to be determined. Evaluating $\varphi_{jn}^{(k)}(y)$ at $y = 0$ in the above equations and recalling K_j in Lemma 5.11.2, we obtain

$$\begin{aligned}
\mathrm{i}\beta_{1n}\varphi_{1n}^{(k)}(0) &= (q_n^{(k)} + \mathrm{i}\alpha_n\varphi_{2n}^{(k)}(0)) - e^{\mathrm{i}\beta_{1n}b}r_{1n}^{(k)} + \int_0^b e^{\mathrm{i}\beta_{1n}z}u_{1n}^{(k)}(z)\mathrm{d}z,\\
\mathrm{i}\beta_{2n}\varphi_{2n}^{(k)}(0) &= (p_n^{(k)} - \mathrm{i}\alpha_n\varphi_{1n}^{(k)}(0)) - e^{\mathrm{i}\beta_{2n}b}r_{2n}^{(k)} + \int_0^b e^{\mathrm{i}\beta_{2n}z}u_{2n}^{(k)}(z)\mathrm{d}z,
\end{aligned}$$

which yields a system of algebraic equations for $\varphi_{jn}^{(k)}(0)$:

$$\mathrm{i}\begin{bmatrix} \beta_{1n} & -\alpha_n \\ \alpha_n & \beta_{2n} \end{bmatrix}\begin{bmatrix} \varphi_{1n}^{(k)}(0) \\ \varphi_{2n}^{(k)}(0) \end{bmatrix} = \begin{bmatrix} v_{1n}^{(k)} \\ v_{2n}^{(k)} \end{bmatrix}, \tag{5.69}$$

where

$$\begin{aligned}
v_{1n}^{(k)} &= q_n^{(k)} - e^{\mathrm{i}\beta_{1n}b}r_{1n}^{(k)} + \int_0^b e^{\mathrm{i}\beta_{1n}z}u_{1n}^{(k)}(z)\mathrm{d}z,\\
v_{2n}^{(k)} &= p_n^{(k)} - e^{\mathrm{i}\beta_{2n}b}r_{2n}^{(k)} + \int_0^b e^{\mathrm{i}\beta_{2n}z}u_{2n}^{(k)}(z)\mathrm{d}z.
\end{aligned}$$

It follows from Cramer's rule again that the linear system has a unique solution which is given by

$$\varphi_{1n}^{(k)}(0) = -\mathrm{i}\left(\frac{\beta_{2n}v_{1n}^{(k)} + \alpha_n v_{2n}^{(k)}}{\alpha_n^2 + \beta_{1n}\beta_{2n}}\right), \quad \varphi_{2n}^{(k)}(0) = -\mathrm{i}\left(\frac{\beta_{1n}v_{2n}^{(k)} - \alpha_n v_{1n}^{(k)}}{\alpha_n^2 + \beta_{1n}\beta_{2n}}\right).$$

Once $\varphi_{jn}^{(k)}(0)$ are determined, $\varphi_{jn}^{(k)}(y)$ can be computed from (5.68a) and (5.68b) explicitly for all k and n.

5.7.4 Leading Terms

For $k = 0$, it follows from (5.62), (5.63), and (5.64) that we obtain

$$u_j^{(0)} = p^{(0)} = q^{(0)} = 0, \quad r_j^{(0)} = \tau_j.$$

Their Fourier coefficients are

$$u_{jn}^{(0)} = p_n^{(0)} = q_n^{(0)} = 0, \quad r_{jn}^{(0)} = \tau_{jn}. \tag{5.70}$$

Substituting (5.70) into (5.69) yields

$$v_{jn}^{(0)} = -e^{\mathrm{i}\beta_{jn}b}\tau_{jn}$$

and

$$\begin{aligned}
\varphi_{1n}^{(0)}(0) &= \left(\frac{\mathrm{i}\beta_{2n}e^{\mathrm{i}\beta_{1n}b}}{\alpha_n^2+\beta_{1n}\beta_{2n}}\right)\tau_{1n} + \left(\frac{\mathrm{i}\alpha_n e^{\mathrm{i}\beta_{2n}b}}{\alpha_n^2+\beta_{1n}\beta_{2n}}\right)\tau_{2n},\\
\varphi_{2n}^{(0)}(0) &= \left(\frac{\mathrm{i}\beta_{1n}e^{\mathrm{i}\beta_{2n}b}}{\alpha_n^2+\beta_{1n}\beta_{2n}}\right)\tau_{2n} - \left(\frac{\mathrm{i}\alpha_n e^{\mathrm{i}\beta_{1n}b}}{\alpha_n^2+\beta_{1n}\beta_{2n}}\right)\tau_{1n}.
\end{aligned} \tag{5.71}$$

Plugging (5.71) into (5.68), we get

$$\begin{aligned}
\varphi_{1n}^{(0)}(y) &= \mathrm{i}\alpha_n K_1(y,\beta_{1n})\varphi_{2n}^{(0)}(0) - K_2(y,\beta_{1n})\tau_{1n}\\
&= M_{11}^{(n)}(y)\tau_{1n} + M_{12}^{(n)}(y)\tau_{2n}, &\text{(5.72a)}\\
\varphi_{2n}^{(0)}(y) &= -\mathrm{i}\alpha_n K_1(y;\beta_{2n})\varphi_{1n}^{(0)}(0) - K_2(y;\beta_{2n})\tau_{2n}\\
&= M_{21}^{(n)}(y)\tau_{1n} + M_{22}^{(n)}(y)\tau_{2n}, &\text{(5.72b)}
\end{aligned}$$

where

$$\begin{aligned}
M_{11}^{(n)}(y) &= -\left(\frac{\mathrm{i}\alpha_n^2 e^{\mathrm{i}\beta_{1n}b}}{\beta_{1n}(\alpha_n^2+\beta_{1n}\beta_{2n})}\right)e^{\mathrm{i}\beta_{1n}y} + \frac{\mathrm{i}e^{\mathrm{i}\beta_{1n}b}}{2\beta_{1n}}(e^{\mathrm{i}\beta_{1n}y}+e^{-\mathrm{i}\beta_{1n}y}),\\
M_{12}^{(n)}(y) &= \left(\frac{\mathrm{i}\alpha_n e^{\mathrm{i}\beta_{2n}b}}{\alpha_n^2+\beta_{1n}\beta_{2n}}\right)e^{\mathrm{i}\beta_{1n}y},\\
M_{21}^{(n)}(y) &= -\left(\frac{\mathrm{i}\alpha_n e^{\mathrm{i}\beta_{1n}b}}{\alpha_n^2+\beta_{1n}\beta_{2n}}\right)e^{\mathrm{i}\beta_{2n}y},\\
M_{22}^{(n)}(y) &= -\left(\frac{\mathrm{i}\alpha_n^2 e^{\mathrm{i}\beta_{2n}b}}{\beta_{2n}(\alpha_n^2+\beta_{1n}\beta_{2n})}\right)e^{\mathrm{i}\beta_{2n}y} + \frac{\mathrm{i}e^{\mathrm{i}\beta_{2n}b}}{2\beta_{2n}}(e^{\mathrm{i}\beta_{2n}y}+e^{-\mathrm{i}\beta_{2n}y}).
\end{aligned}$$

5.7.5 Linear Terms

For $k=1$, it follows from (5.62)–(5.64) that we obtain

$$\begin{aligned}
u_j^{(1)} &= b^{-1}\left[2g\partial_{xx}^2 + 2g'(b-y)\partial_{xy}^2 + g''(b-y)\partial_y + 2\kappa_j^2 g\right]\varphi_j^{(0)},\\
p^{(1)} &= \left(b^{-1}g\partial_x + g'\partial_y\right)\varphi_1^{(0)},\\
q^{(1)} &= -\left(b^{-1}g\partial_x + g'\partial_y\right)\varphi_2^{(0)},\\
r_j^{(1)} &= -b^{-1}g(\mathscr{T}_j\varphi_j^{(0)} + \tau_j).
\end{aligned}$$

Using the convolution theorem and (5.72a)–(5.72b) yields

$$u_{jn}^{(1)}(y) = \sum_{m\in\mathbb{Z}} U_j^{(n,m)}(y) g_{n-m}, \tag{5.73a}$$

$$p_{1n}(y) = \sum_{m\in\mathbb{Z}} P_m(y) g_{n-m}, \tag{5.73b}$$

$$q_{1n}(y) = \sum_{m\in\mathbb{Z}} Q_m(y) g_{n-m}, \tag{5.73c}$$

$$r_{jn}^{(1)}(y) = -b^{-1} \sum_{m\in\mathbb{Z}} \left(R_{jm}(y) + \tau_{jm}\right) g_{n-m}, \tag{5.73d}$$

where

$$\begin{aligned}
U_j^{(n,m)}(y) &= b^{-1}\left[2(\beta_{jm})^2 M_{j1}^{(m)}(y) + (\alpha_m^2 - \alpha_n^2)(b-y)\partial_y M_{j1}^{(m)}(y)\right]\tau_{1m} \\
&\quad + b^{-1}\left[2(\beta_{jm})^2 M_{j2}^{(m)}(y) + (\alpha_m^2 - \alpha_n^2)(b-y)\partial_y M_{j2}^{(m)}(y)\right]\tau_{2m}, \\
P_m(y) &= \mathrm{i}\alpha_m b^{-1}\left(M_{11}^{(m)}(y)\tau_{1m} + M_{12}^{(m)}(y)\tau_{2m}\right) \\
&\quad + \mathrm{i}(\alpha_n - \alpha_m)\left(\partial_y M_{11}^{(m)}(y)\tau_{1m} + \partial_y M_{12}^{(m)}(y)\tau_{2m}\right), \\
Q_m(y) &= -\mathrm{i}\alpha_m b^{-1}\left(M_{21}^{(m)}(y)\tau_{1m} + M_{22}^{(m)}(y)\tau_{2m}\right) \\
&\quad - \mathrm{i}(\alpha_n - \alpha_m)\left(\partial_y M_{21}^{(m)}(y)\tau_{1m} + \partial_y M_{22}^{(m)}(y)\tau_{2m}\right) \\
R_{jm}(y) &= \mathrm{i}\beta_{jm}\left(M_{j1}^{(m)}(y)\tau_{1m} + M_{j2}^{(m)}(y)\tau_{2m}\right).
\end{aligned}$$

When $k = 1$, recalling the expressions of $\varphi_{jn}^{(1)}(0)$ and evaluating (5.68) at $y = b$, we have

$$\begin{aligned}
\varphi_{1n}^{(1)}(b) &= K_1(b;\beta_{1n})(q_n^{(1)} + \mathrm{i}\alpha_n\varphi_{2n}^{(1)}(0)) - K_2(b;\beta_{1n})r_{1n}^{(1)} + \int_0^b K_3(b,z;\beta_{1n})u_{1n}^{(1)}(z)\mathrm{d}z \\
&= \frac{e^{\mathrm{i}\beta_{1n}b}}{\mathrm{i}\beta_{1n}}(q_n^{(1)} + \mathrm{i}\alpha_n\varphi_{2n}^{(1)}(0)) - \frac{e^{\mathrm{i}\beta_{1n}b}}{2\mathrm{i}\beta_{1n}}(e^{\mathrm{i}\beta_{1n}b} + e^{-\mathrm{i}\beta_{1n}b})r_{1n}^{(1)} \\
&\quad + \int_0^b \frac{e^{\mathrm{i}\beta_{1n}b}}{2\mathrm{i}\beta_{1n}}(e^{\mathrm{i}\beta_{1n}z} + e^{-\mathrm{i}\beta_{1n}z})u_{1n}^{(1)}(z)\mathrm{d}z \\
&= \frac{e^{\mathrm{i}\beta_{1n}b}}{(2\mathrm{i}\beta_{1n})(\alpha_n^2 + \beta_{1n}\beta_{2n})}\Bigg(2\beta_{1n}\beta_{2n}q_n^{(1)} + 2\alpha_n\beta_{1n}p_n^{(1)} - 2\alpha_n\beta_{1n}e^{\mathrm{i}\beta_{2n}b}r_{2n}^{(1)} \\
&\quad + (\alpha_n^2 - \beta_{1n}\beta_{2n})e^{\mathrm{i}\beta_{1n}b}r_{1n}^{(1)} - (\alpha_n^2 + \beta_{1n}\beta_{2n})e^{-\mathrm{i}\beta_{1n}b}r_{1n}^{(1)} \\
&\quad + 2\alpha_n\beta_{1n}\int_0^b e^{\mathrm{i}\beta_{2n}z}u_{2n}^{(1)}(z)\mathrm{d}z - 2\alpha_n^2\int_0^b e^{\mathrm{i}\beta_{1n}z}u_{1n}^{(1)}(z)\mathrm{d}z \\
&\quad + (\alpha_n^2 + \beta_{1n}\beta_{2n})\int_0^b (e^{\mathrm{i}\beta_{1n}z} + e^{-\mathrm{i}\beta_{1n}z})u_{1n}^{(1)}(z)\mathrm{d}z\Bigg),
\end{aligned}$$

and

$$\begin{aligned}
\varphi_{2n}^{(1)}(b) &= K_1(b;\beta_{2n})(p_n^{(1)} - \mathrm{i}\alpha_n\varphi_{1n}^{(1)}(0)) - K_2(b;\beta_{2n})r_{2n}^{(1)} + \int_0^b K_3(b,z;\beta_{2n})u_{2n}^{(1)}(z)\mathrm{d}z \\
&= \frac{e^{\mathrm{i}\beta_{2n}b}}{\mathrm{i}\beta_{2n}}(p_n^{(1)} - \mathrm{i}\alpha_n\varphi_{1n}^{(1)}(0)) - \frac{e^{\mathrm{i}\beta_{2n}b}}{2\mathrm{i}\beta_{2n}}(e^{\mathrm{i}\beta_{2n}b} + e^{-\mathrm{i}\beta_{2n}b})r_{2n}^{(1)} \\
&\quad + \int_0^b \frac{e^{\mathrm{i}\beta_{2n}b}}{2\mathrm{i}\beta_{2n}}(e^{\mathrm{i}\beta_{2n}z} + e^{-\mathrm{i}\beta_{2n}z})u_{2n}^{(1)}(z)\mathrm{d}z \\
&= \frac{e^{\mathrm{i}\beta_{2n}b}}{(2\mathrm{i}\beta_{2n})(\alpha_n^2 + \beta_{1n}\beta_{2n})}\Bigg(2\beta_{1n}\beta_{2n}p_n^{(1)} - 2\alpha_n\beta_{2n}q_n^{(1)} + 2\alpha_n\beta_{2n}e^{\mathrm{i}\beta_{1n}b}r_{1n}^{(1)} \\
&\quad + (\alpha_n^2 - \beta_{1n}\beta_{2n})e^{\mathrm{i}\beta_{2n}b}r_{2n}^{(1)} - (\alpha_n^2 + \beta_{1n}\beta_{2n})e^{-\mathrm{i}\beta_{2n}b}r_{2n}^{(1)} - 2\alpha_n\beta_{2n}\int_0^b e^{\mathrm{i}\beta_{1n}z}u_{1n}^{(1)}(z)\mathrm{d}z \\
&\quad - 2\alpha_n^2\int_0^b e^{\mathrm{i}\beta_{2n}z}u_{2n}^{(1)}(z)\mathrm{d}z + (\alpha_n^2 + \beta_{1n}\beta_{2n})\int_0^b (e^{\mathrm{i}\beta_{2n}z} + e^{-\mathrm{i}\beta_{2n}z})u_{2n}^{(1)}(z)\mathrm{d}z\Bigg).
\end{aligned}$$

Substituting (5.73) into (5.68) and evaluating at $y = b$, after tedious but straight forward calculations, we obtain the key identities:

$$\varphi_{1n}^{(1)}(b) = \sum_{m\in\mathbb{Z}} \frac{e^{\mathrm{i}\beta_{1n}b}}{(2\mathrm{i}\beta_{1n})(\alpha_n^2 + \beta_{1n}\beta_{2n})(\alpha_m^2 + \beta_{1m}\beta_{2m})}A_1^{(n,m)}g_{n-m}, \tag{5.74a}$$

$$\varphi_{2n}^{(1)}(b) = \sum_{m\in\mathbb{Z}} \frac{e^{\mathrm{i}\beta_{2n}b}}{(2\mathrm{i}\beta_{2n})(\alpha_n^2 + \beta_{1n}\beta_{2n})(\alpha_m^2 + \beta_{1m}\beta_{2m})}A_2^{(n,m)}g_{n-m}, \tag{5.74b}$$

where

$$
\begin{aligned}
A_1^{(n,m)} =& \Bigg\{ b^{-1}\Bigg[-2\beta_{1n}\beta_{2n}\alpha_m^2 e^{\mathrm{i}(\beta_{1m}+\beta_{2m})b} + \frac{\alpha_n\alpha_m\beta_{1n}}{\beta_{1m}}(\alpha_m^2-\beta_{1m}\beta_{2m})e^{2\mathrm{i}\beta_{1m}b} \\
&+ 2\Big\{\alpha_m\beta_{1n}(\alpha_n\beta_{2m}+\alpha_m\beta_{2n}) + \mathrm{i}b\beta_{1n}\big[\alpha_n\alpha_m\beta_{2m}(\beta_{2n}-\beta_{2m}) \\
&- (\alpha_n\alpha_m)^2 + \beta_{1m}^2\beta_{2m}\beta_{2n}\big]\Big\}e^{\mathrm{i}\beta_{1m}b} - \frac{\alpha_n\alpha_m\beta_{1n}}{\beta_{1m}}(\alpha_m^2+\beta_{1m}\beta_{2m})\Bigg] \\
&- \mathrm{i}\beta_{1n}(\alpha_n-\alpha_m)\Bigg[2\alpha_m\beta_{2m}\beta_{2n}e^{\mathrm{i}(\beta_{1m}+\beta_{2m})b} - \alpha_n(\alpha_m^2-\beta_{1m}\beta_{2m})e^{2\mathrm{i}\beta_{1m}b} \\
&- \alpha_n(\alpha_m^2+\beta_{1m}\beta_{2m})\Bigg]\Bigg\}\tau_{1m} + \Bigg\{ b^{-1}\Bigg[-2\alpha_n\alpha_m^2\beta_{1n}e^{\mathrm{i}(\beta_{1m}+\beta_{2m})b} \\
&- \frac{\alpha_m\beta_{1n}\beta_{2n}}{\beta_{2m}}(\alpha_m^2-\beta_{1m}\beta_{2m})e^{2\mathrm{i}\beta_{2m}b} + 2\Big\{\alpha_m\beta_{1n}\big(\alpha_n\alpha_m-\beta_{1m}\beta_{2n}\big) \\
&+ \mathrm{i}b\beta_{1n}\Big[\alpha_n(\alpha_m^2\beta_{2n}+\beta_{2m}^2\beta_{1m}) + \alpha_m\beta_{1m}(\alpha_n^2+\beta_{1m}\beta_{2n})\Big]\Big\}e^{\mathrm{i}\beta_{2m}b} \\
&+ \frac{\alpha_m\beta_{1n}\beta_{2n}}{\beta_{2m}}(\alpha_m^2+\beta_{1m}\beta_{2m})\Bigg] - \mathrm{i}\beta_{1n}(\alpha_n-\alpha_m)\Bigg[2\alpha_n\alpha_m\beta_{1m}e^{\mathrm{i}(\beta_{1m}+\beta_{2m})b} \\
&+ \beta_{2n}(\alpha_m^2-\beta_{1m}\beta_{2m})e^{2\mathrm{i}\beta_{2m}b} + \beta_{2n}(\alpha_m^2+\beta_{1m}\beta_{2m})\Bigg]\Bigg\}\tau_{2m},
\end{aligned}
$$

and

$$
\begin{aligned}
A_2^{(n,m)} =& \Bigg\{ b^{-1}\Bigg[2\alpha_n\alpha_m^2\beta_{2n}e^{\mathrm{i}(\beta_{1m}+\beta_{2m})b} + \frac{\alpha_m\beta_{1n}\beta_{2n}}{\beta_{1m}}(\alpha_m^2-\beta_{1m}\beta_{2m})e^{2\mathrm{i}\beta_{1m}b} \\
&- 2\Big\{\alpha_m\beta_{2n}(\alpha_n\alpha_m-\beta_{1n}\beta_{2m}) + \mathrm{i}b\beta_{2n}\Big[\alpha_n(\alpha_m^2\beta_{1n}+\beta_{1m}^2\beta_{2m}) \\
&+ \alpha_m\beta_{2m}\big(\alpha_n^2+\beta_{1n}\beta_{2m}\big)\Big]\Big\}e^{\mathrm{i}\beta_{1m}b} - \frac{\alpha_m\beta_{1n}\beta_{2n}}{\beta_{1m}}(\alpha_m^2+\beta_{1m}\beta_{2m})\Bigg] \\
&+ \mathrm{i}\beta_{2n}(\alpha_n-\alpha_m)\Big[2\alpha_n\alpha_m\beta_{2m}e^{\mathrm{i}(\beta_{1m}+\beta_{2m})b} + \beta_{1n}(\alpha_m^2-\beta_{1m}\beta_{2m})e^{2\mathrm{i}\beta_{1m}b} \\
&+ \beta_{1n}(\alpha_m^2+\beta_{1m}\beta_{2m})\Big]\Bigg\}\tau_{1m} + \Bigg\{ b^{-1}\Bigg[-2\beta_{1n}\beta_{2n}\alpha_m^2 e^{\mathrm{i}(\beta_{1m}+\beta_{2m})b} \\
&+ \frac{\alpha_m\alpha_n\beta_{2n}}{\beta_{2m}}(\alpha_m^2-\beta_{1m}\beta_{2m})e^{2\mathrm{i}\beta_{2m}b} + 2\Big\{\alpha_m\beta_{2n}\big(\alpha_n\beta_{1m}+\alpha_m\beta_{1n}\big) \\
&+ \mathrm{i}b\beta_{2n}\Big[\alpha_n\alpha_m\beta_{1m}(\beta_{1n}-\beta_{1m}) - (\alpha_n\alpha_m)^2 + \beta_{2m}^2\beta_{1m}\beta_{1n}\Big]\Big\}e^{\mathrm{i}\beta_{2m}b} \\
&- \frac{\alpha_m\alpha_n\beta_{2n}}{\beta_{2m}}(\alpha_m^2+\beta_{1m}\beta_{2m})\Bigg] - \mathrm{i}\beta_{2n}(\alpha_n-\alpha_m)\Bigg[2\alpha_m\beta_{1n}\beta_{1m}e^{\mathrm{i}(\beta_{1m}+\beta_{2m})b} \\
&- \alpha_n(\alpha_m^2-\beta_{1m}\beta_{2m})e^{2\mathrm{i}\beta_{2m}b} - \alpha_n(\alpha_m^2+\beta_{1m}\beta_{2m})\Bigg]\Bigg\}\tau_{2m}.
\end{aligned}
$$

5.8 Inverse Problem

In this section, we give reconstruction formulas for the inverse problem by dropping the higher order terms in the power series. Moreover, a nonlinear correction scheme is proposed to improve the accuracy of the reconstruction.

5.8.1 Reconstruction Formula

First, we rewrite the power series expansion (5.60) of φ_1 and φ_2 as follows,

$$\varphi_j(x,y) = \varphi_j^{(0)}(x,y) + \varepsilon\varphi_j^{(1)}(x,y) + e_j(x,y), \tag{5.75}$$

where $e_j(x,y) = \mathcal{O}(\varepsilon^2)$ denote the remainder consisting of all the high oder terms. Evaluating (5.75) at $y = b$ and dropping $e_j(x,y)$, we get the linearized equation:

$$\varphi_j(x,b) = \varphi_j^{(0)}(x,b) + \varepsilon\varphi_j^{(1)}(x,b),$$

which, in the frequency domain,

$$\varphi_{jn}(b) = \varphi_{jn}^{(0)}(b) + \varepsilon\varphi_{jn}^{(1)}(b). \tag{5.76}$$

Substituting (5.74) into (5.76) and noting $f = \varepsilon g$, we obtain an infinite dimensional linear system of equations:

$$\sum_{m\in\mathbb{Z}} C_j^{(n,m)} f_{n-m} = \varphi_{jn}(b) - \varphi_{jn}^{(0)}(b),$$

where

$$C_j^{(n,m)} = \frac{e^{\mathrm{i}\beta_{jn}b}}{(2\mathrm{i}\beta_{jn})(\alpha_n^2 + \beta_{1n}\beta_{2n})(\alpha_m^2 + \beta_{1m}\beta_{2m})} A_j^{(n,m)}.$$

In order to obtain a truncated finite dimensional linear systems, the cut-off

$$N_j = \left\lfloor \frac{\eta_j \Lambda}{2\pi} \right\rfloor$$

is chosen such that $|\alpha_n| \leqslant \eta_j$ for all $|n| \leqslant N_j$, where η_j is given by (5.15). In view of the definition of η_j, the density ρ_1 of the elastic slab is crucial to the reconstruction

resolution, a bigger ρ_1 gives a higher resolution. Keeping only the Fourier coefficients of the solution in $[-N_j,\, N_j]$, we obtain the truncated equations

$$C_j s_j = t_j, \tag{5.77}$$

where C_j is the $(2N_j+1)\times(2N_j+1)$ portion of $C_j^{(n,m)}$, and s_j, t_j are $(2N_j+1)$ column vectors given by

$$s_{j,m} = f_m, \quad t_{j,n} = \varphi_{jn}(b) - \varphi_{jn}^{(0)}(b), \quad -N_j \leqslant n, m \leqslant N_j.$$

We observe from (5.54) and (5.74) that when $|m| > N_j$ there could have exponentially amplified errors of $A_j^{(n,m)}$ due to the data noise. Therefore, the equations need to be regularized further by letting $A_j^{(n,m)} = 0$ if $|n-m| > N_j$. Let the solution of (5.77) be given by

$$s_j = C_j^{\dagger} t_j, \tag{5.78}$$

where $C_j^{\dagger}$ denote the Moore-Penrose pseudo-inverse of C_j. Finally, the scattering surface function is reconstructed as follows:

$$f(x) = \mathrm{Re} \sum_{|m|\leqslant N_j} s_{j,m} e^{\mathrm{i}\alpha_m x}. \tag{5.79}$$

5.8.2 Nonlinear Correction Scheme

In the previous subsection, an explicit reconstruction formula (5.79) is given. It is effective for a sufficiently small deformation parameter ε. For a relatively large ε, it is necessary to develop a nonlinear correction scheme to improve the accuracy of the reconstruction.

Firstly, we solve the linearized problem and compute (5.78) to obtain s_j, which is denoted as $s_j^{[0]}$. Let f_0 be the reconstructed surface function by using $s_j^{[0]}$ in (5.79). Next we solve the direct problem using f_0 as the surface function, and evaluate the total field $\boldsymbol{u}$ at $y = a$ denoted by $\boldsymbol{u}^{[f_0]}$. The data $\phi_j^{[f_0]}(x, a)$ is computed from (5.42) by using $\boldsymbol{u}^{[f_0]}$, which is then used to compute $\tau_{jn}^{[f_0]}$ from (5.47), (5.49) and (5.54). We

construct the coefficient matrices $C_j^{[f_0]}$ and the right hand side vectors $t_j^{[f_0]}$ of (5.77) using $\tau_{jn}^{[f_0]}$. Now we have approximated equations:

$$C_j^{[f_0]} s_j^{[0]} = t_j^{[f_0]}.$$

Subtracting the above equation from (5.77) yields

$$C_j s_j = t_j + C_j^{[f_0]} s_j^{[0]} - t_j^{[f_0]},$$

from which we compute the updated Fourier coefficients:

$$s_j^{[1]} = C_j^{\dagger} \left(t_j + C_j^{[f_0]} s_j^{[0]} - t_j^{[f_0]} \right).$$

Then the surface function is updated as follows

$$f_1(x) = \mathrm{Re} \sum_{|m| \leqslant N_j} s_{j,m}^{[1]} e^{\mathrm{i}\alpha_m x}.$$

Repeating the above procedure gives the nonlinear correction scheme:

$$\begin{aligned} s_j^{[l]} &= C_j^{\dagger} \left(t_j + C_j^{[f_{l-1}]} s_j^{[l-1]} - t_j^{[f_{l-1}]} \right), \\ f_l(x) &= \mathrm{Re} \sum_{|m| \leqslant N_j} s_{j,m}^{[l]} e^{\mathrm{i}\alpha_m x}, \quad l = 1, \ldots. \end{aligned}$$

Essentially the above nonlinear correction scheme is similar to Newton's method for solving non-linear equations. From the numerical experiments in the next section, we only need few iterations to obtain accurate reconstructions because good initial guesses are available from the reconstruction formula (5.79) when solving the linearized equation.

5.9 Numerical Experiments

In this section, we present some numerical experiments to show the effectiveness of the proposed method. We solve the direct scattering problem (5.4) to get the synthetic data of the displacement of the total field $\boldsymbol{u}$ by using the finite element method with the perfectly matched layer (PML) technique. Then the measured data

is obtained by interpolating the finite element solution with 500 uniform grid on Γ_a. In order to test the robustness of the proposed method, we add random noise to the data:

$$\boldsymbol{u}_\delta(x_i, a) = \boldsymbol{u}(x_i, a)(1 + \delta \boldsymbol{r}_i),$$

where $x_i = -\Lambda/2 + i\Lambda/500, i = 1, \ldots, 500$, $\boldsymbol{r}_i$ are vectors whose two components are random numbers uniformly distributed on $[-1, 1]$, and δ is the noise level.

In our numerical experiments, the Lamé parameters μ, λ are taken as $\lambda = 2, \mu = 1$. The density ρ_0 of the free space is $\rho_0 = 1$, while the density of the elastic slab ρ_1 is chosen to be three different numbers $\rho_1 = 1.0$, 2.0 and 4.0 in order to compare the reconstruction results. The noise level $\delta = 2\%$. The angular frequency $\omega = 2\pi$. Thus the compressional wavenumber $\kappa_1 = \pi$ and the shear wavenumber $\kappa_2 = 2\pi$, which indicate that $\lambda_1 = 2, \lambda_2 = 1$, where λ_1 and λ_2 are the compressional wavelength and the shear wavelength, respectively. The bottom of the slab is positioned at $y = b = 0.05\lambda_2$ and the top of the slab is put at $y = a = 2.0\lambda_2$. Hence the slab is put in the near-field regime while the data is measured in the far-field regime. The incident wave is generated by (5.2). In all numerical examples, the deformation parameter is fixed at $\varepsilon = 0.01$. According to (5.79), there are two possible choices to obtain the reconstructed surface function f, which are mathematically equivalent. Thus we always take $j = 1$ in (5.77) to compute the Fourier coefficients and to reconstruct the surface.

Example 1. The exact surface profile function is given by

$$g(x) = \frac{1}{5}\sin\left(\frac{20\pi x}{31}\right) - \sin\left(\frac{40\pi x}{31}\right) + \sin\left(\frac{60\pi x}{31}\right),$$

which is a periodic function with the period $\Lambda = 3.1$. This is a simple example as the surface function only contains a few Fourier modes.

Figure 5.2 shows the reconstructed surfaces (dashed line) against the exact surface (solid line). Figure 5.2(a), (b), and (c) plot the reconstructed surfaces by using $\rho_1 = 1.0, 2.0, 4.0$, respectively. Clearly, the reconstruction resolution is increased with respect to ρ_1. For $\rho_1 = 1.0$, the slab is absent and the cut-off $N_1 = 1$. Hence only the

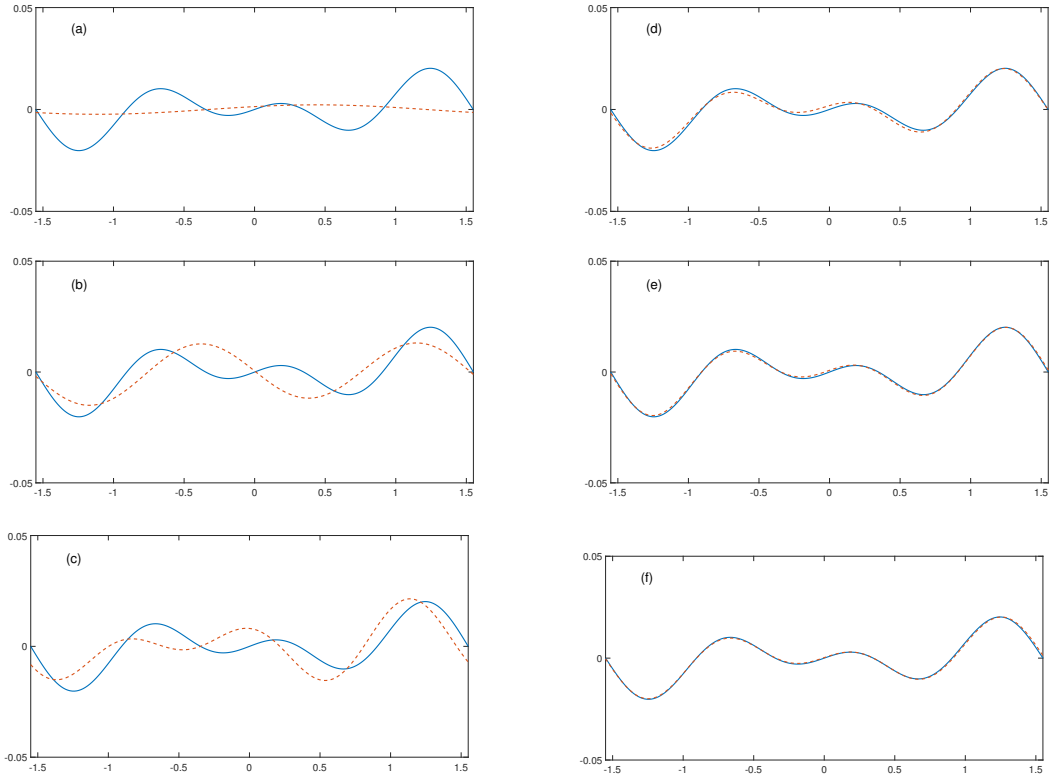

Figure 5.2. Example 1: the reconstructed surface (dashed line) is plotted against the exact surface (solid line). (a) $\rho_1 = 1$; (b) $\rho_1 = 2$; (c) $\rho_1 = 4$; (d) 1 step of nonlinear correction when $\rho_1 = 4$; (e) 2 steps of nonlinear correction when $\rho_1 = 4$; (f) 3 steps of nonlinear correction when $\rho_1 = 4$.

zeroth and first Fourier modes may be reconstructed and the resolution is at most one wavelength. More frequency modes are able to be recovered and the resolution increases to the subwavelength regime by increasing ρ_1. Using Figure 5.2(c) as the initial guess, we adopt the nonlinear correction scheme to improve the reconstruction accuracy. As shown in Figure 5.2(d), (e), and (f), the reconstruction is almost perfect after 3 steps of the iteration, which indicates that the algorithm is effective to improve the accuracy of the reconstruction.

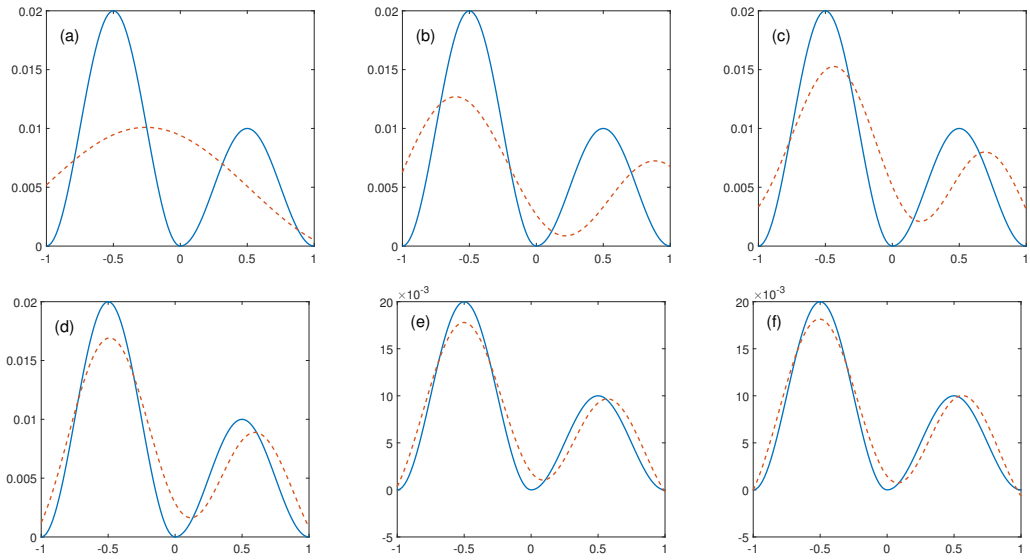

Figure 5.3. Example 2: the reconstructed surface (dashed line) is plotted against the exact surface (solid line). (a) $\rho_1 = 1$; (b) $\rho_1 = 2$; (c) $\rho_1 = 4$; (d) 1 step of nonlinear correction when $\rho_1 = 4$; (e) 2 steps of nonlinear correction when $\rho_1 = 4$; (f) 3 steps of nonlinear correction when $\rho_1 = 4$.

Example 2. Consider the following surface profile function in the interval $[-1, 1]$:

$$g(x) = \begin{cases} 1 - \cos(2\pi x), & -1 \leqslant x < 0, \\ 0.5 - 0.5\cos(2\pi x), & 0 < x \leqslant 1. \end{cases}$$

The period $\Lambda = 2$. Although this function is continuous, it is not smooth since the first derivative is not continuous at $x = 0$. Figure (5.3) shows the reconstructed surface (dashed line) against the exact surface (solid line) for different density ρ_1 and the first three steps of the nonlinear correction. The similar conclusions can be drawn as those for Example 1: the density ρ_1 helps the resolution and the nonlinear correction improve the reconstruction.

5.10 Conclusion

In this chapter, we have proposed an effective mathematical model and developed an efficient numerical method to solve the inverse elastic surface scattering problem by using the far-field data. The key idea is to utilize a slab with larger density to allow more propagating modes to propagate to the far-field zone, which contributes to the reconstruction resolution. The nonlinear correction improves the accuracy by using the initial guess generated from the explicit reconstruction formula. Results show that the proposed method is robust to the data noise.

5.11 Appendix: Second Order Equations

Consider the final value problem of the second order equation in the interval (b, a):

$$u'' + \eta^2 u = 0, \quad b < y < a, \tag{5.80a}$$

$$u = p, \quad y = a, \tag{5.80b}$$

$$u' - \mathrm{i}\beta u = q, \quad y = a, \tag{5.80c}$$

where $0 \neq \eta, \beta, p, q$ are constants.

Lemma 5.11.1 *The final value problem (5.80) has a unique solution which is given by*

$$u(y) = \left(\frac{(\eta+\beta)p - \mathrm{i}q}{2\eta}\right) e^{-\mathrm{i}\eta(a-y)} + \left(\frac{(\eta-\beta)p + \mathrm{i}q}{2\eta}\right) e^{\mathrm{i}\eta(a-y)}.$$

Proof The general solution of the homogeneous second order equation (5.80a) is

$$u(y) = c_1 e^{\mathrm{i}\eta y} + c_2 e^{-\mathrm{i}\eta y},$$

where c_1 and c_2 are constant coefficients to be determined. It follows from the final conditions (5.80b)–(5.80c) that

$$u = p, \quad u' = \mathrm{i}\beta p + q, \quad y = a.$$

Plugging the final values of u and u' into the general solution, we obtain

$$c_1 = \left(\frac{(\eta+\beta)p - \mathrm{i}q}{2\eta}\right) e^{-\mathrm{i}\eta a}, \quad c_2 = \left(\frac{(\eta-\beta)p + \mathrm{i}q}{2\eta}\right) e^{\mathrm{i}\eta a},$$

which completes the proof. ■

Consider the two-point boundary value problem of the second order equation in the interval $(0, h)$:

$$u'' + \beta^2 u = v, \quad 0 < y < h, \tag{5.81a}$$

$$u' = r, \quad y = 0, \tag{5.81b}$$

$$u' - \mathrm{i}\beta u = s, \quad y = h, \tag{5.81c}$$

where $0 \neq \beta, r, s$ are constants.

Lemma 5.11.2 *The two-point boundary value problem* (5.81) *has a unique solution which is given by*

$$u(y) = K_1(y;\beta)r - K_2(y;\beta)s + \int_0^h K_3(y,z;\beta)v(z)\mathrm{d}z,$$

where

$$K_1(y;\beta) = \frac{e^{\mathrm{i}\beta y}}{\mathrm{i}\beta}, \quad K_2(y;\beta) = \frac{e^{\mathrm{i}\beta h}}{2\mathrm{i}\beta}(e^{\mathrm{i}\beta y} + e^{-\mathrm{i}\beta y}),$$

and

$$K_3(y,z;\beta) = \begin{cases} \frac{e^{\mathrm{i}\beta y}}{2\mathrm{i}\beta}(e^{\mathrm{i}\beta z} + e^{-\mathrm{i}\beta z}), & z < y, \\ \frac{e^{\mathrm{i}\beta z}}{2\mathrm{i}\beta}(e^{\mathrm{i}\beta y} + e^{-\mathrm{i}\beta y}), & z > y. \end{cases}$$

Proof A fundamental set of solutions for the second order equation (5.81a) is

$$u_1(y) = e^{\mathrm{i}\beta y}, \quad u_2(y) = e^{-\mathrm{i}\beta y}.$$

A simple calculation yields that the Wronskian $W(u_1, u_2) = -2\mathrm{i}\beta$. It follows from the variation of parameters that the general solution to the inhomogeneous second order equation (5.81a) is

$$u(y) = c_1 e^{\mathrm{i}\beta y} + c_2 e^{-\mathrm{i}\beta y} + \frac{e^{\mathrm{i}\beta y}}{2\mathrm{i}\beta}\int_0^y e^{-\mathrm{i}\beta z}v(z)\mathrm{d}z - \frac{e^{-\mathrm{i}\beta y}}{2\mathrm{i}\beta}\int_0^y e^{\mathrm{i}\beta z}v(z)\mathrm{d}z, \tag{5.82}$$

where c_1 and c_2 are undetermined constants.

Taking the derivative of (5.82), evaluating at $y = 0$, and using the boundary condition (5.81b) give

$$u'(0) = \mathrm{i}\beta(c_1 - c_2) = r. \tag{5.83}$$

It follows from the boundary condition (5.81c) that

$$c_2 = \frac{1}{2\mathrm{i}\beta}\left(\int_0^h e^{\mathrm{i}\beta z} v(z)\mathrm{d}z - se^{\mathrm{i}\beta h}\right). \tag{5.84}$$

Combining (5.83) and (5.84) yields

$$c_1 = c_2 + \frac{r}{\mathrm{i}\beta} = \frac{1}{2\mathrm{i}\beta}\left(\int_0^h e^{\mathrm{i}\beta z} v(z)\mathrm{d}z - se^{\mathrm{i}\beta h}\right) + \frac{r}{\mathrm{i}\beta}. \tag{5.85}$$

Substituting (5.84) and (5.85) into (5.82), we obtain the solution. ■

REFERENCES

[1] T. Arens, A new integral equation formulation for the scattering of plane elastic waves by diffraction gratings, *J. Integral Equations Appl.*, **11** (1999), 275–297.

[2] T. Arens, The scattering of plane elastic waves by a one-dimensional periodic surface, *Math. Methods Appl. Sci.*, **22** (1999), 55–72.

[3] I. Babuška and A. Aziz, *Survey lectures on Mathematical Foundation of the Finite Element Method, in the Mathematical Foundations of the Finite Element Method with Application to the Partial Differential Equations*, ed. by A.Aziz, Academic Press, New York, 1973, 5–359.

[4] I. Babuška and C. Werner, Error estimates for adaptive finite element computations, *SIAM J. Numer. Anal.*, 15 (1978), 736–754.

[5] G. Bao, Finite element approximation of time harmonic waves in periodic structures, *SIAM J. Numer. Anal.*, 32(1995), 1155–1169.

[6] G. Bao, Variational approximation of Maxwell's equations in biperiodic structures, *SIAM J. Appl. Math.*, 57(1997), 364–381.

[7] G. Bao, Z. Chen, and H. Wu, Adaptive finite element method for diffraction gratings, *J. Opt. Soc. Amer. A*, 22(2005), 1106–1114.

[8] G. Bao, L. Cowsar, and W. Masters, eds., Mathematical Modeling in Optical Science, *Frontiers in Appl. Math.*, SIAM, Philadelphia, 2001.

[9] G. Bao, T. Cui, and P. Li, Inverse diffraction grating of maxwell's equations in biperiodic structures, *Opt. Express*, **22**(2014), 4799–4816.

[10] G. Bao, D. C. Dobson, and J. A. Cox, Mathematical studies in rigorous grating theory, *J. Opt. Soc. Amer. A*, 12(1995), 1029–1042.

[11] G. Bao, G. Hu, J. Sun, and T. Yin, Direct and inverse elastic scattering from anisotropic media, *J. Math. Pures Appl.*, 117 (2018), 263–301.

[12] G. Bao and P. Li, Near-field imaging of infinite rough surfaces *SIAM J. Appl.Math.*, **73** (2013), 2162–2187.

[13] G. Bao and P. Li, Convergence analysis in near-field imaging, *Inverse Problems*, **30**(2014), 085008.

[14] G. Bao and P. Li, Near-field imaging of infinite rough surfaces in dielectric media, *SIAM J. Imaging Sci.*, **7** (2014), 867–899.

[15] G. Bao, P. Li, J. Lin, and F. Triki, Inverse scattering problems with multi-frequencies, *Inverse Problems*, 31 (2015), 093001.

[16] G. Bao, P. Li, and H. Wu, An adaptive edge element method with perfectly matched absorbing layers for wave scattering by periodic structures, *Math. Comp.*, 79(2010), 1-34.

[17] G. Bao, P. Li, and Y. Wang, Near-field imaging with far-field data, *Appl. Math. Lett.*, **60**(2016), 36–42.

[18] G. Bao and H. Wu, On the convergence of the solutions of PML equations for Maxwell's equations, *SIAM J. Numer. Anal.*, 43(2005), 2121–2143.

[19] A. Bayliss and E. Turkel, Radiation boundary conditions for numerical simulation of waves, *Comm. Pure Appl. Math.*, 33 (1980), 707–725.

[20] J.-P. Berenger, A perfectly matched layer for the absorption of electromagnetic waves, *J. Comput. Phys.*, 114 (1994), 185–200.

[21] J. H. Bramble and J. E. Pasciak, Analysis of a finite PML approximation for the three dimensional time-harmonic Maxwell and acoustic scattering problems, Math. Comp., 76 (2007), 597–614.

[22] J. H. Bramble, J. E. Pasciak and D. Trenev, Analysis of a finite PML approximation to the three dimensional elastic wave scattering problem, *Math. Comp.*, 79 (2010), 2079–2101.

[23] O. P. Bruno and F. Reitich, Numerical solution of diffraction problems: a method of variation of boundaries, *J. Opt. Soc. Am. A*, **10** (1993), 1168–1175.

[24] J. M. Cascon, C. Kreuzer, R. H. Nochetto, and K. G. Siebert, Quasi-optimal convergence rate for an adaptive finite element method, *SIAM J. Numer. Anal.*, 46(2008), 2524–2550.

[25] A. Charalambopoulos, D. Gintides, and K. Kiriaki, On the uniqueness of the inverse elastic scattering problem for periodic structures, *Inverse Problems*, **17** (2001), 1923–1935.

[26] J. Chen and Z. Chen, An adaptive perfectly matched layer technique for 3-D time-harmonic electromagnetic scattering problems, *Math. Comp.*, 77 (2008),673–698.

[27] X. Chen and A. Friedman, Maxwell's equations in a periodic structure, Trans. Amer. Math. Soc., 323 (1991), 465–507.

[28] Z. Chen and X. Liu, An adaptive perfectly matched layer technique for time-harmonic scattering problems, *SIAM J. Numer. Anal.*, 43 (2005), 645–671.

[29] Z. Chen and H. Wu, An adaptive finite element method with perfectly matched absorbing layers for the wave scattering by periodic structures, *SIAM J.Numer. Anal.*, 41(2003), 799–826.

[30] Z. Chen, X. Xiang and X. Zhang, Convergence of the PML method for elastic wave scattering problems, *Math. Comp.*, 85 (2016), 2687–2714.

[31] T. Cheng, P. Li, and Y. Wang, Near-field imaging of perfectly conducting grating surfaces, *J. Opt. Soc. Am. A*, **30** (2013), 2473–2481.

[32] W. Chew and Q. Liu, Perfectly matched layers for elastodynamics: a new absorbing boundary condition, *J. Comput. Acoust.*, 4 (1996), 341–359.

[33] W. Chew and W. Weedon, A 3D perfectly matched medium for modified Maxwell's equations with stretched coordinates, *Microwave Opt. Techno. Lett.*, 13(1994), 599-604.

[34] P. G. Ciarlet, *Mathematical Elasticity, vol. I : Three-Dimensional Elasticity, Studies in Mathematics and its Applications*, North-Holland, Amsterdam, 1988.

[35] F. Collino and P. Monk, The perfectly matched layer in curvilinear coordinates, SIAM J. Sci. Comput., 19 (1998), 2061–1090.

[36] F. Collino and C. Tsogka, Application of the PML absorbing layer model to the linear elastodynamics problem in anisotropic heterogeneous media, *Geophysics*,66 (2001), 294–307.

[37] D. Colton and R. Kress, *Integral Equation Methods in Scattering Theory,* Wiley, New York, 1983.

[38] D. Colton and R. Kress, *Inverse acoustic and electromagnetic scattering theory*, Springer, New York, 2013.

[39] D. Courjon, *Near-Field Microscopy and Near-Field Optics*, Imperial College Press, London, 2003.

[40] W. Dörfler, A convergent adaptive algorithm for Poisson's equation, *SIAM J. Numer. Anal.*, 33(1996), 1106–1124.

[41] J. Elschner and G. Hu, Variational approach to scattering of plane elastic waves by diffraction gratings, *Math. Methods Appl. Sci.*, **33** (2010), 1924–1941.

[42] J. Elschner and G. Hu, An optimization method in inverse elastic scattering for one-dimensional grating profiles *Commun. Comput. Phys.*, **12**(2012), 1434–1460.

[43] J. Elschner and G. Hu, Scattering of plane elastic waves by three-dimensional diffraction gratings, *Math. Models Methods Appl. Sci.*, **22**(2012), 1150019.

[44] B. Engquist and A. Majda, Absorbing boundary conditions for the numerical simulation of waves, *Math. Comp.*, 31 (1977), 629–651.

[45] G. K. Gächter and M. J. Grote, Dirichlet-to-Neumann map three-dimensional elastic waves, *Wave Motion*, 37 (2003), 293–311.

[46] D. Givoli and J. B. Keller, Non-reflecting boundary conditions for elastic waves, *Wave Motion*, 12 (1990), 261–279.

[47] H. Haddar and R. Kress, On the Fréchet derivative for obstacle scattering with an impedance boundary condition, *SIAM J. Appl. Math.*, 65 (2004), 94–208.

[48] F. D. Hastings, J. B. Schneider, and S. L. Broschat, Application of the perfectly matched layer (PML) absorbing boundary condition to elastic wave propagation, *J. Acoust. Soc. Am.*, 100 (1996), 3061–3069.

[49] Y. He, D. P. Nicholls, and J. Shen, An efficient and stable spectral method for electromagnetic scattering from a layered periodic structure, *J. Comput. Phys.*, 231(2012), 3007–3022.

[50] F. Hecht, New development in FreeFem++, *J. Numer. Math.*, 20 (2012), 251–265.

[51] T. Hohage, F. Schmidt, and L. Zschiedrich, Solving time-harmonic scattering problems based on the pole condition. II: Convergence of the PML method, SIAM J. *Math. Anal.*, 35 (2003), 547–560.

[52] G. C. Hsiao, N. Nigam, J. E. Pasiak, and L. Xu, Error analysis of the DtN-FEM for the scattering problem in acoustic via Fourier analysis, *J. Comput. Appl. Math.*, 235(2011), 4949–4965.

[53] G. Hu, J. Li, H. Liu, and H. Sun, Inverse elastic scattering for multiscale rigid bodies with a single far-field pattern, *SIAM J. Imaging Sci.*, 7 (2014), 1799–1825.

[54] G. Hu, Y. Lu, and B. Zhang, The factorization method for inverse elastic scattering from periodic structures, *Inverse Problems*, **29**(2013), 115005.

[55] M. Grote and J. Keller, On nonreflecting boundary conditions, *J. Comput. Phys.*, 122 (1995), 231–243.

[56] M. Grote and C. Kirsch, Dirichlet-to-Neumann boundary conditions for multiple scattering problems, *J. Comput. Phys.*, 201 (2004), 630–650.

[57] X. Jiang and P. Li, Inverse electromagnetic diffraction by biperiodic dielectric gratings, *Inverse Problems*, **33**(2017), 085004.

[58] X. Jiang and P. Li, An adaptive finite element PML method for the acoustic-elastic interaction in three dimensions, Commun. Comput. Phys.,22 (2017), 1486–1507.

[59] X. Jiang, P. Li, J. Lv, Z. Wang, H. Wu and W. Zheng, An adaptive finite element DtN method for Maxwell's equation in biperiodic structures, submitted.

[60] X. Jiang, P. Li, J. Lv, and W. Zheng, An adaptive finite element PML method for the elastic wave scattering problem in periodic structures, *ESAIM: Math. Model. Numer. Anal.*, 51 (2017), 2017–2047.

[61] X. Jiang, P. Li, J. Lv,and W. Zheng, An adaptive finite element method for the wave scattering with transparent boundary condition, *J. Sci. Comput.*, 72(2017), 936–956.

[62] X. Jiang, P. Li, J. Lv, and W. Zheng, Convergence of the PML solution for elastic wave scattering by biperiodic structures, *Comm. Math. Sci.*, 16 (2018), 985–1014.

[63] X. Jiang, P. Li, and W. Zheng, Numerical solution of acoustic scattering by an adaptive DtN finite element method, *Commun. Comput. Phys.*, 13(2013), 1227–1244.

[64] A. Kirsch, The domain derivative and two applications in inverse scattering theory, *Inverse Problems*, 9 (1993), 81–96.

[65] D. Komatitsch and J. Tromp, A pefectly matched layer absorbing boundary condition for the second-order seismic wave equation, *Geophys. J. Int.*, 154(2003), 146–153.

[66] L. D. Landau and E. M. Lifshitz, *Theory of Elasticity,* Oxford: Pergamon Press, 1986

[67] M. Lassas and E. Somersalo, On the existence and convergence of the solution of PML equations, Computing, 60 (1998), 229–241.

[68] F. Le Louër, On the Fréchet derivative in elastic obstacle scattering, *SIAM J. Appl. Math.*, 72 (2012), 1493–1507.

[69] P. Li and J. Shen, Analysis of the scattering by an unbounded rough surface, *Math. Methods Appl. Sci.*, **35**(2012), 2166–2184.

[70] P. Li and Y. Wang, Near-field imaging of interior cavities, *Commun. Comput. Phys.*, **17** (2015), 542–563.

[71] P. Li and Y. Wang, Near-field imaging of obstacles, *Inverse Probl. Imaging*, **9** (2015), 189–210.

[72] P. Li, Y. Wang, and Y. Zhao, Inverse elastic surface scattering with near-field data, *Inverse Problems*, **31**(2015), 035009.

[73] P. Li, Y. Wang, and Y. Zhao, Convergence analysis in near-field imaging for elastic waves, *Appl. Anal.*, **95** (2016), 2339–2360.

[74] P. Li, Y. Wang, and Y. Zhao, Near-field imaging of biperiodic surfaces for elastic waves, *J. Comput. Phys.*, **324** (2016), 1–23.

[75] P. Li, Y. Wang, Z. Wang, and Y. Zhao, Inverse obstacle scattering for elastic waves, *Inverse Problems*, 32 (2016), 115018.

[76] P. Li and X. Yuan, Inverse obstacle scattering for elastic waves in three dimensions, *Inverse Problems and Imaging*, to appear.

[77] P. Li and X. Yuan, Convergence of an adaptive finite element DtN method for the elastic wave scattering problem, arXiv:1903.03606.

[78] A. Malcolm and D. P. Nicholls, A field expansions method for scattering by periodic multilayered media, *J. Acoust. Soc. Am.*, **129** (2011), 1783–1793.

[79] P. Monk, A posterior error indicators for Maxwell's equations, *J. Comput. Appl. Math.*, 100(1998), 173–190.

[80] P. Monk, *Finite Element Methods for Maxwell's Equations,* Oxford University Press, New York, 2003.

[81] P. Morin, R. H. Nochetto, and K. G. Siebert, Data oscillation and convergence of adaptive FEM, *SIAM J. Numer. Anal.*, 38(2000), 466–488.

[82] J.-C. Nédélec, *Acoustic and Electromagnetic Equations Integral Representations for Harmonic Problems,* Springer, 2000.

[83] J. C. Nédélec and F. Starling, Integral equation methods in a quasi-periodic diffraction problem for the time-harmonic Maxwell's equations, *SIAM J. Math. Anal.*, 22(1997), 1679–1701.

[84] D. P. Nicholls and F. Reitich, Shape deformations in rough-surface scattering: cancellations, conditioning, and convergence, *J. Opt. Soc. Am. A*, **21** (2004), 590–605.

[85] J. A. Ogilvy, *Theory of Wave Scattering from Random Rough Surfaces*, Institute of Physics Publishing, 1991.

[86] R. Petit, ed.,Electromagnetic Theory of Gratings, Springer, 1980.

[87] R. Potthast, Domain derivatives in electromagnetic scattering, *Math. Meth. Appl. Sci.*, 19 (1996), 1157–1175.

[88] P. Rayleigh, On the dynamical theory of gratings, *R. Soc. London Ser. A.*, 79(1907), 399–416.

[89] L. Scott and S. Zhang, Finite element interpolation of nonsmooth functions satisfying boundary conditions, *Math. Comp.*, 54 (1990), 483–493.

[90] A. H. Schatz, An observation concerning Ritz–Galerkin methods with indefinite bilinear forms, *Math. Comp.*, 28 (1974), 959–962.

[91] H. Thomas, Radiation boundary conditions for the numerical simulation of waves, *Acta Numer.*, 8 (1999), 47–106.

[92] E. Turkel and A. Yefet, Absorbing PML boundary layers for wave-like equations, *Appl. Numer. Math.*, 27 (1998), 533–557.

[93] R. Verfürth, A review of a posterior error estimation and adaptive mesh refinement techniques, Teubner, Stuttgart, 1996.

[94] Z. Wang, G. Bao, J. Li, P. Li, and H. Wu, An adaptive finite element method for the diffraction grating problem with transparent boundary condition, *SIAM J. Numer. Anal.*, 53(2015), 1585–1607.

[95] G. N. Watson, *A Treatise on the Theory of Bessel Functions,* Cambridge University Press, Cambridge, UK, 1922.

[96] Y. Wu and Y. Y. Lu, Analyzing diffraction gratings by a boundary integral equation Neumann-to-Dirichlet map method, *J. Opt. Soc. Am. A*, 26(2009), 2444–2451.